UFRRJ

INSTITUTO DE TECNOLOGIA

PROGRAMA DE PÓS-GRADUAÇÃO EM CIÊNCIA E TECNOLOGIA DE ALIMENTOS

TESE

DESENVOLVIMENTO DE EXTRUDADOS EXPANDIDOS À BASE DE CEREAIS INTEGRAIS

JHONY WILLIAN VARGAS SOLÓRZANO

2019

UNIVERSIDADE FEDERAL RURAL DO RIO DE JANEIRO
INSTITUTO DE TECNOLOGIA
PROGRAMA DE PÓS-GRADUAÇÃO EM CIÊNCIA E
TECNOLOGIA DE ALIMENTOS

DESENVOLVIMENTO DE EXTRUDADOS EXPANDIDOS À BASE DE
CEREAIS INTEGRAIS

JHONY WILLIAN VARGAS SOLÓRZANO

Sob a Orientação do Professor Doutor
José Luis Ramírez Ascheri

e Coorientação do Professor Doutor
Carlos Wanderlei Piler de Carvalho

Tese submetida como requisito parcial para obtenção do grau de **Doutor em Ciência e Tecnologia de Alimentos**, no Programa de Pós-Graduação em Ciência e Tecnologia de Alimentos, Área de Concentração em Tecnologia de Alimentos.

Seropédica, RJ
Dezembro de 2019

UNIVERSIDADE FEDERAL RURAL DO RIO DE JANEIRO
INSTITUTO DE TECNOLOGIA
**PROGRAMA DE PÓS-GRADUAÇÃO EM CIÊNCIA E TECNOLOGIA DE
ALIMENTOS**

JHONY WILLIAN VARGAS SOLÓRZANO
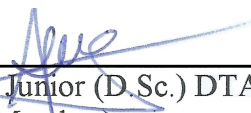
Tese submetida como requisito parcial para obtenção do grau de **Doutor em Ciência e
Tecnologia de Alimentos**, no Programa de Pós-Graduação em Ciência e Tecnologia de
Alimentos, Área de Concentração em Tecnologia de Alimentos.

TESE APROVADA EM 18 DE DEZEMBRO DE 2019.

_____
José Luis Ramírez Ascheri   .Sc.)   mbrapa-CTAA
(Orientador)

_____
José Lucena Barbosa Junior (D.Sc.) DTA-UFRRJ
(Membro)
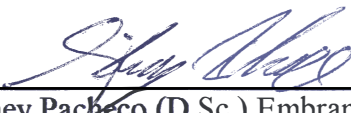
_____
Juarez Vicente (D.Sc.) DTA-UFRRJ
(Membro)

_____
Renata Torrezan (D.Sc.) Embrapa-CTAA
(Membro)

_____
Sidney Pacheco (D.Sc.) Embrapa-CTAA
(Membro)

DEDICATORIA

Para todos os que tem prazer em estudar as grandes obras de Jeová (Salmo 111:2). Para Jeová, meu Deus, Pai e Amigo, o magnifico instrutor que ensina o melhor para nosso próprio benefício e nos guia no caminho que é conveniente para nós (Isaías 48:17). Seus conselhos são maravilhosos e suas realizações são grandiosas (Isaías 28:29). A Ele pertence a glória, a honra e o poder (Apocalipse 4:11), pois Jeová nunca se cansa nem fica exausto, seu entendimento é insondável, dá poder ao cansado e enche de vigor aquele que está sem forças (Isaías 40:28, 29).

AGRADECIMENTOS

RESUMO GERAL

VARGAS-SOLÓRZANO, Jhony Willian. **Desenvolvimento de extrudados expandidos à base de cereais integrais**. 2019. Tese (Doutorado em Ciência e Tecnologia de Alimentos). Instituto de Tecnologia, Universidade Federal Rural do Rio de Janeiro, Seropédica, RJ. 2019.

O consumo de grãos integrais está associado com uma alimentação saudável e incentiva a redução do impacto ambiental, economizando energia da indústria do refino de cereais. Os consumidores optam cada vez mais por produtos processados à base de grãos integrais e preservados por métodos físicos. Neste sentido, o cozimento por extrusão é uma técnica útil para produzir alimentos sem conservantes e para aumentar a gama de produtos à base de grãos integrais. *Snacks* extrudados prontos para consumo produzidos a partir de grãos integrais têm texturas duras e são mais escuros, o que afeta a aceitação sensorial do consumidor. O principal componente que afeta esses atributos é a fibra insolúvel depositada nas camadas de farelo. As partículas de farelo são difíceis de fundir e causam ruptura física do material fundido à saída da matriz do extrusor. A redução do tamanho de partículas do farelo melhora a expansão elástica dos extrudados. Neste trabalho, o efeito negativo das fibras naturais na expansão e nas propriedades de textura de *snacks* extrudados de grãos integrais foi abordado pela redução do tamanho das partículas de farelo, usando dois tipos de moinho (disco e rolo), operados em uma única etapa e sem uma placa de peneiramento, para evitar o entupimento da peneira do moinho. Durante a moagem, os tecidos do farelo e germe são desintegrados e tornam-se parte das superfícies das partículas. Para melhorar o fraccionamento das partículas e a heterogeneidade do tamanho das partículas no material de alimentação, os grãos foram secos antes do processo de moagem. Este passo favoreceu a propagação de tecidos de farelo e germe no material de alimentação. O processo de secagem afetou a fração de amido dos grãos. Os processos de secagem e moagem influenciaram na porosidade interpartícula do material de alimentação. Farinhas integrais mais porosas foram obtidas com o moinho de rolos e, durante sua extrusão, geraram menor resistência ao trabalho realizado pelo parafuso, que foi monitorado por mudanças no torque do motor. Considerando o efeito lubrificante dos lipídios e fibras presentes nas matérias-primas à base de grãos integrais, o teor de água na ração foi fixado em níveis abaixo de 14% (base úmida) para produzir *snacks* extrudados com boas características de expansão e textura.

Palavras-chave: Secagem de alimentos. Moagem de grãos. Processamento agrícola. Processo de extrusão. Produtos de cereais.

GENERAL ABSTRACT

VARGAS-SOLÓRZANO, Jhony Willian. **Development of whole-grain cereals expanded extrudates**. 2019. Thesis (Doctorate in Food Science and Technology). Instituto de Tecnologia, Universidade Federal Rural do Rio de Janeiro, Seropédica, RJ. 2019.

The consumption of whole grains is associated with healthy eating and encourages to reduce the environmental impact by saving energy from the grain refining industry. People increasingly opt for processed products based on whole grains and preserved by physical methods. In that regard, extrusion cooking is a useful technique to produce preservative-free foods and to increase the range of whole-grain based products. Ready-to-eat extruded snacks produced from whole grains have hard textures and are darker, which affects consumer sensory acceptance. The main component that affects these attributes is the insoluble fiber deposited in the bran layers. Bran particles are hard to melt and cause physical rupture of the melt at the die exit. A reduction in the size of the bran particles improves the elastic expansion of the extrudates. In this work, the effect of natural fibers on the expansion and textural properties of whole-grain extruded snacks was addressed by size reducing of the bran particles. This was performed using two types of mill (disc and roller), operated in a one-step and without a screening plate, to prevent clogging of the mill sieve. During grinding, the bran and germ tissues are disintegrated and become part of particle surfaces. To improve the fractionation of particles and the particle-size heterogeneity in the feeding material, the grains were dried before the grinding process. This step favored the spread of bran and germ tissues in the feed material. The drying process affected the starch fraction of the grains. The drying and grinding processes influenced on interparticle porosity of feeding material. More porous wholemeal flours were obtained with the roller mill and during its extrusion, generated lower resistance to the work performed by the screw, which was monitored by changes in the motor torque. Considering the lubricating effect of the lipids and fibers present in the whole-grain based feed materials, the water content in the feed was set to levels below 14% (wet basis) to produce extruded snacks with good expansion and texture characteristics.

Keywords: Food drying. Grain milling. Agricultural processing. Extrusion process. Cereal products.

LIST OF FIGURES

CHAPTER II **Page**

CHAPTER III **Page**

CHAPTER IV   **Page**

CHAPTER V   **Page**

LIST OF TABLES

SUMMARY

INTRODUÇÃO GERAL

Os cereais integrais são fontes ricas de fibras naturais e diversos fitoquímicos depositados principalmente no germe e nas camadas externas do grão. De uma grande variedade de fitoquímicos, quase todos os fenólicos encontram-se esterificados com as fibras. Estes compostos são ainda complexados com polímeros de amido e proteínas para formar uma estrutura alimentar amorfa durante o processamento de cereais por extrusão. A ingestão de extrudados de cereais integrais obtidos através de condições apropriadas de extrusão pode melhorar a saúde intestinal. A formação de amido resistente promovida nesses produtos pode retardar a liberação de açúcares e fornecer ao intestino grosso compostos bioativos protetores associados com as fibras, onde são transformados numa variedade de metabólitos benéficos e logo utilizados pelo organismo na prevenção de doenças. Em alguns casos, o processamento de cereais por extrusão pode aumentar a disponibilidade de fenólicos, de modo que sejam absorvidos no intestino delgado, onde suas propriedades antioxidantes e anti-inflamatórias também podem contribuir na prevenção de doenças.

No entanto, do ponto de vista tecnológico, a incorporação do germe e das camadas externas do grão no material de alimentação se torna um desafio durante o processamento de extrusão. As fibras e lipídios insolúveis que procedem principalmente dessas partes anatômicas afetam adversamente a expansão, a textura e a cor dos extrudados. Devido às suas texturas duras e cores mais escuras, os *snacks* extrudados prontos para o consumo, produzidos a partir de cereais integrais, são menos favoráveis às preferências do consumidor. Por um lado, as fibras insolúveis são difíceis de fundir e causam ruptura física da massa fundida, afetando sua capacidade de expansão na direção radial na saída pela matriz. Por outro lado, lipídios e fibras solúveis, atuam como lubrificantes no material de alimentação, reduzindo as forças de atrito entre as partículas e entre as superfícies internas do extrusor e as partículas. Essa ação lubrificante diminui a viscosidade de cisalhamento do fundido, o que não causa pressão na matriz frontal e, consequentemente, o fluxo de material extrudado não expande.

O grupo de pesquisa em extrusão de alimentos da Embrapa Agroindústria de Alimentos (Rio de Janeiro, Brasil) processa há mais de 20 anos diferentes ingredientes refinados em combinação com subprodutos ricos em fibras, a fim de obter *snacks* extrudados nutritivos. A transformação termomecânica desses materiais é um método físico de preservação que permitiu projetar uma ampla gama de produtos práticos com boas características de expansão e textura. No entanto, os consumidores optam cada vez mais por produtos processados com base em grãos integrais. Assim, no mesmo grupo de pesquisa, um eixo específico de pesquisa foi dedicado ao desenvolvimento de extrudados expandidos de cereais integrais. O laboratório de propriedades físicas localizada na mesma instalação possui dispositivos analíticos e experiência para caracterizar as matérias-primas e os produtos extrudados, com relação ao grau de conversão do amido (propriedades de pasta), análise de tamanho de partícula, densidade aparente, densidade de partícula, densidade sólida, grau de expansão, e textura instrumental.

Em 2012, o projeto FAPERJ nº 21, denominado "Desenvolvimento de processos e produtos de conveniência à base de cereais integrais com e sem glúten, com adição de frutas produzidas no Estado do Rio de Janeiro, obtidas por co-extrusão", ofereceu a possibilidade de projetar produtos com densidade calórica reduzida e incentivar o consumo de frutas e cereais integrais no consumidor brasileiro. A partir dessa ideia de projeto, foi construído um projeto de pesquisa mais específico com relação ao processamento de extrusão monorosca de cereais integrais sem glúten (arroz, milho e sorgo) e cereais integrais associados ao glúten (aveia, centeio e trigo), com uma única exigência: produzir *snacks* extrudados expandidos com textura

crocante. O projeto em menção foi o marco desta tese de doutorado. Desta forma, o presente manuscrito foi estruturado em cinco capítulos, onde cada um foi escrito no formato de publicação científica.

O primeiro capítulo abrange uma revisão de literatura sobre a estrutura dos grãos integrais, secagem de grãos, tipos de moinho e processamento de extrusão com parafuso único. Descreve as principais semelhanças e diferenças na estrutura e composição das partes anatômicas dos cereais em estudo e sua influência nos processos de secagem, moagem e extrusão.

O segundo capítulo apresenta as propriedades físico-químicas dos cereais integrais obtidos por moagem em rolos, onde os grãos foram previamente secos. A caracterização focou as alterações nas propriedades de pasta, distribuição de tamanho de partícula e porosidade interpartículas. O objetivo deste estudo preliminar foi definir condições de secagem adequadas, comparar as propriedades de fluxo das partículas integrais e identificar os materiais de alimentação adequados antes de iniciar os experimentos de extrusão.

O terceiro capítulo está relacionado ao impacto dos tipos de moinho e tipos de cereal, sob condições de extrusão constantes, nas propriedades de expansão e textura dos extrudados. Antes da moagem com discos ou rolos, os grãos foram secos até 6% de umidade (base úmida) a fim de maximizar o fracionamento de suas partes anatômicas. Além disso, foi necessário moer novamente em moinho de martelos, as partículas integrais superiores ao diâmetro correspondendo a 50% mais finas (D_{50} = 500 ou180 μm para os moinhos de discos ou rolos, respectivamente). Esta etapa adicional aprimorou a homogeneidade do tamanho das partículas nos materiais de alimentação. O experimento foi projetado para identificar efeitos principais significativos nas propriedades de expansão e textura dos extrudados.

O quarto capítulo refere-se ao impacto das condições de secagem e moagem do arroz integral, e a umidade de alimentação na porosidade interpartículas do material de alimentação e o torque gerado sob condições de extrusão constante. Antes da moagem com discos ou rolos, os níveis de umidade dos grãos foram estabelecidos em 6 e 9% (base úmida). Em seguida, as partículas de arroz integral foram umedecidas a 11 e 14% (base úmida). Poucos trabalhos publicados correlacionam propriedades físicas do material de alimentação com variáveis dependentes de extrusão. Neste capítulo, materiais de alimentação com alta porosidade interpartículas foram produzidos com moinho de rolos e, quando extrudados, geraram baixos valores de torque.

No último capítulo, foram explorados simultaneamente cinco fatores que provavelmente influenciam no processamento de extrusão de arroz integral: umidade do grão antes da moagem (9 e 11%, base úmida), tipo moinho (disco e rolos), umidade de alimentação (11 e 14%, base úmida), velocidade rotacional do parafuso (150 e 250 rpm) e taxa de alimentação (4 e 6 kg / h). O experimento foi projetado para identificar variáveis independentes significativas (efeitos principais e de interação) e correlacionar variáveis dependentes de extrusão (temperatura da massa fundida, torque e energia mecânica específica) com as propriedades de expansão e textura dos extrudados.

CHAPTER I

EXTRUSION COOKING OF WHOLE-GRAIN CEREALS: A REVIEW

Extrusion Cooking of Whole-Grain Cereals: A Review

Jhony Willian Vargas-Solórzano [a] *, José Luis Ramírez Ascheri [b], Carlos Wanderlei Piler de Carvalho [b]

[a] Postgraduate Program in Food Science and Technology. Federal Rural University of Rio de Janeiro. Rodovia Br 465, km 7, CEP 23890-000, Seropédica, RJ – Brazil.
[b] Embrapa Agroindústria de Alimentos, Food Extrusion and Physical Properties Lab., Avenida das Américas 29501, Guaratiba, CEP 23020-470, Rio de Janeiro, RJ – Brazil.

* Corresponding author: jwvargass@ufrrj.br; vargasjw@gmail.com

ABSTRACT

Extrusion technology is widely used to process cereals, in which macromolecular components mainly starch, proteins, and fibers, undergo physical and chemical modifications. The process has a positive environmental impact since it does not generate by-products. The addition of bran and fiber-rich by-products to a starch/protein-based refined ingredient is a common practice to prepare feed materials to produce fiber-enriched extrudates. The feeding materials from whole-grain cereals include in addition to the bran, the germ fraction. Both the insoluble fibers and lipids that proceed from the bran and germ tissues, adversely affect the texture and color of extrudates, making them less favorable to consumer preferences. To address this industrial challenge, the size fractionation of bran and germ tissues through mechanical milling can be a way to improve the physicochemical compatibility between natural fibers, lipids, proteins, and starch polymers during the melt formation in the compression section of the screw. In this article, the extrusion cooking of whole-grain cereals is reviewed, emphasizing the role of drying of grains, grinder types, and extrusion operative conditions at low feed moistures.

Keywords: Fiber-rich extrudate. Dietary fiber. Drying. Milling. Extrusion

1 INTRODUCTION

Extrusion technology is widely used to process cereals and other starchy and/or proteinaceous raw materials. The major macromolecular components: starch, proteins, and fibers are physically treated without generating by-products. It is a useful technique to obtain clean label products and to increase the range of whole-grain based products. Ready-to-eat extruded snacks are aerated foods considered as shelf-stable, preservative-free, and practical products to offer the consumers owing to their low moisture levels inactivated oxidizing enzymes, bonded lipids, and their easy preparation and/or consumption (O'SHEA; ARENDT; GALLAGHER, 2014; SMITH, 1976). These interesting features are very important for consumers who are increasingly looking for processed products based on whole-grains and preserved by physical methods.

The versatility for generating extruded snacks of attractive appearance and novelty textures is inherently linked to variables related to the raw material, extruder type, screw and die configurations, and operational conditions of the extruder. These variables will establish the physical and chemical modifications of macromolecular components in the melt, mainly starch, proteins, and fibers. Also, these variables will affect the thermal expansion of the air and water vapor embedded in the melt, and hence the porous microstructure of the extrudate and its expansion and texture characteristics.

The design of fiber-rich extrudates usually is performed by adding fiber-rich by-products to refined ingredients obtained from various food sources: refined flours, starch isolates, and protein isolates. The processing of these materials, alone or in combination, is a common strategy for improving the physical, chemical, and nutritional quality of extruded products (CUETO et al., 2018; PITTS et al., 2016). Feeding materials prepared from whole-grain cereals include in addition to the bran, the germ fraction. These materials provide natural lipids, proteins, and fibers that in many cases are not present in the added fiber source.

Nevertheless, the development of fiber-rich extrudates with the expectation of good taste and texture, and that preserve their health benefits, is a challenge because these products have textures and colors that are less favorable to consumer preferences (ROBIN et al., 2012). This occurs mainly due to the insoluble fibers that proceed from the bran particles, which are not melted in the compression section of the screw and reach the metering section. Therefore, the insoluble fibers are conveyed and longitudinally oriented on the way. At the cylindrical section of the die, just before leaving the extruder, the insoluble fibers are close to the starch and protein polymers but in an incompatible way, which hinders the expansion process.

The melt can be considered as a binary system in which the continuous starchy phase surrounds the dispersed phase composed by the minority components, mainly proteins and fibers. In this scenario, air bubbles in the melt act as expansion nuclei of the water vapor at the die exit, whereby the cellular structure formation of the extrudate occurs. The low physicochemical compatibility of insoluble fibers with starch polymers causes physical rupture of the melt, decreasing the extensional forces and resulting in low shear rate and low die pressure. At the die exit, the elastic properties of the melt are hindered, resulting in extrudates with less sectional expansion, with smaller air cells and thicker cell walls. All these features adversely influence on texture and color of the fiber-rich extrudates (AČKAR et al., 2018; YANNIOTIS; PETRAKI; SOUMPASI, 2007).

2 WHOLE-GRAIN CEREALS

Cereal grains are monocotyledon starchy one-seeded fruits composed of three major anatomical parts: pericarp, germ, and endosperm, botanically named caryopses, and are enveloped by a protective coat named hull or husk, composed of the ventral and dorsal glumes known as lemma and palea, respectively (SERNA-SALDIVAR, 2010a, b). During threshing, the hull tightly remains attached to the caryopsis in rice (rough), oats, and barley (husked caryopsis), and it is loosed in the rest of the cereals (naked caryopsis). The rice hull weight ranges from 16–28% of the rough rice weight, is high in cellulose (25%), lignin (30%), arabinoxylans (15%), and its ash (21%) contains about 95% silica, what makes it inedible even for ruminants (DELCOUR; HOSENEY, 2010b; JULIANO; TUAÑO, 2019; SERNA-SALDIVAR, 2010b). The oat hull is dry, brittle at physiological maturity, high in cellulose, hemicellulose, and lignin, and contributes 25–35% of the total grain weight (ZWER, 2017). Oats as husked caryopsis are subjected to hydrothermal treatment by steaming and kilning to inactivate lipases and lipoxygenase that negatively affect the odor and flavor of ground products (GANßMANN; VORWERCK, 1995; SERNA-SALDIVAR, 2010b). Rough rice and heat-treated oats are dehulled by abrasion to yield brown rice and groats, respectively.

The endosperm and germ are covered by three outer tissues: pericarp (or fruit coat), seed coat (or testa), and nucellar epidermis. The endosperm constitutes the largest organ in any cereal grain and is divided into the aleurone layer and starchy endosperm. The seed includes the seed coat, nucellar epidermis, germ, and endosperm. The germ consists of two major parts: scutellum (or cotyledon) and embryonic axis (CHAMPAGNE et al., 2004; GARCÍA-LARA; CHUCK-HERNANDEZ; SERNA-SALDIVAR, 2019; JULIANO; TUAÑO, 2019; SERNA-SALDIVAR; ESPINOSA-RAMÍREZ, 2019). The cereal bran is referred to as the milling by-product containing more of the outer maternal tissues: pericarp, seed coat, nucellar epidermis, and aleurone layer, and variable amounts of the germ and the subaleurone starchy endosperm, depending on the variety of cereal and the milling process (KAMAL-ELDIN, 2016; MILLER; FULCHER, 2011).

The brown rice, oats, rye, and wheat caryopses have an elongated shape, maize has a truncated pyramid shape, and sorghum grains, a flattened spherical shape. Oats and rye are longer and thinner than wheat. Oats, rye, and wheat are covered by numerous trichomes (hair-like bulges), at the apex (the non-embryo end) of the grain (ARENDT; ZANNINI, 2013a; BECHTEL et al., 2009; EVERS; O'BRIEN; BLAKENEY, 1999). Rye grain is more speckled than wheat, and its surface is often wrinkled (SERNA-SALDIVAR, 2010a).

The volume of a single grain can be estimated with equation (1) for rice, oats, rye, wheat, and sorghum, and with equation (2) for maize:

$$V = \frac{4}{3}\pi D_1 D_2 D_3 \tag{1}$$

$$V = \frac{1}{3}\left(B_1 B_2 H - B_3 B_4 (H - H_t)\right) \tag{2}$$

The diameters D_i and B_i, and the truncated height H_t, are dimensions according to Figure 1. The height H in equation (2) can be estimated with equation (3):

$$H = \frac{H_t}{2}\left(\frac{B_1}{B_1 - B_2} + \frac{B_3}{B_3 - B_4}\right) \tag{3}$$
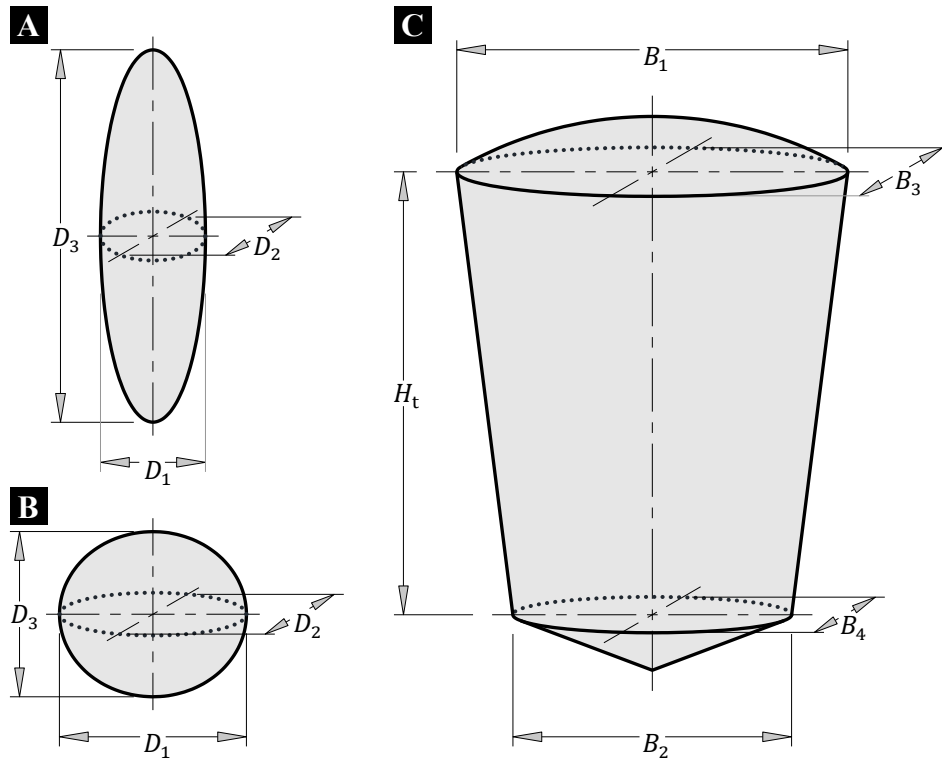
Figure 1. Diameters D_i to estimate the individual volume of grains of (A) Rice, oats, rye, and wheat; (B) Sorghum. Diameters B_i and truncated height H_t to estimate the individual volume of (C) maize grains.

The individual volume and anatomical parts of selected whole-grain cereals are compared in Table 1. The maize grain (dent) is the largest of all cereals and is approximately 3-folds bulkier than sorghum, 2.5-folds than brown rice, 2-folds than oats and rye, and 1.5-folds than hard wheat.

Table 1. Individual volume and anatomical parts of selected cereal grains.

Cereal type	Volume [a] (mm³)	Tip cap	Anatomical components (%) [b]						
				Bran				Endosperm	
			Germ	Outer tissues				Aleurone	Starchy
				Pericarp	Seed coat	Nucellus			
Brown rice	122		3.3	⊢————— 6 —————⊣					91.2
Maize (dent)	316	1.2	12.0	6.0	–	–		2.8	78.0
Sorghum	99		9.4	6.5	–	–		⊢——— 84.2 ———⊣	
Oats (groats)	156		3.7	⊢————— 12 —————⊣					84.3
Rye	153		3.5	12.1	–	–		11.6	72.8
Wheat (hard)	203		3.6	8.2	–	–		6.7	81.5

[a] Estimated according to equations (1 – 3). [b] Source: SERNA-SALDIVAR (2010b).

The transversal section of selected caryopses compared in Table 1, is depicted in Figure 2, wherein the mature grain varies according to the cereal type. The cut crossed the germ in the maize and sorghum grains (Figure 2B, C). The cavity corresponds to the embryonic axis, which is surrounded by the scutellum (GARCÍA-LARA; CHUCK-HERNANDEZ; SERNA-SALDIVAR, 2019; SERNA-SALDIVAR; ESPINOSA-RAMÍREZ, 2019).
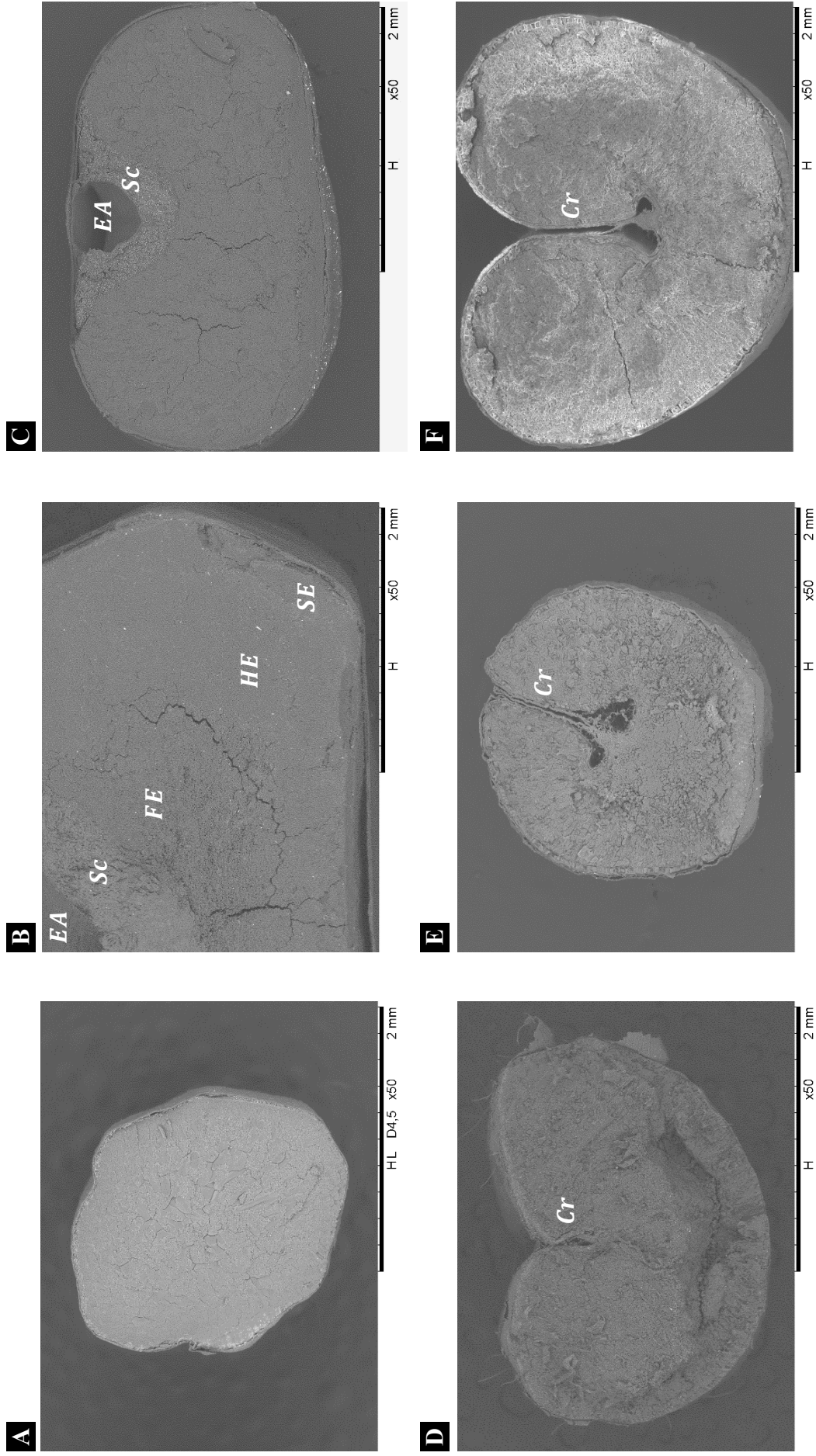
Figure 2. Transversal section images (x50) of whole-grain cereals: (A) brown rice, (B) maize, (C) sorghum, (D) oats, (E) rye, and (F) wheat. *EA*: embryonic axis, *Sc*: scutellum, *FE*: floury endosperm, *HE*: horny endosperm, *SE*: subaleurone endosperm, and *Cr*: crease.

Wheat, rye, and oats have a longitudinal furrow that extends the entire length of the ventral (opposite the germ) side of the grains, named crease (DELCOUR; HOSENEY, 2010b; HOLOPAINEN-MANTILA; RAULIO, 2016). This deep groove extends nearly to the center of the grain (Figure 2D-F), form a hiding place for insects, microorganisms, and dust, and also hinders the performance during grain refinement (DELCOUR; HOSENEY, 2010b). Mold attack is more susceptible when water activity (a_w) levels are higher than 0.65. In terms of mold damage, this limited range of a_w is attained for various cereals at critical moisture contents around 14% (ABDULLAH; NAWAWI; OTHMAN, 2000; POMERANZ; ZELENY, 1971). The low a_w and the enclosed cell wall compartments contribute to the equilibrium of the whole grain, preventing substrates and degrading enzymes from finding each other (DELCOUR; HOSENEY, 2010b). When the outer layers are intact, the grain is protected against mold attack and oxidative and enzymatic deterioration (MIR et al., 2019). However, in all cereals, the outer layers are thinner over the germ than over other parts of the kernel. This feature also makes the germ susceptible to moisture, molds, and insects (POMERANZ; ZELENY, 1971).

2.1 The Germ Structure

The germ (or embryo) is located at the base of the grain on its ventral side in rice, maize and sorghum (JULIANO; TUAÑO, 2019; ROSENTRATER; EVERS, 2018a), and on its dorsal side in oats, rye and wheat (ARENDT; ZANNINI, 2013a, b, c; BECHTEL et al., 2009). The germ plays the role of first reserve tissue for the seed germination, in which it develops the capacity for photosynthesis. As previously mentioned, the germ is constituted of two major parts: the scutellum (or cotyledon) and the embryonic axis. The embryonic axis is composed of the radicle (predecessor of primary roots) and plumule (predecessor of leaves and stems) (GARCÍA-LARA; CHUCK-HERNANDEZ; SERNA-SALDIVAR, 2019; JULIANO; TUAÑO, 2019; SERNA-SALDIVAR; ESPINOSA-RAMÍREZ, 2019). The scutellum, the largest portion of the germ, is located between the starchy endosperm and the embryonic axis, surrounding the latter as a protective shield. It is the organ that secretes hormones and enzymes to the starchy endosperm and absorbs the solubilized nutrients to be supplied to the embryonic axis when germination occurs (ROSENTRATER; EVERS, 2018a). The scutellum is composed of the scutellar parenchyma and the scutellar epithelium. The scutellar parenchyma is structured by roughly spherical cells, rich in lipid bodies, protein bodies (albumins and globulins) containing phytin globoids, lipolytic enzymes, and minerals, much of the latter sequestered as phytate, a cationic salt of inositol hexaphosphoric acid (GARCÍA-LARA; CHUCK-HERNANDEZ; SERNA-SALDIVAR, 2019; JULIANO; TUAÑO, 2019; MILLER; FULCHER, 2011; SERNA-SALDIVAR; ESPINOSA-RAMÍREZ, 2019). The scutellar epithelium is adjacent to the starchy endosperm (the inner edge of the embryo) and has very little phytin. The starchy endosperm along this boundary region has degraded cells and is referred to as the depleted layer, which forms a natural cleavage plane and allows separating the germ under certain processing conditions (CHAMPAGNE et al., 2004; MILLER; FULCHER, 2011).

Table 2 summarizes the partial composition of the anatomical parts of selected cereals. Starch granules are present in the scutellum cells of wheat and sorghum (FOOD STANDARDS AGENCY, 2002; MOHARRAM; YOUSSEF, 1995; SERNA-SALDIVAR; ESPINOSA-RAMÍREZ, 2019), and very little is present in rice, maize, and oats (MILLER; FULCHER, 2011). The germ is relatively rich in sugars (mainly sucrose and raffinose in wheat, arabinose, and glucose in rice), B vitamins (mainly thiamin and niacin), and vitamin E (tocopherols) (DELCOUR; HOSENEY, 2010b; LU; LUH, 1991; SHIBUYA et al., 1985). From among the selected cereals, the maize germ is the richest oil depository, which is composed mainly of triacylglycerides (KUMAR; SINGH, 2019).

Table 2. Chemical composition of selected whole-grain cereals and their anatomical parts.

Component	Cereal type					
	Rice [1]	Maize [2]	Sorghum [3]	Oats [6]	Rye [10]	Wheat [11]

			Whole grain			
Starch	77.2	71.7	73.8	64.2	63.4	65.1
Proteins	8.3-9.7 [a]	9.5	12.3	15.3	8.3	12.8 [13, a]
Lipids	1.9-3.3	4.3	3.6	8.7	1.5	1.22 [14, j]
Dietary fiber	4.5 [b]	9.5	1.93 [4, c]	9.8	16.1	13.8
Ash	1.2-1.7	1.4	1.6	2.0	1.4	1.2-3.0 [15]
Sugars	0.8-1.5	2.6	0.90 [5, d]	0.9-1.3 [7]	3.2 [11]	1.9
			Germ			
Starch	2.1	1.5	13.4			28.7 [16]
Proteins	14.1-20.6 [a]	26.2	18.4	24.2-32.4 [8, e]		34.1 [13, a]
Lipids	16.6-20.5	82.6	28.1	8.5 [7]		8.83 [14, j]
Dietary fiber	13.1 [b]	12	9.11 [4, c]			15.6 [16]
Ash	4.8- 8.7	78.4	9.2			4.2-4.4 [15]
Sugars	8.0-12	69.3	0.12 [5, d]			16.0 [16]
			Endosperm			
	Milled				Flour F1 [h]	Flour
Starch	77.6	98.1	82.5		85.3	82.0
Proteins	6.3-7.1 [a]	73.8	10.5	9.6-17.0 [8, f]	3.9	33.1 [13, a]
Lipids	0.3-0.5	15.4	0.6	53.3 [7, f]	0.5	0.54 [14, j]
Dietary fiber	0.7-2.3 [b]	26	1.5 [4, c]		5.5	3.5
Ash	0.3-0.8	17.9	0.6		0.4	0.5-0.7 [15]
Sugars	0.22- 0.45	28.9	0.16 [5, d]	0.6 [9, g]	5.5 [12, i]	1.7
			Outer layers			
	Bran	Pericarp	Pericarp	Bran	Bran	Bran
Starch	13.8	0.6	3.5	54.4	24.9	22.2
Proteins	11.3-14.9 [a]	2.6	6.0	18.5	12.8	10.8 [13, k]
Lipids	15.0-19.7	1.3	4.9	38.2 [7]	3.0	0.96 [14, j]
Dietary fiber	23.7-28.6 [b]	54	15.36 [4, c]	16.5	40.6	44.9
Ash	6.6-9.9	2.9	3.4	3.1	4.1	5.3-6.2 [15]
Sugars	5.5-6.9	1.2	0.62 [5, d]	2.6-3.4 [7]	7.5 [11]	5.3

[a] Conversion factor: 5.95 for rice, 5.70 for wheat; [b] Neutral detergent fiber; [c] Crude fiber; [d] Water-soluble sugars: xylose, arabinose, glucose, and galactose; [e] Scutellum; [f] Starchy endosperm; [g] Flour; [h] Flour with particles ≤ 150 μm; [i] Free sugars; [j] Nonpolar lipids; [k] Pericarp + testa.

Source: [1] LU e LUH (1991); [2] KUMAR e SINGH (2019); [3] SERNA-SALDIVAR e ESPINOSA-RAMÍREZ (2019); [4] WALL e BLESSIN (1970); [5] KARIM e ROONEY (1972); [6] WELCH (2011); [7] PETERSON (1992); [8] LÁSZTITY (1998); [9] WELCH (1995); [10] NILSSON et al. (1997); [11] KNUDSEN (1997); [12] GLITSØ e BACH KNUDSEN (1999) [13] SHEWRY et al. (2009); [14] POMERANZ e CHUNG (1965); [15] PIIRONEN et al. (2009); [16] FOOD STANDARDS AGENCY (2002).

2.2 The Endosperm Structure

As previously mentioned, in the mature caryopsis the endosperm is composed of two regions: the aleurone layer and the starchy endosperm. The aleurone layer surrounds the starchy endosperm and the outer side of the germ. In wheat, the aleurone layer does separate cleanly from the starchy endosperm, and in rice and oats is tightly bonded to it (CHAMPAGNE et al., 2004; MILLER; FULCHER, 2011). In mature kernels of sorghum, oats, rye, and wheat, the aleurone layer is usually one cell thick, with some exceptions in the crease region for oats (BECHTEL et al., 2009; MILLER; FULCHER, 2011; PARKER, 1981; SERNA-SALDIVAR; ESPINOSA-RAMÍREZ, 2019). In rice, the number of aleurone layers can be between 1-7, being greater in the short-grains than in the slender long-grains (JULIANO; TUAÑO, 2019). Multiple aleurone layers are also known to exist in diverse maize genotypes (GARCÍA-LARA; CHUCK-HERNANDEZ; SERNA-SALDIVAR, 2019).

The aleurone cells represent the only living tissue of the endosperm at maturity, and continue to respire for indefinite periods after harvest (ROSENTRATER; EVERS, 2018a). These cells have thick bilayered walls, large prominent nuclei, and a large number of lipid droplets and aleurone granules, relatively rich in ashes, proteins (albumins and globulins), phytates, water-soluble vitamins (niacin, thiamine, and riboflavin), antioxidant compounds, and hydrolytic enzymes, the latter play a key role in the germination process. The main mineral components associated with cereal phytates are sodium, potassium, magnesium, and calcium (BECHTEL et al., 2009; MEERA; BHASHYAM; ALI, 2011; MOHARRAM; YOUSSEF, 1995; POSNER, 2009). The part that borders the endosperm cavity in the crease region of wheat has modified aleurone cells, and lack aleurone grains (BECHTEL et al., 2009). In oats, the cell walls of the aleurone layer are less thick, as they are in wheat and rye (ROSENTRATER; EVERS, 2018a). In rye, the aleurone cell walls are composed of arabinoxylans (17.1%), lignin (3.9%), β-glucans (3.3%), and cellulose (2%) (GLITSØ; BACH KNUDSEN, 1999).

The starchy endosperm, the largest portion of the endosperm, is a central mass of thin-walled cells filled with the nutrients necessary to sustain the growth of the embryonic axis during germination and seedling growth (ROSENTRATER; EVERS, 2018a). Cell columns of variable size but similar in shape (rounded or polygonal) radiate the endosperm, which allows delimiting regions. From the outside toward the center, the starchy endosperm is divided into subaleurone (or peripheral) and central regions in rice and oats (BECHTEL; POMERANZ, 1978; MILLER; FULCHER, 2011); corneous (or vitreous) and floury regions in maize (GARCÍA-LARA; CHUCK-HERNANDEZ; SERNA-SALDIVAR, 2019); peripheral, corneous, and floury regions in sorghum (SERNA-SALDIVAR; ESPINOSA-RAMÍREZ, 2019); and peripheral, prismatic, and central regions in rye and wheat (BECHTEL et al., 2009; PARKER, 1981). The thin-walled cells that make up the endospermic regions are structures, wherein the cytoplasm and organelles were digested during the final maturation stage, with the amyloplasts prevailing. Amyloplasts are organelles delimited by double membranes, in which the major nutrient: starch, is stored in an insoluble form (BECHTEL; WILSON, 2003; CHAMPAGNE et al., 2004; ROSENTRATER; EVERS, 2018a). Reserve proteins are the second main nutrient in the endosperm cells, providing a source of amino acids for the germinating grain. The concentration of these two nutrients, as well as the cell size and cell wall thickness, vary inversely from the center to the periphery of the starchy endosperm. In the center, large size cells with a thin cell wall, with high starch content and low protein content, predominate. On the contrary, in the periphery predominates small size cells with a thick cell wall, rich in proteins and poor in starch (ROSENTRATER; EVERS, 2018a).

Inside each amyloplast, starch polymers are properly organized as compound or simple granules. Compound starch granules consist of assemblies of small non-fused starch granules, that are easily separated by conventional purification procedures. Single granules are further

classified as uniform and bimodal. The uniform type is composed of a single starch granule that covers the entire amyloplast. The bimodal type contains large (A-type) and small (B-type) simple starch granules that coexist in the same cells (MATSUSHIMA, 2015; PARKER, 1981, 1985). Compound starch granules are present in rice and oats (Figure 3A, D), wherein the grouping of granules reaches up to 60 units in rice and 80 units in oats. The diameter of an individual granule varies from 1.8 to 8 µm in rice and from 2 to 11 µm in oats. The diameter of a cluster of granules varies from 10 to 39 µm in rice and from 10 to 60 µm in oats (JULIANO; TUAÑO, 2019; MILLER; FULCHER, 2011; ROSENTRATER; EVERS, 2018a; SAYAR; WHITE, 2011). Uniform starch granules are present in maize and sorghum (Figure 3B, C), of approximately 10 µm in diameter. Simple starch granules also are observed in oats (Figure 3 D) (BECHTEL; POMERANZ, 1981; SECKINGER; WOLF, 1973). Bimodal simple granules are observed in the rye, wheat (Figure 3E, F), and barley. The large oval A-type granules are of approximately 15 – 20 µm in diameter in the subaleurone cells, and up to 40 µm in diameter in the prismatic endosperm cells. The small spherical B-type granules are less than 10 µm in diameter in both subaleurone and prismatic regions (MATSUSHIMA, 2015; PARKER, 1981, 1985).

Reserve proteins in rice, maize, and sorghum are deposited in membrane-bound protein bodies of 1 – 3 µm in diameter, whose inner is composed of concentric rings of aqueous alcohol-soluble prolamins (BECHTEL; POMERANZ, 1978; SECKINGER; WOLF, 1973). The protein bodies of oats are roughly spherical bodies of 0.2 – 6 µm in diameter in which the salt-soluble globulins predominate (BECHTEL; POMERANZ, 1981; MILLER; FULCHER, 2011). Protein bodies are embedded in variable amounts of protein matrix rich in dilute acid/base-soluble glutelins, which in turn surround the amyloplasts containing starch granules. The subaleurone cells contain numerous protein bodies and a few small starch granules, whereas the central endosperm cells are composed mostly of starch with protein bodies interspersed (BECHTEL; POMERANZ, 1978; BECHTEL; POMERANZ, 1981; SECKINGER; WOLF, 1973).

In rye, protein bodies with less than 1 µm in diameter were only observed in the subaleurone endosperm cells, as cytoplasmic disorganized pockets (PARKER, 1981). Reserve proteins in the mature endosperm of wheat and rye occur as a continuous matrix devoid of protein bodies in which, the starch granules, lipids, and fragments of cytoplasm and disrupted organelles are embedded (PARKER, 1981; SIMMONDS, 1972). In wheat, this continuous matrix contains the gluten-forming proteins: gliadin (prolamin) and glutenin (glutelin). Both proteins will become gluten after milling and dough formation. During wheat endosperm developing, gliadin polymers are accumulated as discrete body vacuoles via the Golgi apparatus and glutenin polymers are accumulate in the lumen of the endoplasmic reticulum. In the ultrastructure of the wheat mature endosperm, protein bodies rich in gliadin are not discernable, only membranous structures of endoplasmic reticulum as cross-linked filaments are interpreted as the glutenin fraction (WRIGLEY; BÉKÉS; BUSHUK, 2006). The continuous matrix in the mature endosperm of rye and wheat grains is formed as a result of the compression and fusion of large protein bodies (diameters up to 20 µm) by the combined effect of starch accumulation and water loss during grain ripening (PARKER, 1981; SIMMONDS, 1972).

In the maize endosperm, this water loss causes shrinkage of the cells. The strong adhesion between proteins and starch results in tightly packed starch granules of polygonal shape, in which the zein bodies (prolamins) make indentations on the starch granules of the corneous endosperm (DELCOUR; HOSENEY, 2010b). The endosperm proteins in maize stand out in quantity among the cereals presented in Table 2. The relative proportion of the various protein groups is about 44% zeins, 25% glutelins, 5% albumins plus globulins, and the remaining protein is mainly a zein fraction (about 17%) cross-linked by disulfide bonds to the glutelins (DELCOUR; HOSENEY, 2010a).
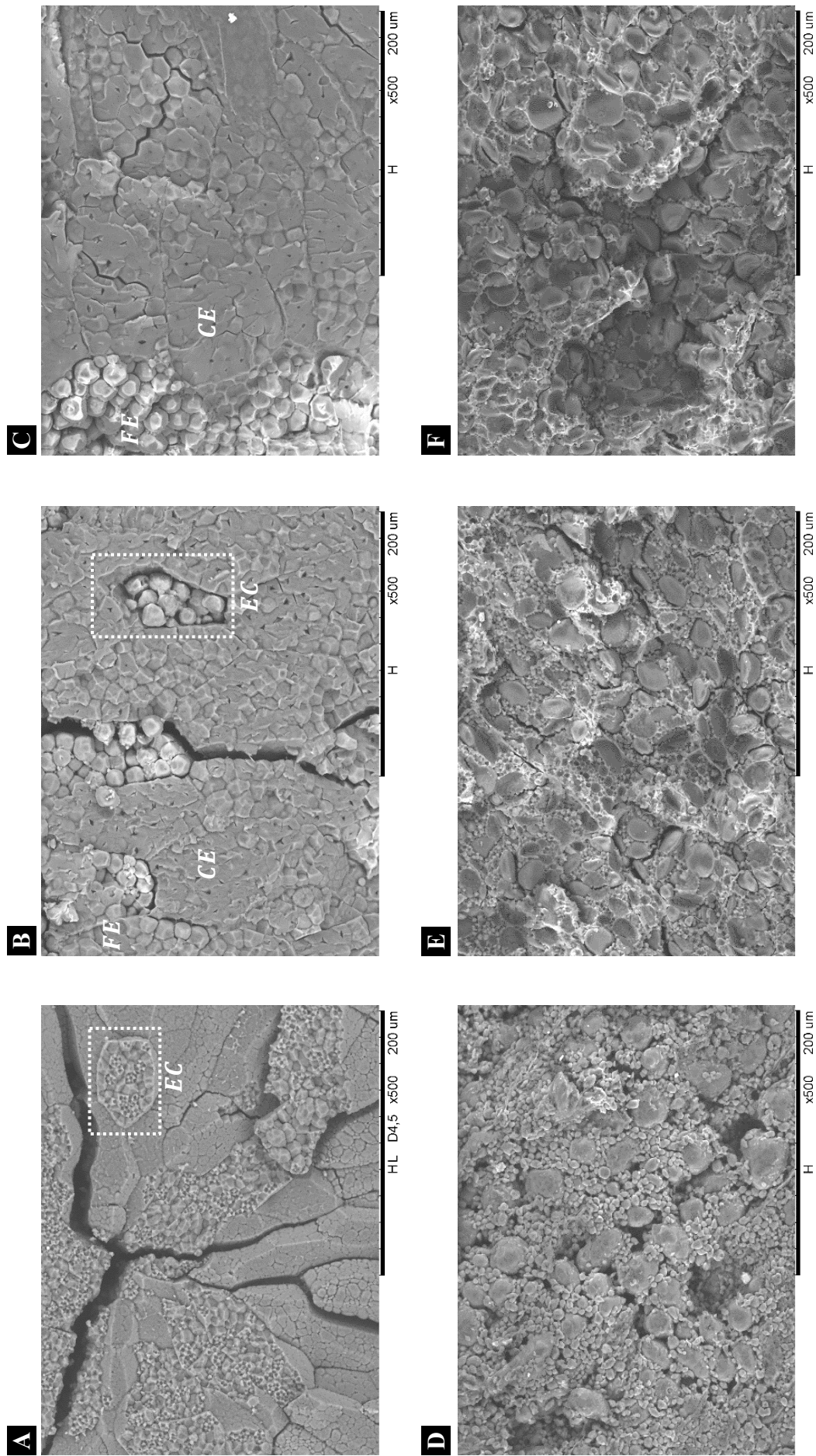
Figure 3. Microphotography of the endosperm structure (x500) of whole-grain cereals: (A) brown rice, (B) maize, (C) sorghum, (D) oats, (E) rye, and (F) wheat. *EC*: endosperm cell containing amyloplasts, *FE*: floury endosperm, and *CE*: corneous endosperm.

The corneous endosperm cells (CE) of maize and sorghum grains are composed of polygonal starch granules, densely compacted by the glutelin matrix, with little or no air spaces (Figure 3B, C). This particular structure present in the corneous endosperm gives the grain hard mechanical and translucent optical properties. The starch granules in the floury endosperm (FE) have spherical shapes in maize and angular shapes in sorghum. The granules are surrounded by a less dense glutelin matrix, that entraps large amounts of air spaces (Figure 3B, C). The revealed structure of the floury endosperm is manifested by their slight mechanical and opaque optical properties (DELCOUR; HOSENEY, 2010b; MOHARRAM; YOUSSEF, 1995; MORA; MILÁN; MILÁN, 2019).

The starchy endosperm of the rye grain is softer than that of hard and soft wheat. Thus the floury content of the rye grains is readily released after grinding (ARENDT; ZANNINI, 2013b). In wheat, the subaleurone cells have about 60 μm in diameter, the prismatic cells are 128 – 200 μm long by 40 – 60 μm wide, and the central cells that occur in the center of the cheeks and have a length of 72 – 144 μm and a width of 69 – l20 μm (BECHTEL et al., 2009). Unlike other cereals, oats endosperm is rich in lipids (more than 53%, Table 2), most of which are neutral lipids with smaller amounts of glycolipids and phospholipids (MILLER; FULCHER, 2011; PETERSON, 1992).

The walls that structure the starchy endosperm cells are constituted of cellulose and noncellulosic polysaccharides, arabinoxylans and (1–3, 1–4)-β-D-glucans as the most abundant components, and xyloglucans and pectins as the less abundant. Variable amounts of protein are also included in these polysaccharides (ROSENTRATER; EVERS, 2018b). The endosperm cell walls of japonica-type rice grains are composed of hemicellulose (49%), pectic substances (27%), α-cellulose (23%), lignin (1%), and protein (18%). In wheat, cell walls are composed mainly of arabinoxylan (70%), (1–3, 1–4)-β-D-glucans (20%), β-glucomannan (7%), cellulose (4%), and protein (0.5%) (SHIBUYA et al., 1985; STONE, 2006). In oats, 30% of (1–3) and 70% of (1–4) β-D-glucans predominate (ARENDT; ZANNINI, 2013a; ROSENTRATER; EVERS, 2018a). In rye, the endosperm cell walls are thicker than those of wheat, especially where they adjoin the aleurone layer and contribute to the high pentosan content of rye flour (PARKER, 1981). In rye, the starchy endosperm cell walls are composed of arabinoxylans (4.2%), β-glucans (0.75%), cellulose (0.4%), and lignin (0.1%) (GLITSØ; BACH KNUDSEN, 1999). Pentosans increase the water-binding capacity and play a vital role in determining the baking quality of rye flour by conferring viscous properties to the dough. However, gluten formation is inhibited by the presence of pentosans, so that protein is a less important factor in baking quality in rye than in wheat doughs (PARKER, 1981).

2.3 The Outer Layers Structure

The outer layers are remnants of the ovary and are metabolically inactive layers at maturity (MILLER; FULCHER, 2011). They comprise three types of cellular tissue: the nucellar epidermis (or nucellus, hyaline layer), the seed coat (or testa), and the pericarp (or fruit coat). In a mature cereal grain, the cellular content in the tissues of the pericarp and the testa disappears, and only the thick walls remain (STONE, 2006).

The nucellar layer is about 7 μm thick, is tightly bound to both the seed coat and the aleurone layer, and surrounds the endosperm and germ. A coating cuticle is present on the outer surface of the nucellar epidermis (DELCOUR; HOSENEY, 2010b; ROSENTRATER; EVERS, 2018a). In oats, rye, and wheat, the nucellar epidermis is composed mostly of arabinoxylan with a low degree of arabinose substitution. This layer is thicker in wheat and rye than in oats (DORNEZ et al., 2011).

The seed coat consists of one or two cellular layers termed suberin, in which corky substances and pigments accumulate. These compounds control the permeability and color of

the grain. In some varieties of sorghum, a pigmented testa may or not be present. The varieties with a pigmented testa are rich in condensed tannins (DYKES et al., 2009; ROSENTRATER; EVERS, 2018a). An outer cuticle, thicker than that of the nucellar epidermis covers the testa (DELCOUR; HOSENEY, 2010b; ROSENTRATER; EVERS, 2018a).

The pericarp is composed of several layers of generally dry empty cells, some maintaining their shape and the integrity of layers, others being shrunken and distorted, leaving large, frequent intercellular spaces (EVERS; MILLAR, 2002). In contrast to the walls of the endosperm and aleurone cells, many of the pericarp and seed coat walls are reinforced with lignin, which gives these walls a strong structure and less digestion capability in the large intestine (STONE, 2006).

The innermost layer of the pericarp, the one that adjoins the testa, is the inner epidermis constituted of an incomplete layer of isolated groups of wormlike cells, also termed as tube cells. Covering this layer is the layer of cross cells, which are arranged side by side in rows, forming a complete layer on the surface of rye and wheat grains (EVERS; MILLAR, 2002; ROSENTRATER; EVERS, 2018a). In sorghum, these two first layers constitute the endocarp (MOHARRAM; YOUSSEF, 1995). The tubular cells are easily breakable. For that reason, the cross cells adhere to the adjoin cuticle to the testa. In maize, rice, and, sorghum the cross cell layer has more elongated and distorted cells, which leaves large spaces. In oats, tube cells and cross cells are indistinguishable from other inner pericarp cells which are all elongated and distorted with no common orientation (EVERS; MILLAR, 2002).

The mesocarp is located outside the cross cells and is composed of parenchymatous cells. In wheat, the parenchyma does not completely cover the kernel. Only in the crease region, the parenchyma remains intact. Persistent isolated parenchymal remains are termed intermediate cells (DELCOUR; HOSENEY, 2010b; EVERS; MILLAR, 2002). Except for sorghum, this tissue autolyzes towards maturity, and the products of digestion are translocated to the endosperm (EVERS; MILLAR, 2002; ROSENTRATER; EVERS, 2018a). In sorghum, this layer is usually composed of 5–6 cell layers, and it is not uncommon to find mesocarps with 10–14 cell layers (EARP; MCDONOUGH; ROONEY, 2004). In some types of sorghum, mesocarp cells with remaining starch granules, persist at maturity. These sorghum grains have a thick pericarp (DYKES; ROONEY, 2006; ROSENTRATER; EVERS, 2018a).

The outermost layer of the pericarp is the outer epidermis (or epicarp) with one or more layers of hypodermis adjoining the intermediate cells and coated by a thin cuticle (EVERS; MILLAR, 2002). In sorghum, the outer epidermis consists of long, thick-walled and rectangular cells, usually contain pigmented material, and the surface of the cuticular layer presents deposits of wax. (EARP; MCDONOUGH; ROONEY, 2004). The hypodermis is absent in oats, and consist of one or two layers thick in wheat and rye, 1 – 3 layers thick in sorghum, and 10 or more layers thick in dent maize and flint maize (EARP; MCDONOUGH; ROONEY, 2004; EVERS; MILLAR, 2002; ROSENTRATER; EVERS, 2018a).

The color of the mature caryopsis varies according to the absence or presence of accumulated pigments in the outer layers, endosperm and germ (BECHTEL et al., 2009; ROSENTRATER; EVERS, 2018a). Phenolic compounds are responsible for the coloration of the outer layers (DYKES; ROONEY, 2007). Carotenoid pigments and phenolics esterified with polysaccharides, proteins, or cell wall constituents, are responsible for the coloration of the endosperm and germ (PIIRONEN et al., 2009). The wheat caryopsis usually is white or red, and less frequently, purple and even black. In maize, yellow and white are the most common kernel colors, and less frequently, red, blue, dark brown, or purple. Rye grains are usually grayish yellow (DELCOUR; HOSENEY, 2010b).

The pericarp color diversity of rice, maize, sorghum, rye, and wheat is partly due to the presence of phenolic acids (mainly ferulic and *p*-coumaric acids) in free form or simple soluble glycosides or esters, and anthocyanins (DYKES; ROONEY, 2007). The pericarp of wheat and

rye also contain alkylresorcinols and lignans (PIIRONEN et al., 2009). Flavanones and the flavone apigenin were reported in the pericarp of sorghum and oats, and avenanthramides unique in oats bran (DYKES; ROONEY, 2007). Cereals also accumulate condensed tannins (responsible for the red coloration) in the mature seed coat: brown rice 0.1%, sorghum 1.5%, maize 0.4%, oats 1.1%, rye 0.6%, and wheat 0.4% (BECHTEL et al., 2009; EVERS; O'BRIEN; BLAKENEY, 1999; SERNA-SALDIVAR; ESPINOSA-RAMÍREZ, 2019). Sorghum types with large proportions of condensed tannins are known as bird resistant (BR), because they are attacked less by birds, owing to the unpalatability of the tannins (ROSENTRATER; EVERS, 2018a). The yellow color of maize and sorghum, and the amber color of some *Triticum durum* wheat cultivars, are the result of carotenoid pigments in the endosperm, mainly lutein, zeaxanthin, and β–carotene (BECHTEL et al., 2009; GARCÍA-LARA; CHUCK-HERNANDEZ; SERNA-SALDIVAR, 2019; SERNA-SALDIVAR; ESPINOSA-RAMÍREZ, 2019).

3 CONVECTIVE AIR DRYING OF CEREAL GRAINS

In convective air drying, when the air flows through a bed of cereal grains, the air supplies the necessary sensible and latent heat of evaporation to the moisture distributed in the grains. The following heat and mass transfer phenomena occur simultaneously: (1) convective heat transfer from the drying air toward the surface of the kernels, (2) conductive heat transfer within the kernel, (3) moisture diffusion in the kernel toward its external surface, and (4) vaporization and convective vapor transfer into the air stream (DINÇER; ZAMFIRESCU, 2016; MAROULIS; KIRANOUDIS; MARINOS-KOURIS, 1995). These four stages are depicted in Figure 4. In the stage (1) the temperature difference between the interface (T_s) and the drying air (T_a) is the driving force for heat transfer in the air boundary layer. In the stage (2) a temperature gradient between the surface (T_s) and core (T_c) is the driving force for the heat conduction in the kernel ($T_s > T_c$). In the stage (3) it is assumed that a moisture concentration gradient between the surface (M_s) and core (M_c) is the sole driving force ($M_c > M_s$). In the stage (4) it is assumed that the partial pressure difference between the interface (P_s) and the drying air (P_a) is the driving force for the mechanism of vapor transfer in the air boundary layer.
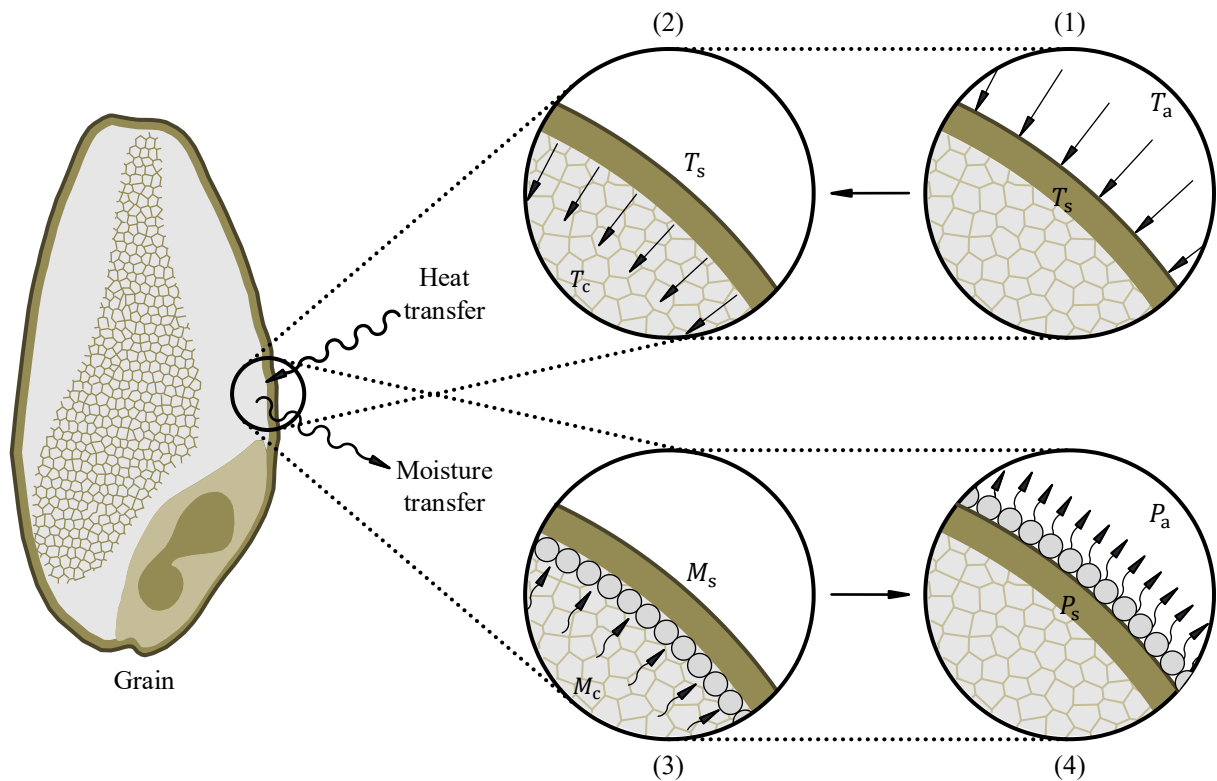
Figure 4. Simultaneous heat and mass transfer phenomena during a convective air-drying process. T: temperature; M: moisture concentration; P: partial pressure; subscripts c, s, and a are referred to the kernel core, kernel surface, and air drying, respectively.

The moisture migration from various parts of the interior to the surface of the kernel is influenced by the endosperm structure, the permeability of the aleurone and outer layers, and the extent of damage to these layers (BALA, 2017a). The pericarp layers play a water-absorbing role during grain tempering, which contributes to hardening the bran layers, and then be easily

removed in the milling process (EVERS; MILLAR, 2002). An inverse behaviour can occur during drying of cereal grains, in which grains become more brittle due to a decrease in tissue adhesive forces that make up the pericarp layers and the intricate network of endosperm cell walls (HOURSTON et al., 2017).

The physical dimensions and 1000-kernel weight are used to describe the physical characteristics of grains and their influence on the drying rate (BALA, 2017a). The 1000-grain weight is a good indicator of the relative size between whole-grain kernels when compared at the same moisture level (SABLANI; RAMASWAMY, 2003). Bulk density is the mass of grains divided by the volume occupied by the grains and intergranular space. Kernel density is the mass of a grain divided by the volume occupied by the grain, that is, excluding the volume of intergranular space (MUIR; .SINHA, 1988).

3.1 The State of Air during Convective Drying

In convective drying, the condition of air changes as part of the process. These changes can be described with the psychometric chart, as depicted in Figure 5. The ambient air (state 1) is heated to the operational dry bulb temperature (T_a) from T_{a1} to T_{a2}. This appears as a horizontal line on the psychometric chart because no moisture is added to the air at this point in the dryer. The specific humidity remains constant ($\omega_1 = \omega_2$). As a result, this increases the saturation temperature (T_s) from T_{s1} to T_{s2} (SUNDERLAND, 2001).
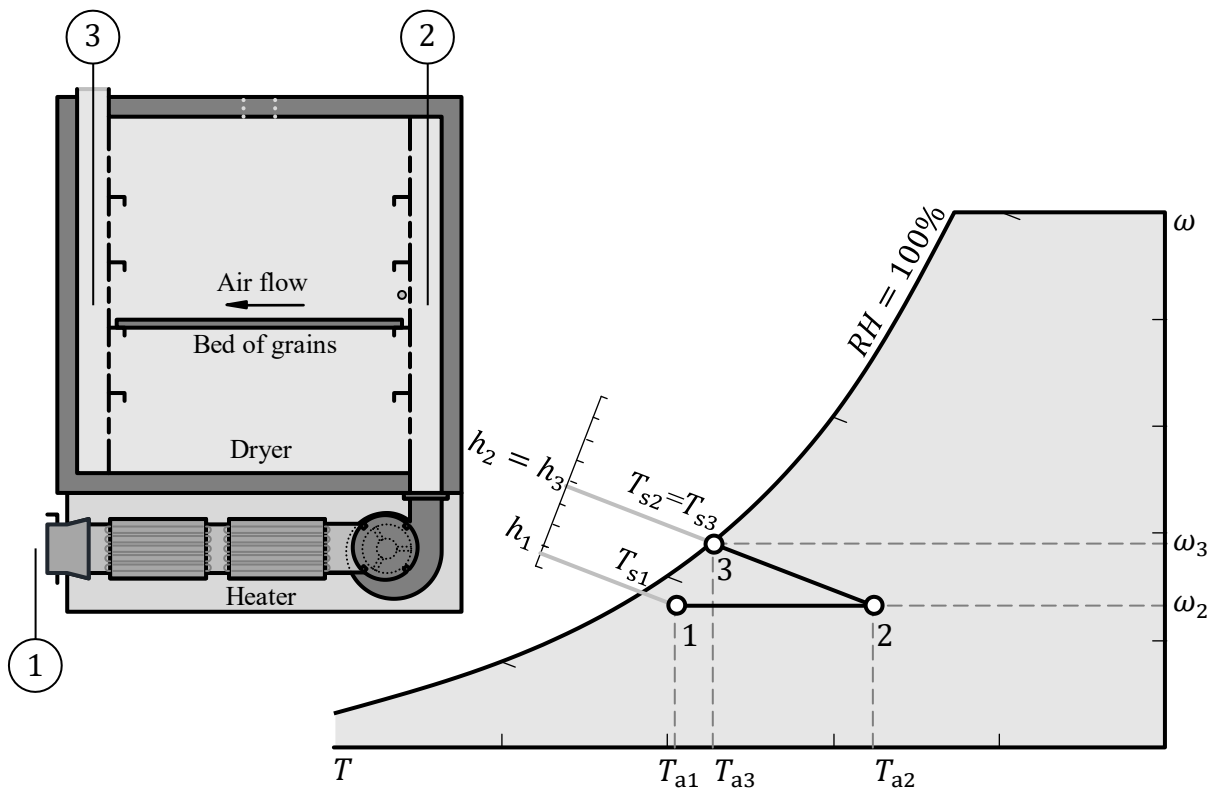
Figure 5. Drying (or adiabatic saturation) process shown on a psychometric chart. Adapted from (SINGH; HELDMAN, 2014a, b). T: temperature; ω: specific humidity; RH: relative humidity; subscripts a and s are referred to the dry bulb and saturation conditions of the air, respectively.

The amount of thermal energy (q) necessary to heat moist air from state 1 to state 2, can be calculated with equation (4) (SINGH; HELDMAN, 2014b):

$$q = \dot{m}(h_2 - h_1) \tag{4}$$

The heated air (state 2) flows like a steady stream through the insulated channel of the dryer containing a bed of grains. In contact with grains, the energy content of the air remains constant ($h_2 = h_3$), but sensible heat is partially exchanged for latent heat to evaporate water from the grains. This is an adiabatic saturation process, where no gain or loss of heat to the surroundings occurs (CENGEL; BOLES, 2015; SINGH; HELDMAN, 2014b). During this process, the moisture content of air increases (the evaporated water is mixed with the airstream) and its temperature decreases. The exhausted air (state 3) exits as saturated air (relative humidity, $RH = 100\%$) at temperature T_{a3}.

3.2 Drying Curves

The variation of moisture content (M, dry basis) when cereal grains are exposed to air of constant temperature and relative humidity is usually measured versus the drying time (t) to perform empirical correlations for the prediction of drying rates (dM/dt) (SUAREZ; VIOLLAZ; CHIRIFE, 1980).

In Figure 6A, the first part of the process (curve A–B) is the stage of warming up of the grains during which the solid surface conditions come into equilibrium with the drying air. This period is governed mostly by transient heat transfer processes. The process B–C shows a reduction of the moisture content which is approximately linear in time. During this phase, the rate of water removal per unit of drying surface is essentially constant (DINÇER; ZAMFIRESCU, 2016). Moisture at point C, where the constant rate period ends, is known as the critical moisture content (M_c). For various cereal grains, the critical moisture content lies around 14% (POMERANZ; ZELENY, 1971). The surface of the grains at point B remains saturated with moisture that comes from the core of the kernels. At point C, this saturated moisture in the surface of the grains is eliminated. This stage is controlled by the heat and/or moisture transfer coefficients, the area exposed to the drying medium, and the difference in temperature and relative humidity between the drying air and the wet surface of the grains (DINÇER; ZAMFIRESCU, 2016). In phase C–E, the drying process occurs under falling rate conditions. The drying curve of cereal grains practically takes place in the falling rate period (BALA, 2017b; VELU et al., 2006). In this period, there is no evaporation at the surface, but rather a diffusion process of the moisture within the kernels followed by a convective mass transfer at the grain surface. The surface temperature begins to rise and continues to do so as drying proceeds, approaching the dry-bulb temperature of the air as the grains approaches dryness (DINÇER; ZAMFIRESCU, 2016). Moisture at point E, where the falling rate period ends, is known as the equilibrium moisture content (M_e). At this point, the vapor pressure of the water within the grains is in equilibrium with the partial pressure of water in the drying air (DELGADO; DA SILVA, 2014). M_e is dependent upon the temperature and relative humidity of the environment and on the variety and maturity of the grain (CHAKRAVERTY; SINGH, 2014).

Figure 6B depicts the changes in drying rate versus moisture content (dry basis) of the grains. This curve is obtained by differentiation of the $M(t)$ curve from Figure 6A. In the period B–C, the rate of drying is constant, which corresponds with the linear reduction of moisture in the evaporative drying stage. In the period C–E, the rate of drying decreases, which corresponds with the sharp decrease of moisture in the diffusive drying stage (DINÇER; ZAMFIRESCU, 2016).

Figure 6C depicts the variation of drying rate versus drying time. The falling rate period begins at M_c, and continues until the moisture content decreases to M_e (SINGH; HELDMAN, 2014a).
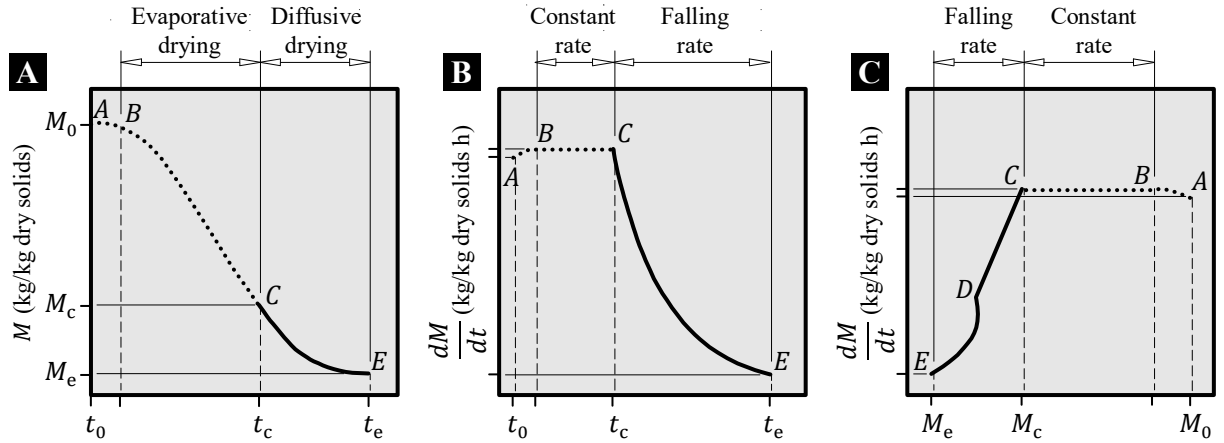
Figure 6. Drying curves. (A) Moisture content (M) versus drying time (t); (B) Drying rate (dM/dt) versus drying time; (C) Drying rate versus moisture content. The curves are for moist material dried at a constant temperature and relative humidity.

Materials can be classified as non-hygroscopic and hygroscopic. For non-hygroscopic materials, M_e is zero (DELGADO; DA SILVA, 2014). Mature cereal grains are hygroscopic materials because water molecules are physically and/or chemically bound to endosperm matrix. The bound moisture is usually found forming hydrogen bonds at the hydroxyl groups around the sugar molecules of the starch polymers. Hydrogen bonds linking water also occurs at the polar amino acid side-chains of water-soluble proteins because these side-chains are uniformly distributed at the surface of the globular protein structures. The bound water to these polymers exerts a vapor pressure less than that of liquid water at the same temperature (BARBOSA-CÁNOVAS; VEGA-MERCADO, 1996).

The drying rate curve in Figure 6C corresponds to hygroscopic materials, where C–D is defined as the first falling rate period, and D–E is the second falling rate period (DELGADO; DA SILVA, 2014). At point D, the entire exposed surface becomes completely unsaturated, and this marks the start of the drying process during which the rate of internal moisture movement controls the drying rate (DINÇER; ZAMFIRESCU, 2016).

3.3 Effective Diffusivity

In the falling rate period, the drying of rate is controlled by a transient mass diffusion and the expressions used to describe the moisture diffusion process are dependent on food shape (SINGH; HELDMAN, 2014a). The mass-transfer Biot number described in equation (5), is a dimensionless group that associates the characteristic dimension of the object (l), the convective mass-transfer coefficient (h_m) for the drying air flowing across the surface of the grains, and the effective moisture diffusivity (D_{eff}).

$$Bi_m = \frac{h_m l}{D_{eff}} \tag{5}$$

D_{eff} represents the conductive term of all moisture transfer mechanisms. This parameter is usually determined from experimental drying curves (ROBERTS; KIDD; PADILLA-ZAKOUR, 2008).

When the hot air velocity is equal to or greater than 1 m/s, external resistances to mass transfer become negligible. Under these conditions, it is ensured that Bi_m in grains will be above 10 (SRIKIATDEN; ROBERTS, 2007). External resistances to mass transfer become

important only for Bi_m less than 10 (VACCAREZZA; LOMBARDI; CHIRIFE, 1974). For an infinite-plate geometry with a thickness of x, l is the half thickness of x, and the relationship used to describe unsteady-state mass transfer is the Fick's second law of diffusion, as shown in equation (6):

$$\frac{\partial M}{\partial t} = D_{\text{eff}} \frac{\partial^2 M}{\partial x^2} \tag{6}$$

The solution of this differential equation was developed by CRANK (1975). Assuming uniform initial moisture distribution, negligible external resistance, negligible temperature gradients, negligible shrinkage during drying, and constant diffusion coefficient, the equation (7) gives the analytical solution for an infinite-plate geometry:

$$\frac{M - M_e}{M_0 - M_e} = \sum_{n=0}^{\infty} \frac{8}{(2n+1)^2 \pi^2} e^{\left(-\frac{(2n+1)^2 \pi^2}{4l^2} D_{\text{eff}}\right) t} \tag{7}$$

where, D_{eff} is the effective moisture diffusivity (m^2/s); l is the half-thickness of the slab with grains (m), and n is a positive integer. In practice, only the first term is used (DOYMAZ, 2007) yielding the equation (8):

$$\frac{M - M_e}{M_0 - M_e} = \frac{8}{\pi^2} e^{\left(-\frac{\pi^2}{4l^2} D_{\text{eff}}\right) t} \tag{8}$$

Linearizing this equation gives equation (9):

$$\ln\left(\frac{M - M_e}{M_0 - M_e}\right) = \ln\left(\frac{8}{\pi^2}\right) + \left(-\frac{\pi^2}{4l^2} D_{\text{eff}}\right) t \tag{9}$$

Thus, D_{eff} is calculated with equation (10), which is derived from the slope of this equation:

$$D_{\text{eff}} = -\frac{4l^2}{\pi^2} (\text{Slope}) \tag{10}$$

4 GRINDING OF CEREAL GRAINS

Grinding or milling of cereal grains is commonly performed to produce refined flour, the ingredient used in making bread, pasta, cakes, cookies, porridge, and extruded snack foods, between many other food products (LI; DHITAL; HASJIM, 2014). Whole-grain flours are increasingly popular because they keep the dietary fiber and bioactive compounds in the end-products. According to the size reduction of bran particles, whole cereal flours also are used for bread production (flours with moderate bran particle size) and non-gluten applications (flours with small bran particle size) (DOBLADO-MALDONADO et al., 2012).

Due to the variation in structure and composition between the anatomical parts of cereal grains, whole-grain flours are composed of irregular particles with various densities different from the density of grains. In cereal processing by extrusion, grains are downsized to produce free-flowing feed materials with appropriate particle sizes. During the grinding process, the grains are stressed by the action of mechanical parts of the grinding machine. Initially, the stress is absorbed internally by the material as strain energy and when it exceeds a critical level, fracture occurs along cleavages or lines of weakness in the grains, and the stored energy is used for the creation of new surfaces. Nevertheless, a large part of the energy is dissipated as heat (GURITNO; HAQUE, 1994).

According to the type of grinder operated, the grinding process increases the surface area of the grains and improve the reactiveness of particles (SHASHIDHAR et al., 2013). Thus, during an extrusion process, particles with large surface areas are easily melted and more starch conversion and more complexes formation between macromolecules and minority compounds can occur.

4.1 Size-Reduction Equipment

Size-reduction machines for dry milling of cereal grains can be classified as grinders, which include hammer mills and impactors, rolling-compression machines, attrition mills, and tumbling mills (MCCABE; SMITH; HARRIOTT, 1993). The grinder type used to produce whole-grain flours can greatly impact the quality of the whole bread (DOBLADO-MALDONADO et al., 2012).

In disc attrition mills, grains are ground between two metal discs with tiles secured to the periphery of them (Figure 7A). One grinding surface rotates (1) and the other is stationary (2). Feed (F) enters through an opening in the hub of the stationary disc. It passes outward through the narrow gap between the discs and discharges from the periphery into a stationary casing (C). Product (P) is collected below (MCCABE; SMITH; HARRIOTT, 1993). The tiles are made of wolfram (tungsten) carbide and have a pattern of sharp parallel ridges arranged almost radially. Tiles are arranged in two concentric rows with different ridges. The coarser ridged tiles form the inner ring so that grains, which pass centrifugally, encounter them before receiving a finer grind by the more finely ridged tiles. The tiles are tapered, with the outside thicker than the inside so grains pass through a narrowing gap between grinding surfaces (ROSENTRATER; EVERS, 2018c). These types of mills make use of shear forces for size reduction. The gap between discs is adjustable, depending on grain size and end-product requirements. A greater degree of shear is achieved when the casing contains two rotating discs that rotate in opposite directions. The combined action of shear and impact forces is performed with the pin-disc mill that carries pins or pegs on the rotating elements (BARBOSA-CÁNOVAS et al., 2005).

In the rolling-compression mills, two or more cylinders revolve towards each other (Figure 7B). The roller milling process for cereal grains comprises a breaking stage with striated rolls and a reduction stage with smooth rolls. In the two first rolling members of the breaking stage, the grains are caught and crushed. The particles from breaker rolls consist of flattened bran flakes with adhering endosperm. Subsequent breaker rolls remove more endosperm and, in the process, particles become smaller flakes. After each breaking stage, the milled products are sieved to separate the bran. The smaller particles comprise mainly endosperm and are conveyed for progressive reduction to flour size, and separation from any remaining bran and germ particles (ROSENTRATER; EVERS, 2018c). The size reduction in these types of mills makes use of compression forces and if the differential speed is maintained, also it is exerted shearing forces. The roller surfaces can carry breaker bars or teeth, as a way to increase friction and facilitate entrapment of particles between the rolls. Toothed-roll mills make use of compression, impact, and shear forces for size reduction (BARBOSA-CÁNOVAS et al., 2005). The differential speed creates a scratching effect rather than a pure pressing action, which results in the production of a higher number of coarse particles (semolina particles) compared to fine particles (flour) (GRUBER; SARKAR, 2012). From the first to the last pair of rolls, the roll gap is set successively narrower as the particle size of the feed material becomes smaller (FANG et al., 1998). The striations in a roll surface help to open up the cereal grain with a scissors-like motion, thus keeping the bran from being broken into smaller pieces (FANG; CAMPBELL, 2002).
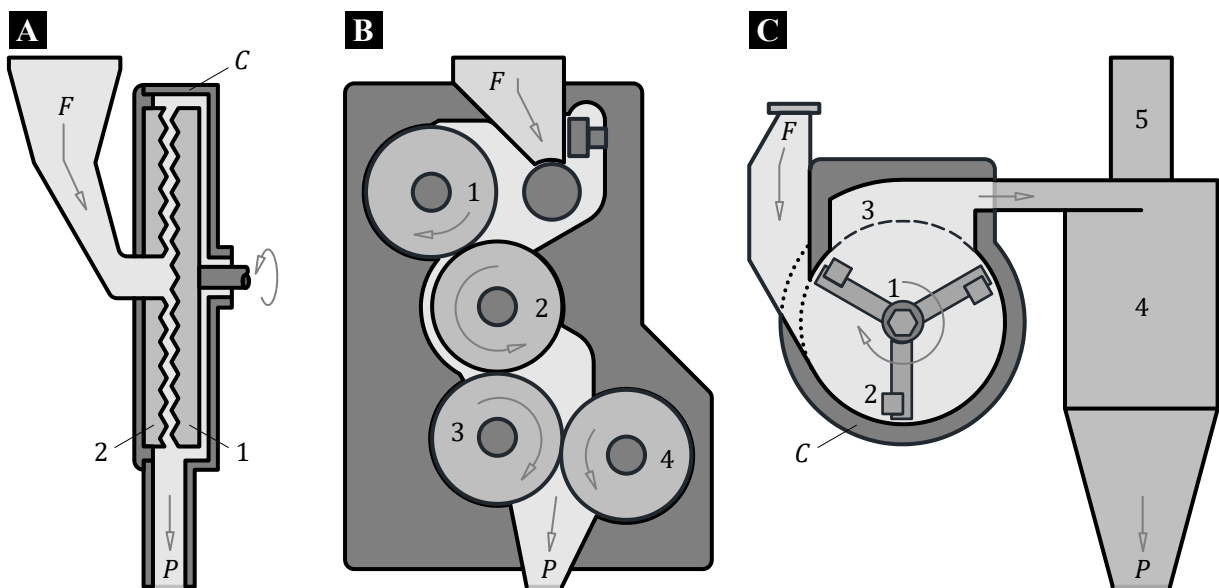
Figure 7. (A) Disc attrition mill; 1: rotating disc; 2: stationary disc. (B) Rolling-compression mill; 1–4: grinding rolls. (C) Hammer mill; 1: hammer; 2: screening plate. F: feed; P: product. Adapted from (BARBOSA-CÁNOVAS et al., 2005; POSNER; HIBBS, 2005a).

Hammer mills (Figure 7C) consist of a disc (1) with swing hammers (2) pinned and equally spaced to it. The disc is coupled to a high-speed rotor turning inside a cylindrical casing (C). Feed (F) dropped into the top of the casing is struck by the swing hammers and it shatters into pieces, which fly against a stationary screening plate (3) inside the casing and break into still smaller fragments. The particles larger than the mesh opening, in turn, are rubbed into powder by the hammers until they get to pass through the opening (BARBOSA-CÁNOVAS et al., 2005; MCCABE; SMITH; HARRIOTT, 1993). The hammer mill creates a high airflow during its operation, which helps push the product out of the mill. So that, most hammer mills

are typically installed with an air system, which includes a cyclone (4) and a filter (5) for fine particle collection (ROSENTRATER; EVERS, 2018d). The hammer mill gives high reduction ratios, mainly due to impact forces, although under choke feeding conditions, attrition forces can also play a part in such reduction. The hammers may be replaced by knives or other devices to give the mill the possibility of handling tough, ductile or fibrous materials (BARBOSA-CÁNOVAS et al., 2005). In most flour mills, hammer mills are used for grinding bran and the desired product size is dictated by the size of the perforations in the screening plate. The forced pass of particles through the perforated screen generates high friction and heat than in other grinders. This causes product degradation and loss of moisture (POSNER; HIBBS, 2005b).

4.2 Grinding Energy

Grinding is a unit operation designed to reduce the size of materials to give a usable form or to separate their components. The material is subjected to mechanical stress leading to an increase in its free energy and fragmentation. The free energy generated can be transformed according to various processes in elastic energy, plastic energy, energy surface and various other forms of energy (BAUDELAIRE, 2013).

In mathematical terms, the energy required to breakage the feed into a ground sample is related to equation (11) (NAPIER-MUNN et al., 1996):

$$dE = -K \frac{dx}{x^n} \tag{11}$$

Where dE is the increment in energy required for grinding, dx is the change in the size of feed into the product, and K is some constant. When $n = 2$, the relation is known as Rittinger's law for brittle materials. After integrating, the constant energy per unit of generated surface area gives the equation (12):

$$E = K \left(\frac{1}{x_2} - \frac{1}{x_1} \right) \tag{12}$$

When $n = 1$, the relation is known as Kick's law. After integrating, the constant energy per unit mass for similar relative reduction gives the equation (13):

$$E = K \ln \frac{x_1}{x_2} \tag{13}$$

When $n = 3/2$, the relation is known as Bond's law. After integrating, the constant energy gives the equation (14):

$$E = 2K \left(\frac{1}{\sqrt{x_2}} - \frac{1}{\sqrt{x_1}} \right) \tag{14}$$

5 EXTRUSION COOKING OF FOODS

Extrusion is the operation of shaping a dough-like material by forcing it through a narrow opening (BERK, 2013; RIAZ, 2000). Extrusion cooking of foods is defined as a thermomechanical process whereby starchy and/or proteinaceous materials are plasticized with water in the range of 10 to 40% (wet basis) and cooked in a tube by the combined effect of pressure changes, heat and mass transfer, and mechanical shear (BERK, 2013; GUY, 2001; SMITH, 1976). It is a single-stage continuous process where several unit operations simultaneously take place, such as grinding of particles, agglomeration, mixing, kneading, conveying, shearing, melting, shaping, dehydration and cooking. The combined action of heat, moisture, and mechanical work promote the transformation of food components in relation to their chemical, physical and nutritional characteristics (BERRIOS; ASCHERI; LOSSO, 2013; CAMIRE, 2001; RIAZ, 2000). Some transformations include irreversible changes in starch granules and starch polymers, denaturation of proteins, complexation of amylose-lipids, protein-lipids, and protein-protein, inhibition of anti-nutritional factors (proteins, indigestible sugars, phytates, and tannins), inactivation of enzymes and transformation of insoluble fibers to water-soluble fibers (BRENNAN et al., 2011; CAMIRE; CAMIRE; KRUMHAR, 1990; LAI; KOKINI, 1991).

The machinery configuration and operational conditions of the extruder allow to establish a range of independent variables during extrusion processing: barrel and die design, screw configuration, temperature profiles, screw speed, and feed rate. The raw ingredient formulation also defines input variables such as feed moisture, particle-size range, biopolymer composition, and proportion of ingredients. All these extruder initial operating conditions create a series of dependent variables in the process, such as residence time, melt temperature, melt pressure, torque, extruded mass flow rate and mechanical energy input.

The particles making the raw materials mainly are composed of starch granules, protein networks, protein bodies, and fibrous cell walls. In the process, the free-flowing particles are compacted and then transformed into a fluid melt (GUY, 2001). The aforementioned entities lose their native and organized structure to form a continuous viscoelastic mass (MORARU; KOKINI, 2003; STEEL et al., 2012).

Starch granules are semicrystalline (FITZGERALD, 2004) and their polymers are thermoplastics, that is, they soften when heated and solidify when cooled (KAZEMZADEH, 2012). Hence, the combined effect of moisture and heat into the extruder promotes the glass transition and melting of starch polymers that structure the amorphous and crystalline regions of a starch granule, respectively. Starch granules can be softened, stretched or disrupted according to the process severity (BRENT et al., 1997).

Proteins are thermosetting materials, that is, they undergo a crosslinking reaction when the temperature is raised above a certain value, forming a three-dimensional network. This network remains intact when the temperature is reduced again (RAUWENDAAL, 2014b). During the extrusion process, proteins go through the glass transition phase, unfolding in their helical structure and aligning themselves along with the rationalized flow of the screws and die (CAMIRE, 1991). In such conditions, the crosslinking reactions cause a textured product in layers, resistant to disintegration after rehydration. Vegetable proteins with high solubility in water, such as soybean, wheat gluten and corn gluten meal, play functional characteristics during extrusion: water absorption capacity, mass elastic capacity (expansion) and ability to retain gas (ligand) (AKDOGAN, 1999).

Fibers and minerals do not go through a glass transition phase at the extrusion process conditions. If heated to a high enough thermal energy, they will bypass the amorphous phase and will decompose (KAZEMZADEH, 2012). All these order-disorder transitions affect the physicochemical properties of the melt, and subsequently the physical characteristics of the extrudate.

5.1 Extruder Elements

A basic nomenclature for the extruder parts is depicted in **Figure 8**. The variation in the screw design can generate high pressure (over 100 bars) and compression of the raw material as well as generate temperatures of over 250°C (KAZEMZADEH, 2012).
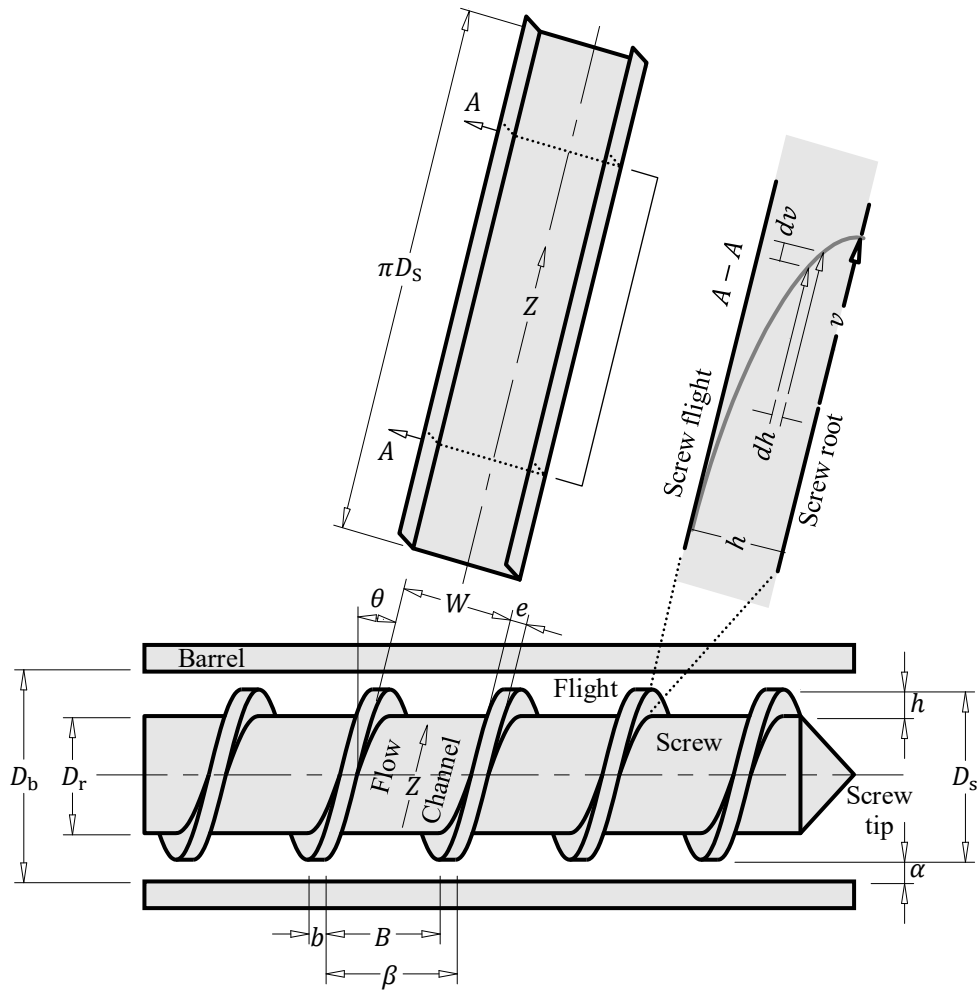
Figure 8. Schematic diagram of the extruder parts and the geometry of the single flighted extruder screw. Adapted from (KAZEMZADEH, 2012).

The barrel diameter (D_b) is referred to as the barrel opening in which the screw is concentrically attached. The screw clearance (2α) is the annular space between the inner surface of the barrel and the outer surface of the screw. The screw diameter (D_s) is calculated with equation (15):

$$D_s = D_b - 2\alpha \tag{15}$$

The root diameter (D_r) is the inner surface of the screw on which the flights are built. It is the base of the shaft that carries the rotational torque. The flight height (h) is referred to as the channel depth, which gradually varies in the compression section of the screw. As the compression ratio of the screw increases, the pressure build-up and temperature increase and the residence time decrease. The degree of starch conversion is promoted at high pressures and temperatures inside the barrel whereas low residence times decrease the degree of starch conversion (CHIRUVELLA; JALURIA; KARWE, 1996). D_r is calculated with equation (16):

$$D_r = D_s - 2h \tag{16}$$

The screw pitch (β) is the axial distance between the leading edge of the flight at the outside diameter and the leading edge of the same flight in front (KAZEMZADEH, 2012). It determines the helix angle (θ) the angle which the flight makes with a plane normal to the axis of the screw. The helix angle primarily determines the extruder output and is calculated with equation (17):

$$\theta = \tan^{-1}\left(\frac{\beta}{\pi D_s}\right) \tag{17}$$

The extruder channel has a rectangular cross-section. The base is obtained by unwinding the helical path of the top of the screw root diameter, that extends from the feed to the discharge end of the screw (KAZEMZADEH, 2012). Thus, the channel length is given by πD_s and the channel width (W) delimit the channel walls of height $h + \alpha$. W comprises from one side of the flight to the next and is determined using equation (18):

$$W = B \cos \theta \tag{18}$$

Where B is the axial distance between the flights. The channel at the top is delimited by the surface of the barrel opening. The width of the screw flight (e) is measured perpendicular to the face of the flight and is determined with equation (19):

$$e = b \cos \theta \tag{19}$$

Where b is the axial flight width. The velocity at the screw tip (v) is the linear velocity of the screw root and is dependent on the diameter of the screw and the rotational screw speed (S_s) of the shaft ($v = \pi D_s S_s$). The shear rate ($\dot{\gamma}$) of the molten material in the melt section of the channel is dependent on the shear characteristics of the screw (YACU, 1985). It can be determined with equation (20):

$$\dot{\gamma} = \frac{d\gamma}{dt} = \frac{dv}{dh} = \frac{\pi D_s S_s}{h} \tag{20}$$

The shear rate and the residence time are increased at low moisture content extrusion processes, resulting in a greater degree of starch conversion, and thus, expansion. At very low feed moisture (below 14% dry basis) the process creates very high shear rates and longer residence times, and thus increases the product temperature. Such conditions are known to cause starch degradation and dextrinization (CHANG; EL-DASH, 2003).

5.2 Single Screw Extruder

The schematic of a single-screw extruder is shown in Figure 9, whose main parts are the drive unit (A–D), the screw (E) and barrel heaters and coolers (F, G), the die (H) and the feeder (I). The drive unit turns the extruder screw at a constant speed over a large speed range and supplies the required amount of torque to the shank of the screw to process the feeding material. The drive motor (A) connected to the gear reducer (C), convert motor rpm to the desired screw rpm (WAGNER; MOUNT; GILES, 2014a). At the entrance to the gearbox is the torque limiting coupling (B), and at the exit is the gearbox connection (D) to the screw shaft (a jaw-type coupling). The torque limiting coupler disengages at a predefined torque limit to protect the motor from damage when the high torque limit is reached (WAGNER; MOUNT; GILES, 2014b).
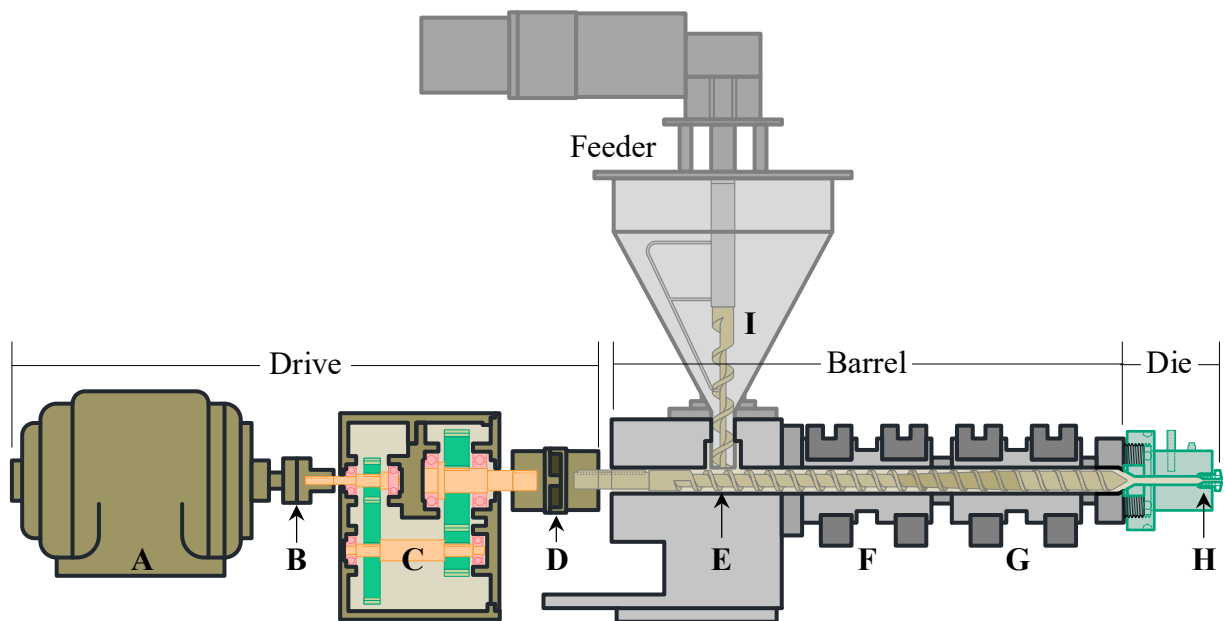
Figure 9. Scheme of a single-screw extruder. The drive unit: (A) motor, (B) torque limiting coupler, (C) gearbox, (D) jaw-type coupling. The barrel: (E) extruder screw, (F) first heater/cooler zone, (G) second heater/cooler zone; The die: (H) circular die; The feeder: (I) feeder screw.

The screw is divided into three distinct geometrical sections with a channel having a variable depth (BOUVIER; CAMPANELLA, 2014). The first section, called the solid conveying section, has deep flights and is partially full of raw material by a frictional drag mechanism, no pressure is developed in this section (RAUWENDAAL, 2014b). Feed materials with a large variation in particle size and shape are likely to cause conveying problems. Single-screw extruders usually are flood fed and flood feeding often results in higher pressures inside the extruder. Feed materials based on whole grains and finely particulate can lead to an agglomeration of particles. This is the case of wholemeal flours of oats and rye, and whole grains ground in a hammer mill. In these cases, it is recommended to opt by starve feeding. In this feeding type, the pressures inside the extruder are lower and can be controlled by adjusting the feed rate and/or the screw speed (RAUWENDAAL, 2014a).

The following section is the compression section, where the material is compressed in a channel of decreasing depth. The screw is full in this section and the mechanical energy required to turn the screw is converted to thermal energy by viscous dissipation. The material also is heated by conductive heat transfer. Both mechanical and thermal energy raises the

temperature until melting occurs (BOUVIER; CAMPANELLA, 2014; HARPER, 1989). In this section, the transition of the solid particles into a viscous fluid melt occurs (RAUWENDAAL, 2014b).

The third screw section is the metering (or pumping) section, wherein the material is ideally in a molten state. This section has shallow flights that generate high shearing conditions and the pressure needed to pump and feed the molten material through the die opening is built up. The mechanical energy dissipated allows the material to be converted into a rheological state which is compatible with satisfactory processing and forming (BOUVIER; CAMPANELLA, 2014).

At the barrel end is attached the die, a block of metal with a specially shaped orifice. The pressure drop across the die causes puffing to occur when the high-temperature water in the product rapidly converts to steam (HARPER, 1989).

6 CONCLUSION AND FUTURE PROSPECTS

The extrusion technology plays a major role in developing whole-grain ready-to-eat extruded snacks. Given that consumers increasingly opt for convenient and healthy food, this technology stands out from others in several aspects, among them, the continuous production of extrudates with a defined glycemic index, according to the degree of starch conversion and complexes formation between the minority components (fibers, lipids, and phenolics) and the starch and protein polymers. Secondly, this research area promotes sustainable and environmentally friendly industrial development. The extrusion technology does not generate by-products and is a useful technique to increase the range of whole-grain based products (clean label products, preservative-free).

The anatomical parts of a cereal grain comprise the outer layers, the germ, and the endosperm. They vary in structure and composition. In the drying of whole-grain cereals, the moisture diffusion from various parts of the interior to the surface of the kernel is influenced by the endosperm structure, the permeability of the aleurone and outer layers, and the extent of damage to these layers.

For various cereal grains, the critical moisture content lies around 14% (wet basis). This moisture level ensures grain storage free of mold growth. The drying curve starting from grains with initial moisture around the critical moisture practically takes place in the falling rate period. In cereal processing by extrusion, grains are downsized to produce free-flowing feed materials with appropriate particle sizes. Feed materials based on whole grains are more heterogeneous because the minor anatomical parts become part of particle surfaces. The drying of whole-grain cereals enhances its fractionation during the grinding process because the fibers distributed in the pericarp layers and the intricate network of endosperm cell walls are more brittle due to a decrease in tissue adhesive forces. The drying of whole-grain cereals can improve the uniformity of the particle-size distribution.

The most important consideration in producing whole-grain particles is selecting the grinder type to be used. The predominant machines for grinding whole-grain cereals are disc, roller, and hammer mills. The shape of the particles in the milled product is inherently bound to the action of mechanical parts of the grinding machine. According to the type of grinder operated, the grinding process increases the surface area of the grains and improve the reactiveness of particles. This is important in an extrusion process, wherein the particles with large surface areas are easily melted and more starch conversion and more complexes formation between macromolecules and minority compounds can occur.

REFERENCES

ABDULLAH, N.; NAWAWI, A.; OTHMAN, I. Fungal spoilage of starch-based foods in relation to its water activity (aw). **Journal of Stored Products Research**. v. 36, n. 1, p. 47-54, 2000.

AČKAR, Đ.; JOZINOVIĆ, A.; BABIĆ, J.; MILIČEVIĆ, B.; PANAK BALENTIĆ, J.; ŠUBARIĆ, D. Resolving the problem of poor expansion in corn extrudates enriched with food industry by-products. **Innovative Food Science & Emerging Technologies**. v. 47, n. 6, p. 517-524, 2018.

AGENCY, F. S. **McCance and Widdowson's The Composition of Foods**. 6th ed. Royal Society of Chemistry: Cambridge, 2002.

AKDOGAN, H. High moisture food extrusion. **International Journal of Food Science and Technology**. v. 34, n. 3, p. 195-207, 1999.

ARENDT, E. K.; ZANNINI, E. Oats. In: ARENDT, E. K.; ZANNINI, E. (Eds.). **Cereal Grains for the Food and Beverage Industries**. Woodhead Publishing: Cambridge, 2013a. p. 243-283.

ARENDT, E. K.; ZANNINI, E. Rye. In: ARENDT, E. K.; ZANNINI, E. (Eds.). **Cereal Grains for the Food and Beverage Industries**. Woodhead Publishing: Cambridge, 2013b. p. 220-243.

ARENDT, E. K.; ZANNINI, E. Wheat and other Triticum grains. In: ARENDT, E. K.; ZANNINI, E. (Eds.). **Cereal Grains for the Food and Beverage Industries**. Woodhead Publishing: Cambridge, 2013c. p. 1-67.

BALA, B. K. Physical and Thermal Properties of Cereal Grains. In: BALA, B. K. (Ed.). **Drying and Storage of Cereal Grains**. 2nd ed. Wiley Blackwell: Chichester, 2017a. p. 55-80.

BALA, B. K. Thin Layer Drying of Cereal Grains. In: BALA, B. K. (Ed.). **Drying and Storage of Cereal Grains**. Wiley Blackwell: Chichester, 2017b. p. 107-145.

BARBOSA-CÁNOVAS, G. V.; ORTEGA-RIVAS, E.; JULIANO, P.; YAN, H. Size reduction. In: **Food Powders: Physical Properties, Processing, and Functionality**. Springer US: Boston, MA, 2005. p. 157-173.

BARBOSA-CÁNOVAS, G. V.; VEGA-MERCADO, H. Dehydration Mechanisms. In: BARBOSA-CÁNOVAS, G. V.; VEGA-MERCADO, H. (Eds.). **Dehydration of Foods**. Springer US: Boston, MA, 1996. p. 101-155.

BAUDELAIRE, E. D. Grinding for food powder production. In: BHANDARI, B. et al. (Eds.). **Handbook of Food Powders**. Woodhead Publishing: Cambridge, 2013. p. 132-149.

BECHTEL, D. B.; ABECASSIS, J.; SHEWRY, P. R.; EVERS, A. D. Development, Structure, and Mechanical Properties of the Wheat Grain. In: KHAN, K.; SHEWRY, P. R. (Eds.). **Wheat Chemistry and Technology**. 4th ed. AACC International Press: St. Paul, 2009. p. 51-95.

BECHTEL, D. B.; POMERANZ, Y. Ultrastructure of the mature ungerminated rice (Oryza

sativa) caryopsis. The starchy endosperm. **American Journal of Botany**. v. 65, n. 6, p. 684-691, 1978.

BECHTEL, D. B.; POMERANZ, Y. Ultrastructure and cytochemistry of mature oat (Avena sativa L.) endosperm. The aleurone layer and starchy endosperm. **Cereal Chemistry**. v. 58, n. 1, p. 61-69, 1981.

BECHTEL, D. B.; WILSON, J. D. Amyloplast Formation and Starch Granule Development in Hard Red Winter Wheat. **Cereal Chemistry**. v. 80, n. 2, p. 175-183, 2003.

BERK, Z. Extrusion. In: BERK, Z. (Ed.). **Food Process Engineering and Technology**. 2nd ed. Academic Press: San Diego, 2013. p. 373-393.

BERRIOS, J. J.; ASCHERI, J. L. R.; LOSSO, J. N. Extrusion processing of dry beans and pulses. In: SIDDIQ, M.; UEBERSAX, M. A. (Eds.). **Dry Beans and Pulses**. Wiley Blackwell: Iowa, 2013. p. 185–203.

BOUVIER, J.-M.; CAMPANELLA, O. H. Extrusion Equipment. In: BOUVIER, J.-M.; CAMPANELLA, O. H. (Eds.). **Extrusion Processing Technology**. John Wiley & Sons, Ltd: Chichester, 2014. p. 13-51.

BRENNAN, C.; BRENNAN, M.; DERBYSHIRE, E.; TIWARI, B. K. Effects of extrusion on the polyphenols, vitamins and antioxidant activity of foods. **Trends in Food Science & Technology**. v. 22, n. 10, p. 570-575, 2011.

BRENT, J. J. L.; MULVANEY, S. J.; COHEN, C.; BARTSCH, J. A. Viscoelastic Properties of Extruded Cereal Melts. **Journal of Cereal Science**. v. 26, n. 3, p. 313-328, 1997.

CAMIRE, M. E. Protein functionality modification by extrusion cooking. **Journal of the American Oil Chemists' Society**. v. 68, n. 3, p. 200-205, 1991.

CAMIRE, M. E. Extrusion and nutritional quality. In: GUY, R. (Ed.). **Extrusion Cooking Technologies and Applications**. Woodhead Publishing: Cambridge, 2001. p. 108-129.

CAMIRE, M. E.; CAMIRE, A.; KRUMHAR, K. Chemical and nutritional changes in foods during extrusion. **Critical Reviews in Food Science and Nutrition**. v. 29, n. 1, p. 35-57, 1990.

CENGEL, Y. A.; BOLES, M. A. Gas–Vapor Mixtures and Air-Conditioning. In: CENGEL, Y. A.; BOLES, M. A. (Eds.). **Thermodynamics: an Engineering Approach**. 8th ed. McGraw-Hill Education: New York, 2015. p. 725-758.

CHAKRAVERTY, A.; SINGH, R. P. Theory of Grain Drying. In: CHAKRAVERTY, A.; SINGH, R. P. (Eds.). **Postharvest Technology and Food Process Engineering**. CRC Press: Boca Raton, 2014. p. 31-74.

CHAMPAGNE, E. T.; WOOD, D. F.; JULIANO, B. O.; BECHTEL, D. B. The rice grain and its gross composition. In: CHAMPAGNE, E. T. (Ed.). **Rice: Chemistry and Technology**. Grain Science References, 3rd ed. American Association of Cereal Chemists, Inc.: St. Paul, 2004. p. 77-107.

CHANG, Y. K.; EL-DASH, A. A. Effects of acid concentration and extrusion variables on some physical characteristics and energy requirements of cassava starch. **Brazilian Journal of**

Chemical Engineering. v. 20, n. 2, p. 129-137, 2003.

CHIRUVELLA, R. V.; JALURIA, Y.; KARWE, M. V. Numerical simulation of the extrusion process for food materials in a single-screw extruder. **Journal of Food Engineering**. v. 30, n. 3, p. 449-467, 1996.

CRANK, J. **The mathematics of diffusion**. 2nd ed. Oxford Science Publications: Glasgow, 1975.

CUETO, M.; FARRONI, A.; RODRÍGUEZ, S. D.; SCHOENLECHNER, R.; SCHLEINING, G.; DEL PILAR BUERA, M. J. F.; TECHNOLOGY, B. Assessing Changes in Enriched Maize Flour Formulations After Extrusion by Means of FTIR, XRD, and Chemometric Analysis. **Food and Bioprocess Technology**. v. 11, n. 8, p. 1586-1595, 2018.

DELCOUR, J. A.; HOSENEY, R. C. Proteins of Cereals. In: DELCOUR, J. A.; HOSENEY, R. C. (Eds.). **Principles of Cereal Science and Technology**. Textbooks, 3rd ed. AACC International, Inc.: St. Paul, 2010a. p. 53-70.

DELCOUR, J. A.; HOSENEY, R. C. Structure of cereals. In: DELCOUR, J. A.; HOSENEY, R. C. (Eds.). **Principles of Cereal Science and Technology**. Textbooks, 3rd ed. AACC International, Inc.: St. Paul, 2010b. p. 1-22.

DELGADO, J. M. P. Q.; DA SILVA, M. V. Food Dehydration: Fundamentals, Modelling and Applications. In: DELGADO, J. M. P. Q.; BARBOSA DE LIMA, A. G. (Eds.). **Transport Phenomena and Drying of Solids and Particulate Materials**. Springer International Publishing: Cham, 2014. p. 69-94.

DINÇER, İ.; ZAMFIRESCU, C. Basics of Drying. In: DINÇER, İ.; ZAMFIRESCU, C. (Eds.). **Drying Phenomena**. John Wiley & Sons, Ltd: Chichester, 2016. p. 67-98.

DOBLADO-MALDONADO, A. F.; PIKE, O. A.; SWELEY, J. C.; ROSE, D. J. Key issues and challenges in whole wheat flour milling and storage. **Journal of Cereal Science**. v. 56, n. 2, p. 119-126, 2012.

DORNEZ, E.; HOLOPAINEN, U.; CUYVERS, S.; POUTANEN, K.; DELCOUR, J. A.; COURTIN, C. M.; NORDLUND, E. Study of grain cell wall structures by microscopic analysis with four different staining techniques. **Journal of Cereal Science**. v. 54, n. 3, p. 363-373, 2011.

DOYMAZ, İ. The kinetics of forced convective air-drying of pumpkin slices. **Journal of Food Engineering**. v. 79, n. 1, p. 243-248, 2007.

DYKES, L.; ROONEY, L. W. Sorghum and millet phenols and antioxidants. **Journal of Cereal Science**. v. 44, n. 3, p. 236-251, 2006.

DYKES, L.; ROONEY, L. W. Phenolic compounds in cereal grains and their health benefits. **Cereal Foods World**. v. 52, n. 3, p. 105-111, 2007.

DYKES, L.; SEITZ, L. M.; ROONEY, W. L.; ROONEY, L. W. Flavonoid composition of red sorghum genotypes. **Food Chemistry**. v. 116, n. 1, p. 313-317, 2009.

EARP, C. F.; MCDONOUGH, C. M.; ROONEY, L. W. Microscopy of pericarp development

in the caryopsis of Sorghum bicolor (L.) Moench. **Journal of Cereal Science**. v. 39, n. 1, p. 21-27, 2004.

EVERS, A. D.; O'BRIEN, L.; BLAKENEY, A. B. Cereal structure and composition. **Australian Journal of Agricultural Research**. v. 50, n. 5, p. 629-650, 1999.

EVERS, T.; MILLAR, S. Cereal Grain Structure and Development: Some Implications for Quality. **Journal of Cereal Science**. v. 36, n. 3, p. 261-284, 2002.

FANG, C.; CAMPBELL, G. M. Stress-Strain Analysis and Visual Observation of Wheat Kernel Breakage During Roller Milling Using Fluted Rolls. **Cereal Chemistry**. v. 79, n. 4, p. 511-517, 2002.

FANG, Q.; HAQUE, E.; SPILLMAN, C. K.; REDDY, P. V.; STEELE, J. L. Energy requeriments for size reduction of wheat using a roller mill. **Transactions of the ASAE**. v. 41, n. 6, p. 1713-1720, 1998.

FITZGERALD, M. Starch. In: **Rice Chemistry and Technology**. 3rd ed. American Association of Cereal Chemists, Inc., 2004. p. 109-141.

GANßMANN, W.; VORWERCK, K. Oat milling, processing and storage. In: WELCH, R. W. (Ed.). **The Oat Crop: Production and Utilization**. Springer Netherlands: Dordrecht, 1995. p. 369-408.

GARCÍA-LARA, S.; CHUCK-HERNANDEZ, C.; SERNA-SALDIVAR, S. O. Development and Structure of the Corn Kernel. In: SERNA-SALDIVAR, S. O. (Ed.). **Corn: Chemistry and Technology**. 3rd ed. AACC International Press: Oxford, 2019. p. 147-163.

GLITSØ, L. V.; BACH KNUDSEN, K. E. Milling of Whole Grain Rye to Obtain Fractions with Different Dietary Fibre Characteristics. **Journal of Cereal Science**. v. 29, n. 1, p. 89-97, 1999.

GRUBER, W.; SARKAR, A. Durum Wheat Milling. In: SISSONS, M. et al. (Eds.). **Durum Wheat Chemistry and Technology**. AACC International Press: St. Paul, 2012. p. 139-159.

GURITNO, P.; HAQUE, E. Relationship Between Energy and Size Reduction of Grains Using a Three-roller Mill. **Transactions of the ASAE**. v. 37, n. 4, p. 1243-1248, 1994.

GUY, R. Raw materials for extrusion cooking. In: GUY, R. (Ed.). **Extrusion Cooking Technologies and Applications**. First ed. Woodhead Publishing: Cambridge, 2001. p. 5-28.

HARPER, J. M. Food extruders and their applications. In: MERCIER, C.; LINKO, P.; HARPER, J. M. (Eds.). **Extrusion Cooking**. American Association of Cereal Chemists. Inc.: St. Paul, 1989. p. 1-16.

HOLOPAINEN-MANTILA, U.; RAULIO, M. Cereal grain structure by microscopic analysis. In: SOZER, N. (Ed.). **Imaging Technologies and Data Processing for Food Engineers**. Springer International Publishing: Cham, 2016. p. 1-39.

HOURSTON, J. E.; IGNATZ, M.; REITH, M.; LEUBNER-METZGER, G.; STEINBRECHER, T. Biomechanical properties of wheat grains: the implications on milling. **Journal of The Royal Society Interface**. v. 14, n. 126, 2017.

JULIANO, B. O.; TUAÑO, A. P. P. Gross structure and composition of the rice grain. In: BAO, J. (Ed.). **Rice Chemistry and Technology**. 4th ed. AACC International Press, 2019. p. 31-53.

KAMAL-ELDIN, A. Dietary Fiber: Bran. In: CABALLERO, B.; FINGLAS, P. M.; TOLDRÁ, F. (Eds.). **Encyclopedia of Food and Health**. Academic Press: Oxford, 2016. p. 378-382.

KARIM, A.; ROONEY, L. W. Characterization of pentosans in sorghum grain. **Journal of Food Science**. v. 37, n. 3, p. 369-371, 1972.

KAZEMZADEH, M. Introduction to extrusion technology. In: MASKAN, M.; ALTAN, A. (Eds.). **Advances in Food Extrusion Technology**. First ed. CRC Press: Boca Raton, 2012. p. 1-21.

KNUDSEN, K. E. B. Carbohydrate and lignin contents of plant materials used in animal feeding. **Animal Feed Science and Technology**. v. 67, n. 4, p. 319-338, 1997.

KUMAR, D.; SINGH, V. Bioethanol Production From Corn. In: SERNA-SALDIVAR, S. O. (Ed.). **Corn: Chemistry and Technology**. 3rd ed. AACC International Press: Oxford, 2019. p. 615-631.

LAI, L. S.; KOKINI, J. L. Physicochemical changes and rheological properties of starch during extrusion. (A review). **Biotechnology Progress**. v. 7, n. 3, p. 251-266, 1991.

LÁSZTITY, R. Oat grain—a wonderful reservoir of natural nutrients and biologically active substances. **Food Reviews International**. v. 14, n. 1, p. 99-119, 1998.

LI, E.; DHITAL, S.; HASJIM, J. Effects of grain milling on starch structures and flour/starch properties. **Starch - Stärke**. v. 66, n. 1-2, p. 15-27, 2014.

LU, S.; LUH, B. S. Properties of the Rice Caryopsis. In: LUH, B. S. (Ed.). **Rice: Volume I. Production/Volume II. Utilization**. Springer US: Boston, MA, 1991. p. 389-419.

MAROULIS, Z. B.; KIRANOUDIS, C. T.; MARINOS-KOURIS, D. Heat and mass transfer modeling in air drying of foods. **Journal of Food Engineering**. v. 26, n. 1, p. 113-130, 1995.

MATSUSHIMA, R. Morphological Variations of Starch Grains. In: NAKAMURA, Y. (Ed.). **Starch: Metabolism and Structure**. Springer Japan: Tokyo, 2015. p. 425-441.

MCCABE, W. L.; SMITH, J. C.; HARRIOTT, P. Size reduction. In: MCCABE, W. L.; SMITH, J. C.; HARRIOTT, P. (Eds.). **Unit Operations of Chemical Engineering**. 5th ed. McGraw-Hill Inc: New York, 1993. p. 960-993.

MEERA, M. S.; BHASHYAM, M. K.; ALI, S. Z. Effect of heat treatment of sorghum grains on storage stability of flour. **LWT - Food Science and Technology**. v. 44, n. 10, p. 2199-2204, 2011.

MILLER, S. S.; FULCHER, R. G. Microstructure and Chemistry of the Oat Kernel. In: WEBSTER, F. H.; WOOD, P. J. (Eds.). **Oats Chemistry and Technology**. 2nd ed. AACC International Press: St. Paul, 2011. p. 77-94.

MIR, S. A.; MANICKAVASAGAN, A.; BOSCO, S. J. D.; SHAH, M. A. Brown rice. In: MIR, S. A.; MANICKAVASAGAN, A.; SHAH, M. A. (Eds.). **Whole Grains. Processing, Product**

Development, and Nutritional Aspects. CRC Press: Boca Raton, 2019. p. 49-69.

MOHARRAM, Y. G.; YOUSSEF, A. M. A. Sorghum grain and quality of its edible products. In: CHARALAMBOUS, G. (Ed.). **Food Flavors: Generation, Analysis and Process Influence**. Developments in Food Science, v. 37A. Elsevier: Amsterdam, 1995. p. 111-146.

MORA, S. R.; MILÁN, A. K. N.; MILÁN, J. C. Maize. In: MIR, S. A.; MANICKAVASAGAN, A.; SHAH, M. A. (Eds.). **Whole Grains. Processing, Product Development, and Nutritional Aspects**. CRC Press: Boca Raton, 2019. p. 87-102.

MORARU, C. I.; KOKINI, J. L. Nucleation and Expansion During Extrusion and Microwave Heating of Cereal Foods. **Comprehensive Reviews in Food Science and Food Safety**. v. 2, n. 4, p. 147-165, 2003.

MUIR, W. E.; .SINHA, R. N. Physical properties of cereal and oilseed cultivars grown in western Canada. **Canadian Agricultural Engineering**. v. 30, n. 1, p. 51-55, 1988.

NAPIER-MUNN, T. J.; MORRELL, S.; MORRISON, R. D.; KOJOVIC, T. Models of comminution processes. In: NAPIER-MUNN, T. J. (Ed.). **Mineral Comminution Circuits: Their Operation and Optimisation**. Julius Kruttschnitt Mineral Research Centre, 1996. p. 10-31.

NILSSON, M.; ÅMAN, P.; HÄRKÖNEN, H.; HALLMANS, G.; KNUDSEN, K. E. B.; MAZUR, W.; ADLERCREUTZ, H. Content of Nutrients and Lignans in Roller Milled Fractions of Rye. v. 73, n. 2, p. 143-148, 1997.

O'SHEA, N.; ARENDT, E.; GALLAGHER, E. Enhancing an Extruded Puffed Snack by Optimising Die Head Temperature, Screw Speed and Apple Pomace Inclusion. **Food and Bioprocess Technology**. v. 7, n. 6, p. 1767-1782, 2014.

PARKER, M. L. The Structure of Mature Rye Endosperm. **Annals of Botany**. v. 47, n. 2, p. 181-186, 1981.

PARKER, M. L. The relationship between A-type and B-type starch granules in the developing endosperm of wheat. **Journal of Cereal Science**. v. 3, n. 4, p. 271-278, 1985.

PETERSON, D. M. Composition and Nutritional Characteristics of Oat Grain and Products. In: MARSHALL, H. G.; SORRELLS, M. E. (Eds.). **Oat Science and Technology**. American Society of Agronomy, Inc.: Madison, 1992. p. 265-292.

PIIRONEN, V.; LAMPI, A.-M.; EKHOLM, P.; SALMENKALLIO-MARTTILA, M.; LIUKKONEN, K.-H. Micronutrients and Phytochemicals in Wheat Grain. In: KHAN, K.; SHEWRY, P. R. (Eds.). **Wheat: Chemistry and Technology**. AACC International Press: St. Paul, 2009. p. 179-222.

PITTS, K. F.; MCCANN, T. H.; MAYO, S.; FAVARO, J.; DAY, L. Effect of the Sugar Replacement by Citrus Fibre on the Physical and Structural Properties of Wheat-Corn Based Extrudates. **Food and Bioprocess Technology**. v. 9, n. 11, p. 1803-1811, 2016.

POMERANZ, Y.; CHUNG, O. The lipid composition of a single wheat kernel and its structural parts. **Journal of Chromatography A**. v. 19, p. 540-550, 1965.

POMERANZ, Y.; ZELENY, L. Biochemical and functional changes in stored cereal grains. **C R C Critical Reviews in Food Technology**. v. 2, n. 1, p. 45-80, 1971.

POSNER, E. S. Wheat flour milling. In: KHAN, K.; SHEWRY, P. R. (Eds.). **Wheat: Chemistry and Technology**. Grain Science References, 4th ed. AACC International, Inc.: St. Paul, 2009. p. 119-152.

POSNER, E. S.; HIBBS, A. N. The Flour Mill Laboratory. In: POSNER, E. S.; HIBBS, A. N. (Eds.). **Wheat Flour Milling**. References Series, 2nd ed. AACC International, Inc.: St. Paul, 2005a. p. 47-100.

POSNER, E. S.; HIBBS, A. N. The Grinding Process. In: POSNER, E. S.; HIBBS, A. N. (Eds.). **Wheat Flour Milling**. References Series, 2nd ed. AACC International, Inc.: St. Paul, 2005b. p. 185-221.

RAUWENDAAL, C. Functional Process Analysis. In: RAUWENDAAL, C. (Ed.). **Polymer Extrusion**. 5th ed. Hanser Publications: Cincinnati, 2014a. p. 255-508.

RAUWENDAAL, C. Introduction. In: RAUWENDAAL, C. (Ed.). **Polymer Extrusion**. 5th ed. Hanser Publications: Cincinnati, 2014b. p. 1-10.

RIAZ, M. N. Introduction to extruders and their principles. In: RIAZ, M. N. (Ed.). **Extruders in Food Applications**. CRC Press: Boca Raton, 2000. p. 1-23.

ROBERTS, J. S.; KIDD, D. R.; PADILLA-ZAKOUR, O. Drying kinetics of grape seeds. **Journal of Food Engineering**. v. 89, n. 4, p. 460-465, 2008.

ROBIN, F.; DUBOIS, C.; PINEAU, N.; LABAT, E.; THÉODULOZ, C.; CURTI, D. Process, structure and texture of extruded whole wheat. **Journal of Cereal Science**. v. 56, n. 2, p. 358-366, 2012.

ROSENTRATER, K. A.; EVERS, A. D. Botanical aspects. In: ROSENTRATER, K. A.; EVERS, A. D. (Eds.). **Kent's Technology of Cereals (Fifth Edition)**. Woodhead Publishing: Cambridge, 2018a. p. 205-266.

ROSENTRATER, K. A.; EVERS, A. D. Chemical components and nutrition. In: ROSENTRATER, K. A.; EVERS, A. D. (Eds.). **Kent's Technology of Cereals (Fifth Edition)**. Woodhead Publishing: Cambridge, 2018b. p. 267-368.

ROSENTRATER, K. A.; EVERS, A. D. Dry-milling technology. In: ROSENTRATER, K. A.; EVERS, A. D. (Eds.). **Kent's Technology of Cereals (Fifth Edition)**. Woodhead Publishing: Cambridge, 2018c. p. 421-514.

ROSENTRATER, K. A.; EVERS, A. D. Feed and industrial uses for cereals. In: ROSENTRATER, K. A.; EVERS, A. D. (Eds.). **Kent's Technology of Cereals (Fifth Edition)**. Woodhead Publishing: Cambridge, 2018d. p. 785-837.

SABLANI, S. S.; RAMASWAMY, H. S. Physical and thermal properties of cereal grains. In: CHAKRAVERTY, A. et al. (Eds.). **Hanbook of Postharvest Technology**. Marcel Dekker, Inc.: New York, 2003. p. 17-40.

SAYAR, S.; WHITE, P. J. Oat Starch: Physiochemical Properties and Function. In:

WEBSTER, F. H.; WOOD, P. J. (Eds.). **Oats Chemistry and Technology**. 2nd ed. AACC International Press: St. Paul, 2011. p. 77-94.

SECKINGER, H. L.; WOLF, M. J. Sorghum protein ultrastructure as it relates to composition. **Cereal Chemistry**. v. 50, n. 4, p. 455-464, 1973.

SERNA-SALDIVAR, S. O. Cereal Grains. The Staff of Life. In: SERNA-SALDIVAR, S. O. (Ed.). **Cereal Grains. Properties, Processing, and Nutritional Attributes**. Food Preservation Technology Series. CRC Press: Boca Raton, 2010a. p. 1-42.

SERNA-SALDIVAR, S. O. Grain Development, Morphology, and Structure. In: SERNA-SALDIVAR, S. O. (Ed.). **Cereal Grains. Properties, Processing, and Nutritional Attributes**. Food Preservation Technology Series. CRC Press: Boca Raton, 2010b. p. 109-128.

SERNA-SALDIVAR, S. O.; ESPINOSA-RAMÍREZ, J. Grain Structure and Grain Chemical Composition. In: TAYLOR, J. R. N.; DUODU, K. G. (Eds.). **Sorghum and Millets: Chemistry, Technology and Nutritional Attributes**. 2nd ed. AACC International Press, 2019. p. 85-129.

SHASHIDHAR, M. G.; MURTHY, T. P. K.; GIRISH, K. G.; MANOHAR, B. Grinding of Coriander Seeds: Modeling of Particle Size Distribution and Energy Studies. **Particulate Science and Technology**. v. 31, n. 5, p. 449-457, 2013.

SHEWRY, P. R.; D'OVIDIO, R.; LAFIANDRA, D.; JENKINS, J. A.; MILLS, E. N. C.; BÉKÉS, F. Wheat Grain Proteins. In: KHAN, K.; SHEWRY, P. R. (Eds.). **Wheat: Chemistry and Technology**. AACC International Press: St. Paul, 2009. p. 223-298.

SHIBUYA, N.; NAKANE, R.; YASUI, A.; TANAKA, K.; IWASAKI, T. Comparative Studies on Cell Wall Preparations from Rice Bran, Germ and Endosperm. **Cereal Chemistry Journal**. v. 62, n. 4, p. 252-258, 1985.

SIMMONDS, D. H. The ultrastructure of the mature wheat endosperm. **Cereal Chemistry**. v. 49, n. 2, p. 212-222, 1972.

SINGH, R. P.; HELDMAN, D. R. Dehydration. In: SINGH, R. P.; HELDMAN, D. R. (Eds.). **Introduction to Food Engineering (Fifth Edition)**. Academic Press: San Diego, 2014a. p. 675-710.

SINGH, R. P.; HELDMAN, D. R. Psychrometrics. In: SINGH, R. P.; HELDMAN, D. R. (Eds.). **Introduction to Food Engineering (Fifth Edition)**. Academic Press: San Diego, 2014b. p. 593-616.

SMITH, O. B. Extrusion Cooking. In: ALTSCHUL, A. M. (Ed.). **New Protein Foods**. Academic Press, 1976. p. 86-121.

SRIKIATDEN, J.; ROBERTS, J. S. Moisture Transfer in Solid Food Materials: A Review of Mechanisms, Models, and Measurements. **International Journal of Food Properties**. v. 10, n. 4, p. 739-777, 2007.

STEEL, C. J.; LEORO, M. G. V.; SCHMIELE, M.; FERREIRA, R. E.; CHANG, Y. K. Thermoplastic Elastomers. In: EL-SONBATI, A. Z. (Ed.). **Thermoplastic Extrusion in Food Processing**. First ed. InTech: Rijeka, Croatia, 2012. p. 265-290.

STONE, B. A. Cell walls of cereal grains. **Cereal Foods World**. v. 51, n. 2, p. 62-65, 2006.

SUAREZ, C.; VIOLLAZ, P.; CHIRIFE, J. Diffusional analysis of air drying of grain sorghum. **International Journal of Food Science and Technology**. v. 15, n. 5, p. 523-531, 1980.

SUNDERLAND, R. Hot Air Dryers. In: LUSAS, E. W.; ROONEY, L. W. (Eds.). **Snack foods processing**. 1st ed. CRC Press: Boca Raton, 2001. p. 205-223.

VACCAREZZA, L. M.; LOMBARDI, J. L.; CHIRIFE, J. Heat transfer effects on drying rate of food dehydration. **The Canadian Journal of Chemical Engineering**. v. 52, n. 5, p. 576-579, 1974.

VELU, V.; NAGENDER, A.; PRABHAKARA RAO, P. G.; RAO, D. G. Dry milling characteristics of microwave dried maize grains (Zea mays L.). **Journal of Food Engineering**. v. 74, n. 1, p. 30-36, 2006.

WAGNER, J. R.; MOUNT, E. M.; GILES, H. F. Single Screw Extruder: Equipment. In: WAGNER, J. R.; MOUNT, E. M.; GILES, H. F. (Eds.). **Extrusion: The Definitive Processing Guide and Handbook**. 2nd ed. William Andrew Publishing: Oxford, 2014a. p. 17-46.

WAGNER, J. R.; MOUNT, E. M.; GILES, H. F. Twin Screw Extruder Equipment. In: WAGNER, J. R.; MOUNT, E. M.; GILES, H. F. (Eds.). **Extrusion: The Definitive Processing Guide and Handbook**. 2nd ed. William Andrew Publishing: Oxford, 2014b. p. 125-148.

WALL, J. S.; BLESSIN, C. W. Composition of sorghum plant and grain. In: WALL, J. S.; ROSS, W. M. (Eds.). **Sorghum Production and Utilization: Major Feed and Food Crops in Agriculture and Food Series**. Avi Publishing Company Inc.: Westport, 1970. p. 118-166.

WELCH, R. W. The chemical composition of oats. In: WELCH, R. W. (Ed.). **The Oat Crop: Production and Utilization**. Springer Netherlands: Dordrecht, 1995. p. 279-320.

WELCH, R. W. Nutrient Composition and Nutritional Quality
of Oats and Comparisons with Other Cereals. In: WEBSTER, F. H.; WOOD, P. J. (Eds.). **Oats Chemistry and Technology**. 2nd ed. AACC International Press: St. Paul, 2011. p. 95-107.

WRIGLEY, C.; BÉKÉS, F.; BUSHUK, W. Gluten: a balance of gliadin and glutenin. In: WRIGLEY, C.; BÉKÉS, F.; BUSHUK, W. (Eds.). **Gliadin and Glutenin: The Unique Balance of Wheat Quality**. AACC International Press: St Paul, 2006. p. 3-32.

YACU, W. A. Modeling a twing screw co-rotating extruder. **Journal of Food Process Engineering**. v. 8, n. 1, p. 1-21, 1985.

YANNIOTIS, S.; PETRAKI, A.; SOUMPASI, E. Effect of pectin and wheat fibers on quality attributes of extruded cornstarch. **Journal of Food Engineering**. v. 80, n. 2, p. 594-599, 2007.

ZWER, P. Oats: Grain-Quality Characteristics and Management of Quality Requirements. In: WRIGLEY, C.; BATEY, I.; MISKELLY, D. (Eds.). **Cereal Grains**. 2nd ed. Woodhead Publishing: Cambridge, 2017. p. 235-256.

Transition Chapter I to Chapter II

The overview of the structure of whole grains, drying of grains, grinder types, and the extrusion process, has allowed selecting suitable conditions of drying and grinding processes for the production of wholemeal particles and their subsequent extrusion process for the production of expanded extrudates. It was highlighted that single-screw extruders are quite used by the industrial sector, for being a low-cost and green technology.

Whole-grain cereals are promising raw materials for the production of nutritious extruded snacks due to their compounds associated with the outer layers and the germ: natural fibers, phytochemicals, proteins, and lipids. It is expected that differences in structure and composition between cereals reflect different behaviors during the drying and grinding processes.

Since 1996, the research group of the laboratory of food extrusion and physical properties located in the facilities of Embrapa Agroindústria de Alimentos (Rio de Janeiro, Brazil) has been working with thermoplastic extrusion technology in food applications. Based on this accumulated knowledge, extrusion cooking technology was used to produce whole-grain based extrudates that retain their quality attributes.

In that regard, the research was oriented on the physical characterization of wholemeal particles obtained from different cereal types, wherein the grains were previously dried up to moisture levels of 9 and 6% (wet basis), to increase the fractionation of the grain anatomical parts and obtain more homogeneous feed materials. It is important to understand the behavior of a feed material before exploring any extrusion processing parameter.

Therefore, in the next chapter, a series of physicochemical analyses (pasting properties, bulk density, particle density, interparticle porosity, and particle-size distribution) were performed to compare the flow properties of the wholemeal particles and identify the adequate feeding materials.

CHAPTER II

PHYSICOCHEMICAL PROPERTIES OF WHOLEMEAL CEREAL PARTICLES. EFFECT OF DRYING OF GRAINS

Physicochemical Properties of Wholemeal Cereal Particles. Effect of Drying of Grains

Jhony Willian Vargas-Solórzano [a] *, José Luis Ramírez Ascheri [b], Carlos Wanderlei Piler de Carvalho [b].

[a] Postgraduate Program in Food Science and Technology. Federal Rural University of Rio de Janeiro. Rodovia Br 465, km 7, CEP 23890-000, Seropédica, RJ – Brazil.
[b] Embrapa Agroindústria de Alimentos, Food Extrusion and Physical Properties Lab., Avenida das Américas 29501, Guaratiba, CEP 23020-470, Rio de Janeiro, RJ – Brazil.

* Corresponding author: jwvargass@ufrrj.br; vargasjw@gmail.com

ABSTRACT

Whole-grain cereal particles are granular solids composed of disintegrated tissues of endosperm, outer layers, and germ. The latter fractions become part of particle surfaces and affect the size, shape and chemical composition of the individual particles that structure a particulate food. The objective of this work was to evaluate the drying process effect at 60 °C of six whole-grain cereal (caryopses without a crease: rice, maize, and sorghum and caryopses with a crease: oats, rye, and wheat), on changes in the starch fraction of the kernels through their pasting properties, and changes in the morphology of the particles through their interparticle porosities and particle-size distributions. The grains were dried from an initial moisture content in the range of 11.5–13.8%, up to 9% and 6% (wet basis) and then roller milled at constant operating parameters. Maize was the grain hard to dry ($D_{eff} = 4.18 \times 10^{-10}$ m^2/s) and oats dried faster ($D_{eff} = 7.35 \times 10^{-10}$ m^2/s). The drying processing induced slight physical modifications to the starch fraction of all grains. Rye and sorghum were the most prone to undergo starch damage. The drying process could be used for inducing resistant starch formation by decreasing the gelatinization peak in the RVA viscosity profiles. The ground products from rye and oats presented the highest interparticle porosity. A reduction in grain moisture up to 6% decreased the interparticle porosity of rye from 77.4 to 72.8%, and for oats from 75.1 to 71.1%. Brown rice, sorghum, dried-maize, and dried-wheat presented particles with a unimodal distribution. Oats, rye, non-dried maize, and non-dried wheat presented particles with a bimodal distribution. The particle-size distribution span was shortened by previously drying the grains. Brown rice showed the narrowest particle-size distribution and rye the widest distribution. This work contributed to understanding the impact of the drying of cereal grains on the physical properties of the wholemeal particles derived from them. Few published works linked physical properties to extrudability of feed materials. In the present study, feed materials from grains dried up to 6% showed reduced D_{90} values. A less coarse fraction in the feed materials ensures acceptable flux of particles in the conveying section.

Keywords: Particulate food. Physical property. Drying. Milling.

1 INTRODUCTION

Cereal grains are monocotyledon starchy one-seeded fruits composed of three major anatomical parts: pericarp, germ, and endosperm, botanically named caryopses which are enveloped by a protective coat named hull or husk (SERNA-SALDIVAR, 2010a, b). This outer cover is a woody, siliceous, and non-edible material (CHAMPAGNE et al., 2004; MIR et al., 2019).

During threshing, the hull tightly remains attached to the caryopsis in rice (rough rice or paddy), and it is loosed in wheat, rye, maize, and sorghum. Brown rice is obtained by removing the hull with a dehulling machine. The low water activity and the enclosed cell wall compartments contribute to the equilibrium of the whole grain, preventing substrates and degrading enzymes from finding each other (DELCOUR; HOSENEY, 2010). When the pericarp layers are intact, they protect the grain against mold attack and oxidative and enzymatic deterioration (MIR et al., 2019).

Cereal milling operations as part of the production of refined products generate about 30% of by-products that are not directly used (SERNA-SALDIVAR, 2010a). The refined products vary according to the cereal type: polished or white rice; grits or dry-milled fractions of maize; pearled or kibbled grains of sorghum and wheat; refined flours of sorghum and wheat. Oats and rye usually are commercialized as whole roasted grains (groats) and roasted-grain flours. Cereals are processed by grinding using different types of mills based on rollers, hammer, disc, and stone (APRODU; BANU, 2017). In the roller milling process, the bran and germ are separated from the endosperm followed by gradual size reduction of the endosperm. Roller milling is more economical and flexible, produces less heat and thus less destruction to chemical components (LIU et al., 2015).

In a grinding process, grains are subjected to mechanical stress before the breakage. The stress is mostly stored as elastic energy (according to the type of mill) and is lost when grains fracture (BAUDELAIRE, 2013) giving rise to particles of different shapes. This process is dependent on the grain hardness and grain composition. Different cereal types have different nature of protein network medium that surround the starch granules in the grain endosperm, and different thickness and composition of cell walls of the amyloplasts that make up the endosperm. The endosperm is the largest part, where protein and starch are stored as reserve tissues (SERNA-SALDIVAR, 2010a). Thick endosperm cell walls are related to more arabinoxylan polymers, which have high water absorption capacity (DELCOUR; HOSENEY, 2010).

In the production of refined wheat flour, where the primary objective is to separate the pericarp, the grains are tempered to moistures around 15% to break the pericarp into coarse particles. On the other hand, in the production of flours based on whole grains, the objective is to break the pericarp into fine particles to obtain a more homogeneous particle-size distribution. Drying the grains up to 6% (wet basis) allows for greater breakage of the pericarp. Wholemeal flours intended for making extruded expanded products should display high interparticle porosity. The shape of the particles and therefore, their interparticle porosity is governed by the type of mill used. The porosity of the particles may also be influenced by the water content of the cereal grain before grinding. Wholemeal porous flours deliver more air into the extruder tube. Thus, pressure buildup during material compression will generate a higher pressure gradient at the outlet through the front die. High-pressure gradients between the inside and outside of the die extruder allow for ultrafast cooling with the consequent formation of expanded amorphous extrudates (WAGNER; MOUNT; GILES, 2014).

The present work aimed to characterize six wholemeal cereal particles. The grains were previously dried before grinding. The pasting properties of the starch fraction, the particle-size distribution, and the interparticle porosity of the wholemeal milled products were evaluated as a function of the grain moisture reduction.

2 MATERIALS AND METHODS

2.1 Cereal Grains

Whole grains of brown rice (light brown pericarp), hulled and stabilized oats, rye, and wheat were kindly donated by S.L. Alimentos (Mauá da Serra, PR, Brazil). Yellow maize grains (included its tip cap), was donated by Indústrias Granfino (Nova Iguaçú, RJ, Brazil). Sorghum cultivar BRS 310 (red pericarp, with low tannin) was supplied by Embrapa Maize and Sorghum (Sete Lagoas, MG, Brazil). Foreign materials, broken grains, and other types of grains were separated with a Clipper Office Tester 400/B (A.T. Ferrell Co., Bluffton, USA). The grains remained stored in a cold chamber (~7 °C) and where used in batches to perform the drying experiments and to obtain wholemeal cereal particles, according to Figure 1.
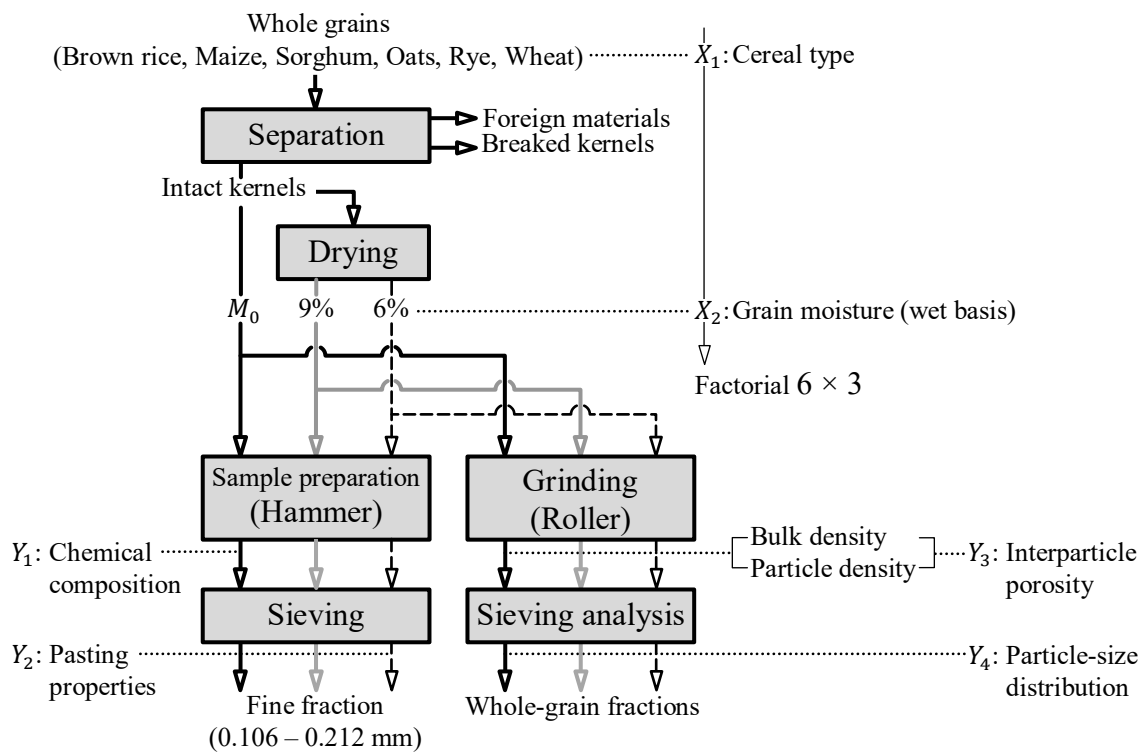
Figure 1. Drying pretreatment of whole-grain cereals before roller milling, linking the analysis performed in each step and the planned experiment. M_0: initial moisture, X_i: independent variables, Y_i: dependent variables.

2.2 Chemical Composition, Soluble Protein, and Minerals

Intact kernels of each cereal (Figure 2) were sampled, then size reduced in a hammer type mill (Lab Mill 3100, Perten Instruments AB, Huddinge, Sweden) without its screening plate (Figure 1). Then, the proximate composition of the powdered samples were analyzed in duplicate following the official methods of analysis of AOAC (2005): water content (method 925.09), ash content (method 923.03), total nitrogen (method 2001.11), total protein (using conversion factors (MOSSÉ, 1990): 5.17 for rice, 5.65 for maize and sorghum, 5.36 for oats and 5.33 for rye and wheat), lipids (method 945.38), and dietary fiber (method 985.29).

Figure 2. Intact kernels of whole-grain cereals used in the present studio. (A): Rice; (B) Maize; (C): Sorghum; (D): Oats; (E): Rye; (F): Wheat.

Starch was obtained by difference from the other sample components. The quantification of soluble protein was measured using the Bradford dye-binding method (BRADFORD, 1976). The mineralization of the dry ash residues was performed in a closed-vessel microwave digestion system, following the 999.10 method, item 9.1.08 (AOAC, 2005). The quantification of minerals (mg/Kg): sodium (Na), potassium (K), magnesium (Mg), calcium (Ca), manganese (Mn), iron (Fe), zinc (Zn), copper (Cu), phosphorus (P) and chromium (Cr) was performed by inductively coupled plasma-optical emission spectroscopy (ICP-OES), according to the 990.08 method, item 9.2.39 (AOAC, 2005).

2.3 Drying of Grains

Thin-layer drying experiments were performed in a drying oven with air circulation and renewal SL102 (SOLAB, São Paulo, Brazil) operated at 60.0 ± 0.5 °C of dry-bulb temperature, 1.0 ± 0.1 m/s of air velocity and $26 \pm 2\%$ of relative humidity. The temperatures and relative humidities of the ambient air and drying air were monitored by a Traceable® Hygrometer Thermometer Dew Point (Cole-Parmer, Vernon Hills, USA). The dry-bulb temperature and relative humidity of the ambient air were 29.7 ± 2.8 °C and $82.0 \pm 16.5\%$, respectively. Intact kernels of each cereal type were placed in a rectangular tray of $330 \times 360 \times 10$ mm. Then, the bed of grains was weighted at intervals of $30 - 40$ min to build drying curves.

The moisture content of grains was measured at the beginning and end of the drying experiments, by the 925.09 oven method (AOAC, 2005). The moisture content at intermediate drying stages was calculated from the initial moisture and the water evaporated during drying. The moisture content at the kernel surface in equilibrium with the surrounding drying air was assumed after a prolonged drying period (until to observe a no measurable weight loss) and was considered as the equilibrium moisture content.

2.4 Drying Time and Effective Moisture Diffusivity

Considering an immediate temperature equilibrium between the kernels and the drying chamber, the semi-empirical Page model given in equation (1) was used to predict the drying time to achieve grain moisture reductions to the levels of 9 and 6% (wet basis) (PARTI, 1993):

$$MR = \frac{M - M_e}{M_0 - M_e} = e^{-(k)t^N} \tag{1}$$

Where MR is the moisture ratio, M is the moisture at any time t during drying (in kg/kg dry solids), M_0 is the initial moisture content, M_e is the equilibrium moisture content, and k and N are drying rate constants, determined from the intercept and slope respectively, of the normalized drying curve. The Page model was selected because it computed the highest coefficient of determination (R^2) in comparison to other thin-layer drying models (ROBERTS; KIDD; PADILLA-ZAKOUR, 2008).

For air velocity streams ≥ 1 m/s, the Biot number for mass transfer is above 10, thus, the external resistances to mass transfer can be neglected (SRIKIATDEN; ROBERTS, 2007) and taking into account only the internal mass transfer resistances for long drying time, the first term of the series solution of the theoretical diffusion Fick model for an infinite-plate geometry given in equation (2) can be used to determine the effective moisture diffusivity (SINGH; HELDMAN, 2014):

$$MR = \frac{M - M_e}{M_0 - M_e} = \frac{8}{\pi^2} e^{-\left(\frac{\pi^2}{4l^2}D_{\text{eff}}\right)t} \tag{2}$$

Where D_{eff} is the effective moisture diffusivity (in m²/s), and l is the half-thickness of the slab with grains (in m). D_{eff} was determined from the slope of the normalized plot of $\ln(MR)$ vs time, in the interval of $MR = 0.1 - 0.6$ (ROBERTS; KIDD; PADILLA-ZAKOUR, 2008), according to the equation (3):

$$D_{eff} = -\frac{4l^2}{\pi^2}(\text{slope}) \tag{3}$$

2.5 Pasting Properties

Changes in the starch fraction by the drying process were verified through the pasting properties. Samples of grains non-exposed to drying and dried grains were size reduced in a hammer type Lab Mill 3100 without its screening plate (Figure 1). The powdered samples were sieved and particles of $106 - 212$ μm were used to prepare suspensions, by adding 3 g of sample (moisture content adjusted to 14%, wet basis) to 25 g of distilled water (CHEN, 2014). Viscosity profiles as a function of time-temperature were performed in a Rapid Visco Analyser (RVA) Series 4 (Newport Scientific, Warriewood, Australia), in duplicate. Stirring-time protocol was set according to standard procedures and a two-step heating protocol was set (BOUVIER; CAMPANELLA, 2014). From the viscosity curves, the following pasting characteristics were determined: pasting onset, trough viscosity, gelatinization peak, gelation peak, and breakdown viscosity.

2.6 Grinding of Grains

Grains from three moisture content (initial moisture, 9%, and 6%) were ground in a roller type mill (Quadrumat Junior, Brabender, Duisburg, Germany) without the sieving drum. Then, particle-size distribution by mass was performed to evaluate the drying effect. The characteristics of the four rollers assembled in the roller mill are presented in Table 1. They had identical diameter and height and corrugated surfaces that varied between $5 - 16$ striations per centimeter. The differential speed for the rollers 1 and 3 was maintained in 2.3:1 and for the rollers 2 and 4, in 1:1. The grinder worked without a screening plate and grains were fed at a feed rate of 7.9 kg/h (POSNER; HIBBS, 2005).

Table 1. Characteristics of the rollers assembled in the laboratory mill Quadrumat Junior.

Roller n°	Roller dimension (cm)		Striations/cm	Differential speed
	Diameter	Height		
1	7	3	5	2.3:1
2	7	3	10	1:1
3	7	3	16	2.3:1
4	7	3	15	1:1

2.7 Mass Flow Rate

Two hundred grams of each particulate sample was fed into the hopper of a single-screw volumetric feeder (Brabender, Duisburg, Germany). The screw speed was varied at three levels (10, 15 and 20 rpm) and particles were collected at the outlet for 1 min (YANNIOTIS; PETRAKI; SOUMPASI, 2007). Then, by linear interpolation, it was calculated the screw speed in the feeder that corresponds to a mass flow rate of 4 kg/h, for each particulate sample.

2.8 Bulk Density of Particles

The loose bulk density of particles (ρ_b) was determined as the non-compacted sample mass, freely poured in a container of known volume (ORTEGA-RIVAS, 2008). The bed of particles was obtained by placing a graduated cylinder with the top leveled to 50 cm^3 under the outlet of a single-screw volumetric feeder (Brabender, Duisburg, Germany) and then, dropping 50 g of sample at 4 kg/h.

2.9 Particle Density and Interparticle Porosity

The solid phase volume (which excludes all open and closed pores) and skeletal volume (which is the closed-pores) of individual particles that structure a particulate material were determined by the gas displacement method in a pycnometer system AccuPyc II 1340 (Micromeritics, Norcross, USA), using helium as displacement medium. Then, the sum of the volumes was used as the total volume of the particles to calculate the particle density. The interparticle porosity was estimated according to equation (4) (MAROUSIS; SARAVACOS, 1990; ORTEGA-RIVAS, 2008).

$$\nu = \left(1 - \frac{\rho_b}{\rho_p}\right) 100\% \tag{4}$$

ρ_b and ρ_p are the bulk and particle densities of the particulate material, respectively.

2.10 Particle-Size Distribution

A RO-TAP sieve shaker RX-29-10 (W.S. Tyler, Mentor, USA) and a set of stainless steel sieves with progressively smaller openings were used. Sieves were selected taking into account that segregation of particles must follow a log-normal distribution. A hundred grams of particulate material described in item 2.2.6 were segregated for 10 min. Particle-size distribution curves based on cumulative mass percentage were generated, from which the diameter (in μm) corresponding to 10%, 50%, and 90% finer were obtained (D_{10}, D_{50}, and D_{90}, respectively). The small particles size (fine, D_{10}), the large particles size (coarse, D_{90}), and the uniformity of the distribution were used to characterize the particle-size distributions. The uniformity of the distribution was calculated according to equation (5) (DODDS, 2013).

$$\text{Uniformity} = \frac{\sigma}{D_{av}} \tag{5}$$

D_{av} is the average particles size by mass and σ is the standard deviation and were calculated according to equations (6) and (7), respectively:

$$D_{av} = \frac{\sum m_i D_i}{\sum m_i} \tag{6}$$

$$\sigma = \sqrt{\frac{\sum m_i (D_i - D_{av})^2}{\sum m_i}} \tag{7}$$

m_i and D_i are the mass in class (in g) and the average class size (in μm), respectively.

2.11 Experimental Design and Data Analysis

A 6×3 factorial experiment replicated twice was conducted. The independent variables were X_1 = cereal type (brown rice, maize, sorghum, oats, rye, and wheat), and X_2 = moisture of grains before roller milling (6%, 9%, and initial moisture, wet basis). The impact of the studied factors was evaluated on the starch fraction (pasting properties) and the wholemeal particles (bulk density, particle density, interparticle porosity, and particle-size distribution).

Factorial ANOVA (analysis of variance) was performed on responses. The null hypothesis was rejected when the probability value (p-value) for the statistic F_0 was less than 5% of significance level (α). The total and partial sum of squares in the ANOVA were estimated according to the least-squares methodology (MONTGOMERY, 2013). The significance of each source in the ANOVA was performed according to the partial F test. To depict the impact of the factors on responses, the multiple range test of Tukey, with $\alpha = 0.05$, was included in the interaction plots.

The goodness of fit for each drying model was evaluated by minimizing the sum of squared deviations using non-linear regression analysis. A value of 0.1 for all parameters was set as initial conditions. The GRG Nonlinear method provided in the Solver add-in of Microsoft Excel was used as the solving method (LANG et al., 2009). The relative percent error also was computed as an indicator of the goodness of fit of a model. *PE* below 10% indicates a good fit (ROBERTS; KIDD; PADILLA-ZAKOUR, 2008).

3 RESULTS AND DISCUSSION

3.1 Chemical Composition, Soluble Protein, and Minerals

The proximate chemical composition and soluble protein of the whole-grain cereals are presented in Table 2. The macronutrients: dietary fiber, protein, and starch, varied according to the cereal type. The free-gluten cereals (brown rice, maize, and sorghum) presented the lowest content of dietary fiber (5.82 vs. 13.34%), protein (7.83 vs. 13.25%) and soluble protein (1.56 vs. 4.14%). Starch was high in this group of cereals (> 67% vs. < 61%) outstanding brown rice (> 74%). Among the cereals associated with gluten, the fiber content in the rye was almost two folds than the others, and total protein in oats and wheat were the highest. However, the soluble protein in the latter was lower than in rye. Despite rye is genetically related to wheat, it generally contains less starch and protein than wheat, but more dietary fiber (ARENDT; ZANNINI, 2013). The fat content varied widely among the studied cereals, outstanding oats, and maize. The proportions between starch, proteins, and lipids play an important role in the extrudability of feeding materials. A starch content greater than 60% is required to obtain extrudates with good expansion. Lipids act as plasticizers in the extrusion cooking processes. Levels between 0.5 to 1.0% protect starch granule degradation by the mechanical shearing action during a low moisture extrusion. Less degraded starch granules give a higher viscosity in the fluid melt. Above to 2-3%, lipids are smeared out on the biopolymers, decreasing the melt viscosity. Quantities < 3% have a low effect on the extrudate expansion at the die, while amounts over 5% result in rapid decreases of extrudate expansion (ILO; SCHOENLECHNER; BERGHOFE, 2000; ZASYPKIN et al., 1992). Proteins and amylose-rich starches also restrict expansion because these polymers are prone to form crosslinks, thus increasing the melt viscosity. At the die exit, the high extensibility of the continuous polymers matrix will produce extrudates with poor expansion and thick cell walls (ALLEN; CARPENTER; WALSH, 2007; DE MESA et al., 2009; ZASYPKIN et al., 1992).

Whole-grain oat is mainly appreciated by its advantageous macronutrient composition: lipids with total fatty acids composed of 40 and 36% of oleic and linoleic acids, respectively; proteins with a favorable composition of essential amino acids, and dietary fibers with a higher soluble fraction (roughly 40% of β-glucan) relative to other cereal grains (MENON et al., 2016; MULTARI et al., 2018). However, from an extrudability point of view, its high-fat content (> 5%) restricts the extrudate expansion. Brahma, Weier and Rose (2016), reported sectional expansion indexes of oat extrudates in the range of 1.25 to 2.69.

The caryopses without a crease presented the lowest content of ash (1.29 vs. 1.91%). Ashes represent the total mineral content and are mainly concentrated in the aleurone cells and the scutellar parenchyma of the cereal grain. Ash content is positively correlated with phenolic acids content of the bran and polyphenol oxidase activity. From this relationship, it is believed that this enzyme is located in the bran layer (HATCHER; KRUGER, 1997).

The mineral composition is presented in Table 3, where it is observed that potassium, magnesium and phosphorous, outstand in quantity. Much of the minerals, mainly sodium, potassium, magnesium, and calcium are found forming phytates (cationic salts of inositol hexaphosphoric acid) in the mature cereal grains (BECHTEL et al., 2009; MEERA; BHASHYAM; ALI, 2011; POSNER, 2009). The starch fraction of the cereals is associated with phosphorus, mainly in the form of phospholipids and phosphate monoesters. Phospholipids form water-insoluble complexes with amylose during heating (SRICHUWONG et al., 2005).

Table 2. Approximate chemical composition and soluble protein of six whole-grain cereal.

Cereal	Water g/100 g	Ash g/100 g	Total nitrogen g/kg	Total protein g/100 g	Fat g/100 g	Dietary fiber g/100 g	Starch g/100 g	Soluble protein g/100 g
Rice	12.55±0.08	1.60±0.33	12.65±0.01 [a]	6.54±0.04	1.27±0.08	2.58±0.10	74.73±0.47	1.14±0.04
Maize	11.53±0.01	1.11±0.01	12.70±0.00	7.18±0.00	4.26±0.13	7.81±0.08	67.99±0.21	1.82±0.07
Sorghum	11.37±0.04	1.16±0.01	15.50±0.01	8.76±0.08	3.49±0.10	7.06±0.13	68.02±0.08	1.72±0.08
Oats	10.31±0.04	1.98±0.01	24.50±0.01	13.13±0.08	5.19±0.19	10.37±0.17	58.07±0.42	3.19±0.37
Rye	10.82±0.05	1.97±0.00	20.85±0.02	11.11±0.12	1.72±0.09	18.55±0.09	54.97±0.17	5.41±0.12
Wheat	10.81±0.07	1.77±0.00	23.80±0.01	12.69±0.08	1.90±0.05	11.37±0.08	60.47±0.29	3.83±0.02

[a] Mean ± standard deviations of duplicate measurements.

Table 3. Mineral composition of six whole-grain cereal.

Cereal	Sodium mg/kg	Potassium mg/kg	Magnesium mg/kg	Calcium mg/kg	Manganese mg/kg	Iron mg/kg	Zinc mg/kg	Cooper mg/kg	Phosphorus mg/kg
Rice	2.37±0.07	210.96±0.19	108.68±1.65	5.76±0.12 [a]	2.28±0.06	1.12±0.09	1.83±0.00	0.33±0.00	278.24±7.94
Maize	1.95±0.15	294.98±2.81	81.15±1.13	1.77±0.17	0.39±0.01	1.81±0.02	1.85±0.04	0.18±0.00	215.58±1.72
Sorghum	2.36±0.15	282.72±5.87	117.78±1.19	10.70±0.08	1.53±0.02	6.67±0.08	1.50±0.00	0.27±0.00	236.64±2.25
Oats	2.79±0.11	395.53±20.45	148.94±9.61	56.82±4.19	6.54±0.48	4.65±0.30	3.04±0.18	0.50±0.03	484.05±32.96
Rye	2.52±0.08	520.28±10.65	121.44±1.25	36.69±1.71	2.71±0.07	3.92±0.04	2.90±0.04	0.50±0.01	387.18±11.64
Wheat	2.66±0.04	363.04±6.21	135.83±4.16	31.76±0.97	4.45±0.09	5.35±0.22	3.60±0.06	0.52±0.01	352.69±7.25

[a] Mean ± standard deviations of duplicate measurements.

3.2 Drying Time and Effective Moisture Diffusivity

The drying curves for the whole-grain cereals studied are displayed in Figure 3, wherein it is observed a typical case of moisture loss in the diffusive drying region. In Table 4 it is summarized the initial moisture content (M_0), the moisture at the set levels, the equilibrium moisture (M_e), and the drying time prediction to reach the set moisture levels. The initial moisture of the grains was below the critical moisture content (M_c). For various cereal grains, M_c in terms of mold attack lies around 14% (POMERANZ; ZELENY, 1971). M_0 influences the initial drying rate and thus, the drying time. A higher M_0 promotes a greater concentration gradient and thus, a higher driving force for mass transport would result (NGUYEN; PRICE, 2007). M_0 was similar for brown rice, oats, and wheat ($p \geq 0.05$). Maize presented the lowest (11.51%) and rye the highest (13.80%). These differences affected the initial drying rate to a lesser extent. Conversely, the size and shape of the grain and the differences in structure and chemical composition between grains influenced the drying rates to a greater extent according to the cereal type. The endosperm structure, the permeability of the aleurone and outer layers, and the extent of damage to these layers influence the moisture migration from various parts of the interior to the surface of the kernel (BALA, 2017a).

M_e was different in all grains ($p < 0.05$). This could be attributed to the degree with which water molecules are physically and/or chemically bound to starch and protein polymers in the endosperm matrix (BARBOSA-CÁNOVAS; VEGA-MERCADO, 1996). Water in this state is part of the bound moisture, which exerts less equilibrium vapor pressure than that of the pure water at the same temperature. The bound moisture is also contained in the endosperm cell walls, in loose chemical combination with the cellulosic material (CHAKRAVERTY; SINGH, 2014).

The semi-empirical drying rate constants of the Page model for each cereal type are given in Table 5. For all models, the coefficient of determination (R^2) was above 0.99 and the relative percent error (PE) ranged between 0.67% and 2.04%. A PE below 10% provides models with good predictions. The k value can be associated inversely with the endosperm hardness. In the drying of three grape seed varieties, higher k values were found for the "*Cab Franc*" variety. This was attributed to the fact that these seeds were softened by a fermentation process (ROBERTS; KIDD; PADILLA-ZAKOUR, 2008). Thus, maize was the grain hard to dry ($k = 5.54 \times 10^{-3}$ 1/min), reaching the highest drying period to set the moisture level to 6% (14.68 ± 0.93 h). On the other hand, oats grain dried faster ($k = 11.53 \times 10^{-3}$ 1/min) than the other grains studied (3.12 ± 0.03 h). The drying rate also is interpreted in terms of differences in the effective moisture diffusivity (D_{eff}) between grains, summarized in Table 5. Maize had the lowest D_{eff} value (4.18×10^{-10} m²/s), whereas oats presented the highest (7.35×10^{-10} m²/s). The moisture movement from the core to the surface of grain occurs in a liquid and/or vapor state(BALA, 2017b). To reach to the grain surface, moisture must cross the outer layers of the grain. Differences in the pericarp thickness among cereals and within an individual kernel could explain in part these variations in the drying rate curves.
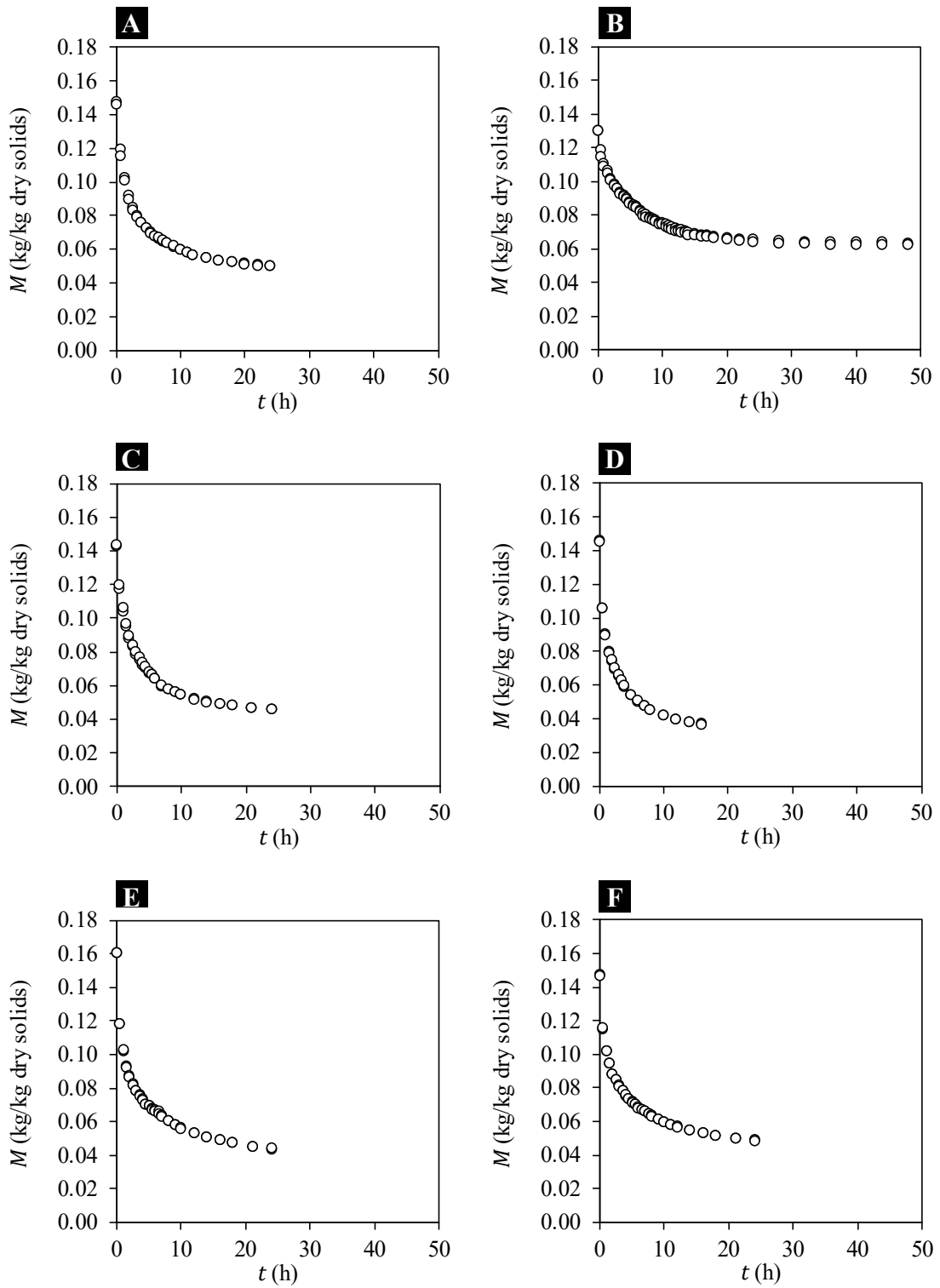
Figure 3. Drying curves of whole-grain cereals in a convective drying oven at 60 °C. M: moisture content (dry basis). t: drying time.

Table 4. Initial moisture, moisture at the set levels, equilibrium moisture, and drying time prediction of six whole-grain cereal.

Cereal	Initial moisture M_0 (%, wb)	1st moisture level M_9 (%, wb)	Time to reach t_9 (h)	t_6 (h)	2nd moisture level M_6 (%, wb)	Equilibrium moisture M_e (%, wb)
Brown rice	12.78 ± 0.08 [b]	9.29 ± 0.10 [ab]	1.47 ± 0.10 [b]	7.24 ± 0.05 [b]	6.32 ± 0.05 [b]	4.73 ± 0.03 [b]
Maize	11.51 ± 0.03 [d]	9.36 ± 0.08 [a]	2.42 ± 0.14 [a]	15.25 ± 1.72 [a]	6.57 ± 0.09 [a]	5.92 ± 0.05 [a]
Sorghum	12.48 ± 0.03 [c]	9.32 ± 0.07 [ab]	1.32 ± 0.09 [b]	5.83 ± 0.09 [b]	6.08 ± 0.04 [cd]	4.35 ± 0.02 [d]
Oats	12.66 ± 0.04 [b]	8.92 ± 0.03 [c]	0.70 ± 0.01 [c]	3.05 ± 0.02 [c]	5.95 ± 0.04 [d]	3.52 ± 0.02 [f]
Rye	13.80 ± 0.03 [a]	9.04 ± 0.03 [bc]	1.50 ± 0.71 [b]	6.13 ± 0.14 [b]	6.23 ± 0.02 [bc]	4.17 ± 0.02 [e]
Wheat	12.78 ± 0.01 [b]	9.09 ± 0.08 [abc]	1.22 ± 0.00 [b]	7.30 ± 0.10 [b]	6.15 ± 0.06 [bcd]	4.59 ± 0.02 [c]

M: moisture content in wet basis. t: drying time. Subscripts 9 and 6 refer to set moisture levels at 9% and 6%. Values with different lowercase letters in a same column, differ from each other according to the Tukey test.

Table 5. Effective diffusivities, semi-empirical constants, and model prediction evaluation of the Page model for the six whole-grain cereal.

Cereal	Page equation k (1/min) × 10⁻³	N	R^2	PE	Effective moisture diffusivity D_{eff} (m²/s) × 10⁻¹⁰	R^2
Brown rice	8.73 ± 0.31 [c]	0.656 ± 0.029 [bc]	0.9979	1.22	5.11 ± 0.24 [c]	0.9803
Maize	5.54 ± 0.07 [d]	0.716 ± 0.012 [a]	0.9976	0.98	4.18 ± 0.07 [d]	0.9971
Sorghum	8.22 ± 0.38 [c]	0.691 ± 0.018 [ab]	0.9994	0.67	6.02 ± 0.10 [b]	0.9953
Oats	11.53 ± 0.07 [a]	0.619 ± 0.005 [cd]	0.9981	2.04	7.35 ± 0.27 [a]	0.9960
Rye	11.24 ± 0.15 [a]	0.526 ± 0.003 [e]	0.9970	1.95	4.56 ± 0.06 [cd]	0.9809
Wheat	9.84 ± 0.06 [b]	0.571 ± 0.003 [de]	0.9981	1.21	4.73 ± 0.01 [c]	0.9890

R^2: coefficient of determination. k and N: drying constants. PE: relative percent error. Values with different lowercase letters in a same column, differ from each other according to the Tukey test.

3.3 Pasting Properties

The changes in viscosity of whole-grain cereal suspensions as a function of time and temperature are displayed in Figure 4. The viscosity profile of wheat was the only curve with high noise in the viscosity record (Figure 4F). This can be attributed to the fibers deposited in the bran particles with sizes in the range of 0.106 to 0.212 mm, which perform a cutting action when the starch swelling process starts. The drying process did not affect the pasting onset in rice, maize, and oats ($p \geq 0.05$), but did it in the dried sorghum (Figure 4C). The drying process did not affect the trough viscosity on rice and maize ($p \geq 0.05$). However, in sorghum, oats, and rye, the trough viscosity decreased (Figure 4C, D, E). No starch swelling events were observed at the holding times of 25 °C and 60 °C for brown rice, maize, sorghum, and oats. These observations rule out the possibility of any cold solubilization and starch conversion by heat transfer effect in prolonged drying periods. Moreover, in the rye, this behavior was marked in both holding temperatures. There was observed a slight increment of viscosity before onset time during pasting formation of sorghum. This event can be associated with the presence of broken or damaged starches in the sorghum slurry (BOUVIER; CAMPANELLA, 2014).

3.4 Bulk Density

Individual particles of wholemeal cereals are porous solids with irregular shapes and voids between them usually containing open pores (cracks, flaws, hollows), and closed pores (BARBOSA-CÁNOVAS et al., 2005). Besides, the moisture content can affect the number of interparticle contact points structuring a bed of particles, by altering the interaction forces between particles close to one another, thereby affecting its bulk volume (BARBOSA-CÁNOVAS; JULIANO, 2005).

The volume of particles including the solid and liquid phase, the open and closed pores, and the voids between particles was used to compute the bulk density of wholemeal cereals, which varied from 320 to 488 kg/m^3 (Figure 5). Variations in bulk density of brown rice (478 $\pm$ 8 kg/m^3), maize (444 $\pm$ 9 kg/m^3) and sorghum (422 $\pm$ 5 kg/m^3) were negligible with changes in grain moisture in the studied range ($p \geq 0.05$). Rye particles from non-dried grains yielded the lowest bulk density (323 $\pm$ 4 kg/m^3, $p < 0.05$). Bulk density in the group of caryopses with a crease (oats, rye, and wheat) increased as grain moisture was reduced, which was more noticeable in the rye ($p < 0.05$). Oats bulk density increased only when grain moisture was reduced to 6% and for wheat, it was necessary to reduce the grain moisture to just 9% ($p < 0.05$).
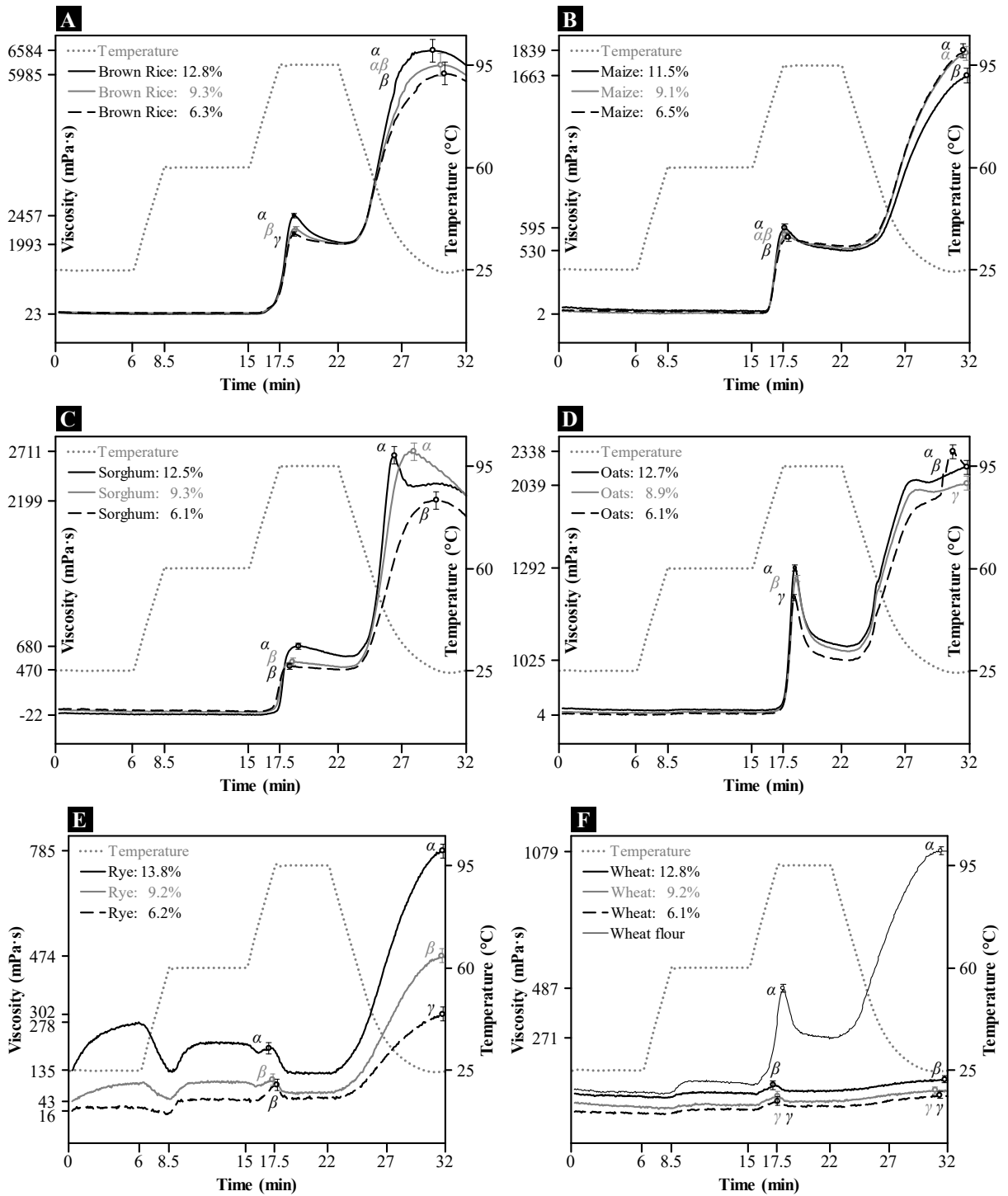
Figure 4. Effect of the drying processing on paste viscosity profiles of suspensions of whole-grain cereals. (A): Rice; (B) Maize; (C): Sorghum; (D): Oats; (E): Rye; (F): Wheat.
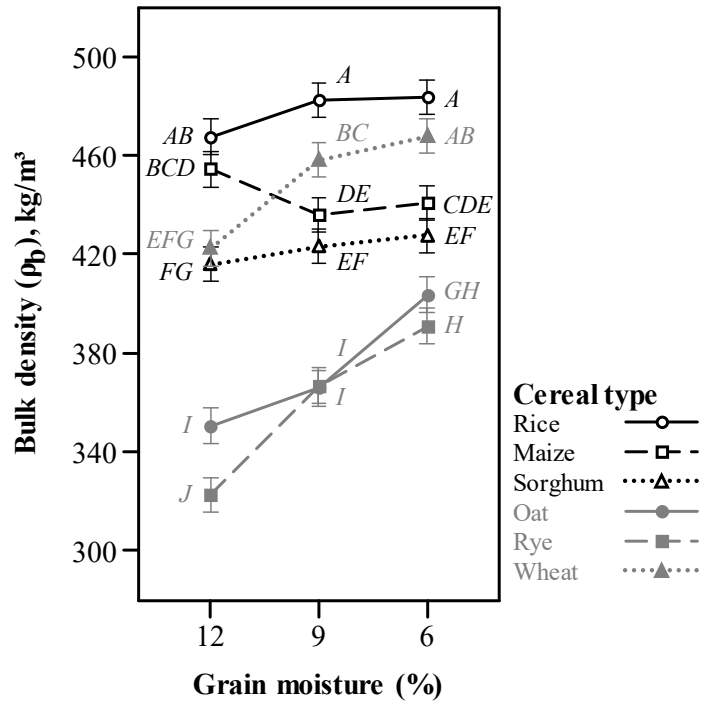
Figure 5. Drying processing effect on the bulk density of wholemeal cereals.

Differences in bulk density of wholemeal cereals can be attributed to the composition and structure of bran layers and subaleurone region in each cereal type. These anatomical parts differ in relative toughness and friability, giving different breakage patterns during the roller milling (FISTES; TANOVIC, 2007). According to the degree of arabinoxylan cross-linking in cell walls, and the intrinsic properties of the walls, these anatomical parts are reduced in flat fragments (PEYRON et al., 2002) or can remain attached to the particle surfaces, thereby affecting shape and size of particles, and consequently the bulk volume. As grains were dried, friability of bran layers and subaleurone cell wall regions were increased, which in turn during the grinding process were generated more fine particles. Fine particles are packed more efficiently, reducing interparticle spaces and thus, increasing bulk density.

3.5 Particle Density

The volume of particles excluding the open pores but including the closed pores was used to compute the particle density of wholemeal cereals (LOZANO; ROTSTEIN; URBICAIN, 1980), which varied from 1394 to 1468 kg/m^3 (Figure 6). The particle density of brown rice (1462 ± 4 kg/m^3) and sorghum (1422 ± 2 kg/m^3) was similar to changes in grain moisture in the explored range ($p \geq 0.05$). Oats particles from dried grains yielded the lowest particle densities (1396 ± 1 kg/m^3, $p < 0.05$). Maize particle density decreased and wheat particle density increased, only when grain moisture was reduced to 6% ($p < 0.05$). Rye particle density was higher at 9% grain moisture.
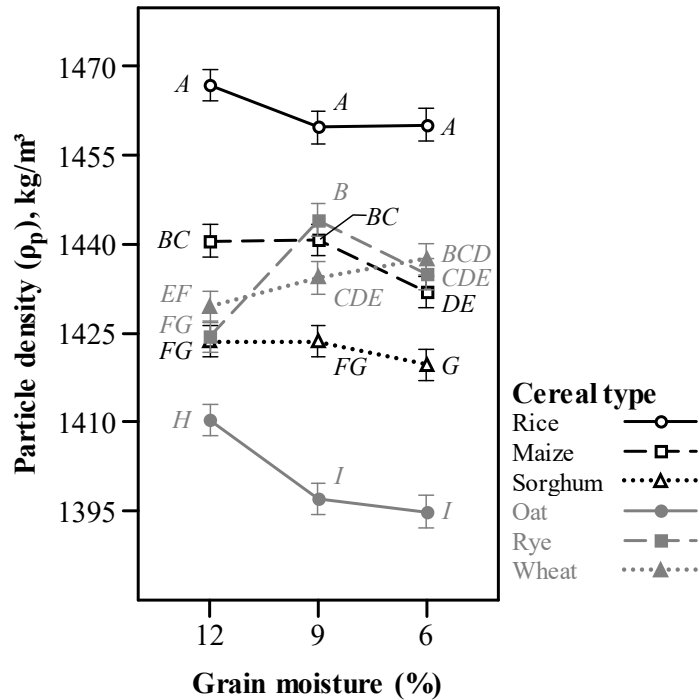
Figure 6. Drying processing effect on particle density of wholemeal cereals.

Differences in particle density of wholemeal cereals, mainly between brown rice and oat groats can be attributed to the composition and degree of closed pores present in the particles. The compound starch granules in brown rice are polygonal aggregates tightly packed (20 – 60 polygonal granules), whereas in oats groats they are spherical structures (possibly 80 or more granules) with individual free granules present in the spaces among the aggregates (ROSENTRATER; EVERS, 2018a). This latter characteristic in oats groats would be contributing to increase closed pores within the oats particles and consequently to decrease particle density.

3.6 Interparticle Porosity

A particulate food based on ground whole-grain cereal is an assembly of particles in which the void spaces between the particles are surrounded by air and partially filled with water. A food structured by discrete particles can be considered as a three-phase system: solid-water-air. Interparticle porosity of different wholemeal products obtained with a roller mill, varied between 66.6% and 77.5% (Figure 7). As in the case of bulk density, variations in interparticle porosity of brown rice (67.3 ± 0.7 %), maize (69.1 ± 0.6 %) and sorghum (70.3 ± 0.4 %) was negligible with changes in grain moisture in the studied range ($p \geq 0.05$).

Rye particles from non-dried grains yielded the highest interparticle porosity (77.4 ± 0.3 %, $p < 0.05$). Bulk porosity in the group of caryopses with a crease decreased as grain moisture was reduced, which was more noticeable in the rye ($p < 0.05$). Oats interparticle porosity decreased only when grain moisture was reduced to 6% and for wheat, it was necessary to reduce the grain moisture to just 9% ($p < 0.05$).

This can be attributed to the degree with which the outer layers, the aleurone layer, and the cell walls of the subaleurone region are disintegrated during the grinding process and become part of the surface of the particles. In rye, the endosperm cell walls are thicker than those of wheat, especially in the subaleurone region (PARKER, 1981).
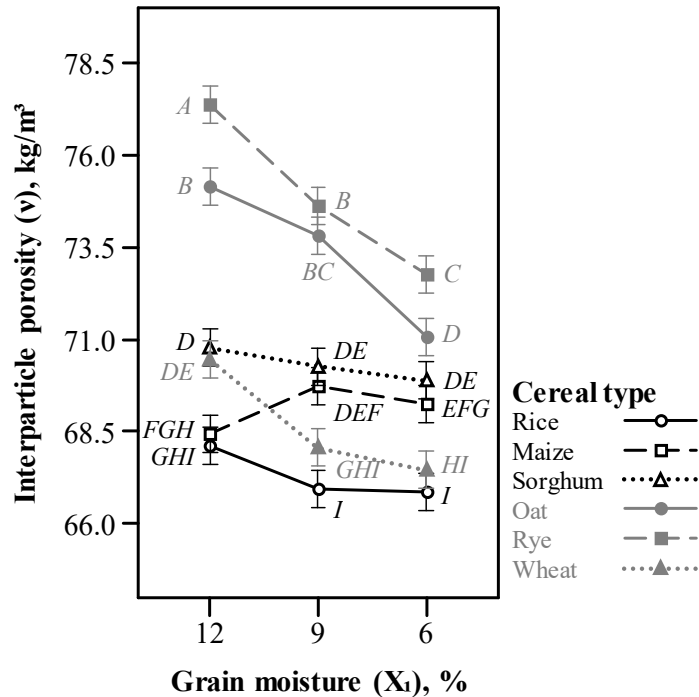
Figure 7. Drying processing effect on interparticle porosity of wholemeal cereals.

Differences in endosperm cell wall composition can also explain this variability in the interparticle porosity of wholemeal cereals. Oats is rich in β-D-glucans while rye and wheat, in arabinoxylans (GLITSØ; BACH KNUDSEN, 1999; ROSENTRATER; EVERS, 2018b). A decrease in the interparticle porosity of rye and oats by the drying effect can be associated with a decrease in the tissue-adhesive forces that structure the pericarp layers and the intricate network of endosperm cell walls (HOURSTON et al., 2017). Thus, these grains became more brittle and their smaller size particles resulting from the grinding process were less bulky.

3.7 Particle-Size Distribution

In roller mills, sequential rotating wheels allow progressive size reduction of the grains in the mating surfaces. The particles are subjected to successive compressions on corrugated surfaces of the rolls and other particles. The process of grinding with roller mill increases the surface area of particles and homogeneity of particle size (coefficient of uniformity close to 1) when comparing to the process with disc mill. These characteristics improve blend homogeneity and dissolution of particles in a suspension (HICKEY; GIOVAGNOLI, 2018).

The sieving analysis results and frequency distribution curves by mass were summarized in **Annexes A–C**. Regardless of the drying conditions of the grains, brown rice and sorghum had unimodal distributions, in the range of 63–500 μm and 90–1000 μm respectively, whereas oats and rye presented bimodal distributions, in the range of 75–2830 μm. A bimodal distribution was also observed in wheat and maize particles from grains that were not previously dried before milling (non-dried grains). From the undersize cumulative distribution curves (Figure 8–10), it was extracted the following particle-size parameters (**Annexes A–C**): the fine particles fraction (D_{10}), the coarse particles fraction (D_{90}), and the coefficient of uniformity of the distribution (Un).

The undersize cumulative distribution curves for rice and oats are shown in Figure 8. Oat wholemeal particles presented bimodal distributions at ~ 1000 and 200 μm. The coarse fraction (~ 1000 μm) decreased as a function of the moisture reduction. The fine fraction (~ 200
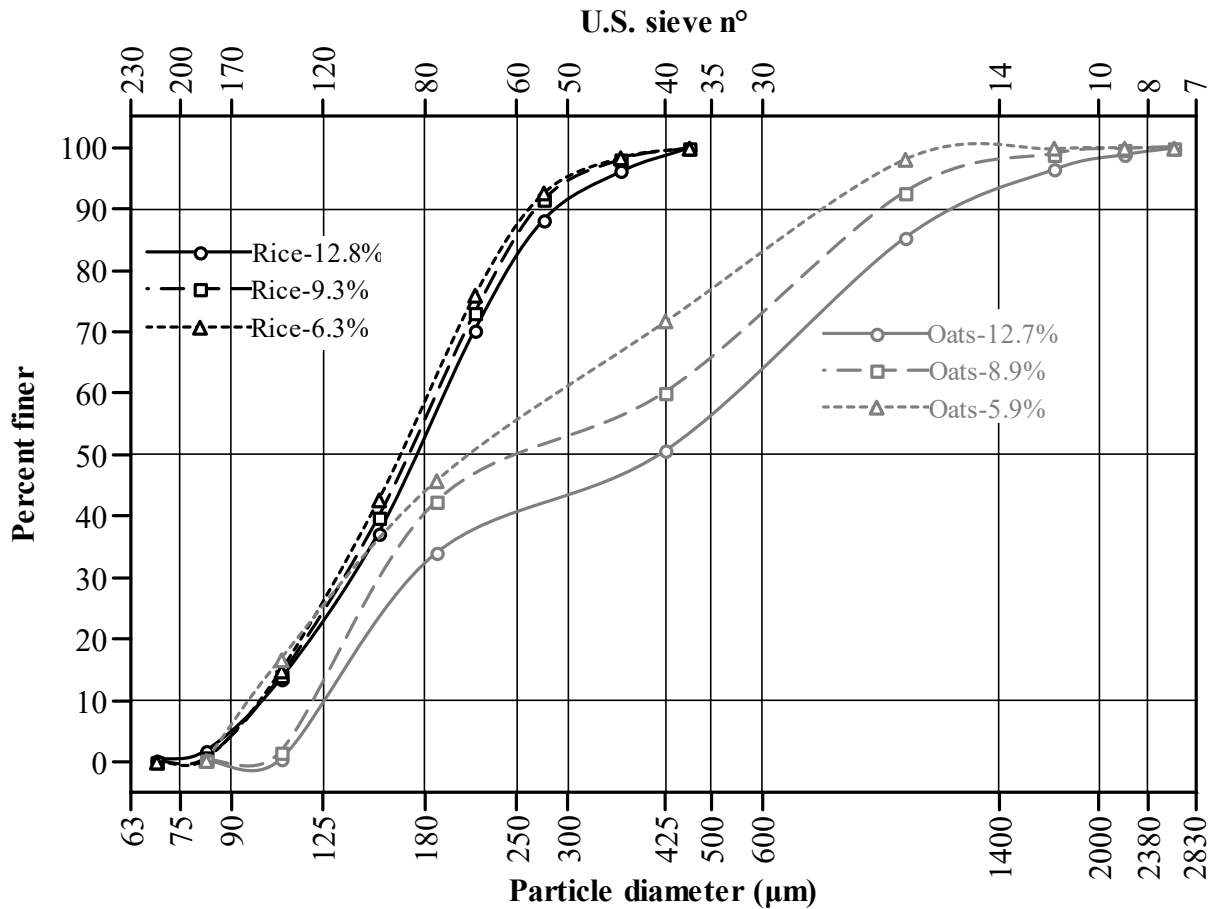
Figure 8. Undersize cumulative distribution curve for rice and oats.

μm) increased with a change in grain moisture from initial moisture to 9%. However, this fine fraction decreased with a further change in grain moisture from 9 to 6%. As drying progressed, the modes were kept at ~ 1000 and 200 μm. Rice wholemeal particles presented a unimodal distribution at ~ 200 μm. The drying process did not affect the content of this fine fraction. Oat particles presented wider distributions than sorghum particles.

As drying progressed, D_{90} decreased significantly and to a greater extent in oats (from 1287 to 823 μm) than in brown rice (from 294 to 266 μm). Reduction in D_{10} values was more noticeable in dried oats up to 6% moisture content. For brown rice, D_{10} did not change as a function of grain moisture reduction.

Endosperm particles represent almost all of the whole-grain based granular material. Compound starch granules present in rice and oats endosperm, contribute to the fine particles fraction of the wholemeal ground product. Endosperm oat also is composed of simple bimodal starch granules. The bimodal type contains large (A-type) and small (B-type) simple starch granules that coexist in the same cells (MATSUSHIMA, 2015). Both, the A and B starch granules in oats endosperm contributed to structuring coarse (~ 1000 μm) and fine (~ 190 μm) wholemeal particles, as observed in Figure 8. These two populations of particle-size decreased (more percent finer) as drying progressed.

The undersize cumulative distribution curves for maize and sorghum are shown in Figure 9. Maize wholemeal particles from non-dried grains presented a bimodal distribution at ~ 400 and 200 μm. Maize presented distributions slightly wider than sorghum. The curves for both types of cereal overlapped as drying progressed. In maize, the coarse fraction (~ 400 μm) decreased and the fine fraction (~ 200 μm) increased as a function of the moisture reduction.

Sorghum
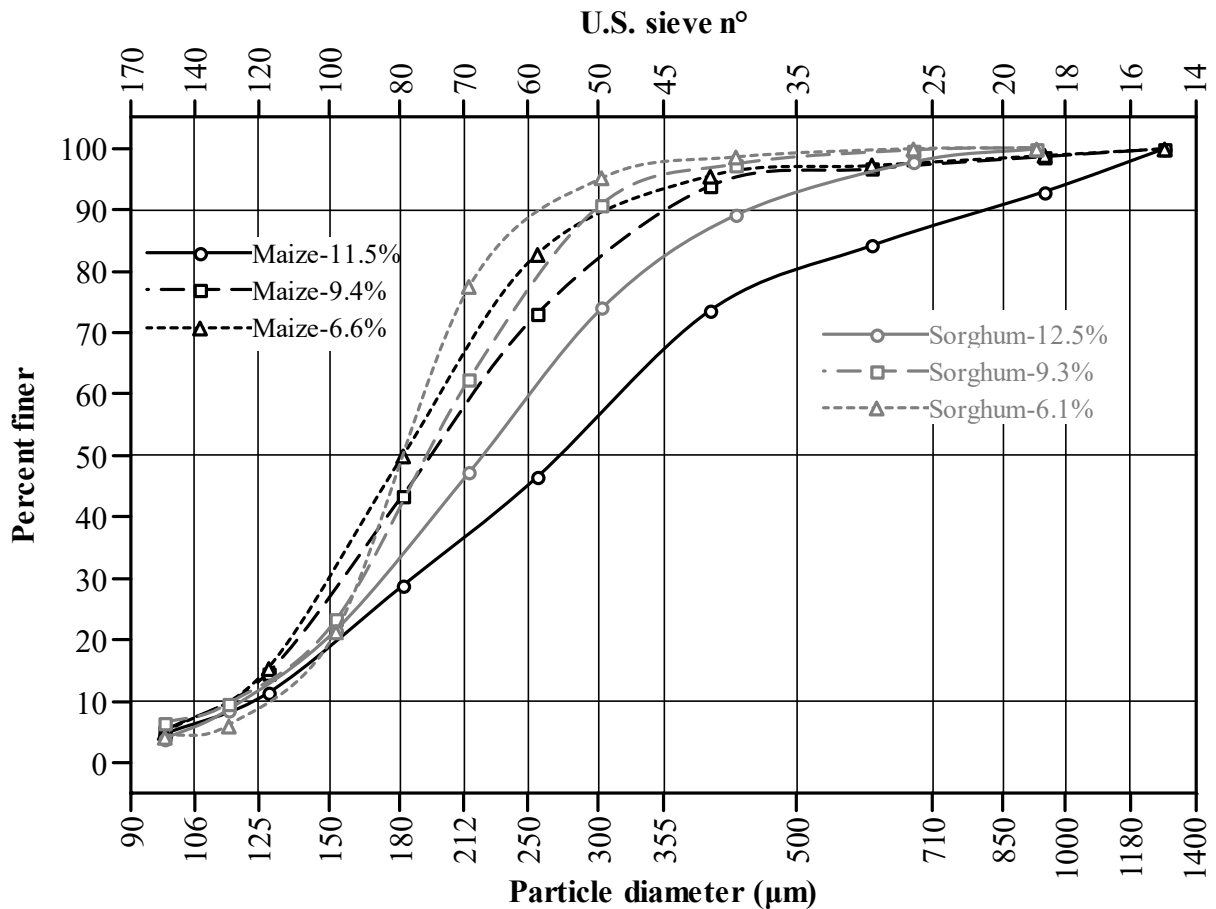
Figure 9. Undersize cumulative distribution curve for maize and sorghum.

wholemeal particles from non-dried grains presented a unimodal distribution of fine particles at ~ 260 μm. This fraction sharply increased as drying progressed while the mode was slightly reduced to ~ 220 μm. As drying progressed, D_{90} decreased significantly and to a greater extent in maize (from 830 to 337 μm) than in sorghum (from 449 to 270 μm). The drying process had a little effect on D_{10} values, which ranged from 113 to 128 μm for both types of cereal and irrespective of the moisture level reduction.

The undersize cumulative distribution curves for rye and wheat are shown in Figure 10. Wheat wholemeal particles from non-dried grains presented a bimodal distribution at ~ 1125 and 180 μm. The coarse fraction (~ 1125 μm) decreased and the fine fraction (~ 170 μm) increased as a function of the moisture reduction. The distribution of wheat particles from dried grains changed to unimodal distributions, with no reductions in the mode. Rye wholemeal particles presented a bimodal distribution of coarse particles at ~ 1000 μm and fine particles at ~ 275 μm. These fractions sharply decreased and increased respectively, as drying progressed while the mode was kept. As drying progressed, D_{90} decreased significantly and to a greater extent in the rye (from 1161 to 515 μm) than in wheat (from 685 to 368 μm).
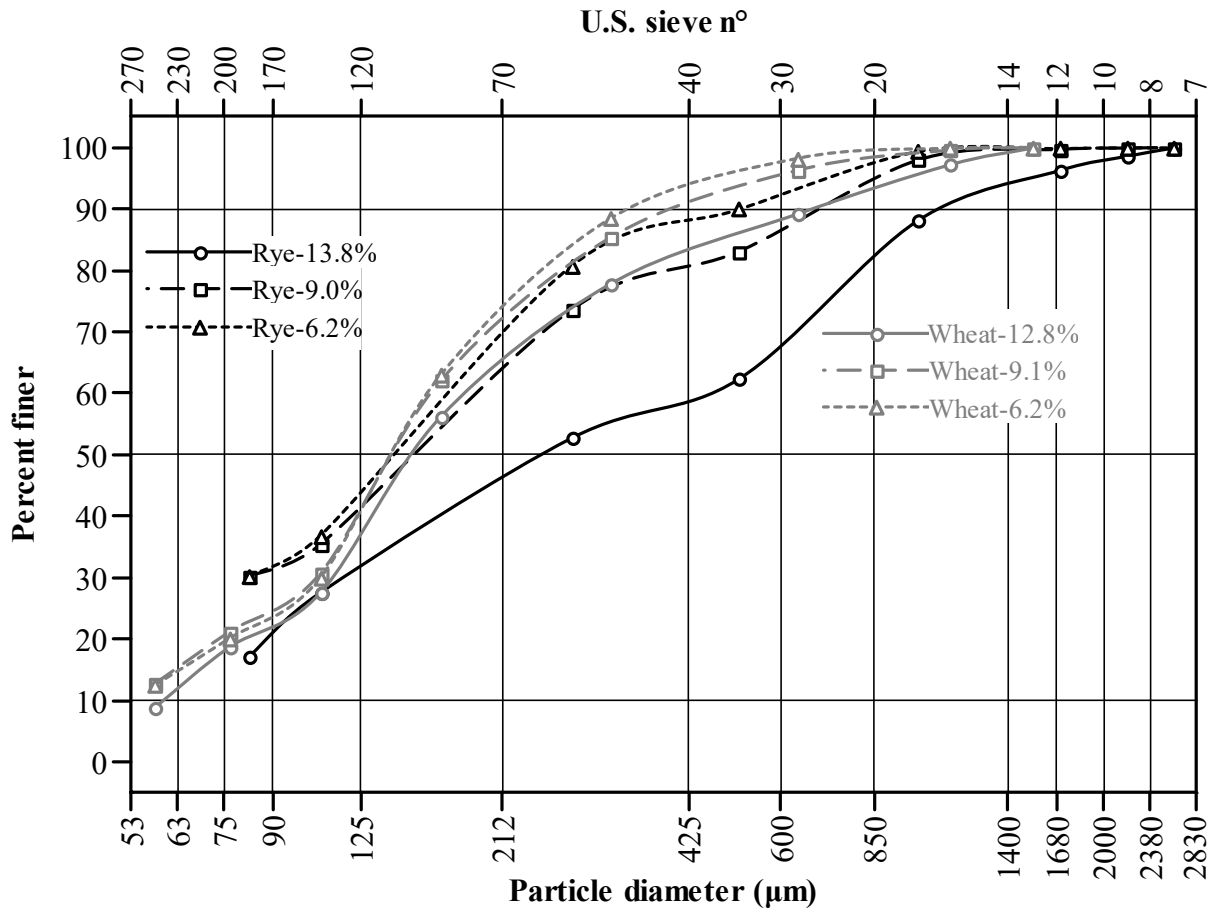
Figure 10. Undersize cumulative distribution curve for rye and wheat.

These differences in the particle-size distribution between cereals can be attributed to the structure and composition of the starchy endosperm, which during the grinding process it is disintegrated and becomes most of the particles. The starchy endosperm in the rye is softer than that of hard and soft wheat, and its floury content is readily released after grinding (ARENDT; ZANNINI, 2013). Maize and sorghum present corneous endosperm that confers these grains hard mechanical and translucent optical properties (MORA; MILÁN; MILÁN, 2019). And more than 53% of the lipids in oats is located in its endosperm (MILLER; FULCHER, 2011). All these characteristics influenced the particle-size distributions.

4 CONCLUSION

The effect of drying at 60 °C on six whole-grain cereal was evaluated. Maize was the grain hard to dry (D_{eff} = 4.18 × 10^{-10} m^2/s) and it was necessary a drying period of 14.68 ± 0.93 h to reach 6% moisture content. Oats dried faster (D_{eff} = 7.35 × 10^{-10} m^2/s) and took only 3.12 ± 0.03 h to reach 6% moisture content. The drying process did not affect the trough viscosity on rice and maize, but in sorghum, oats, and rye, the trough viscosity decreased. Only rye suspensions presented solubilization and/or water absorption at the holding temperatures of 25 and 60 °C. The drying processing decreased the gelatinization peak of the starch fraction in all cereals, being markedly noticeable in brown rice and oats. As drying progressed, the gelation peak decreased in brown rice, sorghum, and rye. In maize and dried-oats up to 6%, the gelation peaks increased. These results evidenced that hot air drying induced slight physical modifications to the starch fraction of the grains, being rye and sorghum prone to undergo starch damage. Since decrements in the gelatinization peak are associated with more amylose content, the drying process could be used for inducing resistant starch formation. The porosity of wholemeal particles varied according to the cereal type. Rice had the lowest values, whereas rye presented the highest. The drying process significantly decreased the interparticle porosity of wholemeal particles from rye, oats, and wheat. The drying effect did not change the interparticle porosity in the other cereals. Brown rice, sorghum, dried-maize, and dried-wheat presented particles with a unimodal distribution. Oats, rye, non-dried maize, and non-dried wheat presented particles with a bimodal distribution. Brown rice showed the narrowest particle-size distribution and rye the wider. From an extrudability point of view, feed materials should present high homogeneity in the particles to ensure an acceptable flux of particles in the conveying section of the screw. The flux of particles was improved when grains were dried up to 6% moisture content due to reductions in D_{90} values.

REFERENCES

ALLEN, K. E.; CARPENTER, C. E.; WALSH, M. K. Influence of protein level and starch type on an extrusion-expanded whey product. **International Journal of Food Science and Technology**. v. 42, n. 8, p. 953-960, 2007.

AOAC. **Official Methods of Analysis of AOAC International**. 18th ed. AOAC International: Gaithersburg, 2005.

APRODU, I.; BANU, I. Milling, functional and thermo-mechanical properties of wheat, rye, triticale, barley and oat. **Journal of Cereal Science**. v. 77, p. 42-48, 2017.

ARENDT, E. K.; ZANNINI, E. Rye. In: ARENDT, E. K.; ZANNINI, E. (Eds.). **Cereal Grains for the Food and Beverage Industries**. Woodhead Publishing: Cambridge, 2013. p. 220-243.

BALA, B. K. Physical and Thermal Properties of Cereal Grains. In: BALA, B. K. (Ed.). **Drying and Storage of Cereal Grains**. 2nd ed. Wiley Blackwell: Chichester, 2017a. p. 55-80.

BALA, B. K. Thin Layer Drying of Cereal Grains. In: BALA, B. K. (Ed.). **Drying and Storage of Cereal Grains**. Wiley Blackwell: Chichester, 2017b. p. 107-145.

BARBOSA-CÁNOVAS, G. V.; JULIANO, P. Physical and chemical properties of food powders. In: ONWULATA, C. (Ed.). **Encapsulated and Powdered Foods**. CRC Press: Boca Raton, 2005. p. 39-71.

BARBOSA-CÁNOVAS, G. V.; ORTEGA-RIVAS, E.; JULIANO, P.; YAN, H. Particle Properties. In: **Food Powders: Physical Properties, Processing, and Functionality**. Springer US: Boston, MA, 2005. p. 19-54.

BARBOSA-CÁNOVAS, G. V.; VEGA-MERCADO, H. Dehydration Mechanisms. In: BARBOSA-CÁNOVAS, G. V.; VEGA-MERCADO, H. (Eds.). **Dehydration of Foods**. Springer US: Boston, MA, 1996. p. 101-155.

BAUDELAIRE, E. D. Grinding for food powder production. In: BHANDARI, B. et al. (Eds.). **Handbook of Food Powders**. Woodhead Publishing: Cambridge, 2013. p. 132-149.

BECHTEL, D. B.; ABECASSIS, J.; SHEWRY, P. R.; EVERS, A. D. Development, Structure, and Mechanical Properties of the Wheat Grain. In: KHAN, K.; SHEWRY, P. R. (Eds.). **Wheat Chemistry and Technology**. 4th ed. AACC International Press: St. Paul, 2009. p. 51-95.

BOUVIER, J.-M.; CAMPANELLA, O. H. Quality analysis of extrusion-textured food products. In: BOUVIER, J.-M.; CAMPANELLA, O. H. (Eds.). **Extrusion Processing Technology**. John Wiley & Sons, Ltd: Chichester, 2014. p. 311-349.

BRADFORD, M. M. A rapid and sensitive method for the quantitation of microgram quantities of protein utilizing the principle of protein-dye binding. **Analytical Biochemistry**. v. 72, n. 1, p. 248-254, 1976.

BRAHMA, S.; WEIER, S. A.; ROSE, D. J. Effects of selected extrusion parameters on

physicochemical properties and in vitro starch digestibility and β-glucan extractability of whole grain oats. **Journal of Cereal Science**. v. 70, p. 85-90, 2016.

CHAKRAVERTY, A.; SINGH, R. P. Theory of Grain Drying. In: CHAKRAVERTY, A.; SINGH, R. P. (Eds.). **Postharvest Technology and Food Process Engineering**. CRC Press: Boca Raton, 2014. p. 31-74.

CHAMPAGNE, E. T.; WOOD, D. F.; JULIANO, B. O.; BECHTEL, D. B. The rice grain and its gross composition. In: CHAMPAGNE, E. T. (Ed.). **Rice: Chemistry and Technology**. Grain Science References, 3rd ed. American Association of Cereal Chemists, Inc.: St. Paul, 2004. p. 77-107.

CHEN, H. H. Investigation of Properties of Long-grain Brown Rice Treated by Low-pressure Plasma. **Food and Bioprocess Technology**. v. 7, n. 9, p. 2484-2491, 2014.

DE MESA, N. J. E.; ALAVI, S.; SINGH, N.; SHI, Y.-C.; DOGAN, H.; SANG, Y. Soy protein-fortified expanded extrudates: Baseline study using normal corn starch. **Journal of Food Engineering**. v. 90, n. 2, p. 262-270, 2009.

DELCOUR, J. A.; HOSENEY, R. C. Structure of cereals. In: DELCOUR, J. A.; HOSENEY, R. C. (Eds.). **Principles of Cereal Science and Technology**. Textbooks, 3rd ed. AACC International, Inc.: St. Paul, 2010. p. 1-22.

DODDS, J. Techniques to analyse particle size of food powders. In: BHANDARI, B. et al. (Eds.). **Handbook of Food Powders**. Woodhead Publishing: Cambridge, 2013. p. 309-338.

FISTES, A.; TANOVIC, G. Effect of smooth roll grinding conditions on reduction of sizings in the wheat flour milling process. In: PLETNEY, V. (Ed.). **Focus on Food Engineering Research and Developments**. Nova Science Publishers, Inc.: New York, 2007. p. 453-466.

GLITSØ, L. V.; BACH KNUDSEN, K. E. Milling of Whole Grain Rye to Obtain Fractions with Different Dietary Fibre Characteristics. **Journal of Cereal Science**. v. 29, n. 1, p. 89-97, 1999.

HATCHER, D. W.; KRUGER, J. E. Simple Phenolic Acids in Flours Prepared from Canadian Wheat: Relationship to Ash Content, Color, and Polyphenol Oxidase Activity. **Cereal Chemistry**. v. 74, n. 3, p. 337-343, 1997.

HICKEY, A. J.; GIOVAGNOLI, S. Powder and particle-dependent traditional manufacturing processes (Unit Operations). In: **Pharmaceutical Powder and Particles**. Springer International Publishing: Cham, 2018. p. 61-71.

HOURSTON, J. E.; IGNATZ, M.; REITH, M.; LEUBNER-METZGER, G.; STEINBRECHER, T. Biomechanical properties of wheat grains: the implications on milling. **Journal of The Royal Society Interface**. v. 14, n. 126, 2017.

ILO, S.; SCHOENLECHNER, R.; BERGHOFE, E. Role of lipids in the extrusion cooking processes. **Grasas y Aceites**. v. 51, n. 1-2, p. 97-110, 2000.

LANG, W.; DEJMA, C.; SIRISANSANEEYAKUL, S.; SAKAIRI, N. Biosorption of nonylphenol on dead biomass of Rhizopus arrhizus encapsulated in chitosan beads. **Bioresource Technology**. v. 100, n. 23, p. 5616-5623, 2009.

LIU, C.; LIU, L.; LI, L.; HAO, C.; ZHENG, X.; BIAN, K.; ZHANG, J.; WANG, X. Effects of different milling processes on whole wheat flour quality and performance in steamed bread making. **LWT - Food Science and Technology**. v. 62, n. 1, Part 1, p. 310-318, 2015.

LOZANO, J. E.; ROTSTEIN, E.; URBICAIN, M. J. Total porosity and open-pore porosity in the drying of fruits. **Journal of Food Science**. v. 45, n. 5, p. 1403-1407, 1980.

MAROUSIS, S. N.; SARAVACOS, G. D. Density and Porosity in Drying Starch Materials. **Journal of Food Science**. v. 55, n. 5, p. 1367-1372, 1990.

MATSUSHIMA, R. Morphological Variations of Starch Grains. In: NAKAMURA, Y. (Ed.). **Starch: Metabolism and Structure**. Springer Japan: Tokyo, 2015. p. 425-441.

MEERA, M. S.; BHASHYAM, M. K.; ALI, S. Z. Effect of heat treatment of sorghum grains on storage stability of flour. **LWT - Food Science and Technology**. v. 44, n. 10, p. 2199-2204, 2011.

MENON, R.; GONZALEZ, T.; FERRUZZI, M.; JACKSON, E.; WINDERL, D.; WATSON, J. Oats—From Farm to Fork. In: HENRY, J. (Ed.). **Advances in Food and Nutrition Research**, v. 77. Academic Press, 2016. p. 1-55.

MILLER, S. S.; FULCHER, R. G. Microstructure and Chemistry of the Oat Kernel. In: WEBSTER, F. H.; WOOD, P. J. (Eds.). **Oats Chemistry and Technology**. 2nd ed. AACC International Press: St. Paul, 2011. p. 77-94.

MIR, S. A.; MANICKAVASAGAN, A.; BOSCO, S. J. D.; SHAH, M. A. Brown rice. In: MIR, S. A.; MANICKAVASAGAN, A.; SHAH, M. A. (Eds.). **Whole Grains. Processing, Product Development, and Nutritional Aspects**. CRC Press: Boca Raton, 2019. p. 49-69.

MONTGOMERY, D. C. Fitting regression models. In: **Design and analysis of experiments**. 8th ed. Wiley: Hoboken, 2013. p. 449-477.

MORA, S. R.; MILÁN, A. K. N.; MILÁN, J. C. Maize. In: MIR, S. A.; MANICKAVASAGAN, A.; SHAH, M. A. (Eds.). **Whole Grains. Processing, Product Development, and Nutritional Aspects**. CRC Press: Boca Raton, 2019. p. 87-102.

MOSSÉ, J. Nitrogen-to-protein conversion factor for ten cereals and six legumes or oilseeds. A reappraisal of its definition and determination. Variation according to species and to seed protein content. **Journal of Agricultural and Food Chemistry**. v. 38, n. 1, p. 18-24, 1990.

MULTARI, S.; PIHLAVA, J.-M.; OLLENNU-CHUASAM, P.; HIETANIEMI, V.; YANG, B.; SUOMELA, J.-P. Identification and Quantification of Avenanthramides and Free and Bound Phenolic Acids in Eight Cultivars of Husked Oat (Avena sativa L) from Finland. **Journal of Agricultural and Food Chemistry**. v. 66, n. 11, p. 2900-2908, 2018.

NGUYEN, M.-H.; PRICE, W. E. Air-drying of banana: Influence of experimental parameters, slab thickness, banana maturity and harvesting season. **Journal of Food Engineering**. v. 79, n. 1, p. 200-207, 2007.

ORTEGA-RIVAS, E. Bulk Properties of Food Particulate Materials: An Appraisal of their Characterisation and Relevance in Processing. **Food and Bioprocess Technology**. v. 2, n. 1, p. 28, 2008.

PARKER, M. L. The Structure of Mature Rye Endosperm. **Annals of Botany**. v. 47, n. 2, p. 181-186, 1981.

PARTI, M. Selection of Mathematical Models for Drying Grain in Thin-Layers. **Journal of Agricultural Engineering Research**. v. 54, n. 4, p. 339-352, 1993.

PEYRON, S.; CHAURAND, M.; ROUAU, X.; ABECASSIS, J. Relationship between bran mechanical properties and milling behaviour of durum wheat (Triticum durum Desf.). Influence of tissue thickness and cell wall structure. **Journal of Cereal Science**. v. 36, n. 3, p. 377-386, 2002.

POMERANZ, Y.; ZELENY, L. Biochemical and functional changes in stored cereal grains. **C R C Critical Reviews in Food Technology**. v. 2, n. 1, p. 45-80, 1971.

POSNER, E. S. Wheat flour milling. In: KHAN, K.; SHEWRY, P. R. (Eds.). **Wheat: Chemistry and Technology**. Grain Science References, 4th ed. AACC International, Inc.: St. Paul, 2009. p. 119-152.

POSNER, E. S.; HIBBS, A. N. The Flour Mill Laboratory. In: POSNER, E. S.; HIBBS, A. N. (Eds.). **Wheat Flour Milling**. References Series, 2nd ed. AACC International, Inc.: St. Paul, 2005. p. 47-100.

ROBERTS, J. S.; KIDD, D. R.; PADILLA-ZAKOUR, O. Drying kinetics of grape seeds. **Journal of Food Engineering**. v. 89, n. 4, p. 460-465, 2008.

ROSENTRATER, K. A.; EVERS, A. D. Botanical aspects. In: ROSENTRATER, K. A.; EVERS, A. D. (Eds.). **Kent's Technology of Cereals (Fifth Edition)**. Woodhead Publishing: Cambridge, 2018a. p. 205-266.

ROSENTRATER, K. A.; EVERS, A. D. Chemical components and nutrition. In: ROSENTRATER, K. A.; EVERS, A. D. (Eds.). **Kent's Technology of Cereals (Fifth Edition)**. Woodhead Publishing: Cambridge, 2018b. p. 267-368.

SERNA-SALDIVAR, S. O. Cereal Grains. The Staff of Life. In: SERNA-SALDIVAR, S. O. (Ed.). **Cereal Grains. Properties, Processing, and Nutritional Attributes**. Food Preservation Technology Series. CRC Press: Boca Raton, 2010a. p. 1-42.

SERNA-SALDIVAR, S. O. Grain Development, Morphology, and Structure. In: SERNA-SALDIVAR, S. O. (Ed.). **Cereal Grains. Properties, Processing, and Nutritional Attributes**. Food Preservation Technology Series. CRC Press: Boca Raton, 2010b. p. 109-128.

SINGH, R. P.; HELDMAN, D. R. Dehydration. In: SINGH, R. P.; HELDMAN, D. R. (Eds.). **Introduction to Food Engineering (Fifth Edition)**. Academic Press: San Diego, 2014. p. 675-710.

SRICHUWONG, S.; SUNARTI, T. C.; MISHIMA, T.; ISONO, N.; HISAMATSU, M. Starches from different botanical sources II: Contribution of starch structure to swelling and pasting properties. **Carbohydrate Polymers**. v. 62, n. 1, p. 25-34, 2005.

SRIKIATDEN, J.; ROBERTS, J. S. Moisture Transfer in Solid Food Materials: A Review of Mechanisms, Models, and Measurements. **International Journal of Food Properties**. v. 10, n. 4, p. 739-777, 2007.

WAGNER, J. R.; MOUNT, E. M.; GILES, H. F. Extrusion Process. In: WAGNER, J. R.; MOUNT, E. M.; GILES, H. F. (Eds.). **Extrusion: The Definitive Processing Guide and Handbook**. 2nd ed. William Andrew Publishing: Oxford, 2014. p. 3-11.

YANNIOTIS, S.; PETRAKI, A.; SOUMPASI, E. Effect of pectin and wheat fibers on quality attributes of extruded cornstarch. **Journal of Food Engineering**. v. 80, n. 2, p. 594-599, 2007.

ZASYPKIN, D. V.; YURYEV, V. P.; ALEXEYEV, V. V.; TOLSTOGUZOV, V. B. Mechanical properties of the products obtained by the thermoplastic extrusion of potato starch-soybean protein mixtures. **Carbohydrate Polymers**. v. 18, n. 2, p. 119-124, 1992.

Transition Chapter II to Chapter III

Feed materials intended for extrusion must present free-flowing (non-cohesive) behavior, that is, they must consist of particles with no tendency towards agglomeration or to form lumps. This specification is fulfilled when the particle size exceeds about 100 μm and when lipid content is less than 5%.

Based on the results obtained in the chemical composition, wholemeal oats presented the highest content in lipids (5.19%). The oats endosperm is soft because the lipid compounds are mainly distributed in the starchy endosperm and during milling, they are smeared out on the starch, proteins, and fibers. However, the lubricant effect of lipids was hindered by incompatibility with soluble β-glucan polymers, also present in oats. Furthermore, the smallest B-type starch granules in oats particles could have increased the interparticle adhesion and extruder-surfaces adhesion. Starch granules in oats are in groups of about 80 units (compound granules of 10 – 60 μm in diameter) and the diameter of an individual granule varies from 2 to 11 μm. These characteristics made the wholemeal oats a non-extrudable material. The wholemeal particles from rice, maize, sorghum, rye, and wheat presented characteristics of a uniform free-flowing material before extrusion and were selected as the most suitable for the production of extruded snacks.

In the next chapter, the impact of grinding conditions of whole-grain cereals on the expansion and texture properties of extruded snacks was addressed. The research focused on the use of two mill types (disc and roller) on the five selected cereal. Before the extrusion step, a maximum fractionation of the grain anatomical parts was sought in the feed material so before grinding, the grains were dried up to 6% moisture content (wet basis). In the extrusion step, through trial-and-error experimentations, the screw profile, the temperature profile, screw speed, feed rate, and feed moisture were fixed to process the ground products at the same extrusion conditions. Once the extrusion process was carried out at constant operational parameters, the characterization of the extruded products was carried out.

CHAPTER III

EFFECT OF CEREAL TYPE AND MILL TYPE ON EXPANSION AND TEXTURE PROPERTIES OF WHOLE-GRAIN CEREAL EXTRUDED SNACKS

Effect of Cereal Type and Mill Type on Expansion and Texture Properties of Whole-Grain Cereal Extruded Snacks

Jhony Willian Vargas-Solórzano [a] *, José Luis Ramírez Ascheri [b], Carlos Wanderlei Piler de Carvalho [b].

[a] Postgraduate Program in Food Science and Technology. Federal Rural University of Rio de Janeiro. Rodovia Br 465, km 7, CEP 23890-000, Seropédica, RJ – Brazil.
[b] Embrapa Agroindústria de Alimentos, Food Extrusion and Physical Properties Lab., Avenida das Américas 29501, Guaratiba, CEP 23020-470, Rio de Janeiro, RJ – Brazil.

* Corresponding author: jwvargass@ufrrj.br; vargasjw@gmail.com

ABSTRACT

The development of fiber-rich extrudates with the expectation of good taste and texture, and that preserve their nutritional benefits, is a challenge because of these products have textures and colors that are less favorable to consumer preference. This occurs mainly due to the insoluble fibers and lipids that proceed from the bran and germ fractions, respectively. Bran particles are hard to melt and cause physical rupture of the molten material at the die exit, and lipids exert a lubricant effect in the stream of particles being sheared and compressed in the screw channel. The objective of this work was to evaluate the cereal type (rice, maize, sorghum, rye, and wheat) and mill type (disc and roller) effects on changes in the expansion and texture properties of whole-grain cereal extruded snacks. The grains were dried up to 6% moisture content (wet basis) to improve the fractionation of the grains (reduced D_{90} values). The dried grains were disc and roller milled at constant operating parameters. The particles upper to the D_{50} value were ground again in a hammer mill. Then, the particles of both streams were mixed and moistened to 11% (wet basis). The moist particles were processed in a single-screw extruder at constant operating conditions. Irrespective of the cereal type, particles from roller mill required higher screw speeds in the volumetric feeder than disc mill products, to deliver a mass flow rate of 4 kg/h inside of the extruder. At this feed rate, the degree of screw filling and interparticle porosity was higher for the roller-milled products than for the disc-milled ones. The disc-milled maize particles produced extrudates with the highest volumetric expansion (13.66). The roller-milled brown rice particles produced extrudates with the highest sectional expansion (11.12). The disc-milled rye particles produced extrudates with the highest average puncturing force (6.17 N) and the highest crispness work (0.82 N·mm). Brown rice extrudates produced from roller-milled particles and maize extrudates produced from roller or disc-milled particles showed the lowest average puncturing forces (~ 1.89 N) and the lowest crispness work (~ 0.24 N·mm). This work contributed to select an appropriate combination of cereal type and mill type to produce extrudates with varying degrees of expansion and texture. These characteristics, as well as the flavor and color, could be improved by producing multi-grain extrudates based on rice and maize.

Keywords: Whole grain. Grinder. Milling. Physical properties.

1 INTRODUCTION

In extrusion cooking experiments, the feeding material usually is based on refined ingredients rich in starches and proteins, and the addition of by-products rich in dietary fiber is a frequent practice to incorporate these removed components from whole grains. Few works start the extrusion processing from whole grains, and in general, the feed material is obtained using a particular type of mill. Grinding or milling of cereal grains is commonly performed to produce refined flour, the ingredient used in making bread, pasta, cakes, cookies, porridge, and extruded snack foods, between many other food products (LI; DHITAL; HASJIM, 2014). Whole-grain flours are increasingly popular because they keep the dietary fiber and bioactive compounds in the end-products. According to the size reduction of bran particles, whole cereal flours also are used for bread production (flours with moderate bran particle size) and non-gluten applications (flours with small bran particle size) (DOBLADO-MALDONADO et al., 2012).

Due to the variation in structure and composition between the anatomical parts of cereal grains, whole-grain ground products are composed of irregular particles with various densities different from the density of grains. In cereal processing by extrusion, grains are downsized to produce free-flowing feed materials with appropriate particle sizes. During the grinding process, the grains are stressed by the action of mechanical parts of the grinding machine. Initially, the stress is absorbed internally by the material as strain energy and when it exceeds a critical level, fracture occurs along cleavages or lines of weakness in the grains, and the stored energy is used for the creation of new surfaces. Nevertheless, a large part of the energy is dissipated as heat (GURITNO; HAQUE, 1994).

The physical changes in a feed material as a result of the grinding conditions can be quantified by its interparticle porosity. The interparticle space in a particulate food is influenced by the morphology of its particles, that is, the size, distribution, and shape of the individual particles structuring the particulate food (DODDS, 2013). These characteristics will determine the degree of hydration during the preconditioning moisture and the degree of compaction and melting rate of the particles in the compression section of the screw. During the compression–melting process, air volumes released from pores, present at the inter- and intra-granular voids, are trapped in the mass (CISNEROS; KOKINI, 2002). The air trapped in the consolidated solid particles would contribute to decrease the thermal conductivity, influencing on the melting rate of the particles. Likewise, air bubbles trapped in the melt may act as expansion nuclei of the water vapor at the die outlet. Thus, the thermal expansion of the air and water vapor embedded in the melt could be affected by the interparticle porosity of feed material, and likewise, the cellular structure formation of the extrudate and its expansion and texture characteristics.

Furthermore, according to the type of grinder operated, the grinding process increases the surface area of the grains and improve the reactiveness of particles (SHASHIDHAR et al., 2013). Thus, during an extrusion process, particles with high surface areas are easily melted (the heat transfer is more effective from the surface to the center of the particle) and, more starch conversion and complexes formation between macromolecules and minority compounds can occur. In extrusion processes at very low moisture content, the particles are mainly melted by mechanical shearing and secondarily by heat conduction (BOUVIER; CAMPANELLA, 2014). Both energy inputs cause the melting of crystallites structuring the starch granules, protein bodies, protein networks, and fibers present in the cell walls of the endosperm and bran (VERGNES; VILLEMAIRE, 1987). The starch and protein polymers are easy to melt, while the insoluble fibers are hard to melt. The unmelted insoluble fibers derived from the bran

particles reach the metering section of the screw and are conveyed and longitudinally oriented on the way. At the cylindrical section of the die, just before leaving the extruder, the insoluble fibers are close to the starch and protein polymers but in an incompatible way, causing decreased extensional forces and resulting in low shear rate and low die pressure. At the die exit, the elastic properties of the melt are hindered due to the physical rupture of the melt, resulting in extrudates with less sectional expansion, with smaller air cells and thicker cell walls. All these features adversely influence on texture and color of the fiber-rich extrudates (AČKAR et al., 2018; YANNIOTIS; PETRAKI; SOUMPASI, 2007).

To address this industrial challenge, the size fractionation of bran and germ tissues through mechanical milling can be a way to improve the physicochemical compatibility between natural fibers, lipids, proteins, and starch polymers during the melt formation. A reduction in the size of the bran particles improved the elastic expansion of the rye bran extrudates (ALAM et al., 2014).

The objective of this work was to evaluate the effects of cereal type and grinder type on changes in the expansion and texture properties of whole-grain cereal extruded snacks. Feeding materials based on whole grains of rice, maize, sorghum, rye, and wheat were prepared. The size reduction of these whole grains was performed in two types of mill (disc and roller). Besides, the drying of the grains previously to the grinding process was carried out to improve the breakage of the grains and the distribution of the minor anatomical parts on the new surfaces of the particles generated. The particle-size distribution and the interparticle porosity were determined as a way to characterize the feed materials. The expansion and texture properties were measured to characterize the extrudates.

2 MATERIALS AND METHODS

2.1 Wholemeal Cereal Particles Preparation

From a total of 4 kg of cleaned and intact kernels of whole-grain cereals of brown rice, sorghum, maize, rye and wheat, the initial water content was determined. Therefore, 1.1 kg of each cereal type was dried in a tray dryer at 60 °C up to 6% of moisture content (wet basis). Afterward, the grains were ground either in a disc mill (DM) or a roller mill (RM). The wholemeal particles upper to the diameter corresponding to 50% finer (D_{50}) were ground again in a hammer mill (Figure 1). Then, the particles of both streams were manually mixed, moistened to 11% (wet basis), and kept at refrigeration temperature during 16 h to ensure a uniform distribution of moisture in the feed material. After this time, 0.3 kg of each sample was separated to determine the mass flow rate, the bulk density and the solid density. Before the extrusion process, the moisture in the feed was checked. The remaining portions of moistened particles, according to the cereal type and grinder type used, were divided into two equal sub-portions and a code was assigned to each according to a 5 × 2 factorial experiment.
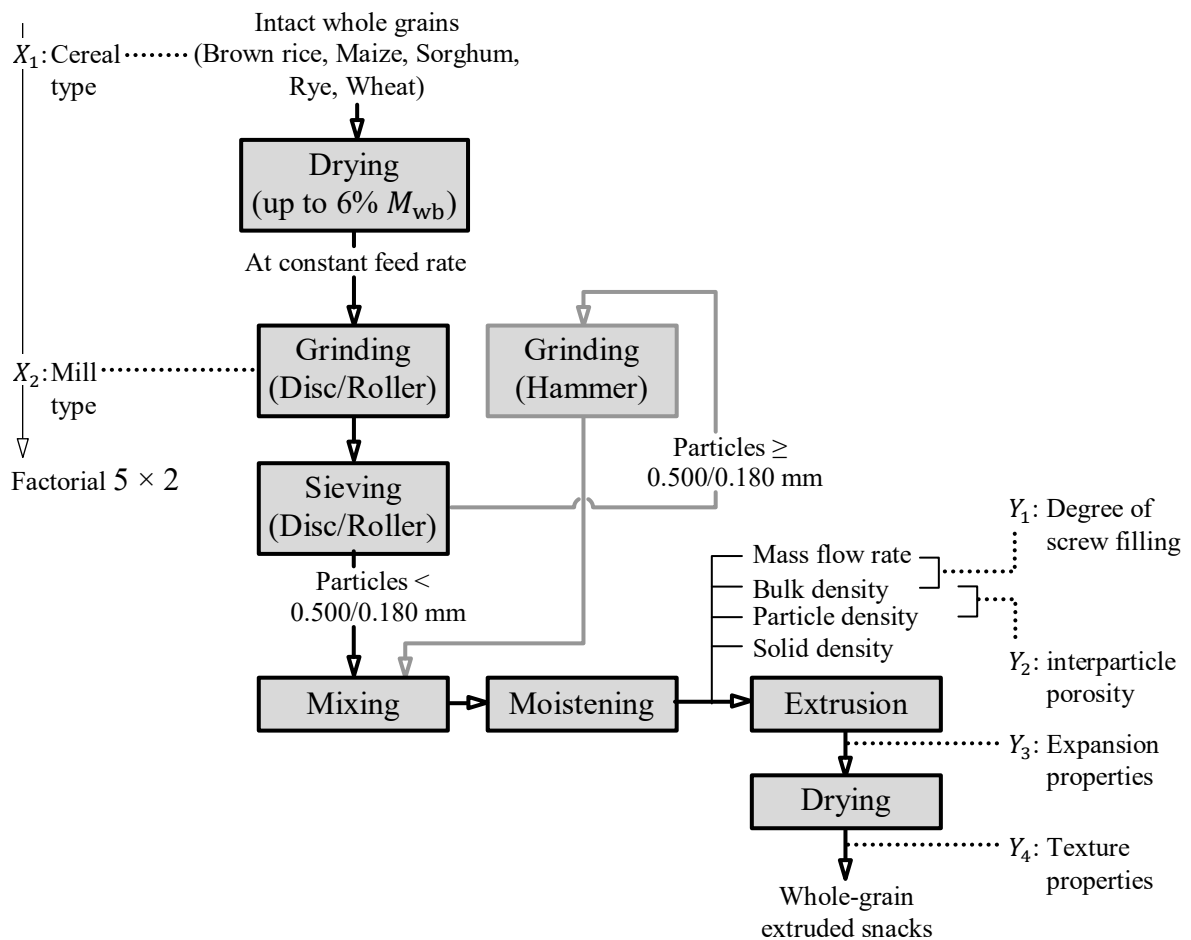
Figure 1. Drying pretreatment of whole-grain cereals before disc and roller milling, linking the analysis performed in each step and the planned experiment. X_i: independent variables, Y_i: dependent variables.

2.2 Mass Flow Rate

A hundred grams of each moistened sample was fed into the hopper of a single-screw volumetric feeder (Brabender, Duisburg, Germany). The screw speed was varied at three levels (10, 15 and 20 rpm) and particles were collected at the outlet for 1 min (YANNIOTIS; PETRAKI; SOUMPASI, 2007). Then, by linear interpolation, it was calculated the screw speed in the feeder that corresponds to a mass flow rate ($\dot{m}$) of 4 kg/h, for each moistened sample.

2.3 Bulk Density of Particles

The loose bulk density of particles (ρ_b) was determined as the non-compacted sample mass, freely poured in a container of known volume (ORTEGA-RIVAS, 2008). The bed of particles was obtained by placing a graduated cylinder with the top leveled to 50 cm^3 under the outlet of a single-screw volumetric feeder (Brabender, Duisburg, Germany) and then, dropping 50 g of a sample at 4 kg/h.

2.4 Solid Density, Particle Density, and Interparticle Porosity

The solid phase volume (which excludes all open and closed pores) and skeletal volume (which is the closed-pores) of individual particles that structure a particulate material were determined in duplicate measurements by the gas displacement method in a pycnometer system AccuPyc II 1340 (Micromeritics, Norcross, USA), using helium as displacement medium. The solid volume was used to calculate the solid density and the sum of the solid and skeletal volumes was used as the total volume of particles to calculate the particle density. The interparticle porosity was estimated according to equation (1) (MAROUSIS; SARAVACOS, 1990; ORTEGA-RIVAS, 2008).

$$\nu = \left(1 - \frac{\rho_b}{\rho_p}\right) 100\% \tag{1}$$

ρ_b and ρ_p are the bulk and particle densities of the particulate material, respectively.

2.5 Degree of Screw Filling

The degree of particles filling in the extruder conveying section was calculated as the ratio of sectional areas of particles flow and extruder channel, according to equation (2):

$$DSF = \frac{\left(\frac{\dot{m}}{\rho_b \pi D_s S_s}\right)}{W\left(\frac{D_b - D_r}{2}\right)} \times 100\% \tag{2}$$

S_s is the screw speed and W is the axial channel width of the extruder. D is diameter and subscripts s, b, and r, are screw, barrel, and root in the conveying section, respectively.

2.6 Extrusion Processing

The extrusion process was conducted using constant operating parameters. The equipment used was a single-screw extruder (Brabender, 19/20 DN, 832500) composed of a barrel with an L/D ratio of 20:1, with grooves along its inner surface, with two electrical heating

zones set at 50 and 90 °C, and provided with an air cooling system (Brabender, ELMO-G, 673420). The screw coupled to the extruder had a compression ratio of 5:1, and the horizontal rod die mounted at the front end of the extruder had a single hole (diameter of 3 mm). This rod die was the third extruder zone, electrically heated to 120 °C. The moistened samples were fed into the feeding zone by a single-screw funnel type volumetric feeder (Brabender, 625415,394). The extruder operated at a constant temperature profile, constant screw speed (200 rpm), and constant feed rate (4 kg/h). The samples (labeled sub-portions) were fed to the extruder in random order.

2.7 Expansion Properties

From each extrusion trial, a total of twenty extruded pieces was randomly selected, which were then cross-sectioned at both ends. The length l and diameters d_i both at the center and ends of each piece were measured using a digital caliper (ZAAS Precision, Curitiba, Brazil). The sectional expansion index (SEI) was then calculated according to equation (3) (ALVAREZ-MARTINEZ; KONDURY; HARPER, 1988).

$$SEI = \left(\frac{D}{D_0}\right)^2 \tag{3}$$

where D is the average of the diameters D_i; D_0 is the hole diameter at the cylindrical die. The mass m of the previous samples was registered using an analytical balance (Mettler Toledo, AG204, Switzerland) and the apparent density of extruded pieces (ρ_e) was then calculated using equation (4).

$$\rho_e = \frac{4\,m}{\pi\,D^2 l} \tag{4}$$

The longitudinal expansion index (LEI) was calculated according to equation (5) (ALVAREZ-MARTINEZ; KONDURY; HARPER, 1988).

$$LEI = \left(\frac{\rho_m}{\rho_e}\right)\frac{1}{SEI}\left(\frac{1 - w_m}{1 - w_e}\right) \tag{5}$$

where ρ is the material density, w is the water content fraction, and subscripts m is melt product and e is the extruded product. ρ_m was estimated as the solid density and measured according to the item 3.2.4. w_m and w_e were determined in duplicate measurements using the 925.09 oven method (AOAC, 2005). The volumetric expansion index (VEI) was obtained from equation (6) (ALVAREZ-MARTINEZ; KONDURY; HARPER, 1988).

$$VEI = SEI(LEI) \tag{6}$$

2.8 Texture Properties

Samples used to determine expansion properties were dried in an oven with air circulation at 60 °C (WTB Binder, Tuttlinger, Germany) up to 4% moisture content. Afterward, pieces were cooled in a desiccator up to room temperature. The mechanical properties of samples were then performed on a texture analyzer TA-XT Plus (Stable Micro Systems, Surrey, England) using the puncture test (BOUVIER; CAMPANELLA, 2014). The analyzer was equipped with a 50 kg load cell and a 2 mm diameter stainless steel cylinder probe. A crosshead

speed of 5 mm/s was applied. When the probe reached a contact force of 0.196 N on the sample surface, the puncturing was initiated at 1 mm/s until a depth of 50% of the sample diameter. The peak compression forces (N) and time (min) at which a sample was punctured, were measured from the force-time curve, recorded and analyzed by the Exponent software program (version 4.0.13.0).

2.9 Experimental Design and Data Analysis

A 5×2 factorial experiment replicated twice was conducted. The independent variables were X_1 = cereal type (brown rice, maize, sorghum, rye, and wheat), and X_2 = grinder type (disc mill and roller mill). The impact of the studied factors was evaluated on the particles entering the conveying section of the extruder screw (mass flow rate, degree of screw filling and interparticle porosity) and on the expanded extrudates (expansion and texture properties).

Factorial ANOVA (analysis of variance) was performed on responses. The null hypothesis was rejected when the probability value (p-value) for the statistic F_0 was less than 5% of significance level (α). The total and partial sum of squares in the ANOVA were estimated according to the least-squares methodology (MONTGOMERY, 2013). The significance of each source in the ANOVA was performed according to the partial F test. To depict the impact of the factors on responses, the multiple range test of Tukey, with $\alpha = 0.05$, was included in the interaction plots.

3 RESULTS AND DISCUSSION

3.1 Mass Flow Rate

To set a mass flow rate of 4 kg/h, the screw speed of the volumetric feeder was adjusted according to the cereal type and grinder type, as shown in Figure 2.
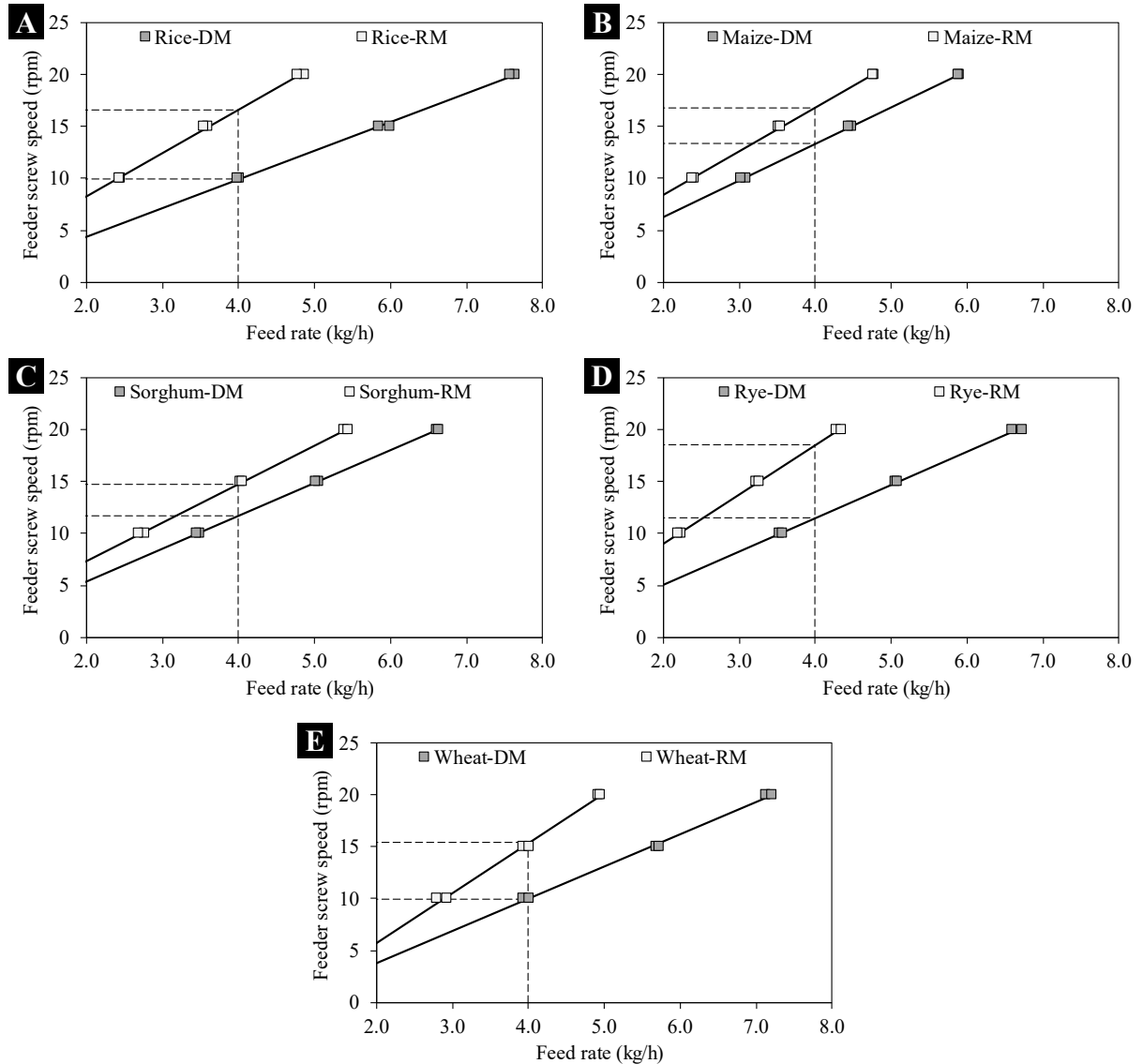
Figure 2. Linear interpolation to calculate the screw speed of the volumetric feeder corresponding to a mass flow rate of 4 kg/h. DM: disc mill; RM: roller mill. (A): Rice; (B) Maize; (C): Sorghum; (D): Rye; (E): Wheat.

Irrespective of the cereal type, particles produced with the roller mill required higher screw speeds in the volumetric feeder than the disc mill produced particles, to deliver a mass flow rate of 4 kg/h inside of the extruder. At feed rates greater than 4 kg/h, the changes in screw speed were less sensitive (less slope on the trend line) for the particles derived from elongated-

shape grains such as wheat, rye, and brown rice, and milled in disc mill (Figure 2A, D, E) than the particles derived from grains maize and sorghum (Figure 2B, C).

A less slope on the trend line can be interpreted as less variability in the interparticle porosity of the feed material. Rounded particles are compacted better and have less interparticle space. It seems that elongated grains milled in disc mill, produce particles with a more spherical shape, due to the mechanical action of the grinder contact elements. In disc mills, grains are ground between two metal discs with tiles secured to the periphery of them. The tiles have a tapered pattern of sharp parallel ridges arranged radially in two concentric rows. The feed is performed in the center of the stator-disc and grains pass centrifugally outward through the narrow gap between the discs by the rotor-disc action. The grains first encounter the coarser ridged tiles that form the inner ring, before receiving a finer grind by the more finely ridged tiles that form the outer ring (MCCABE; SMITH; HARRIOTT, 1993; ROSENTRATER; EVERS, 2018).

3.2 Degree of Screw Filling and Interparticle Porosity of the Feeding Materials

For the calculus of the degree of particles filling in the extruder conveying section, it was used the following constant values in the equation (2): S_s = 200 rpm, W = 14 mm, D_S = 19 mm, D_b = 20 mm, and D_r = 14.75 mm. A feed rate of 4 kg/h filled the screw in the conveying section between 23 and 39%, according to the cereal type and grinder type (Figure 3A). For all cereal and grinder types studied, the range of screw filling operated at 4 kg/h can be classified as a starve feeding process, which can be inferred that the pressures inside the extruder were lower. Single-screw extruders usually are flood fed and flood feeding often results in higher pressures inside the extruder (RAUWENDAAL; GONZALEZ-NUNEZ; RODRIGUE, 2017). Starve feeding is recommended for materials prone to agglomerate. Agglomeration of particles can occur in finely particulate materials, rich in lipids, as in the case of oats and rye particles, or whole-grains ground in a hammer mill. The starve feeding can be controlled by adjusting the feed rate and/or the extruder screw speed.

In all studied cereals, the degree of screw filling and interparticle porosity was higher for the roller milled products than for the disc milled ones (Figure 3A, B; $P < 0.05$). The roller milled rye particles presented the highest interparticle porosity (72.9%), and the disc milled brown rice particles, the lowest (54.7%). The interparticle porosity had a satisfactory positive correlation (–0.9879, $P < 0.05$) with the degree of screw filling (Figure 3C). The variability on interparticle porosity as a function of the combined action of cereal type and grinder type can be used to prepare feeding materials with a variable degree of extrusion cooking because the degree of screw filling (hence, the interparticle porosity) can be associated with the pressure build-up inside the extruder.
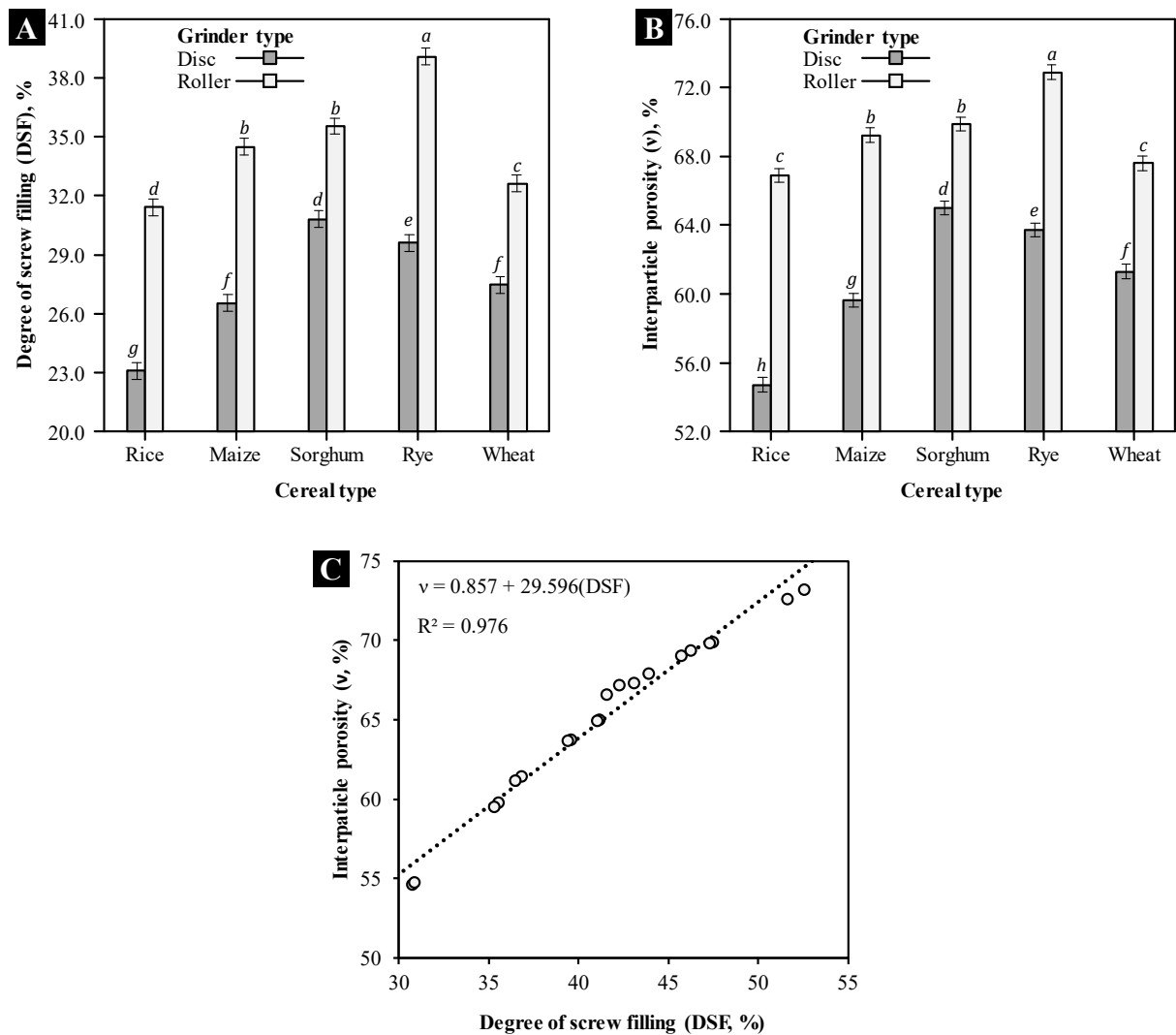
Figure 3. Effects of cereal type and grinder type on (A) Degree of screw filling (*DSF*) in the conveying section of the extruder; (B) Interparticle porosity (*v*) of the feed material. (C) Correlation between *v* and *DSF*. Values with different lowercase letters differ from each other according to the Tukey test.

3.3 Expansion Properties of Extrudates

The scanned images of expanded extrudates for all cereal and grinder type combinations (5 × 2 factorial design) are depicted in **Annex D**. Sorghum and rye extrudates were the darkest, whereas brown rice and wheat extrudates, the lightest. The brown rice extrudates showed large coalescing air cells. In the rye extrudates, the distribution of air cells was more homogeneous than in the other extrudates. The outer surface of the sorghum and rye extrudates was more wrinkled than the others.

Feed materials based on brown rice, sorghum and wheat, and ground in a roller mill produced extrudates with lower apparent densities than their disc mill equivalent products (Figure 4A). An opposite trend was observed for the apparent density of maize extrudates. Grinder type was negligible on the apparent density of rye extrudates ($p \geq 0.05$). Irrespective of the grinder type, maize extrudates presented the lowest apparent density.
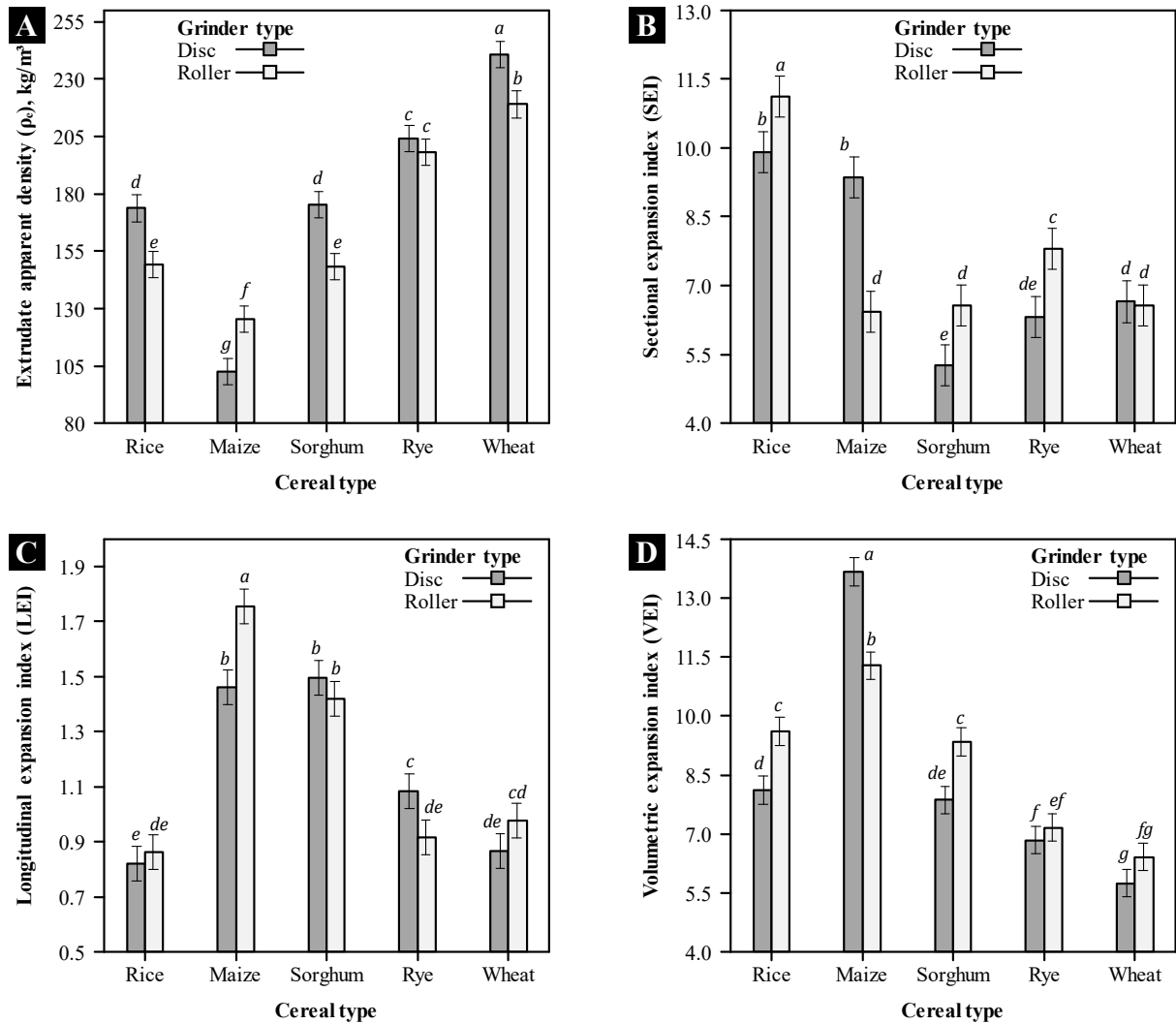
Figure 4. Effects of cereal type and grinder type on (A) Extrudate apparent density (ρ_e); (B) Sectional expansion index (*SEI*); (C) Longitudinal expansion index (*LEI*); (D) Volumetric expansion index (*VEI*). Values with different lowercase letters differ from each other according to the Tukey test.

The highest sectional expansion index (*SEI*) was obtained with feeding materials based on brown rice and ground in the roller mill (Figure 4B, $P < 0.05$). Roller milled feed materials showed higher *SEI* than disc milled products, for brown rice, sorghum, and rye. *SEI* of maize extrudates displayed opposite behavior. Grinder type was negligible on *SEI* of wheat extrudates ($p \geq 0.05$). The highest longitudinal expansion index (*LEI*) was obtained with feeding materials based on maize and ground in the roller mill (Figure 4C, $P < 0.05$). The sorghum particles (irrespective of grinder type) and disc milled products of maize presented similar *LEI* values ($p \geq 0.05$). The lubricant effect of insoluble fibers and lipids present in maize could have plasticized in a greater extend the melt, decreasing its shear viscosity. At the die exit, the viscous properties of the melt are enhanced, giving rise to extrudates with high *LEI*. The volumetric expansion index (*VEI*) is associated with the specific volume of the melt stream, before and after extrusion. Feeding materials prepared with different cereals and grinders, and then extruded at constant operational variables, significantly modified the extrudates *VEI* (between 5.7 and 14.0, Figure 4D). The highest volumetric expansion was obtained with feeding materials based on maize and ground in disc mill ($p < 0.05$).

3.4 Texture Properties of Extrudates

The highest average puncturing force (F_p) was obtained with feeding materials based on rye and ground in disc mill (Figure 5A, $P < 0.05$). Physically, F_p corresponds to the overall force required to puncture the whole extrudate (BOUVIER; CAMPANELLA, 2014). This means that maize extrudates had air pores with thin and smooth walls, that is, air cell structures easy to puncture.
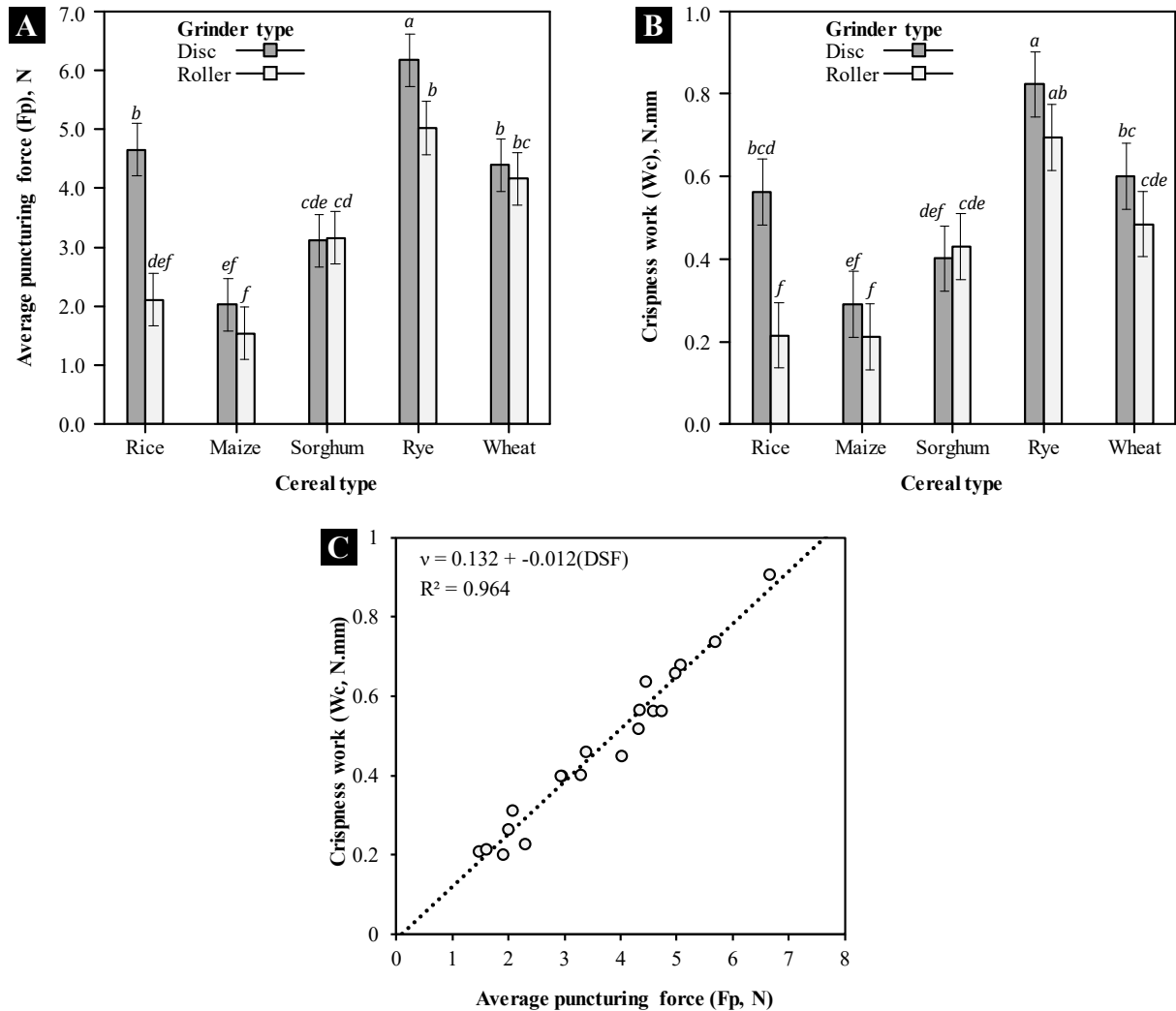
Figure 5. Puncture force parameters of whole-grain extrudates. (A) Average puncturing force (F_p); (B) Crispness work (W_c). (D) Correlation between W_c and F_p. Values with different lowercase letters differ from each other according to the Tukey test.

Crispness work (W_C) represents the average work needed for structural rupture. F_p and W_C varied proportionally, which had a satisfactory positive correlation (-0.9818, $p < 0.05$) (Figure 5C). W_C can be associated to the energy required to fracture and reduce the extrudate into small pieces during consumption (BOUVIER; CAMPANELLA, 2014). In this sense, rye extrudates were the harder, and maize extrudates, the lighter.

4 CONCLUSION

The cereal type and grinder type effects on the physical characteristics of the feed material and the expansion and texture properties of whole-grain cereal extruded snacks were evaluated. Irrespective of the cereal type, particles from roller mill required higher screw speeds in the volumetric feeder than disc mill products, to deliver a mass flow rate of 4 kg/h inside of the extruder. At this feed rate, the particles filled the conveying section of the screw between 23 and 39%, according to the cereal and grinder types used. The degree of screw filling was positively correlated with the interparticle porosity of the feed material ($r = + 0.9879$). The degree of screw filling and interparticle porosity was higher for the roller-milled products than for the disc-milled ones. The roller-milled rye particles presented the highest interparticle porosity (72.9%), and the disc-milled brown rice particles, the lowest (54.7%). The grinder type affected the apparent density and all expansion indexes in maize extrudates. The disc-milled maize particles produced extrudates with the highest volumetric expansion (13.66). In brown rice and sorghum extrudates, the grinder type did not influence on the longitudinal expansion. The roller-milled brown rice particles produced extrudates with the highest sectional expansion (11.12). In rye extrudates, the grinder type did not influence on the apparent density and volumetric expansion. The roller-milled sorghum and rye particles produced extrudates with higher sectional and volumetric expansions than the disc-milled particles. In wheat extrudates, the grinder type did not affect all expansion indexes, and the disc-milled wheat particles produced the highest extrudate apparent density (240.6 kg/m^3). The average puncturing force was positively correlated with the crispness work ($r = + 0.9818$). The grinder type affected the average puncturing force in rice and rye extrudates, and the crispness work only in rice extrudates. The disc-milled rye particles produced extrudates with the highest average puncturing force (6.17 N) and the highest crispness work (0.82 N·mm). Brown rice extrudates produced from roller-milled particles and maize extrudates produced from roller or disc-milled particles showed the lowest average puncturing forces (~ 1.89 N) and the lowest crispness work (~ 0.24 N·mm). The variability on interparticle porosity as a function of the combined action of cereal type and grinder type can be used for preparing feed materials with a variable degree of extrusion cooking because the degree of screw filling (hence, the interparticle porosity) can be associated with the pressure build-up inside the extruder. Furthermore, according to the degree of extrusion cooking and properly blends of multi-grains with higher proportions in rice and maize could be possible to optimize the expansion and texture properties of whole-grain cereal extruded snacks.

REFERENCES

AČKAR, Đ.; JOZINOVIĆ, A.; BABIĆ, J.; MILIČEVIĆ, B.; PANAK BALENTIĆ, J.; ŠUBARIĆ, D. Resolving the problem of poor expansion in corn extrudates enriched with food industry by-products. **Innovative Food Science & Emerging Technologies**. v. 47, n. 6, p. 517-524, 2018.

ALAM, S. A.; JÄRVINEN, J.; KIRJORANTA, S.; JOUPPILA, K.; POUTANEN, K.; SOZER, N. Influence of Particle Size Reduction on Structural and Mechanical Properties of Extruded Rye Bran. **Food and Bioprocess Technology**. v. 7, n. 7, p. 2121-2133, 2014.

ALVAREZ-MARTINEZ, L.; KONDURY, K. P.; HARPER, J. M. A General Model for Expansion of Extruded Products. **Journal of Food Science**. v. 53, n. 2, p. 609-615, 1988.

AOAC. **Official Methods of Analysis of AOAC International**. 18th ed. AOAC International: Gaithersburg, 2005.

BOUVIER, J.-M.; CAMPANELLA, O. H. Quality analysis of extrusion-textured food products. In: BOUVIER, J.-M.; CAMPANELLA, O. H. (Eds.). **Extrusion Processing Technology**. John Wiley & Sons, Ltd: Chichester, 2014. p. 311-349.

CISNEROS, F. H.; KOKINI, J. L. A generalized theory linking barrel fill length and air bubble entrapment during extrusion of starch. **Journal of Food Engineering**. v. 51, n. 2, p. 139-149, 2002.

DOBLADO-MALDONADO, A. F.; PIKE, O. A.; SWELEY, J. C.; ROSE, D. J. Key issues and challenges in whole wheat flour milling and storage. **Journal of Cereal Science**. v. 56, n. 2, p. 119-126, 2012.

DODDS, J. Techniques to analyse particle size of food powders. In: BHANDARI, B. et al. (Eds.). **Handbook of Food Powders**. Woodhead Publishing: Cambridge, 2013. p. 309-338.

GURITNO, P.; HAQUE, E. Relationship Between Energy and Size Reduction of Grains Using a Three-roller Mill. **Transactions of the ASAE**. v. 37, n. 4, p. 1243-1248, 1994.

LI, E.; DHITAL, S.; HASJIM, J. Effects of grain milling on starch structures and flour/starch properties. **Starch - Stärke**. v. 66, n. 1-2, p. 15-27, 2014.

MAROUSIS, S. N.; SARAVACOS, G. D. Density and Porosity in Drying Starch Materials. **Journal of Food Science**. v. 55, n. 5, p. 1367-1372, 1990.

MCCABE, W. L.; SMITH, J. C.; HARRIOTT, P. Size reduction. In: MCCABE, W. L.; SMITH, J. C.; HARRIOTT, P. (Eds.). **Unit Operations of Chemical Engineering**. 5th ed. McGraw-Hill Inc: New York, 1993. p. 960-993.

MONTGOMERY, D. C. Fitting regression models. In: **Design and analysis of experiments**. 8th ed. Wiley: Hoboken, 2013. p. 449-477.

ORTEGA-RIVAS, E. Bulk Properties of Food Particulate Materials: An Appraisal of their

Characterisation and Relevance in Processing. **Food and Bioprocess Technology**. v. 2, n. 1, p. 28, 2008.

RAUWENDAAL, C.; GONZALEZ-NUNEZ, R.; RODRIGUE, D. Polymer Processing: Extrusion. In: **Encyclopedia of Polymer Science and Technology**. 2017. p. 1-67.

ROSENTRATER, K. A.; EVERS, A. D. Dry-milling technology. In: ROSENTRATER, K. A.; EVERS, A. D. (Eds.). **Kent's Technology of Cereals (Fifth Edition)**. Woodhead Publishing: Cambridge, 2018. p. 421-514.

SHASHIDHAR, M. G.; MURTHY, T. P. K.; GIRISH, K. G.; MANOHAR, B. Grinding of Coriander Seeds: Modeling of Particle Size Distribution and Energy Studies. **Particulate Science and Technology**. v. 31, n. 5, p. 449-457, 2013.

VERGNES, B.; VILLEMAIRE, J. P. Rheological behaviour of low moisture molten maize starch. **Rheologica Acta**. v. 26, n. 6, p. 570-576, 1987.

YANNIOTIS, S.; PETRAKI, A.; SOUMPASI, E. Effect of pectin and wheat fibers on quality attributes of extruded cornstarch. **Journal of Food Engineering**. v. 80, n. 2, p. 594-599, 2007.

Transition Chapter III to Chapter IV

Summarizing chapter III, according to the mill type, the grinding conditions of grains dried up to 6% (wet basis) were established as follow:

- Disc mill: gap between discs fixed at aperture 0, feed rate of 7.9 kg/h,
- Roller mill: four sets of rolls with 5, 10, 16, and 15 striations per cm, with differential speeds maintained at 2.3:1, 1:1, 2.3:1, 1:1, feed rate of 7.9 kg/h

And, after trial-and-error experimentations, the extrusion runs were performed under the following conditions:

- Screw profile: compression ratio of 5:1,
- Temperature profile: 50, 90, and 120°C, starting from the feeder zone to the die,
- Screw speed: 200 rpm,
- Feed rate: 4 kg/h,
- Feed moisture: 11%

These conditions allowed comparing the expansion degree of the extrudates and its resultant texture properties.

The sectional expansion index (SEI) of the extruded snacks was found to vary between 5.22 to 11.20 and their corresponding puncturing forces (F_p) between 1.47 to 6.66 N. In one hand, when comparing the cereal types, the brown rice extrudates presented the highest SEI (10.51) and intermediate values of F_p (3.38 N). On the other hand, when comparing the grinder types, variations in SEI and F_p were not significant.

Accordingly, in chapter IV these drying, grinding, and extrusion conditions were used for brown rice, with some modifications: the grain moisture levels before grinding were explored in the range of 6 to 9% (wet basis), the feed moisture levels were explored in the range of 11 to 14% (wet basis), and the screw speed was fixed at 150 rpm. The experiment was designed to correlate the interparticle porosity of the feed material (dependent of factors before extrusion) and the in-line measurement of torque during the extrusion process.

CHAPTER IV

IMPACT OF THE PRETREATMENT OF GRAINS ON THE INTERPARTICLE POROSITY OF FEED MATERIAL AND THE TORQUE SUPPLIED DURING THE EXTRUSION OF BROWN RICE

Impact of the Pretreatment of Grains on the Interparticle Porosity of Feed Material and the Torque Supplied during the Extrusion of Brown Rice

Jhony Willian Vargas-Solórzano [a] *, José Luis Ramírez Ascheri [b], Carlos Wanderlei Piler de Carvalho [b], Cristina Yoshie Takeiti [b], Melicia Cintia Galdeano [b].

[a] Postgraduate Program in Food Science and Technology. Federal Rural University of Rio de Janeiro. Rodovia Br 465, km 7, CEP 23890-000, Seropédica, RJ – Brazil.
[b] Embrapa Agroindústria de Alimentos, Food Extrusion and Physical Properties Lab., Avenida das Américas 29501, Guaratiba, CEP 23020-470, Rio de Janeiro, RJ – Brazil.

* Corresponding author: jwvargass@ufrrj.br; vargasjw@gmail.com

ABSTRACT

The objective of this work was to evaluate the effects of drying, grinder type, and moistening conditions on the interparticle porosity of feed material and the torque supplied to the screw during the single-screw extrusion processing of brown rice. The grains were dried at 60 °C up to moisture contents of 9 and 6% and then milled using two grinder types (disc and roller). The milled products were moistened at levels to produce extruded snacks (11 and 14%). Irrespective of drying the grains, lower particle diameters in the fine and coarse fractions, and narrower distributions were obtained by grinding brown rice in a roller mill than in a disc mill. The disc mill products presented lower interparticle porosity and generated higher torque values than the roller mill products. A reduction in grain moisture from 9 to 6% only decreased the interparticle porosity of disc mill products and increased the torque. An increase in feed moisture from 11 to 14% only increased the interparticle porosity of roller mill products and decreased the torque regardless of grain moisture. This work contributed to understanding the impact of the morphology of the particles in the torque variability during the extrusion processing of brown rice. Few published works correlate physical properties of the feed material with extrusion dependent variables. In the present study, feed materials with high interparticle porosity were produced with roller mill and when extruded they generated low variabilities in the torque.

1 INTRODUCTION

The consumption of brown rice and other whole grains is associated with healthy eating. People increasingly opt for processed products based on whole grains and preserved by physical methods. With promising results, diverse technologies are being applied to stabilize brown rice in storage, to shorten its cooking time, and improve its cooking qualities (BOOTKOTE; SOPONRONNARIT; PRACHAYAWARAKORN, 2016; CHEN, 2014; DING et al., 2015; HUANG; ZHANG; BHANDARI, 2019; KIM et al., 2015; ZHU et al., 2016).

Extrusion cooking was applied, alone or in combination with a germination treatment or enzyme technology, to increase the range of brown rice based novel foodstuffs (MA et al., 2019; MARTI; SEETHARAMAN; PAGANI, 2010; OHTSUBO et al., 2005; WANG et al., 2016; XU et al., 2015) or to produce ready-to-eat extruded brown rice snacks (GONZÁLEZ et al., 2013; GUJRAL et al., 2012; PARDHI et al., 2019; SINGH GUJRAL; SINGH, 2002). The extruded brown rice snacks can be considered as shelf-stable, nutritious and practical products to offer the consumers because they have low levels of moisture and include the bran and germ fractions, rich in insoluble fibers, proteins, lipids, phytonutrients, and minerals.

Few published works correlate physical properties of the feed material (such as particle size range, bulk density, and interparticle porosity) with extrusion dependent variables (such as motor torque, specific mechanical energy, and die pressure). The grinder type as an independent variable greatly affects the physical properties of the feed material (BARBOSA-CÁNOVAS et al., 2005) and extrusion dependent variables (MATHEW; HOSENEY; FAUBION, 1999). In the aforementioned experiments, the feeding material was prepared using a particular type of mill. Usually, the grains fed to the mill are reduced in size to particles smaller or equal to the mesh opening coupled to the mill. In the process, the particles are subjected to stress and fracture several times, until traversing the screening plate. In the case of brown rice grinding, the sticky bran will clog the mill sieves (JULIANO, 1985), and in a short period and due to the overheating effect, particulate materials based on brown rice could become rancid and develop off-flavors.

On the other hand, the moisture content and its distribution in the pericarp, germ, and endosperm affect deformation and breakage of grains (BARBOSA-CÁNOVAS et al., 2005). In wheat milling, grain moisture preconditioning is important to allow better pericarp separation from the endosperm. By drying the grain, it becomes more brittle due to a decrease in tissue-adhesive forces that make up the pericarp layers and the intricate network of endosperm cell walls (HOURSTON et al., 2017).

According to the drying and grinding conditions, the bran and germ tissues are disintegrated and become part of particle surfaces. This combined action defines the morphology of the particles (BADMUS; RAJI; AKINOSO, 2013; SHASHIDHAR et al., 2013), which in turn will affect the degree of hydration during the preconditioning moisture. It is important to reduce the bran particles size in the feeding material to not hinder the elastic properties of the melt. Bran particles cause physical rupture of the melt at the die exit due to the low adhesion properties with starch polymers (ROBIN et al., 2012a). A reduction in the size of the rye bran particles, which constituted a feeding material with 29% in total dietary fibers, improved the elastic expansion of the rye bran extrudates (ALAM et al., 2014).

Natural fibers, and lipids present in the brown rice, and water added to set the feed moisture act as lubricants in the feed material. They affect the resistance to work performed by the screw during the extrusion process (DING et al., 2005; SINGH; GAMLATH; WAKELING, 2007; XU et al., 2015), being necessary to set low levels of feed moisture to enhance the

expansion of the extrudates. The snacks produced in the aforementioned experiments explored feed moistures greater than or equal to 14% (wet basis). Ding et al. (2005) researched below this value but using polished rice as feeding material.

In this work, it was proposed to study the drying and grinding conditions to prepare feeding materials based on brown rice. The grains were dried before grinding, at the maximum recommended temperature for milling wheat (BALA, 2017), up to moisture levels of 9 and 6% (wet basis) to enhance the fractionation of the grains. The grinding was performed in two types of mill (disc and roller), both without a screening plate to obtain milled products in a one-step process. To produce extruded expanded products and considering the lubricating effect of the lipids and fibers present in the brown rice, the milled products were moistened at levels of 11 and 14% (wet basis).

The physical changes of a feed material as a result of drying, grinding, and moistening conditions can be quantified by its interparticle porosity. The interparticle space in a particulate food is influenced by the morphology of its particles. According to Dodds (2013), it is referred to the size, distribution, and shape of the individual particles structuring the particulate food. These characteristics will determine the degree of compaction and melting rate of the particles along the helical channel, in the compression section of the extruder. During the compression–melting process, air volumes released from pores, present at the inter- and intra-granular voids, are trapped in the mass (CISNEROS; KOKINI, 2002). The air trapped in the consolidated solid particles would contribute to decrease the thermal conductivity, influencing on the melting rate of the particles. Likewise, air bubbles trapped in the melt may act as expansion nuclei of the water vapor at the die outlet, wherein the cellular structure formation of the extrudate occurs.

In the production of extruded snacks, the cereal flours and/or grits are cooked at very low moisture content (usually below 20%) in which the solids are mainly melted by mechanical shearing and secondarily by heat conduction (BOUVIER; CAMPANELLA, 2014). Thus, the transformation of starch and other components in the solid particles occurs by melting of the crystallites (VERGNES; VILLEMAIRE, 1987). The melt viscosity development can be directly verified through the motor torque variation, a very sensitive extrusion variable that measures the energy absorbed by a feed material due to the shear exerted by the extruder screw and die orifice (AKDOGAN, 1996). Extruding at constant operational variables (screw speed, feeding rate, and temperature profile in the barrel), torque signals will depend on feed material characteristics. Since single-screw extruders are flood fed, interparticle porosity is a way to characterize the aspect of a feed material and can be linked to the torque supplied to the screw during the extrusion process.

The overall objective of this work was to understand the relationship between interparticle porosity of ground brown rice and the consequent torque supplied during the single-screw extrusion processing. The specific objectives of this research were to evaluate the effects of drying of grains, grinder type, and feed moisture. The drying conditions were evaluated via bulk density of grains and pasting properties; the drying and grinding conditions via the particle-size distribution of the milled products; and the drying, grinding, and moistening conditions via the interparticle porosity and the torque supplied in the process.

2 MATERIAL AND METHODS

2.1 Material and Chemical Composition

Brown rice of light brown pericarp, cultivar Tropical, was kindly donated by S. L. Alimentos (Mauá da Serra, Brazil). The length and length/width ratio of ten grains were 7.41 ± 0.32 mm and 3.74 ± 0.19, respectively, which according to Sinija, Sulochana and Shwetha (2017) correspond to a long slender category of grains. Foreign materials, broken grains, and other types of grains were separated with a Clipper Office Tester 400/B (A.T. Ferrell Co., Bluffton, USA). From 40 kg of intact kernels, 400 g was sampled to perform chemical composition. The sampled grains were size reduced in a hammer type mill (Lab Mill 3100, Perten Instruments AB, Huddinge, Sweden) without its screening plate. Next, the proximate composition of the powdered sample was analyzed in duplicate following the AOAC methods (AOAC, 2005). The sample had, in wet basis, 12.78% of initial moisture (925.09 oven method), 7.25% of proteins (2001.11 method for total nitrogen; factor 5.75 for convert to total protein), 1.27% of fat (945.38 method), 2.57% of dietary fiber (985.29 method), and 1.59% of ash (923.03 method). Fourteen kilograms of the remaining grains were separated for hot air drying. The remaining grains were labeled as grains non-exposed to drying and were used to perform bulk density of grains, pasting properties, and particle-size distribution from two grinder types, following the procedures shown in Figure 1.
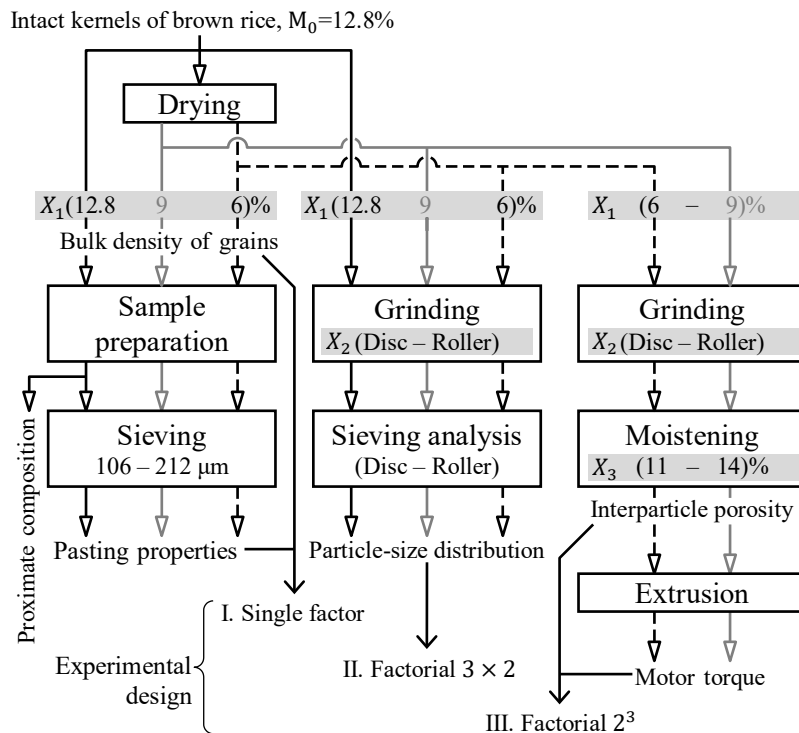
Figure 1. Pretreatment of brown rice for extrusion, linking the analysis performed in each step and the planned experiments. X_1: grain moisture before grinding, X_2: grinder type, and X_3: feed moisture.

2.2 Drying of Grains

The grains separated for hot air drying (14 kg) were split into twelve portions of 1100 g each. Six portions were dried up to 9% of moisture content (wet basis), and the other six up to 6% of moisture content (wet basis), by using a laboratory tray dryer SL102 (SOLAB, São Paulo, Brazil). The temperature and relative humidity of the ambient air and drying air were monitored by a Traceable® Hygrometer Thermometer Dew Point (Cole-Parmer, Vernon Hills, USA). The temperature and relative humidity of the ambient air were 29.71 ± 2.79 °C and $82.01 \pm 16.51\%$, respectively. The dryer operated at 60 ± 0.5 °C air temperature, $26 \pm 2\%$ relative humidity, and 1 ± 0.1 m/s air velocity. Each portion of dried grains was stored in polyethylene bags at ambient temperature for further analysis and processing.

2.3 Moisture Content and Bulk Density of Grains

The grain moisture reduction to the set levels was achieved based on its initial moisture (12.8%, wet basis) and changes in the mass of a bed of grains (1100 g of grains were placed in a rectangular tray of $330 \times 360 \times 10$ mm). Moisture content and bulk density of grains were measured at the beginning and end of the drying experiments. Moisture content was analyzed in duplicate by the 925.09 oven method (AOAC, 2005) and bulk density was determined in quadruplicate according to the method of Joshi, Mohapatra and Joshi (2014) with some modifications. Grains were sampled from different portions of dried grains (200 g each). The non-compacted mass of grains was obtained by freely pouring the grains from 20 cm of height, in a graduated cylinder with the top leveled to 200 cm³. Any excess material in the upper part of the cylinder was horizontally leveled; its external surface was carefully cleaned with a brush and then weighed.

2.4 Pasting Properties

Changes in the starch fraction by the drying process were verified through the pasting properties. Grains from three moisture content (initial moisture: 12.8%, 9%, and 6%, wet basis) were sampled twice from different portions. Each sample (6×100 g) was size reduced in a hammer type Lab Mill 3100 without its screening plate (Figure 1). The powdered samples were sieved and the fraction within 106–212 µm was used to prepare suspensions, by adding 3 g of sample (moisture content adjusted to 14%, wet basis) to 25 g of distilled water (BECKER; HILL; MITCHELL, 2001; CHEN, 2014). Viscosity profiles as a function of time-temperature were performed in a Rapid Visco Analyser (RVA) Series 4 (Newport Scientific, Warriewood, Australia), in duplicate. Stirring time protocol was set according to standard procedures, and a two-step heating protocol was set as shown in Figure 2E (BOUVIER; CAMPANELLA, 2014). From the viscosity curves, the following pasting characteristics were determined: pasting onset, trough viscosity, gelatinization peak, gelation peak, and breakdown viscosity.

2.5 Grinding Process

Grains from three moisture content (initial moisture: 12.8%, 9%, and 6%, wet basis) were ground in a one-step process either in a disc type mill (Lab Mill 3600, Perten Instruments AB, Huddinge, Sweden) fixed at aperture 0 (minimum distance between the stationary disc and the rotating disc) or in a roller type mill (Quadrumat Junior, Brabender, Duisburg, Germany) without the sieving drum (Figure 1). The rotor and stator discs of the disc mill had 11 cm diameter, with sharp steel protrusions in their surfaces, arranged in 10 and 9 arm spirals, respectively. The four sets of rolls assembled in the roller mill had 7 cm diameter and 3 cm

height. Their surfaces were corrugated and had 5, 10, 16, and 15 striations per centimeter, respectively. The differential speed of the rolls was maintained at 2.3:1, 1:1, 2.3:1, and 1:1, respectively. Both grinders worked without a screening plate and grains were fed to the grinders at a feed rate of 7.9 kg/h. The drying and grinding effects were evaluated via particle-size distribution of the milled products.

2.6 Particle-Size Distribution

Particle-size distribution was carried out by sieving analysis according to ASABE Standards (2008) in triplicate measurements. Grains from different moisture content were sampled three times from different portions. Each sample (9×250 g) was split into two equal portions. One was ground in a disc mill, and the other one in a roller mill, following the procedures of "Grinding Process". A RO-TAP sieve shaker RX-29-10 (W.S. Tyler, Mentor, USA) and a set of stainless steel sieves (U.S. series) with progressively smaller openings were used. Sieves were selected taking into account that particles segregation must follow a log-normal distribution. A hundred grams of particulate material described in "Grinding Process" were segregated for 10 min. Then, according to Dodds (2013), particle-size distribution curves based on cumulative mass percentage were generated (Figure 3A), from which the diameter (in μm) corresponding to 10%, 50%, and 90% finer were obtained (D_{10}, D_{50}, and D_{90}, respectively). The small particles size (fine, D_{10}), the large particles size (coarse, D_{90}), and uniformity were used to characterize the particle-size distributions. The uniformity of the distribution was calculated according to equation (1) (DODDS, 2013).

$$\text{Uniformity} = \frac{\sigma}{D_{av}} \tag{1}$$

D_{av} is the average particles size by mass and σ is the standard deviation. They were calculated according to equations (2) and (3), respectively.

$$D_{av} = \frac{\sum m_i D_i}{\sum m_i} \tag{2}$$

$$\sigma = \sqrt{\frac{\sum m_i (D_i - D_{av})^2}{\sum m_i}} \tag{3}$$

m_i and D_i are the mass in class (in g) and the average class size (in μm), respectively.

2.7 Microstructural Characteristics

Morphological observations of samples (transversal section of whole grains and particles segregated from the sieve analysis) were performed in a benchtop scanning electron microscope (SEM) TM3000 (Hitachi HighTechnologies Corporation, Tokyo, Japan) at 15 kV accelerating voltage. Samples were directly placed on aluminum stubs with sticky double-sided conductive metal tape. For the cross-sectional observation, grains were fractured at about its midsection (transverse axis). Then, the tip of the fractured grain was mounted on the stub and examined at a magnification of $\times 500$. For the observation of the particles, a small quantity of particles carefully was poured on the stub, making a thin layer of approximately 16 mm^2, and examined at a magnification of $\times 50$. The acquisition of the images was performed by TM3000 Microscope software version 02-01 (Hitachi High-Tech, Tokyo, Japan).

2.8 Moistening Process

The remaining dried grains from different portions (with moisture contents of 6% and 9%, wet basis) were split into 16 portions of 600 g, and each one was ground as previously described in "Grinding Process" (Figure 1). Eight portions (four by each grain moisture level) were ground in a disc mill and the other eight, in a roller mill. The milled products from the same grain moisture level and grinder type were then moistened in duplicate to 11 and 14% (wet basis). The amount of water (W) to adjust the feed moisture to the established levels (M_p), was calculated according to the equation (4).

$$W = F \left(\frac{M_p - M_f}{100 - M_p} \right) \tag{4}$$

F and M_f are the amount and moisture content of particles after grinding, respectively. The particles were moistened and mixed manually in a plastic bag for about 3 min avoiding the formation of lumps and allowed to equilibrate at room temperature for 24 h before extrusion. Afterward, they were analyzed concerning their moisture content, bulk density, and particle density. The densities were used to calculate the interparticle porosity.

2.9 Bulk Density of Particles

The loose bulk density of particles (ρ_b) was determined in quadruplicate (two replicates by each moist sample portion) according to Ortega-Rivas (2008), as the non-compacted sample mass, freely poured in a graduated cylinder with the top leveled to 50 cm^3. The bed of particles was obtained by placing the graduated cylinder under the outlet of a single-screw volumetric feeder (Brabender, Duisburg, Germany) and then dropping 50 g of sample at 4 kg/h. The feeding rate (kg/h) was calculated by interpolating rotational speed curves (rpm) as a function of particulate mass, collected in 1 min.

2.10 Particle Density and Interparticle Porosity

The solid-phase volume (which excludes all open and closed pores) and skeletal volume (which is the closed pores) of individual particles that structure a particulate material were determined by the gas displacement method in a pycnometer system AccuPyc II 1340 (Micromeritics, Norcross, USA), using helium as displacement medium, according to Webb (2001). Then, the sum of the volumes was used as the total volume of the particles to calculate the particle density. The interparticle porosity was estimated according to equation (5) (MAROUSIS; SARAVACOS, 1990; ORTEGA-RIVAS, 2008).

$$\nu = \left(1 - \frac{\rho_b}{\rho_p} \right) 100\% \tag{5}$$

ρ_b and ρ_p are the bulk and particle densities of the particulate material, respectively.

2.11 Extrusion Process

The extrusion trials were performed in a single-screw extruder 19/20 DN 832500 (Brabender, Duisburg, Germany), composed of an internal grooved barrel, with two electric heating zones (set to 50 and 90 °C), and an L/D ratio of 20:1. The third electric heating zone

was a horizontal rod die mounted at the end of the extruder barrel (set to 120 °C). This frontal die was constituted of two inner compartments: a conical section (reduction in diameter from 19.05 to 7.94 mm and 12.70 mm in length) and a cylindrical section (57.15 mm in length). The cylindrical die at the horizontal rod tip had 3.0 mm in diameter and 14.29 mm in length. The set temperature profile was kept by an air cooling system ELMO-G 673420 (Brabender, Duisburg, Germany). The standard screw attached to the barrel had a 19 mm diameter and compression ratio of 5:1. The extruder was mounted on a universal-docking station 670237.001 (Brabender, Duisburg, Germany) to ensure that the screw shaft couples to a torque rheometer drive unit Plasti-Corder® Lab-Station (Brabender, Duisburg, Germany). The Brabender extruder program for Windows WINEXT, version 4.4.0 (Brabender, Duisburg, Germany) was used to set the operational variables: heating zones temperature (50, 90, and 120 °C) and screw speed (150 rpm), as well as to record net torque values (N m). Moist samples ("Moistening Process") were fed into the feeding zone by a single-screw volumetric feeder (Brabender, Duisburg, Germany). The feeding rate (kg/h) was previously set at 4 kg/h.

2.12 Experimental Design

Three experimental designs, each replicated twice, were performed to evaluate the impact of the studied factors, according to Figure 1. The design I was a single-factor experiment to evaluate the drying process. The factor was X_1 = moisture of grains before grinding (6%, 9%, and initial moisture: 12.8%, wet basis). Dependent variables were the bulk density of grains and pasting properties. Design II was a 3×2 factorial experiment to evaluate the drying and grinding processes. The factors were X_1 (6%, 9%, and initial moisture) and X_2 = grinder type (DM: disc mill, and RM: roller mill). Dependent variables were size parameters: D_{10}, D_{90}, and uniformity. Design III was a 2^3 factorial experiment to evaluate the drying, grinding and moistening processes. The factors were X_1 (6% and 9%), X_2 (DM and RM) and X_3 = moisture of particles before extrusion (11 and 14%, wet basis). The levels of X_3 were selected aiming to obtain expanded products by extrusion cooking and based on previous trials. Dependent variables were interparticle porosity and motor torque. All experimental trials within each design were carried out in random order.

2.13 Data Analysis

One-way ANOVA (analysis of variance) was performed on responses from design I and factorial ANOVA on responses from designs II and III. The null hypothesis was rejected when the probability value (p-value) for the statistic F_0 was less than 5% of significance level (α). In the 2^3 design, first-order polynomial models with two and three interactions were tested. The sum of squares in the ANOVAs and regression coefficients of the models were estimated according to the least-squares methodology (MONTGOMERY, 2013b). The significance of each regression coefficient in a model was performed according to the partial F test. Testing for lack of fit and R^2 for prediction based on PRESS (prediction error sum of squares) were used as criteria for model adequacy checking and predictive capability of the regression model, respectively (MONTGOMERY, 2013b). To depict the impact of the factors on responses, the multiple range test of Tukey, with $\alpha = 0.05$, was included in the graphs from the experiment I, and in the main and interaction plots from experiments II and III.

3 RESULTS AND DISCUSSION

3.1 Effect of Drying Process on Pasting Properties

The initial moisture content of the grains was $12.78 \pm 0.08\%$. After a drying period of 2.87 ± 0.07 h or 12.63 ± 0.04 h, the moisture of grains was $9.29 \pm 0.10\%$ or $6.32 \pm 0.05\%$, respectively. The closing of cracks in the endosperm (**Figure 2**A–C) and the increment in bulk density of dried grains ($p < 0.05$, **Figure 2**D), evidenced the shrinkage of grains exposed to drying. A shrunken grain is the result of sequential contractions of its compound starch granules inside each amyloplast, due to water desorption that took place from the amorphous channels in the granules (FITZGERALD, 2004).
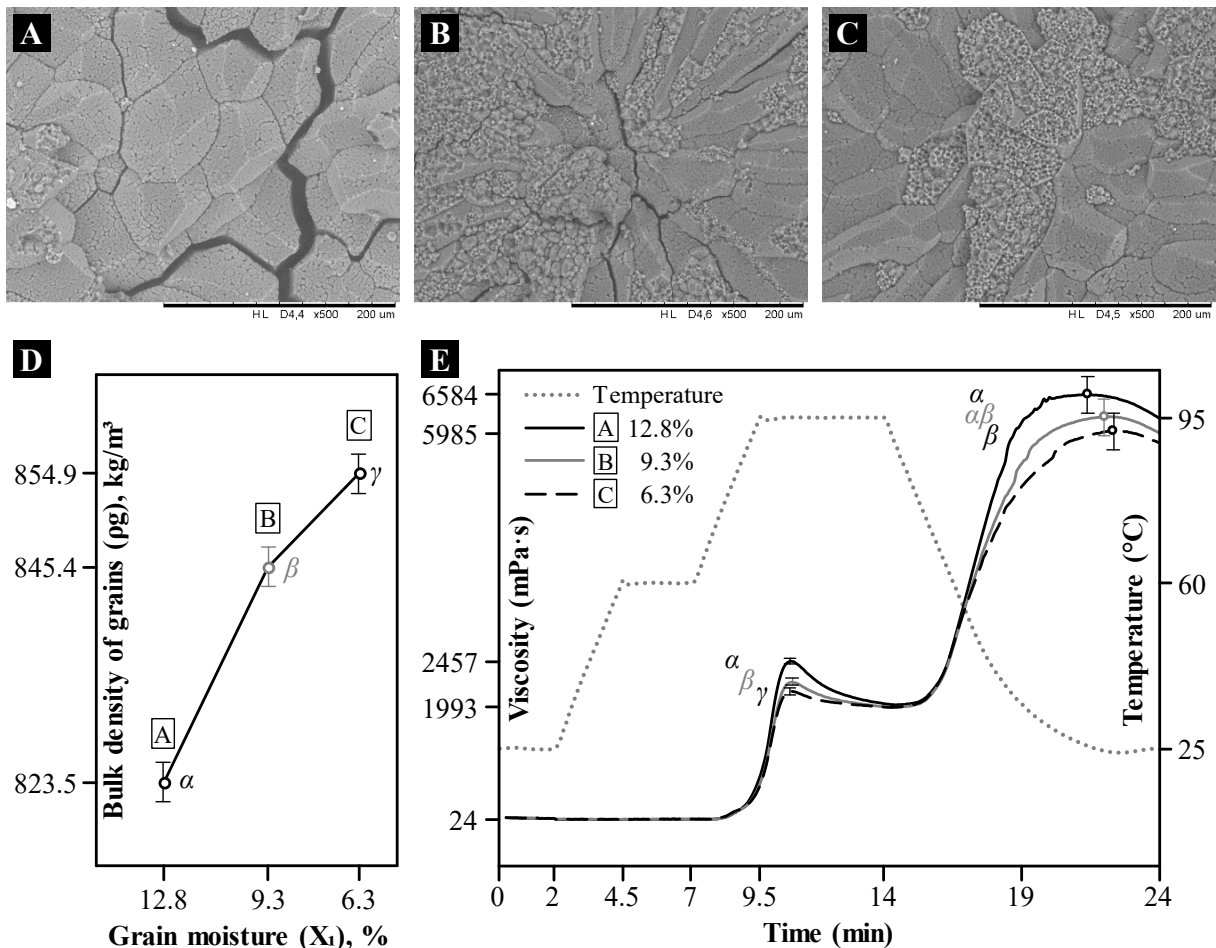
Figure 2. Microphotography ($\times$ 500) of the floury endosperm of brown rice grains from variable moisture content: (A) 12.78%, (B) 9.29%, and (C) 6.32%. (D) Bulk density of grains. (E) Paste viscosity profiles. Values with different Greek letters differ from each other according to the Tukey test.

According to the viscosity profiles (**Figure 2**E), the drying process did not affect the pasting onset (at 8.3 min and 77.8 °C) and the trough viscosity (at 14.3 min and 91 °C). No

97

starch swelling events were observed at the initial holding times of 25 °C and 60 °C. These observations rule out the possibility of any cold solubilization and starch conversion by heat transfer effect in prolonged drying periods. There was not observed any slight increment of viscosity before the onset time of pasting formation, which is associated with the presence of broken or damaged starches in the slurry (BOUVIER; CAMPANELLA, 2014). The drying process did affect the gelatinization peak (at 10.6 min and 95 °C) and the gelation peak (at 21.7 min and 25 °C). Peak viscosity decreased from 2457 to 1993 mPa·s, and breakdown viscosity did it from 676 to 248 mPa·s, as a result of the reduction in the moisture of grains from 12.78 to 6.32%. Chen (2014), also found a significant decrease in peak viscosity (from 2758 to 2643 mPa·s) when brown rice was treated with low-pressure plasma, operated at 2 kV. He claimed that plasma treatment reduced the integrity of the starch granular structure, causing the granules to lose their rigidity. In our case, the integrity of starch granules was kept, because of the gelatinization peak did not move to the left in the viscosity curves. After the gelation peaks, viscosity decreased significantly as a consequence of the thixotropic effects on the suspension induced by continuous stirring (BOUVIER; CAMPANELLA, 2014).

The decrease in the gelatinization peak can be attributed to the obstruction of the surface pores and/or of the channels that extend from these pores to the center of a starch granule. During the drying process, perhaps part of the lipids was diffused from the germ to the endosperm, according to the exposure time to drying. The formation of complexes on the surface of the granules would have caused this obstruction, increasing the granule rigidity, and consequently, the degree of granule swelling would have restricted during pasting formation. Besides, the restricted channels would have interfered with the degree of amylose leached, since the peak of gelation in the cooling stage of the suspension was also affected, mainly when grain moisture was reduced to 6.32% ($p < 0.05$). Channels are thought to facilitate the exchange of water to and from the starch granule and to provide exit points for amylose as it leaches out the granule during starch gelatinization (FITZGERALD, 2004).
These results showed that hot air drying induced slight physical modifications to the starch fraction of brown rice. Since decrements in the gelatinization peak are associated with more amylose content (SRICHUWONG et al., 2005), the drying process could be used for inducing resistant starch formation.

3.2 Effect of Drying and Grinding Processes on Particle-Size Distribution

The dried solid feeding helps to consume less energy during grinding. As the moisture content of solids is reduced, the dried product becomes brittle and, therefore, less resistant to grinding forces (WALDE et al., 2002). In a grinding process, grains are subjected to mechanical stress before the breakage. The stress is mostly stored as elastic energy (according to the type of mill) and is lost when grains fracture (BAUDELAIRE, 2013) giving rise to particles of different shapes.

Brown rice grains, with a moisture content of 12.78%, 9.29%, and 6.32%, were ground in a disc mill (DM) and a roller mill (RM), to study the pattern of particle-size distribution. Log-normal distributions by mass were achieved with nominal aperture sizes that ranged between 150 and 1400 μm for products from DM and between 75 and 425 μm for products from RM (Figure 3A). The average particles size by mass ± the average standard deviation of the distributions was 688 ± 319 μm for the DM products, and 210 ± 79 μm for the RM products.

The two-way ANOVA analysis (Table 1) confirmed the significant effects of grain moisture (X_1) and grinder type (X_2) on all size parameters ($p < 0.05$), and likewise the significant X_1X_2 interaction effect on small particles diameter (D_{10}), and uniformity.

Irrespective of grain moisture, the ground material in DM yielded significantly higher D_{10} values than the RM did (Figure 3B). In the disc type mill, D_{10} was significantly reduced
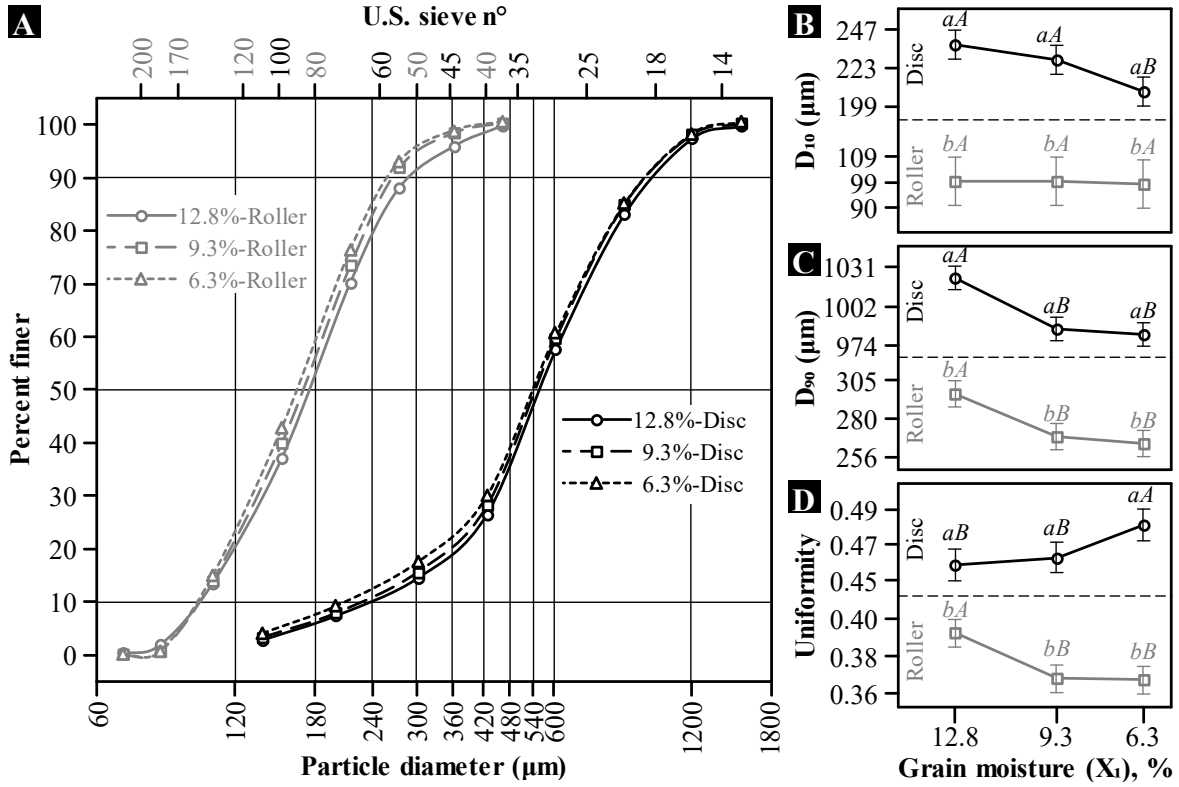
Figure 3. (A) Particle-size distribution curves; (B) Small particles diameter, D_{10}; (C) Large particles diameter, D_{90}; (D) Uniformity of the distribution. Values with different uppercase letters in the abscissa, and different lowercase letters in the ordinate, differ from each other according to the Tukey test.

only by changing grain moisture from 12.78 to 6.32%. The disappearance of cracks in the endosperm of the grains dried up to 6.32% moisture content (**Figure 2**C), may have helped to further fracture the grains, giving rise to low D_{10} values. In the roller type mill, the grain moisture effect was negligible on D_{10} because of grains were forced to pass through three contact areas, causing gradual particle size reduction.

Table 1. Analysis of variance (ANOVA) of independent variables and regression coefficients of linear models with interactions for responses from designs II and III.

	Statistical significance [a]							Regression coefficients			
	p-value of size parameters			ν		Ω			ν		Ω
Source	D_{10}	D_{90}	U	Source	*p*-value	Source	*p*-value				
X_1	**0.0150**	**<0.0001**	**<0.0001**	Model	**<0.0001**	Model	**<0.0001**	$\hat{\beta}_0$	61.587	$\hat{\beta}_0$	27.171
X_2	**<0.0001**	**<0.0001**	**0.0325**	X_1	**0.0007**	X_1	0.2367	$\hat{\beta}_1$	0.379	$\hat{\beta}_1$	-0.428
X_1X_2	**0.0209**	0.4798	**0.0010**	X_2	**<0.0001**	X_2	**0.0002**	$\hat{\beta}_2$	5.967	$\hat{\beta}_2$	-2.128
				X_3	**0.0014**	X_3	**<0.0001**	$\hat{\beta}_3$	0.341	$\hat{\beta}_3$	-3.920
				X_1X_2	**0.0025**	X_1X_2	**0.0075**	$\hat{\beta}_{12}$	-0.308	$\hat{\beta}_{12}$	1.189
				X_2X_3	**0.0032**	X_1X_3	**0.0187**	$\hat{\beta}_{23}$	0.296	$\hat{\beta}_{13}$	-0.984
				Lack of fit	0.2817	Lack of fit	0.6747	R^2_{Pred}	0.9961	R^2_{Pred}	0.8922

[a] Values significant at the 5% level are printed in bold-faced type. D_{10}: small particles diameter. D_{90}: large particles diameter. U: uniformity. ν: Interparticle porosity. Ω: Motor torque. X_i: Coded factors for grain moisture (X_1), grinder type (X_2), and feed moisture (X_3). R^2_{Pred}: R^2 for prediction.

Regardless of grain moisture, the ground material in DM also yielded significantly higher D_{90} values (large particle diameters) than the RM did (**Figure 3C**). Whatever type of mill used, the grains exposed to drying reduced significantly the D_{90} quantile. During the grinding process, cracks in the endosperm of the grains non-exposed to drying (**Figure 2A**), could have caused an increase in the amount of coarse particles (high D_{90} values).

The uniformity of the distribution was higher for products from DM (wider distributions) than products from RM (narrower distributions), irrespective of grain moisture (**Figure 3D**). In the RM products, uniformity decreased when dried grains were fed to the mill. In the DM products, uniformity increased only when dried grains with a moisture content of 6.32% were fed.

During a grinding process, new surfaces are created in which the size and shape of particles are influenced by the mill contact elements. Thus, the minor anatomical parts of the grain were differently distributed in the particulate material. In disc mills, whole grains are fed in the center of a stator disc and undergo instantly extensive shear by a rotor disc that operates at high speed. The particles are transported radially and in the course, subjected to successive impacts on the sharp steel protrusions found in both discs and on other particles, giving rise to coarse particles (high D_{10} and D_{90} values) of sub-angular to sub-rounded shapes (Figure 4A). In the DM products, the bran remained linked to the surface of the coarse particles (Figure 4A, sieve nº 18).
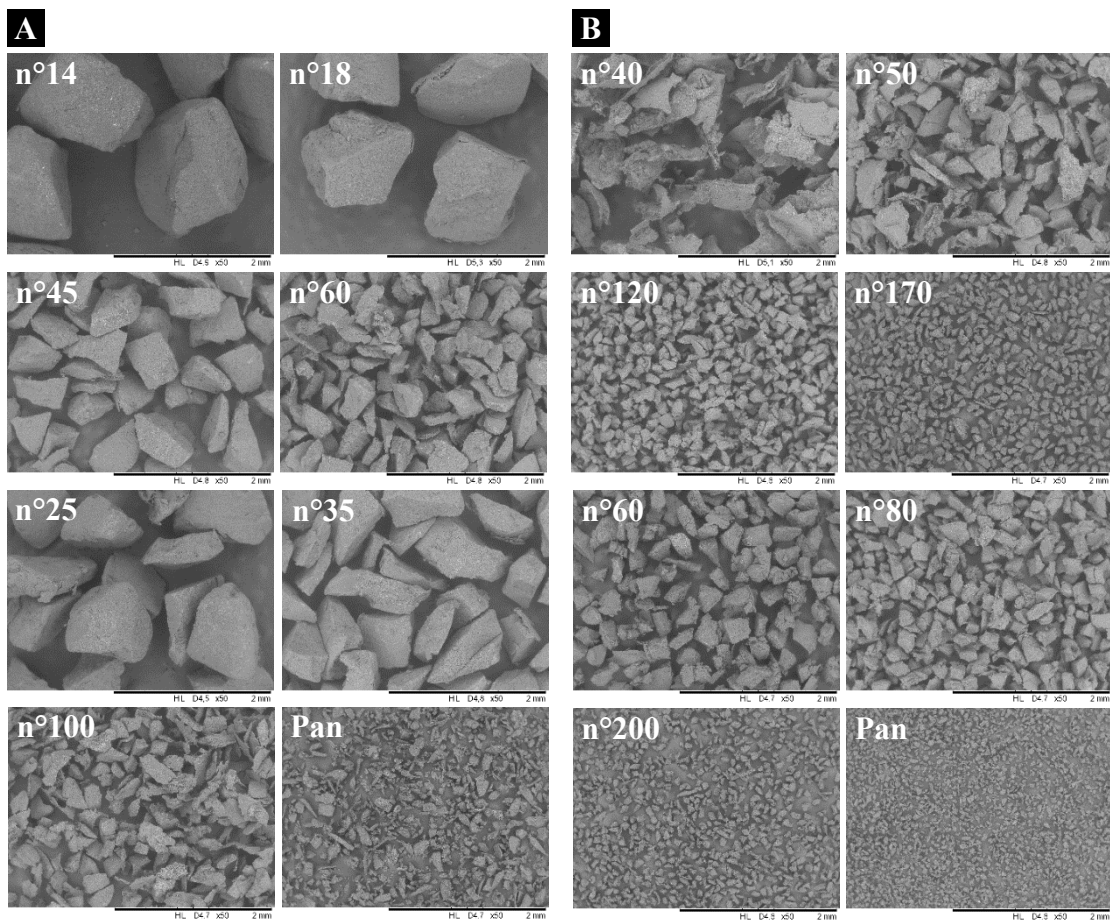
Figure 4. Microphotography ($\times$ 50) of brown rice particles, from grains non-exposed to drying, retained above sieves selected for the following: (A) Disc mill, *DM*; (B) Roller mill, *RM*.

Differently, in roller mills, sequential rotating wheels allow progressive size reduction of the grains in the mating surfaces. The particles are subjected to successive compressions on corrugated surfaces of the rolls and other particles (HICKEY; GIOVAGNOLI, 2018). Variations in the striations per centimeter and differential speed of the rolls led to fine particles (low D_{10} and D_{90} values) of angular to sub-angular shapes (Figure 4B). In the RM products, the bran was part of flaky particles in the coarse fraction (Figure 4B, sieve nº 40).

3.3 Effect of Pretreatment Conditions on Interparticle Porosity

A feeding material based on ground brown rice is an assembly of particles in which the void spaces between the particles are surrounded by air and partially filled with water. After the moistening step, the average moisture of brown rice particles was $11.32 \pm 0.15\%$ or $14.46 \pm 0.29\%$, according to the wetted condition. The moist samples presented an average particle density of 1457 ± 5 kg/m^3, and the average bulk density was 645 ± 11 kg/m^3 for the DM products and 474 ± 11 kg/m^3 for the RM products. Variations in bulk density of particulate foods are mainly caused by moisture content and particle size. For the grinding of yam slices using an attrition mill, Badmus, Raji and Akinoso (2013) previously dried the slices between 8 and 24% moisture content (wet basis). The moisture content in the feeding significantly influenced the bulk density of the yam flour, which ranged between 540 and 660 kg/m^3.

Changes in moisture can affect the number of interparticle contact points structuring a bed of particles, by altering the interaction forces between particles close to one another, thereby affecting their bulk porosity (BARBOSA-CÁNOVAS; JULIANO, 2005). Accordingly, the moist samples before the extrusion process resulted in interparticle porosity (ν) values between 54.6% and 68.6%.

From the factorial ANOVA analysis (Table 1), interparticle porosity significantly was influenced by all main effects and by the X_1X_2 and X_2X_3 interaction effects ($p < 0.05$). The non-significant terms (X_1X_3 and $X_1X_2X_3$) were used to compute the lack of fit of the model. Taking into account the non-significant lack of fit (p-value > 0.05), the linear model with interactions provided an adequate approximation for the true response surface of interparticle porosity, within the region of experimentation. The five predictors in the model were necessary terms (adjusted R^2 of 0.9977) to explain the interparticle porosity variability. The fitting model had a PRESS value of 2.27, which computed a prediction R^2 of 0.9961, a very satisfactory predictive capability. It is expected this model to explain more than 99% of the variability in predicting new interparticle porosity values.

Grinder type had a greater influence in the brown rice pretreatment, accounting for more than 98% on the interparticle porosity variability. The DM products presented lower values than the RM products (Figure 5B). The RM produces smaller and irregularly shaped particles (**Figure 4B**), which hinders their agglomeration, giving rise to a higher interparticle porosity. On the contrary, the particles coming from the DM are larger and rounded (**Figure 4A**), facilitating their agglomeration, resulting in a lower interparticle porosity.

By changing grain moisture from 9.29 to 6.32%, interparticle porosity decreased (**Figure 5A**). This effect was pronounced for the DM products and was negligible for the RM products (**Figure 5D**). This can be associated with a decrease in the D_{10} value (**Figure 3B**) which computed a correlation coefficient of $+ 0.8194$ ($p < 0.05$). Sub-rounded and small particles will agglomerate close to one another, resulting in a bed of particles with low interparticle porosity. The reduction in grain moisture could also lead to an increased rounding degree to the extent that the grains were fed drier. Rounded morphology particles have more sphericity and pack more tightly than angular particles (DODDS, 2013).

By changing feed moisture from 11.32 to 14.46%, interparticle porosity increased (**Figure 5C**). This effect was pronounced for the RM products and was negligible for the DM

products (**Figure 5E**). This can be attributed to the morphology of the particles that structure a RM product, in which more divided materials with larger specific surface areas outstand (**Figure 4B**). By the sequential action of the corrugated surfaces on the rolls, it seems that amyloplasts grouped in a particle are broken to a greater extend, increasing the open pores in the surface of the particles. These open pores were filled with water in the moistening process. It is possible that the subsequent moisture diffusion inward the compound granules have caused volume variations, according to the degree of wetting, giving rise to changes in interparticle porosity.
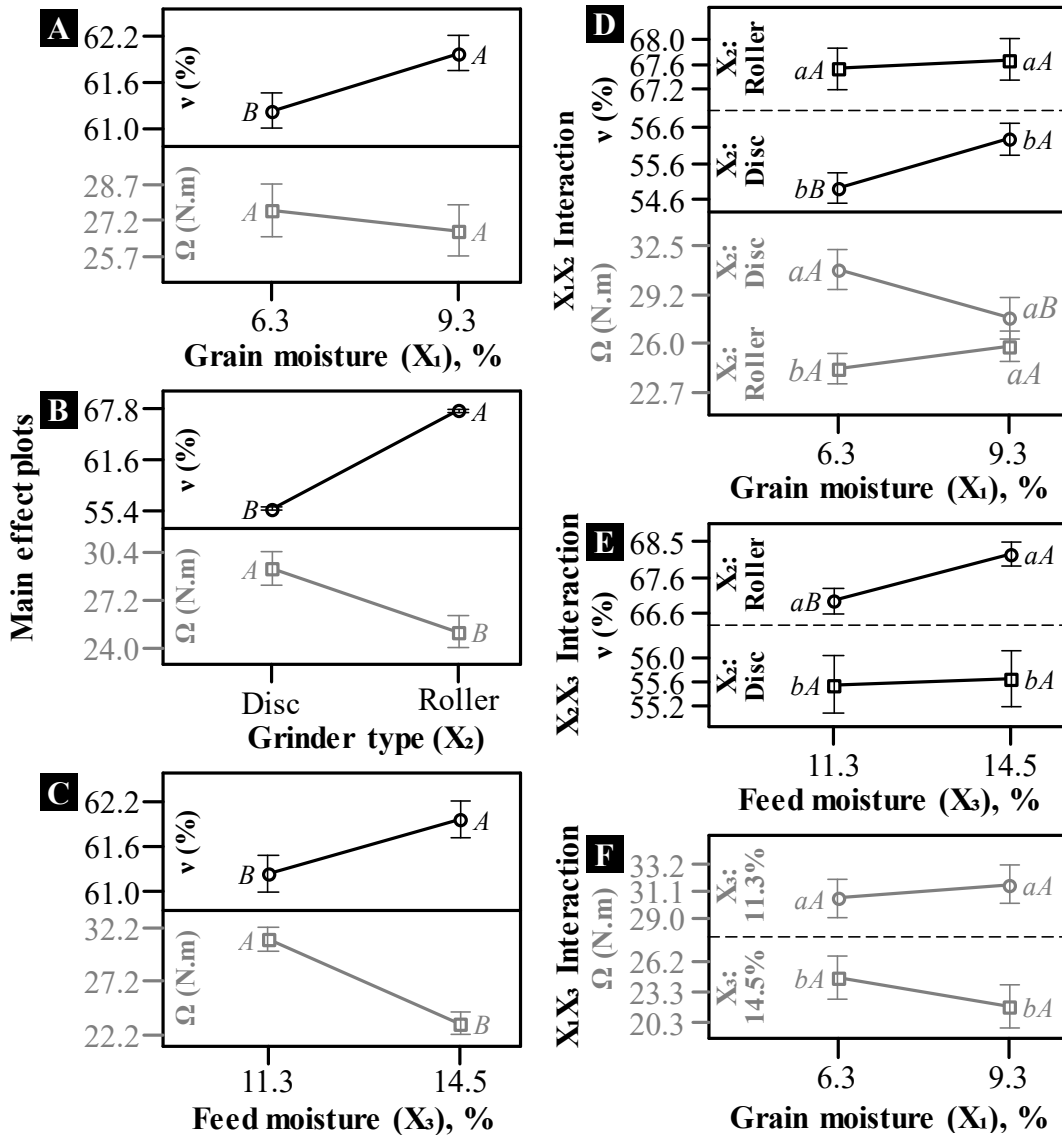
Figure 5. Effect of pretreatment conditions on interparticle porosity (ν) and motor torque (Ω): (A–C) Main effect plots; (D–F) Interaction plots. Values with different uppercase letters in the abscissa, and different lowercase letters in the ordinate, differ from each other according to the Tukey test.

3.4 Effect of Pretreatment Conditions on Motor Torque

The torque (Ω) supplied to the screw during the extrusion process of ground brown rice ranged between 20.0 and 34.4 N·m. Since interaction terms involving grain moisture before milling (X_1) were significant in the ANOVA analysis (Table 1), this non-significant term was left in the model to preserve hierarchy (MONTGOMERY, 2013a). The other non-significant terms (X_2X_3 and $X_1X_2X_3$) were dropped from the full model resulting in a reduced model with non-significant lack of fit (p-value > 0.05). The five predictors in the model were necessary terms (adjusted R^2 of 0.9368) to explain the torque variability. The reduced model had a PRESS value of 40.46, leading to a value of R^2_{Pred} of 0.8922. This model is suitable to predict new torque values (> 89% of the variability) in the range of the studied conditions for process characterization purposes. The torque had a satisfactory negative correlation (– 0.8952, p-value < 0.05) with interparticle porosity of RM ground products, but a poor negative correlation (– 0.3912, p-value ≥ 0.05) with interparticle porosity of DM ground products. This means that RM ground products are more suitable for correlating the interparticle porosity and the torque. This can be attributed to its narrower particle-size distribution with low particle diameters in the fine and coarse fractions.

The torque variability at constant extrusion operational variables was mainly influenced by the grinder type used to prepare feed materials and the feed moisture, which accounted for more than 19% and 65% respectively. The DM ground products generated higher torque values than the RM ground products (**Figure 5B**), which was further increased by changing grain moisture before grinding from 9.29 to 6.32% (**Figure 5D**). However, the change in grain moisture was negligible in the torque variability for the RM ground products.

DM materials could have been compacted more than RM materials in the compression section due to geometric differences between its particles, previously discussed. Consolidated solid particles present high cohesive strength. Cohesion or interparticle attraction is responsible for the caking of the particles during processing (ORTEGA-RIVAS, 2008), which can affect the transition of the solid particles into a fluid melt. During the extrusion process at very low moisture content, frictional forces arising from the screw mechanical shearing cause the melting of crystallites structuring the starch granules, protein bodies, protein networks, and fibers present in the cell walls of the endosperm and bran. Starch polymers and proteins are easy to melt; meanwhile, insoluble fibers are hard to melt. According to the size and shape of particles, the melt viscosity development in the extruder and motor torque changes will occur. If there is still remaining material in solid-state that reaches the metering section, the partially melted material would cause an extra increase in the shear viscosity of the melt. Zhang and Hoseney (1998) reported that coarse and untempered corn particles were not melted completely during extrusion. This is less likely to occur with fine particles in the feed material, in which the heat transfer is more effective from the surface to the center of the particle. The fine particles in the RM ground products could have produced easy-to-pump molten materials in the metering section, causing the torque to decrease. This observed effect on torque was similar to that reported by Wang et al. (2017), wherein the feed materials, based on blends of corn starch and cherry pomace powder fractionated at various particle sizes, affected the torque. The treatment with the smallest particle size had the lowest torque values.

By changing feed moisture from 11.32 to 14.46%, the torque decreased (**Figure 5C**), irrespective of grain moisture (**Figure 5F**). The water content in the feed is the main lubricating agent to decrease the frictional forces that feed material causes in the annular space between the screw and the extruder barrel. The fiber and fat contents in the brown rice particles also performed a lubricant effect, by lowering the die pressure (SINGH GUJRAL; SINGH, 2002), as a result of a decrease in the shear viscosity of the melt, which, in turn, will require less torque to work the material in the screw channel (AKDOGAN, 1996; ROBIN et al., 2012b). Due to

the fiber and fat contents present in feed materials based on brown rice, it was necessary to extrude at low feed moistures to get expanded extrudates, as was performed in the study of O'shea, Arendt and Gallagher (2014), in which the feed moisture of blends, based on cornflour enriched with apple pomace, was fixed at 10.5% (wet basis), resulting in extruded snacks with good expansion characteristics.
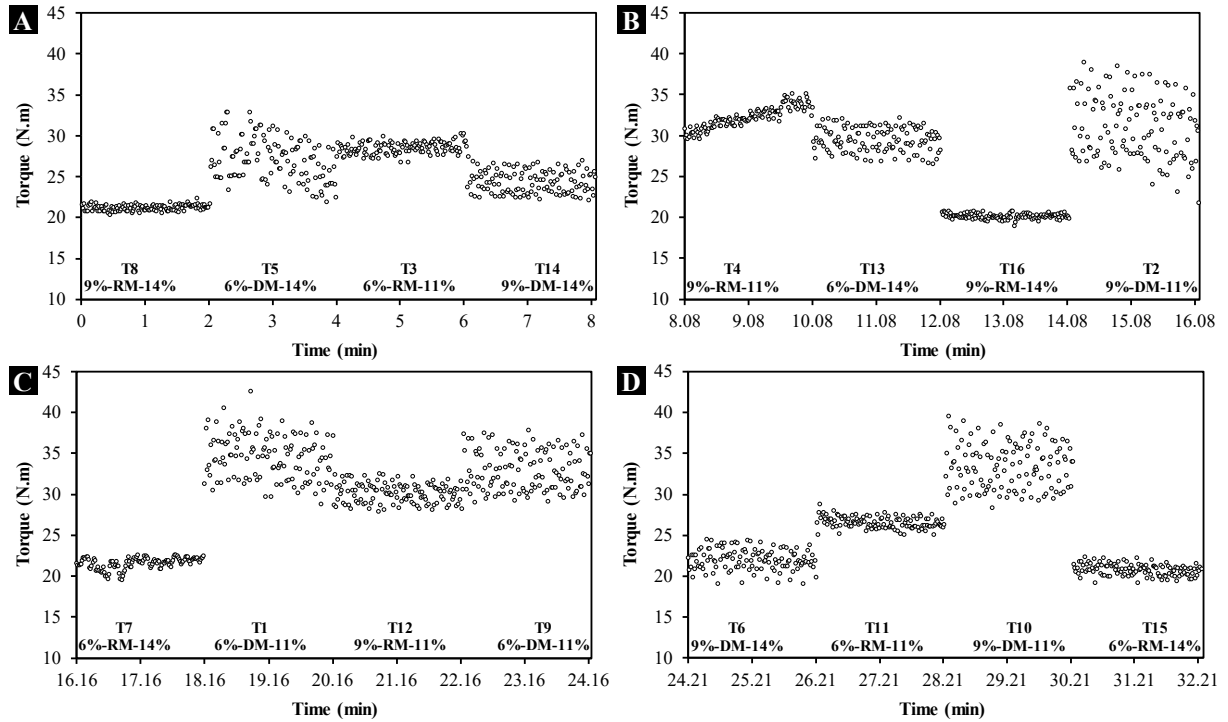
Figure 6. A–D: Torque values plot registered in random order during the extrusion experiment at constant barrel temperature profile (50, 90, and 120 °C), screw speed (150 rpm) and feeding rate (4 kg/h). Grain moisture before milling varied between 6 and 9%. The feed material was obtained with two grinder types: Disc mill (*DM*) and Roller mill (*RM*). Feed moisture varied between 11 and 14%.

The variability in torque was high with the disc mill products as feeding material (**Figure 6A–D**). This can be attributed to a wider particle-size distribution showed by these products, which ranged from 138 to 1545 μm, as compared to the roller mill products, which ranged from 69 to 463 μm (**Figure 3A**). **Figure 6** also reveals that the particulate materials of both mill types produced a greater variability in torque when the feed moisture was 11%. This behavior can influence the expansion and texture of extruded products. The feed materials produced with the roller mill and moistened to 14%, generated less variability in torque, which will produce extrudates with more uniform air cell structures and will reflect the quality of the extrudates.

4 CONCLUSION

The roller mill ground products were more suitable for a negative correlation between the interparticle porosity of feed material and the torque supplied to the screw during the extrusion processing of brown rice ($r = -0.8952$). The drying process increased the bulk density of the grains and caused slight physical modifications in the brown rice starch fraction, by decreasing the gelatinization peak and gelation peak in the RVA viscosity profiles. The use of disc and roller mills to grind brown rice affected the particle-size distributions, the interparticle porosity, and the torque. Independent of drying the grains, the roller mill materials presented narrower particle-size distributions with lower particle diameters in the fine (D_{10}) and coarse (D_{90}) fractions than the disc mill materials. The disc mill materials presented lower interparticle porosity and generated higher torque values than the roller mill materials, which was further decreased the interparticle porosity and increased the torque, by changing grain moisture before milling from 9 to 6%. However, the change in grain moisture was negligible in the interparticle porosity and the torque for the roller mill materials. By changing feed moisture from 11 to 14%, only the interparticle porosity of roller mill materials increased. The torque decreased with an increment in feed moisture, irrespective of grain moisture before milling. According to the grinder type and feed moisture, brown rice particles exhibited different behavior during the extrusion process. High torque instability was observed when disc mill materials were processed in a single-screw extruder at low feed moisture. In contrast, stable torque was achieved using roller mill materials extruded at 14% of feed moisture. For obtaining extrudates with good expansion, it is recommended to prepare brown rice using roller mill at 11% of feed moisture. These findings could reflect the degree of anisotropy of the extrudates according to the sample preparation. Feed materials with high interparticle porosity could produce extrudates less anisotropic (low and stable torque), contributing to more efficient energy use.

REFERENCES

AKDOGAN, H. Pressure, torque, and energy responses of a twin screw extruder at high moisture contents. **Food Research International**. v. 29, n. 5, p. 423-429, 1996.

ALAM, S. A.; JÄRVINEN, J.; KIRJORANTA, S.; JOUPPILA, K.; POUTANEN, K.; SOZER, N. Influence of Particle Size Reduction on Structural and Mechanical Properties of Extruded Rye Bran. **Food and Bioprocess Technology**. v. 7, n. 7, p. 2121-2133, 2014.

AOAC. **Official Methods of Analysis of AOAC International**. 18th ed. AOAC International: Gaithersburg, 2005.

ASABE STANDARDS. **Method of determining and expressing fineness of feed materials by sieving**. In. ANSI/ASAE S319.4. American Society of Agricultural and Biological Engineers: Michigan, 2008.

BADMUS, A. A.; RAJI, A. O.; AKINOSO, R. Effect of Process Parameters on Work Index, Milling Efficiency and Some Technological Properties of Yam Flour Using Attrition Mill. **Food and Bioprocess Technology**. v. 6, n. 1, p. 160-168, 2013.

BALA, B. K. Principles of drying. In: BALA, B. K. (Ed.). **Drying and Storage of Cereal Grains**. 2nd ed. Wiley Blackwell: Chichester, 2017. p. 1-3.

BARBOSA-CÁNOVAS, G. V.; JULIANO, P. Physical and chemical properties of food powders. In: ONWULATA, C. (Ed.). **Encapsulated and Powdered Foods**. CRC Press: Boca Raton, 2005. p. 39-71.

BARBOSA-CÁNOVAS, G. V.; ORTEGA-RIVAS, E.; JULIANO, P.; YAN, H. Size reduction. In: **Food Powders: Physical Properties, Processing, and Functionality**. Springer US: Boston, MA, 2005. p. 157-173.

BAUDELAIRE, E. D. Grinding for food powder production. In: BHANDARI, B. et al. (Eds.). **Handbook of Food Powders**. Woodhead Publishing: Cambridge, 2013. p. 132-149.

BECKER, A.; HILL, S. E.; MITCHELL, J. R. Milling—A Further Parameter Affecting the Rapid Visco Analyser (RVA) Profile. **Cereal Chemistry**. v. 78, n. 2, p. 166-172, 2001.

BOOTKOTE, P.; SOPONRONNARIT, S.; PRACHAYAWARAKORN, S. Process of Producing Parboiled Rice with Different Colors by Fluidized Bed Drying Technique Including Tempering. **Food and Bioprocess Technology**. v. 9, n. 9, p. 1574-1586, 2016.

BOUVIER, J.-M.; CAMPANELLA, O. H. Quality analysis of extrusion-textured food products. In: BOUVIER, J.-M.; CAMPANELLA, O. H. (Eds.). **Extrusion Processing Technology**. John Wiley & Sons, Ltd: Chichester, 2014. p. 311-349.

CHEN, H. H. Investigation of Properties of Long-grain Brown Rice Treated by Low-pressure Plasma. **Food and Bioprocess Technology**. v. 7, n. 9, p. 2484-2491, 2014.

CISNEROS, F. H.; KOKINI, J. L. A generalized theory linking barrel fill length and air bubble

entrapment during extrusion of starch. **Journal of Food Engineering**. v. 51, n. 2, p. 139-149, 2002.

DING, C.; KHIR, R.; PAN, Z.; ZHAO, L.; TU, K.; EL-MASHAD, H.; MCHUGH, T. H. Improvement in Shelf Life of Rough and Brown Rice Using Infrared Radiation Heating. **Food and Bioprocess Technology**. v. 8, n. 5, p. 1149-1159, 2015.

DING, Q.-B.; AINSWORTH, P.; TUCKER, G.; MARSON, H. The effect of extrusion conditions on the physicochemical properties and sensory characteristics of rice-based expanded snacks. **Journal of Food Engineering**. v. 66, n. 3, p. 283-289, 2005.

DODDS, J. Techniques to analyse particle size of food powders. In: BHANDARI, B. et al. (Eds.). **Handbook of Food Powders**. Woodhead Publishing: Cambridge, 2013. p. 309-338.

FITZGERALD, M. Starch. In: **Rice Chemistry and Technology**. 3rd ed. American Association of Cereal Chemists, Inc., 2004. p. 109-141.

GONZÁLEZ, R. J.; PASTOR CAVADA, E.; VIOQUE PEÑA, J.; TORRES, R. L.; DE GREEF, D. M.; DRAGO, S. R. Extrusion Conditions and Amylose Content Affect Physicochemical Properties of Extrudates Obtained from Brown Rice Grains. **International Journal of Food Science**. v. 2013, p. 1-8, 2013.

GUJRAL, H. S.; SHARMA, P.; KUMAR, A.; SINGH, B. Total phenolic content and antioxidant activity of extruded brown rice. **International Journal of Food Properties**. v. 15, n. 2, p. 301-311, 2012.

HICKEY, A. J.; GIOVAGNOLI, S. Powder and particle-dependent traditional manufacturing processes (Unit Operations). In: **Pharmaceutical Powder and Particles**. Springer International Publishing: Cham, 2018. p. 61-71.

HOURSTON, J. E.; IGNATZ, M.; REITH, M.; LEUBNER-METZGER, G.; STEINBRECHER, T. Biomechanical properties of wheat grains: the implications on milling. **Journal of The Royal Society Interface**. v. 14, n. 126, 2017.

HUANG, M.-s.; ZHANG, M.; BHANDARI, B. Assessing the 3D Printing Precision and Texture Properties of Brown Rice Induced by Infill Levels and Printing Variables. **Food and Bioprocess Technology**. v. 12, n. 7, p. 1185-1196, 2019.

JOSHI, N. D.; MOHAPATRA, D.; JOSHI, D. C. Varietal Selection of Some Indica Rice for Production of Puffed Rice. **Food and Bioprocess Technology**. v. 7, n. 1, p. 299-305, 2014.

JULIANO, B. O. Rice properties and processing. **Food Reviews International**. v. 1, n. 3, p. 423-445, 1985.

KIM, M. Y.; LEE, S. H.; JANG, G. Y.; LI, M.; LEE, Y. R.; LEE, J.; JEONG, H. S. Influence of Applied Pressure on Bioactive Compounds of Germinated Rough Rice (Oryza sativa L.). **Food and Bioprocess Technology**. v. 8, n. 10, p. 2176-2181, 2015.

MA, J.; KAORI, F.; MA, L.; GAO, M.; DONG, C.; WANG, J.; LUAN, G. The effects of extruded black rice flour on rheological and structural properties of wheat-based dough and bread quality. **International Journal of Food Science and Technology**. v. 54, n. 5, p. 1729-1740, 2019.

MAROUSIS, S. N.; SARAVACOS, G. D. Density and Porosity in Drying Starch Materials. **Journal of Food Science**. v. 55, n. 5, p. 1367-1372, 1990.

MARTI, A.; SEETHARAMAN, K.; PAGANI, M. A. Rice-based pasta: A comparison between conventional pasta-making and extrusion-cooking. **Journal of Cereal Science**. v. 52, n. 3, p. 404-409, 2010.

MATHEW, J. M.; HOSENEY, R. C.; FAUBION, J. M. Effects of corn sample, mill type, and particle size on corn curl and pet food extrudates. **Cereal Chemistry**. v. 76, n. 5, p. 621-624, 1999.

MONTGOMERY, D. C. The 2^k factorial design. In: **Design and analysis of experiments**. 8th ed. Wiley: Hoboken, 2013a. p. 233-303.

MONTGOMERY, D. C. Fitting regression models. In: **Design and analysis of experiments**. 8th ed. Wiley: Hoboken, 2013b. p. 449-477.

O'SHEA, N.; ARENDT, E.; GALLAGHER, E. Enhancing an Extruded Puffed Snack by Optimising Die Head Temperature, Screw Speed and Apple Pomace Inclusion. **Food and Bioprocess Technology**. v. 7, n. 6, p. 1767-1782, 2014.

OHTSUBO, K. i.; SUZUKI, K.; YASUI, Y.; KASUMI, T. Bio-functional components in the processed pre-germinated brown rice by a twin-screw extruder. **Journal of Food Composition and Analysis**. v. 18, n. 4, p. 303-316, 2005.

ORTEGA-RIVAS, E. Bulk Properties of Food Particulate Materials: An Appraisal of their Characterisation and Relevance in Processing. **Food and Bioprocess Technology**. v. 2, n. 1, p. 28, 2008.

PARDHI, S. D.; SINGH, B.; NAYIK, G. A.; DAR, B. N. Evaluation of functional properties of extruded snacks developed from brown rice grits by using response surface methodology. **Journal of the Saudi Society of Agricultural Sciences**. v. 18, n. 1, p. 7-16, 2019.

ROBIN, F.; DATTINGER, S.; BOIRE, A.; FORNY, L.; HORVAT, M.; SCHUCHMANN, H. P.; PALZER, S. Elastic properties of extruded starchy melts containing wheat bran using on-line rheology and dynamic mechanical thermal analysis. **Journal of Food Engineering**. v. 109, n. 3, p. 414-423, 2012a.

ROBIN, F.; DUBOIS, C.; PINEAU, N.; LABAT, E.; THÉODULOZ, C.; CURTI, D. Process, structure and texture of extruded whole wheat. **Journal of Cereal Science**. v. 56, n. 2, p. 358-366, 2012b.

SHASHIDHAR, M. G.; MURTHY, T. P. K.; GIRISH, K. G.; MANOHAR, B. Grinding of Coriander Seeds: Modeling of Particle Size Distribution and Energy Studies. **Particulate Science and Technology**. v. 31, n. 5, p. 449-457, 2013.

SINGH GUJRAL, H.; SINGH, N. Extrusion behaviour and product characteristics of brown and milled rice grits. **International Journal of Food Properties**. v. 5, n. 2, p. 307-316, 2002.

SINGH, S.; GAMLATH, S.; WAKELING, L. Nutritional aspects of food extrusion: a review. **International Journal of Food Science and Technology**. v. 42, n. 8, p. 916-929, 2007.

SINIJA, V. R.; SULOCHANA, S.; SHWETHA, M. S. Engineering properties of brown rice from selected indian varieties. In: MANICKAVASAGAN, A.; SANTHAKUMAR, C.; VENKATACHALAPATHY, N. (Eds.). **Brown Rice**. Springer International Publishing: Cham, 2017. p. 45-65.

SRICHUWONG, S.; SUNARTI, T. C.; MISHIMA, T.; ISONO, N.; HISAMATSU, M. Starches from different botanical sources II: Contribution of starch structure to swelling and pasting properties. **Carbohydrate Polymers**. v. 62, n. 1, p. 25-34, 2005.

VERGNES, B.; VILLEMAIRE, J. P. Rheological behaviour of low moisture molten maize starch. **Rheologica Acta**. v. 26, n. 6, p. 570-576, 1987.

WALDE, S. G.; BALASWAMY, K.; VELU, V.; RAO, D. G. Microwave drying and grinding characteristics of wheat (Triticum aestivum). **Journal of Food Engineering**. v. 55, n. 3, p. 271-276, 2002.

WANG, L.; DUAN, W.; ZHOU, S.; QIAN, H.; ZHANG, H.; QI, X. Effects of extrusion conditions on the extrusion responses and the quality of brown rice pasta. **Food Chemistry**. v. 204, p. 320-325, 2016.

WANG, S.; KOWALSKI, R. J.; KANG, Y.; KISZONAS, A. M.; ZHU, M.-J.; GANJYAL, G. M. Impacts of the Particle Sizes and Levels of Inclusions of Cherry Pomace on the Physical and Structural Properties of Direct Expanded Corn Starch. **Food and Bioprocess Technology**. v. 10, n. 2, p. 394-406, 2017.

WEBB, P. A. Volume and density determinations for particle technologists. **Micromeritics Instrument Corp**. v. 2, n. 16, p. 01-16, 2001.

XU, E.; WU, Z.; LONG, J.; WANG, F.; PAN, X.; XU, X.; JIN, Z.; JIAO, A. Effect of Thermostable α-Amylase Addition on the Physicochemical Properties, Free/Bound Phenolics and Antioxidant Capacities of Extruded Hulled and Whole Rice. **Food and Bioprocess Technology**. v. 8, n. 9, p. 1958-1973, 2015.

ZHANG, W.; HOSENEY, R. C. Factors affecting expansion of corn meals with poor and good expansion properties. **Cereal Chemistry**. v. 75, n. 5, p. 639-643, 1998.

ZHU, S. M.; HU, F. F.; RAMASWAMY, H. S.; YU, Y.; YU, L.; ZHANG, Q. T. Effect of High Pressure Treatment and Degree of Milling on Gelatinization and Structural Properties of Brown Rice. **Food and Bioprocess Technology**. v. 9, n. 11, p. 1844-1853, 2016.

Transition Chapter IV to Chapter V

Summarizing chapter IV, the grinding conditions in both mill types (disc and roller) to mill grains dried up to 6 and 9% (wet basis) and the extrusion runs at two feed moisture levels (11 and 14%, wet basis), were performed as described in chapter III.

These conditions allowed correlating the interparticle porosity of the feed material with the torque readings of the melt, which correspond to the non-expanded extrudate just before leaving the extruder.

Grain moisture before milling only affected the interparticle porosity (ν) and the torque (Ω) of disc mill products (a change from 6 to 9%, decreased ν and increased Ω). Feed moisture only affected ν of roller mill products (a change from 11 to 14%, increased Ω). The torque decreased with an increment in feed moisture, irrespective of grain moisture before milling. High torque instability was observed when disc mill materials were processed at low feed moisture. In contrast, stable torque was achieved using roller mill materials extruded at 14% of feed moisture. Feed materials with high interparticle porosity could produce extrudates less anisotropic (low and stable torque).

In chapter V, the brown rice processing was carried out according to these drying, grinding, and extrusion conditions, but exploring the grain moisture levels before milling in the range of 9 to 11% (wet basis), and in addition to these variables, the experiment was complemented with the following extrusion conditions: the screw speed was explored in the range of 150 to 250 rpm, and the feed rate of particles in the range of 4 to 6 kg/h. The experiment was designed to identify major independent variables and to correlate extrusion dependent variables (melt temperature, torque, and specific mechanical energy) with the expansion and texture properties of the extrudates.

CHAPTER V

EFFECT OF DRYING, MILLING, FEED MOISTURE, FEED RATE AND SCREW SPEED ON BROWN RICE SINGLE-SCREW EXTRUSION

Effect of drying, milling, feed moisture, feed rate and screw speed on brown rice single-screw extrusion

Jhony Willian Vargas-Solórzano [a] *, José Luis Ramírez Ascheri [b], Carlos Wanderlei Piler de Carvalho [b].

[a] Postgraduate Program in Food Science and Technology. Federal Rural University of Rio de Janeiro. Rodovia Br 465, km 7, CEP 23890-000, Seropédica, RJ – Brazil.
[b] Embrapa Agroindústria de Alimentos, Food Extrusion and Physical Properties Lab., Avenida das Américas 29501, Guaratiba, CEP 23020-470, Rio de Janeiro, RJ – Brazil.

* Corresponding author: jwvargass@ufrrj.br; vargasjw@gmail.com

ABSTRACT

Brown rice extruded snacks were obtained in a single-screw extruder. Five factors were investigated in a 2_V^{5-1} design with the objective of correlate extrusion dependent variables with the expansion and texture properties of brown rice extrudates. The five factors were X_1 = grain moisture before grinding (9% and 11%), X_2 = milling type (disc, roller), X_3 = feed moisture (11 and 14%), X_4 = screw speed (150 and 250 rpm), and X_5 = feed rate (4 and 6 kg/h). The important effects that emerged for torque were X_3, X_4, and X_5. Highest torques were achieved with X_3 and X_4 at the low level and, X_5 at the high-level. The specific mechanical energy (SME) was only influenced by the main effects of X_3 and X_4. SME increased when brown rice was processed at the low-level of X_3 and at the high level of X_4. Expansion properties were influenced by the main effects of X_2, X_3 and X_4, and only the X_3X_4 interaction was important for sectional expansion. Highest expansion indexes were obtained with grains milled in a roller mill (X_2, roller) and when X_3 was at the low-level and X_4 at the high-level. The average puncturing force of extrudates (F_p) presented dependence of X_2, X_4 and X_5. Lowest puncturing forces were obtained with grains milled in a roller mill and when X_4 was at the high-level and X_5 at the low-level. A positive correlation was observed between torque and F_p. SME positively correlated with expansion properties and presented a power-law correlation with apparent density. Linear models based on significant independent variables made possible the prediction and consequently the design of brown rice extruded snacks with acceptable expansion and texture characteristics.

Keywords: Whole grain. Extrusion cooking. Expansion property. Instrumental texture.

1 INTRODUCTION

The intake of foods rich in dietary fibers is associated with decreased risks of obesity, metabolic syndrome, diabetes, and coronary heart disease (SONG et al., 2014). The health benefits of dietary fibers promote a high demand to develop novelty products that diversify the tastes and textures without losing the nutritional attributes. Extrusion technology is widely used to process cereals and is a useful technique to increase the range of whole-grain based products. Besides, this technology does not generate by-products, performs physical and chemical modifications on macromolecular components, mainly starch, proteins, and fibers, producing preservative-free foods. These features are very important for consumers, whose increasingly are looking for processed products based on whole grains and preserved by physical methods.

Traditional extruded snacks based on white rice are rich in carbohydrates from the endosperm and poor in nutrients from bran and germ. Thiamin content in rice grains with light brown pericarp is some four times higher than for white rice. This variety also provides some phenolic acid content, mainly ferulic and p-coumaric acids, both linked via ester bonds: ferulic acid to the arabinoxylans of aleurone cell walls and p-coumaric acid to the lignins of pericarp outermost cell walls (ZHOU et al., 2004). However, the extrusion cooking process with high-temperature profiles can develop phenolic decarboxylation and processing at high moisture contents can promote phenols polymerization (BRENNAN et al., 2011). There is also the possibility of these compounds to undergo complexes-formation with the major components of the grain: starch and protein polymers. The minority components in brown rice act as reactant ingredients in a natural way and the final content of them will depend on the process severity during extrusion cooking. Despite all, the brown rice extrudates will retain its advantage over the white rice extrudates.

The rate of complexes formation by using thermo-mechanical cooking is little understood. Flour components are simultaneously subjected to shear forces combined with moisture and heat. These conditions promote a broad interval of physical modifications and/or complexation of minority components with macromolecules, reflecting on the performance of expansion and texture characteristics.

To increase the nutrient density of rice-based expanded extrudates, many works were performed by adding rice bran or vegetable sub-products mixed with a protein source (ALAM; PATHANIA; SHARMA, 2016; DEHGHAN-SHOAR; HARDACRE; BRENNAN, 2010; LIU et al., 2011; SINGH; SEKHON; SINGH, 2007; YAĞCı; GÖĞÜŞ, 2008). To the present, some studios were focused on the extrusion of brown rice (PARDHI et al., 2019; PASTOR-CAVADA et al., 2011; SUMARGO et al., 2016). In all cases, these fiber-fortified products impacted adversely on the expansion and texture characteristics of final products. These results could be attributed to a cumulative plasticizing effect: barrel temperature profile and chemical composition of whole flours, mainly fiber and fat contents.

This work contributes information on extrusion cooking processing of rice grains with light brown pericarp. The approach was to modify previously the raw material before extrusion, such as drying the grains and using different mills, to reduce bran particle size and consequently, to uniform the particle-size distribution of the wholemeal particles. These treatments in combination with input variables at extrusion, allowed to produce expanded products as an alternative form of intake of dietary fibers, polyphenols, natural pigments, thiamin and minerals in the diet. Moreover, flours starting from these direct expanded products could be used as ingredients to produce a variety of interesting foods, of attractive color and tasty.

2 MATERIAL AND METHODS

2.1 Material and Chemical Composition

Intact kernels of whole rice of long grains with light brown pericarp were provided by S. L. Alimentos (Mauá da Serra, PR, Brazil). A total of 16 kg of cleaned grains were used and 0.4 kg was separated to perform chemical composition according to the methods of the AOAC (2005), sulfur amino acids according to Liu et al. (1995) and the 992.12 method of the AOAC (2005), soluble proteins according to the dye-binding method of Bradford (1976), and minerals following the methods–items: 999.10–9.1.08 and 990.08–9.2.39 of the AOAC (2005). All these chemical compounds are summarized in Table 1. Remaining grains were divided into two parts and each one was dried in a tray drier until reaching water contents of 9% and 11% (wet basis). Afterward, dried grains were divided into two parts and each one was milled either in a disc mill (DM, LM3600, Perten Instruments AB, Huddinge, Sweden) fixed into aperture 0 or in a roller mill (RM, QU-J, Brabender Quadrumat Junior, Duisburg, Germany) without the sieving drum. At once, the brown rice particles were humidified either to 11% and 14% of water content, totalizing eight flour rice samples pre-conditioned for the extrusion process (Figure 1). Portions of 0.3 kg of each sample pre-conditioned were separated to perform mass flow rate and solid density.
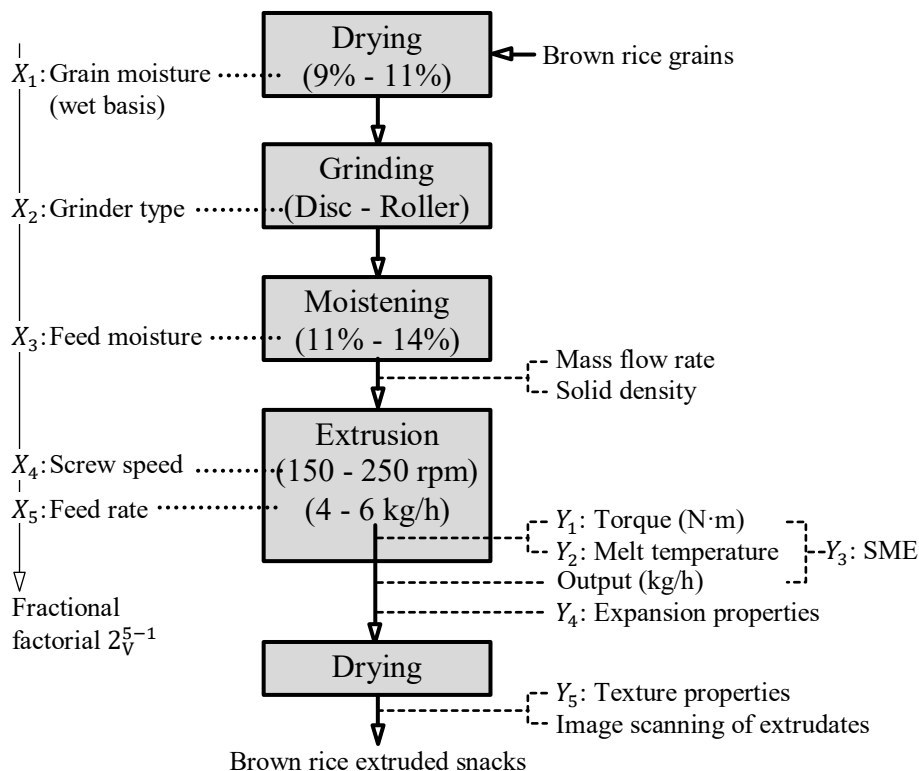
Figure 1. Pretreatment of brown rice (drying, grinding and moistening) following single-screw extrusion (screw speed and feed rate), linking the planned experiment and the analysis performed in each step. X_i: independent variables (····), Y_i: dependent variables (---).

Table 1. Proximate composition, sulphurated amino acids, and minerals of brown rice of light pericarp.

Proximate composition (g/100 g, dry basis)		Mineral composition (mg/kg, dry basis)	
Ash	1.82 ± 0.33 [a]	Sodium	2.72 ± 0.07
Total protein	8.32 ± 0.04	Potassium	241.24 ± 0.19
Fat	1.45 ± 0.08	Magnesium	124.28 ± 1.65
Dietary fiber	2.95 ± 0.10	Calcium	6.59 ± 0.12
Starch	85.46 ± 0.47	Manganese	2.61 ± 0.06
Soluble protein (g/100 g, dry basis)		Iron	1.28 ± 0.09
	1.16 ± 0.04	Zinc	2.09 ± 0.00
Sulphurated amino acids (g/kg, dry basis)		Copper	0.38 ± 0.00
Cysteine	0.46 ± 0.01	Phosphorus	318.17 ± 7.94
Methionine	0.43 ± 0.02		

[a] Mean ± standard deviations of duplicate measurements.

2.2 Mass Flow Rate

A hundred grams of each moistened sample was fed into the hopper of a single-screw volumetric feeder (Brabender, Duisburg, Germany). The screw speed was varied at three levels (8, 16 and 24 rpm) and particles were collected at the outlet for 1 min. Then, by linear interpolation, it was calculated the screw speed in the feeder that corresponds to mass flow rates of 4 and 6 kg/h, according to the moistened sample and the proposed experimental design.

2.3 Solid Density

The solid phase volume (which excludes all open and closed pores) of individual particles that structured a feed material was determined by the gas displacement method in a pycnometer system AccuPyc II 1340 (Micromeritics, Norcross, USA), using helium as displacement medium. Then, this volume was used to calculate the solid density of the preconditioned materials for extrusion. The solid density varied slightly according to the grinder type and feed moisture, which was used to estimate the melt mass density (ρ_m), and subsequently to estimate the longitudinal expansion (ALVAREZ-MARTINEZ; KONDURY; HARPER, 1988).

2.4 Extrusion Conditions

The extrusion trials were performed in a single-screw extruder 19/20 DN 832500 (Brabender, Duisburg, Germany), composed of a barrel with two electrical heating zones, an L/D ratio of 20:1 and provided with grooves along its inner surface. The barrel temperature profile was set at 50 and 90 °C. An air cooling system ELMO-G 673420 (Brabender, Duisburg, Germany) was used to keep it close to these temperature levels. A horizontal rod die was mounted at the front end of the extruder. This was the third extruder zone, electrically heated at 120 °C. The rod die had two inner compartments: a conic section (diameter reduction from 19.05 to 7.94 mm and 12.7 mm length) and a cylindrical section (57.15 mm length). The cylindrical die at the horizontal rod tip had a 3.0 mm diameter and 14.29 mm length. The standard screw attached to the barrel had a 19.05 mm diameter and a compression ratio of 5:1. The extruder was mounted on a universal-docking station 670237.001 (Brabender, Duisburg, Germany) to ensure that the screw shaft couples to the drive unit Plasti-Corder® Lab-Station (Brabender, Duisburg, Germany). The Brabender extruder program for Windows WINEXT,

version 4.4.0 (Brabender, Duisburg, Germany) was used to set the screw speed and heating zones temperature, as well as to record extrusion responses: motor torque and melt temperature. The preconditioned samples were fed into the feeding zone by a single-screw volumetric feeder (Brabender, Duisburg, Germany). The feed rate of the volumetric feeder and the extruder screw speed were varied according to a 2_V^{5-1} fractional factorial experiment.

2.5 Extrusion Dependent Variables

The melt temperature was measured with a stock temperature thermocouple fitted after the second zone, near the screw tip (Thermometrics, Type J, Northridge, USA). Real torque values (N·m) were measured with a Plasti-Corder® torque rheometer (Duisburg, Germany) coupled into the drive unit. The specific mechanical energy (SME) was then calculated according to equation (1).

$$SME = \frac{T_o \times 2\pi \times S_s \times n}{\dot{m}} \tag{1}$$

where T_o is the actual screw torque (N·m), S_s is the actual screw speed (rpm) and $\dot{m}$ the mass flow rate of extruded product (kg/min). $\dot{m}$ was computed by collecting samples to the extruder output, in plastic bags for 30 s. The collected mass was registered on an SB12001 semi-analytical balance (Mettler Toledo, Switzerland).

2.6 Expansion Properties

From each extrusion trial, a total of twenty extruded pieces was randomly selected, which were then cross-sectioned at both ends. The length L and diameters D_i both at the center and ends of each piece were measured using a digital caliper (ZAAS Precision, Curitiba, Brazil). The sectional expansion index (SEI) was then calculated according to equation (2) (ALVAREZ-MARTINEZ; KONDURY; HARPER, 1988).

$$SEI = \left(\frac{D}{D_0}\right)^2 \tag{2}$$

where D is the average of the diameters D_i; D_0 is the hole diameter at the cylindrical die. The mass m of the previous samples was registered using an analytical balance (Mettler Toledo, AG204, Switzerland) and the apparent density of extruded pieces (ρ_e) was then calculated using equation (3).

$$\rho_e = \frac{4\,m}{\pi\,D^2 L} \tag{3}$$

The longitudinal expansion index (LEI) was calculated according to equation (4) (ALVAREZ-MARTINEZ; KONDURY; HARPER, 1988).

$$LEI = \left(\frac{\rho_m}{\rho_e}\right)\frac{1}{SEI}\left(\frac{1 - w_m}{1 - w_e}\right) \tag{4}$$

where ρ is the material density, w is the water content fraction, and subscripts m and e are melt and extruded products, respectively. w_m and w_e were determined in duplicate measurements using the 925.09 oven method (AOAC, 2005). The volumetric expansion index (VEI) was obtained from equation (5) (ALVAREZ-MARTINEZ; KONDURY; HARPER, 1988).

$$VEI = SEI(LEI) \tag{5}$$

and the porosity of the extruded samples ε was obtained from equation (6) (ROBIN et al., 2012).

$$\varepsilon = \left(1 - \frac{1}{VEI}\right) 100\% \tag{6}$$

2.7 Texture Properties

Samples used to determine expansion properties were dried in an oven with air circulation at 60 °C (WTB Binder, Tuttlinger, Germany) up to 4% moisture content. Afterward, pieces were cooled in a desiccator up to room temperature. The mechanical properties of samples were then performed on a texture analyzer TA-XT Plus (Stable Micro Systems, Surrey, England) using the puncture test. The analyzer was equipped with a 50 kg load cell and a 2 mm diameter stainless steel cylinder probe. A crosshead speed of 5 mm/s was applied. When the probe reached a contact force of 0.196 N on the sample surface, the puncturing was initiated at 1 mm/s until a depth of 50% of the sample diameter. The peak compression forces (N) and time (min) at which a sample was punctured, were measured from the force-time curve, recorded and analyzed by the software program Exponent, version 4.0.13.0.

2.8 Experimental Design and Data Analysis

A one-half fraction of the 2_V^{5-1} design with the principal fraction as the first group of runs was conducted (**Annex E**). The independent variables were X_1 = grain moisture before milling (9% and 11%), X_2 = milling type (disc, roller), X_3 = feed moisture (11% and 14%), X_4 = screw speed (150 rpm and 250 rpm), and X_5 = feed rate (4 kg/h and 6 kg/h). These levels were selected according to preliminary trials and taking into account extruder limitations and their operating capability. The quantitative independent variables were coded according to equation (7), where x_i denotes the coded variable and X_i is the actual value to be coded.

$$x_i = \frac{X_i - \dfrac{\left(X_{i\,high} + X_{i\,low}\right)}{2}}{\dfrac{\left(X_{i\,high} - X_{i\,low}\right)}{2}} \tag{7}$$

The orthogonal coding of X_2 was –1 for disc mill and +1 for roller mill. All extrusion trials in the design matrix were carried out in random order. Dependent variables were: process properties of extrusion and physical properties of extruded products. The estimation of regression coefficients and the total and partial sum of squares were performed by the method of least squares (MONTGOMERY, 2013a). The estimation of important effects in a single response was performed according to the Lenth method (LENTH, 1989). Afterward, complete and replicated factorial designs were obtained by projecting 2^{5-1} fractions into 2^{5-h} factorials with 2^{h-1} replicates and with h removed negligible factors ($h < 5 - 1$) (MONTGOMERY, 2013b). First-order regression models with interactions were used as approximating functions, to explore the relationship between significant factors and a single response. Hypothesis testings about each model parameters were summarized in tables of analysis of variance (ANOVA). The null hypothesis was rejected when the p-value for the statistic F₀ was less than $\alpha = 0.05$ and $\alpha = 0.10$. Model adequacy checking was performed by residual analysis and testing for lack of fit (MONTGOMERY, 2013a). The adjusted models were then used to generate contour plots. The overlaying of contour plots allowed to find optimum process variables ranges that maximizes expansion properties and minimize SME and F_p.

3 RESULTS AND DISCUSSION

Responses obtained from the 2_V^{5-1} design (**Annex E**) are presented in Table 2. The magnitude and importance of the 15 effect estimates from this experiment were displayed as Pareto charts, with the reference line outlining the margin of error according to α (LENTH, 1989). The red reference line is for $\alpha = 0.05$ and the blue reference line is for $\alpha = 0.10$.

3.1 Effect of Process Conditions on Extrusion Dependent Variables

3.1.1 Melt temperature

Melt temperature (T_m) only was affected by feed moisture (X_3, Figure 2A) and increased with X_3 at the low-level (Figure 2B). The input variable X_3 negatively affected T_m.
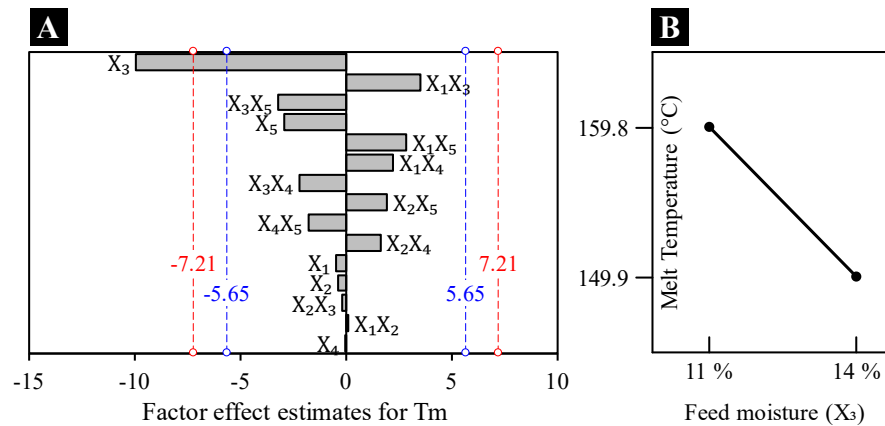
Figure 2. (A): Pareto chart of standardized effects; (B): main effect plot for melt temperature (T_m).

3.1.2 Torque

In the single-screw cooking extruders, the drive unit supplies the required amount of torque to the shank of the extruder screw attached to it (RAUWENDAAL, 2014). Motor torque provides a direct indication of the energy absorbed by a feed material due to the shear exerted by the extruder screw and the die orifice. It is a very sensitive indicator, in which fluctuations in torque values during an extrusion process indicates erratic feeding, surging, and plugging (AKDOGAN, 1996).

The important effects that emerged for torque were X_3, X_4, and X_5 (Figure 3A). Highest torques were achieved with X_3 and X_4 at the low level and, X_5 at the high-level (Figure 3A–D). The input variables X_3 and X_4 negatively affected the torque, whereas X_5 positively influenced on the torque.

118

Table 2. Extrusion dependent variables during the brown rice processing in a single-screw extruder and bulk expansion properties of brown rice extrudates.

Run [1]	Extrusion dependent variables [2]			Bulk expansion properties [3]					Texture properties [3]		
	T_m °C	T_o N·m	SME kJ/kg	ρ_e kg/m³	SEI	LEI	VEI	ε %	F_p N	N_o	S N·mm
1	161.4±0.9	40.8±2.7	370.5±24.1	219.4±9.7	9.82±0.29	0.65±0.02	6.36±0.28	84.24±0.69	7.59±1.47	43.5±4.5	37.86±7.40
2	155.0±1.3	31.9±3.8	392.7±46.6	223.1±10.0	10.02±0.26	0.63±0.02	6.29±0.28	84.07±0.71	6.18±0.96	52.0±5.6	31.03±4.95
3	160.2±0.7	28.1±1.0	368.3±13.0	170.4±8.6	10.74±0.36	0.77±0.02	8.22±0.42	87.80±0.62	3.61±0.62	53.0±1.5	18.41±2.80
4	158.2±1.6	38.3±1.7	365.7±16.3	193.2±8.0	10.67±0.53	0.67±0.02	7.19±0.30	86.07±0.58	8.65±2.14	47.0±6.0	42.69±9.86
5	156.3±3.8	20.0±3.0	252.9±37.6	1160.3±79.4	2.25±0.15	0.55±0.02	1.25±0.09	19.37±5.51	6.99±3.07	13.3±5.2	18.10±7.60
6	150.7±0.7	28.2±1.3	253.1±11.9	804.6±43.1	3.05±0.17	0.57±0.01	1.75±0.09	42.73±3.07	7.74±2.65	18.4±5.4	22.18±7.37
7	146.8±0.9	27.8±0.7	271.6±6.9	402.2±32.7	5.44±0.33	0.64±0.02	3.50±0.27	71.27±2.34	6.75±1.52	37.8±4.4	25.69±5.85
8	150.1±0.8	20.9±0.5	265.1±5.8	455.8±32.8	4.92±0.27	0.63±0.03	3.10±0.23	67.54±2.34	4.51±1.11	30.1±3.1	16.25±4.10
9	164.3±1.4	20.2±2.4	445.3±53.9	155.0±7.5	11.31±0.57	0.79±0.01	8.97±0.43	88.82±0.54	3.19±0.84	49.9±5.8	17.13±4.15
10	158.9±1.0	27.5±2.8	406.4±42.0	167.0±5.0	12.21±0.38	0.68±0.01	8.30±0.24	87.95±0.36	5.81±1.43	57.5±6.5	31.69±7.49
11	161.2±2.2	26.6±0.8	420.3±12.2	135.3±2.0	12.19±0.54	0.83±0.03	10.13±0.15	90.12±0.15	4.47±1.08	44.5±3.7	24.37±5.98
12	159.2±1.6	21.6±1.3	456.0±27.1	136.0±5.9	12.61±0.35	0.81±0.02	10.21±0.43	90.19±0.42	1.98±0.40	59.5±6.2	11.06±2.25
13	139.2±3.4	21.1±1.9	334.3±30.0	333.6±22.4	6.75±0.28	0.62±0.02	4.22±0.28	76.19±1.60	5.19±1.88	35.2±9.6	21.64±8.09
14	154.3±1.5	14.2±1.5	308.3±31.5	300.2±11.2	6.81±0.07	0.68±0.02	4.64±0.17	78.43±0.80	3.21±0.52	39.6±6.3	13.50±2.07
15	151.0±0.0	16.2±0.7	337.1±14.9	254.0±11.3	8.01±0.26	0.69±0.01	5.49±0.25	81.77±0.81	3.69±0.52	41.8±6.1	16.44±2.06
16	150.5±1.3	20.4±0.3	308.0±5.2	255.7±10.4	7.81±0.27	0.70±0.01	5.45±0.22	81.63±0.75	3.99±1.13	46.2±6.0	17.94±4.99

[1] Extrusion trials ordered according to the principal fraction of a 2_V^{5-1} factorial design. [2] Mean ± standard deviation of recorded data during 5 min. [3] Mean ± standard deviation of twenty extrudate pieces. T_m: melt temperature at the die, T_o: torque, SME: specific mechanical energy. ρ_e: apparent density of the extrudate, SEI: sectional expansion index, LEI: longitudinal expansion index, VEI: volumetric expansion index, ε: porosity of the extrudate. F_p: average puncturing force, N_o: number of peaks, S: integral of the curve.

119
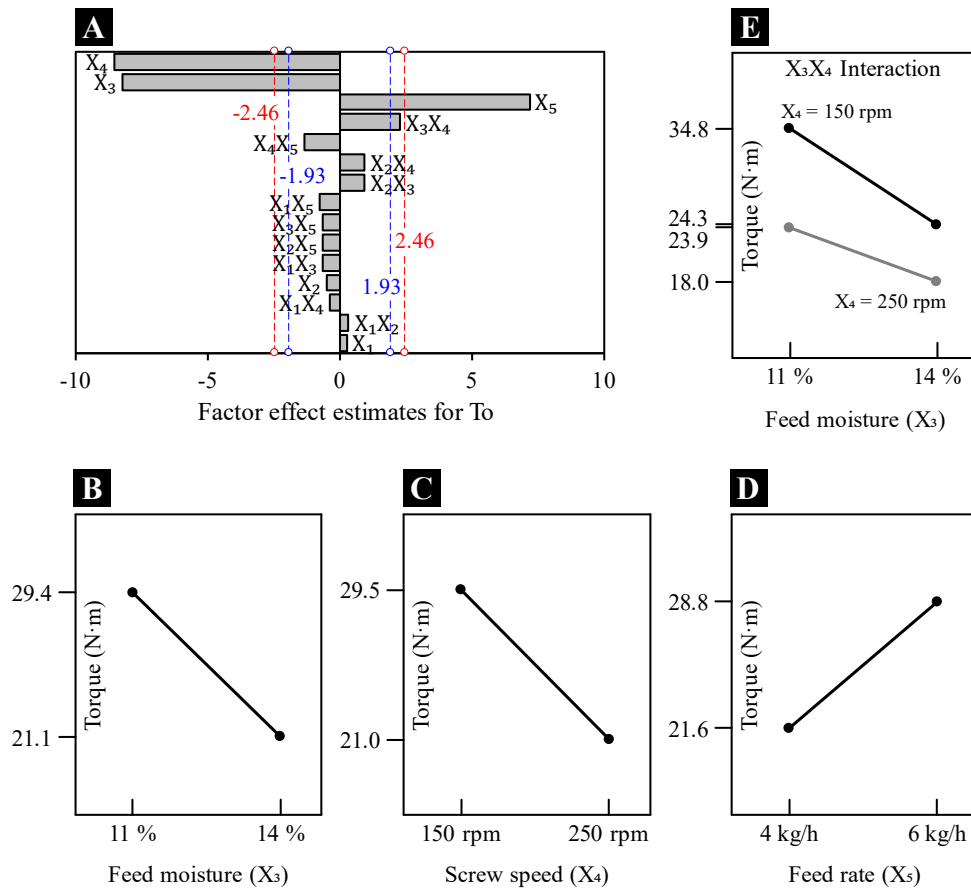
Figure 3. (A) Pareto chart of standardized effects for torque (T_o); (B–D): main effect plots; (E): interaction plot when $\alpha = 0.10$.

According to the X_3X_4 interaction (Figure 3E), the feed moisture X_3 had little effect at high screw speed but a large positive effect at low screw speed. High torque values are associated with the fast wear of the screw flights. During each screw revolution, 10% of the screw surface area comes in contact with the barrel surface (WAGNER; MOUNT; GILES, 2014). Hence, it is desirable to minimize the screw wear during extrusion processing. The lowest torque of brown rice extrudates would appear to be obtained when X_2 and X_4 are at the high level and X_3 is at the low level.

3.1.3 Specific mechanical energy

The mechanical energy required to turn the screw is converted to thermal heat by viscous dissipation, raising the temperature of the melt (HARPER, 1989). It is related to the viscosity of the molten mass. Melt viscosity affects directly the resistance to work performed by screws on the feed material. Polymer type and their interactions with minority compounds present in feeding materials based on whole-grain cereals could influence melt/glass transition temperatures of mass and consequently on melt viscosity (VARGAS-SOLÓRZANO et al., 2014).

The variables X_3 and X_4 were the only ones that influenced SME (Figure 4A). The process SME increased when it was operated with X_3 at the low level and X_4 at the high-level (Figure 4B, C). The input variable X_3 negatively affected SME, whereas X_4 positively influenced on SME.
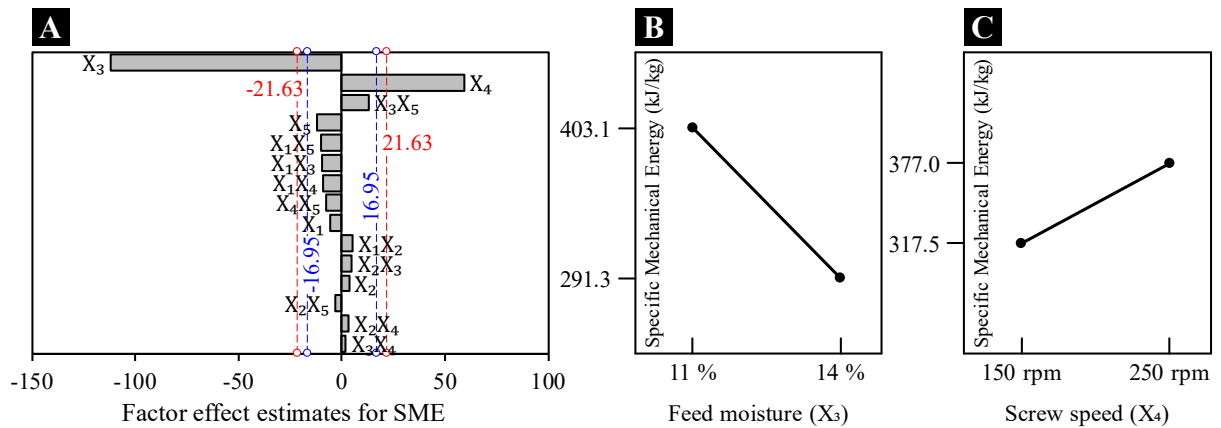
Figure 4. (A): Pareto chart of standardized effects for specific mechanical energy (*SME*); (B) and (C): main effect plots.

3.2 Effect of Process Conditions on Expansion Properties of Extrudates

The scanned images of expanded extrudates for all combinations of the 2_V^{5-1} design are depicted in **Annex F**. The brown rice extrudates processed at conditions of feed moisture - screw speed of 14% - 150 rpm were the darkest and showed holes in its external surfaces. These holes were generated by the explosion of air bubbles and water vapor and the subsequent contraction of the melt leaving the die. The other treatments showed a lighter color. The brown rice extrudates processed at 11% of feed moisture showed more homogeneous air cells and smooth external surfaces.

3.2.1 Apparent density

The main effects of X_3 and X_4 were potentially important for apparent density when $\alpha = 0.05$, whereas the main effect of X_2 and the interaction effect between X_3X_4 also were significant for $\alpha = 0.10$ (Figure 5A). The apparent density of brown rice extrudates (ρ_e) decreased when it was processed with X_3 at the low-level and X_4 at the high-level (Figure 5C, D). Conversely to SME, the input variable X_4 negatively affected ρ_e, whereas X_3 positively affected it and on a larger scale.

Feed materials prepared with the roller mill produced extrudates with lower apparent densities (Figure 5B). From the X_3X_4 interaction (Figure 5E), the feed moisture X_3 had little effect at high screw speed but a large positive effect at low screw speed. Therefore, the lowest apparent density of brown rice extrudates would appear to be obtained when X_2 and X_4 are at the high-level and X_3 is at the low-level. This combination also generates low torque values (**Figure 3E**).
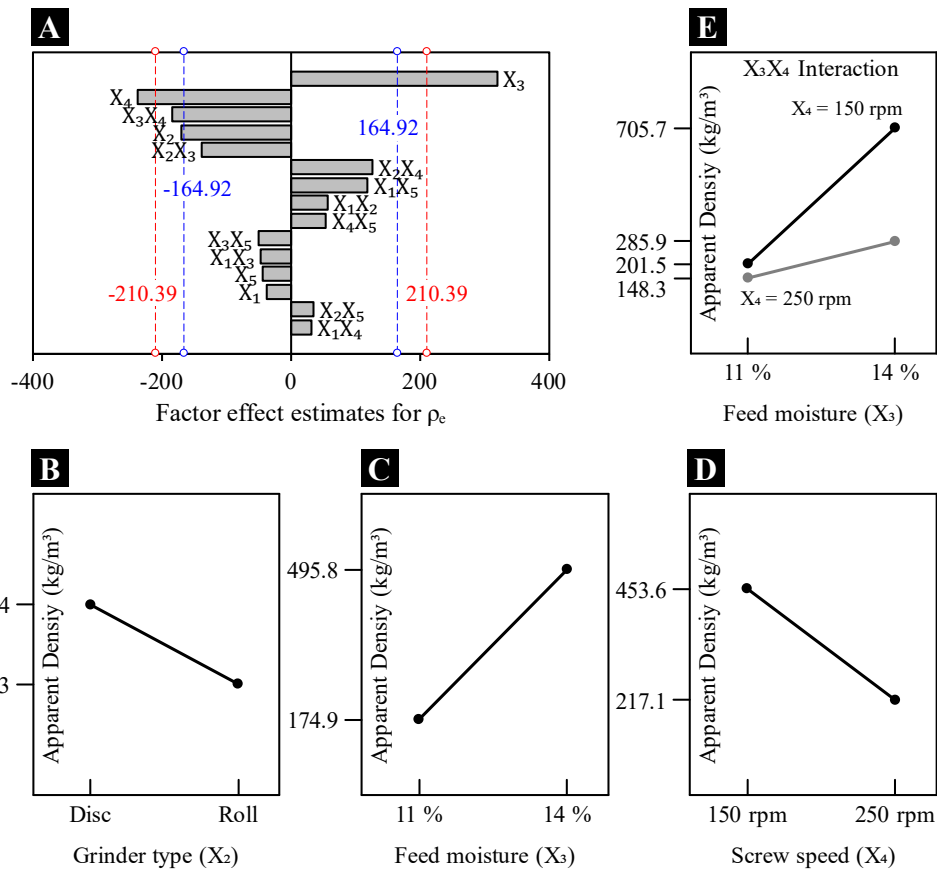
Figure 5. (A): Pareto chart of standardized effects for apparent density (ρ_e); (C) and (D): main effect plots for $\alpha = 0.05$; (B) and (E): main and interaction effect plots when $\alpha = 0.10$.

3.2.2 Sectional expansion index

Sectional expansion index (*SEI*) is highly influenced by the melt temperature, melt elasticity, and die geometry (BOUZAZA; ARHALIASS; BOUVIER, 1996). During its flow through the die insert, the melt stores energy. Small insert diameters generate more pressure and store higher melt energy. This energy is released in the radial direction when the compressed melt emerges the die (ALVAREZ-MARTINEZ; KONDURY; HARPER, 1988). Low carbohydrate content, high crude fiber, high fat, and high tannin contents found in whole-grain sorghum of light brown pericarp, yielded extrudates with low sectional expansion (VARGAS-SOLÓRZANO et al., 2014).

The Pareto chart of the effect estimates, from the analysis of *SEI* is shown in **Figure 6A**. The important effects that emerged from this response were the main effects of X_2, X_3 and X_4 and the X_3X_4 interaction for both α values. The highest sectional expansion was obtained when brown rice was ground in a roller mill ($X_2 = +1$) and when X_3 was at the low-level and X_4 at the high-level (Figure 6B–D). This combination also generates low torque values (**Figure 3E**). Conversely to ρ_e, the input variable X_4 positively affected *SEI*, whereas X_3 negatively influenced it and on a larger scale.
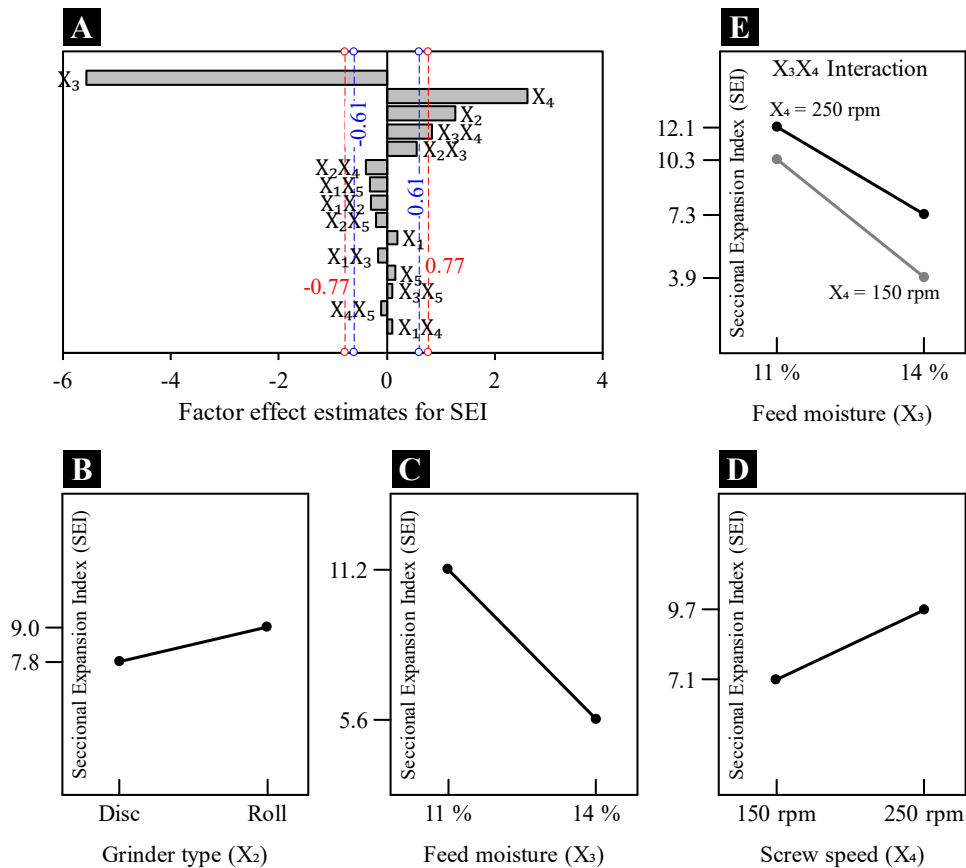
Figure 6. (A): Pareto chart of standardized effects for sectional expansion index (*SEI*); (B–D): main effect plots; (E): interaction effect plot.

From the X_3X_4 interaction (**Figure 6E**), the change in screw speed X_4 had a similar effect with feed moisture conditioned to 11%. In these conditions, the sectional expansion increased above 10. On the contrary, the change in X_4 with feed moisture fixed in 14% had a large positive effect (*SEI* increased from 3.9 to 7.3).

3.2.3 Longitudinal expansion index

The longitudinal expansion is highly influenced by the melt viscosity. It is associated with the velocity of the melt stream, before and after expansion. Extruded product velocity at the extruder outlet is related to the production yield. The longitudinal expansion increases at the expense of diametral expansion (ALVAREZ-MARTINEZ; KONDURY; HARPER, 1988). When insoluble fibers are present in the melt stream, the fibers in the interior of the die are oriented longitudinally throughout the cylindrical section, just before leaving the extruder. The low physicochemical compatibility of insoluble fibers with starch polymers causes physical rupture of the melt, decreasing the extensional forces and resulting in low shear rate and low die pressure. At the die exit, the elastic properties of the melt are hindered, giving rise to extrudates with high longitudinal expansion, with smaller air cells and thicker cell walls.

The longitudinal expansion index (*LEI*) was influenced by the main effects of X_2, X_3 and X_4 (Figure 7A). Feed materials prepared with roller mill, moistened to 11%, fed in the range of 4 to 6 kg/h, and processed at 250 rpm of screw speed, yielded the highest longitudinal expansion (Figure 7B–D). This combination allows the maximization of both extrudate expansion and yield production.

123
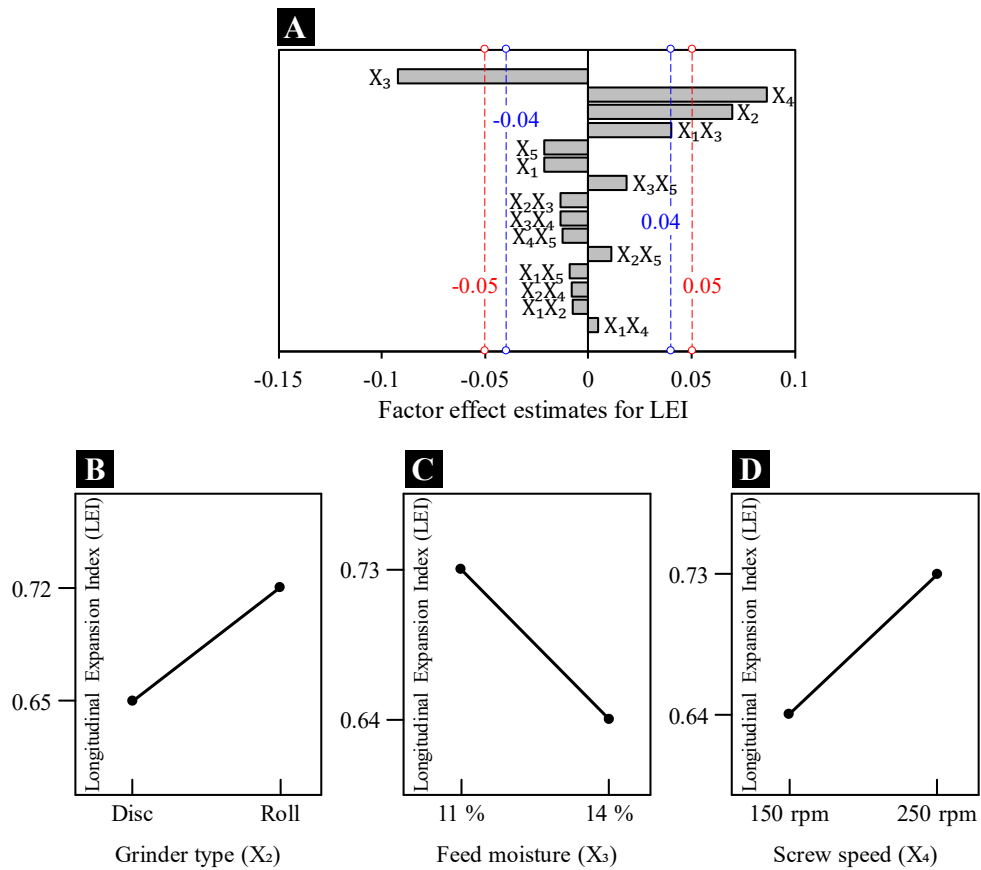
Figure 7. (A): Pareto chart of standardized effects for longitudinal expansion index (*LEI*); (B–D): main effect plots.

3.2.4 Volumetric expansion index

The volumetric expansion index (*VEI*) is associated with the specific volume of the melt stream, before and after extrusion. Changing the extrusion conditions significantly modified the *VEI* of the samples (between 1.2 and 10.2). The *VEI* was highly influenced by the main effects of X_2, X_3 and X_4, even at 95% of confidence interval (Figure 8A).
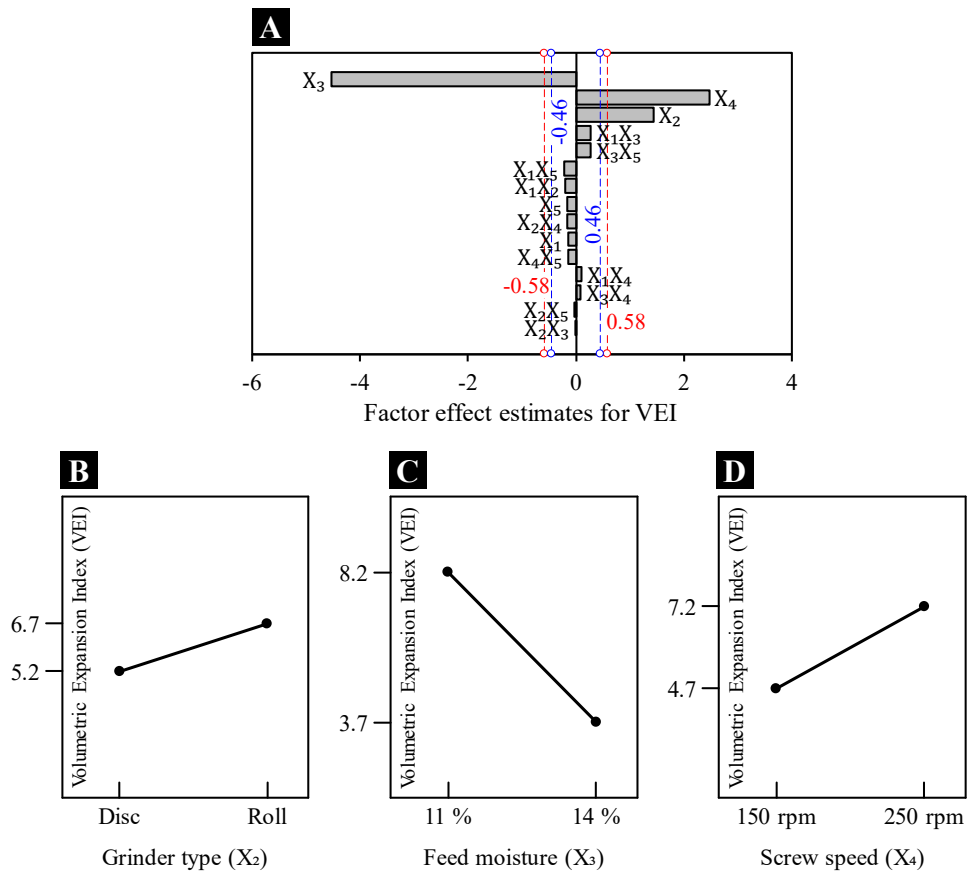
Figure 8. (A): Pareto chart of standardized effects for volumetric expansion index (*VEI*); (B–D): main effect plots.

The highest volumetric expansion was obtained when brown rice was ground in a roller mill ($X_2 = +1$) and when X_3 was at the low-level and X_4 at the high-level (Figure 8B–D). This combination is in agreement with high sectional expansion indexes and low torque values (**Figure 3E**). The feed moisture X_4 was the most important input variable, affecting *VEI* in a linear negative behaviour. X_2 and X_3 influenced *VEI* to a lesser extent a linear positive behaviour.

3.2.5 Porosity of extrudates

At 95% confidence interval, the main effects of X_3 and X_4 were potentially important for porosity (**Figure 9**A). The input variable X_2 and the interaction X_3X_4 had significant effects when the confidence interval was reduced to 90%. The extruded product porosity was maximized when it was processed with X_2 at the high level (Roller), X_3 at the low level (14%), and X_4 at the high-level (250 rpm) (Figure 9A–C).
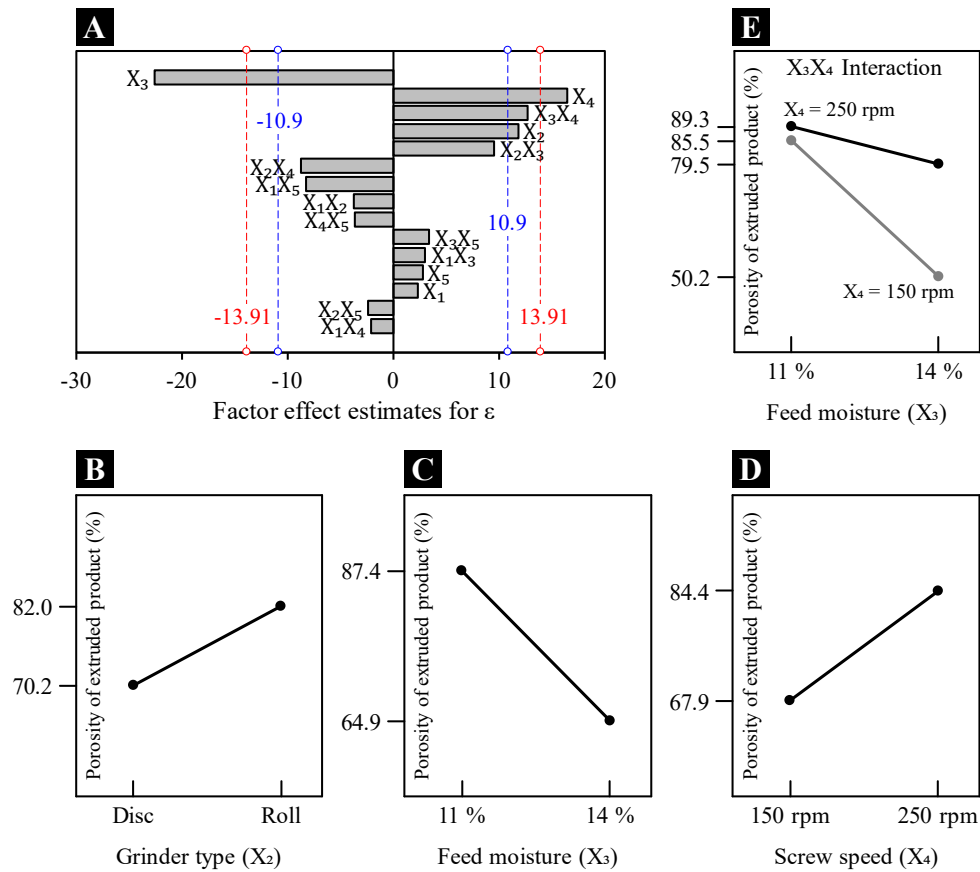
Figure 9. (A): Pareto chart of standardized effects for extruded product porosity (ε); (B–D): main effect plots; (E): interaction effect plot.

Considering the X_3X_4 interaction (Figure 9E), the change in screw speed X_4 had a similar effect with feed moisture conditioned to 11%. In these conditions, the extrudate porosity increased above 85%. On the contrary, the change in X_4 with feed moisture set to 14% had a large positive effect (ε increased from 50.2 to 79.5%).

The effect of process conditions on the expansion properties of extruded brown rice can be investigated by the expansion chart shown in Figure 10. The isotropic expansion occurs when the expansion is uniform in all directions. In the case of extruded brown rice, most of the samples showed a favored sectional expansion index with $SEI^{0.5} \gg LEI$. Of all extruded samples, the sample extruded at the condition $T5$ [$X_1(9\%)$-X_2(Disc)-$X_3(14\%)$-X_4(150 rpm)-X_5(4 kg/h)] showed a closer expansion to isotropy ($LEI/SEI^{0.5} = 0.37$). On the contrary, the sample extruded at the condition $T10$ [$X_1(11\%)$-X_2(Disc)-$X_3(11\%)$-X_4(250 rpm)-X_5(6 kg/h)] was the most anisotropic ($LEI/SEI^{0.5} = 0.19$) and can be compared to sample $T3$ [$X_1(9\%)$-X_2(Roller)-$X_3(11\%)$-X_4(150 rpm)-X_5(4 kg/h)]. Both samples displayed the same volumetric expansion (8.2 vs. 8.3) meaning the same porosity. Other pairs of samples, such as $T15$–$T16$, $T1$–$T2$, and $T11$–$T12$, also showed the same porosity.
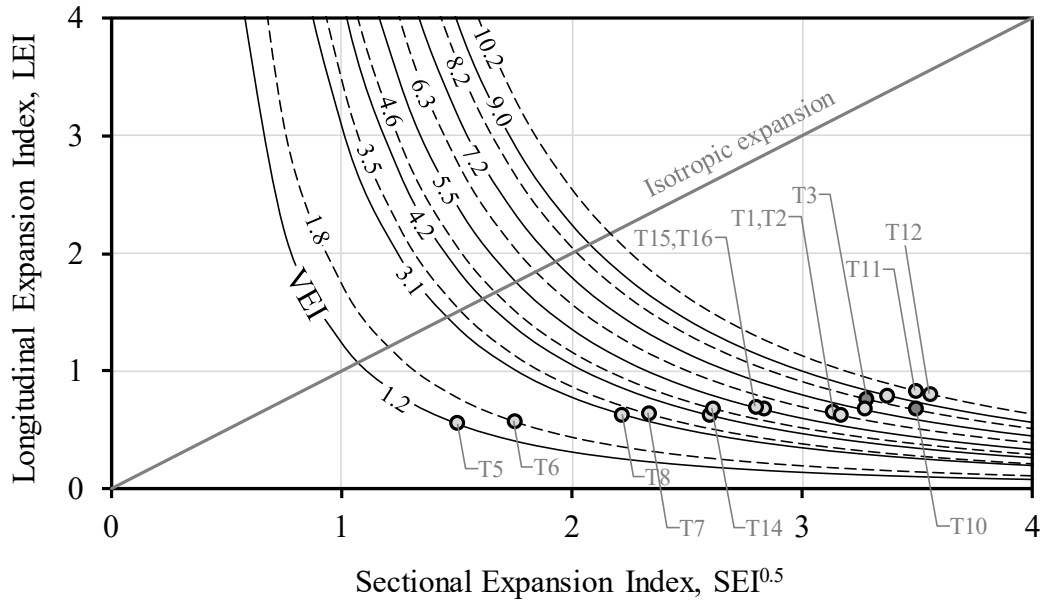
Figure 10. Expansion chart displaying the longitudinal expansion index (*LEI*) vs. sectional expansion index (*SEI*) of extruded whole wheat flour at different conditions.

3.3 Effect of Process Conditions on Texture Properties of Extrudates

3.3.1 Average puncturing force

Average puncturing force (F_p) presented dependence of X_2, X_4 and X_5 for $\alpha = 0.05$ (Figure 11A). When the confidence interval was reduced to 90%, the X_1X_3 and X_3X_5 interactions emerged as significant effects. Since the main effects of X_1 and X_5 were not significant, these interactions can be associated with uncontrolled factors. Lowest puncturing forces were obtained with grains milled in a roller mill and when X_4 was at the high-level and X_5 at the low-level (Figure 11B–D).
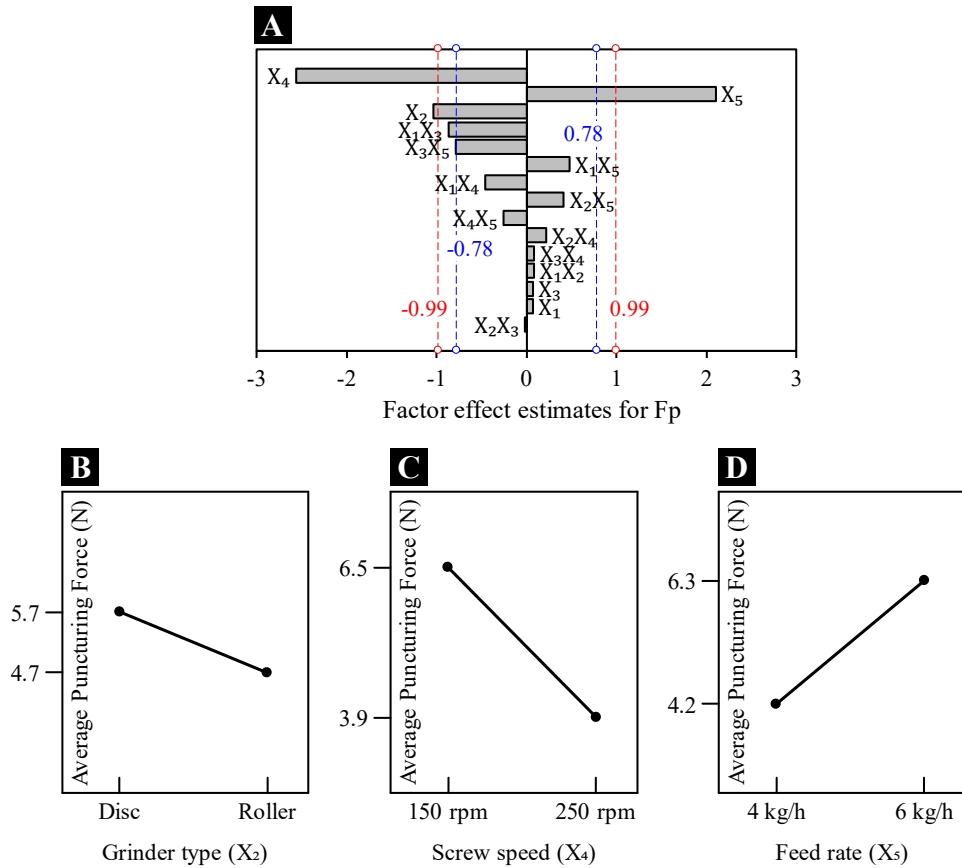
Figure 11. (A): Pareto chart of standardized effects for average puncturing force (F_p); (B–D): main effect plots; (E): interaction effect plot.

It is desirable to minimize F_p, which is associated with the crispness and hardness of the extrudate. Changing the extrusion conditions significantly modified the average puncturing force (2.0 to 8.7 N) of the samples. Moisture contents below to 6% ensure crispness preservation of the extrudates. A slight increase of moisture above that level may lead to a drastic decrease of crispness and, beyond 10 – 12% (wet basis), the crispness of extrudates may be completely lost (BOUVIER; CAMPANELLA, 2014). Since all samples were previously dried up to 4% moisture content (wet basis), the hardness variability is associated with the porous microstructure of the extrudate and its expansion characteristics. Expanded extrudates have more amorphous starch regions in their structure, with larger air cells and thinner cell walls, resulting in extrudates with low hardness.

3.3.2 Number of peaks

For an expanded extrudate, the force-time curve is not smooth but rather the force rises to a peak and then falls back. The observed peaks in the force-time curve have been attributed to successive cell wall breakage of the extrudate structure while the force drops of each peak remain low (BOUVIER; CAMPANELLA, 2014). In the cases when the force rises to zero or rises to larger values, these events are associated with the breakage of the extruded crust.

The number of peaks (N_o) only was affected by feed moisture (X_3, Figure 12A). N_o increased with X_3 at the low-level (Figure 12B). The input variable X_3 negatively affected N_o. Melt temperature and N_o were linearly correlated.
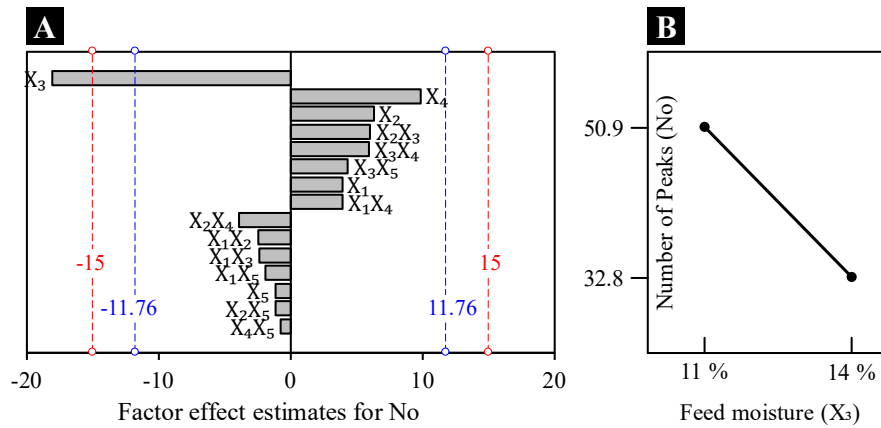
Figure 12. (A): Pareto chart of standardized effects for the number of peaks (N_o); (B): main effect plot.

3.3.3 Integral of the curve

The integral of the curve is an indication of the energy required to fracture and reduce the extrudate to small pieces during consumption (BOUVIER; CAMPANELLA, 2014). Harder extrudates rise the puncture force, leading to high values for the integral of the force-time curve. It takes greater energy/work to reduce a harder extrudate into small pieces to be able to consume it. Changing the extrusion conditions significantly modified the integral of the curve (11.1 to 42.7 N·mm) of the samples.

At 95% confidence interval, the integral of the curve (S) only was dependent of X_5 (Figure 13A). For $\alpha = 0.10$, the main effects of X_3 and X_4 emerged as significant terms. S is minimized with X_3 and X_4 at the high level, and X_5 at the low-level (Figure 13B–D).
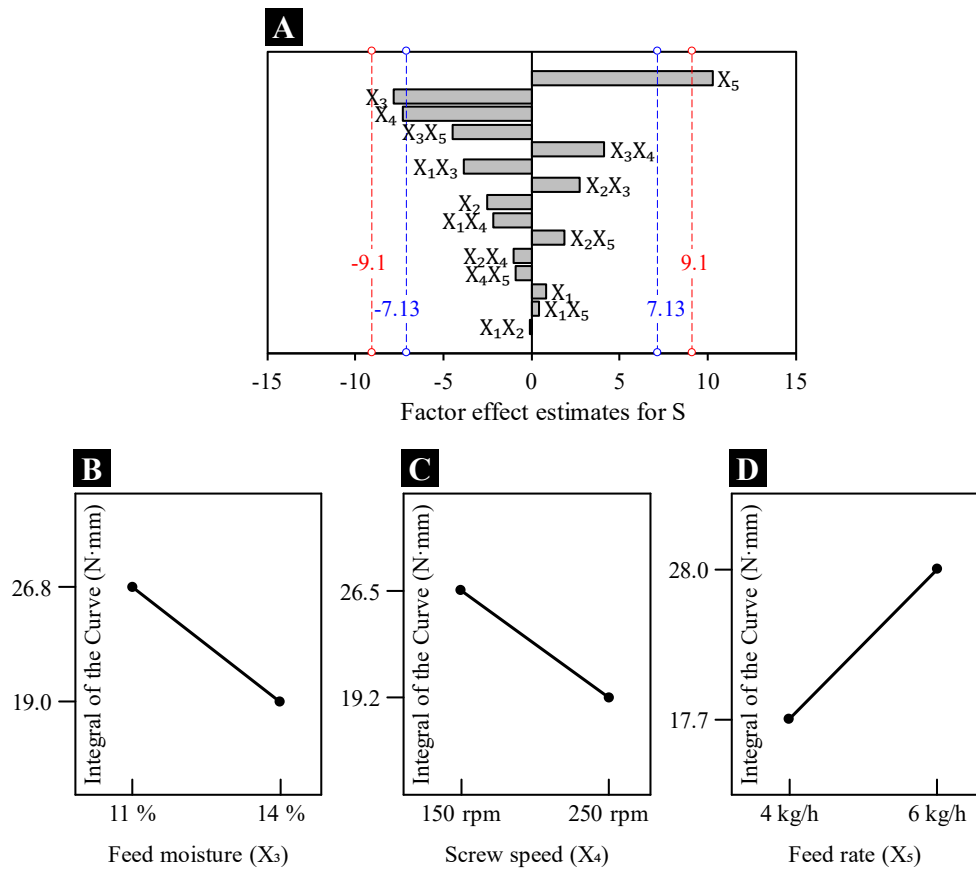
Figure 13. (A): Pareto chart of standardized effects for integral of the curve (S); (B–D): main effect plots.

4 CONCLUSION

The 2_V^{5-1} design provided excellent information concerning the main effects and two-factor interactions. From the five studied independent variables and with an error probability of 0.10, grain moisture before grinding in the levels of 9 to 12% was negligible. The average puncturing force of brown rice extrudates was independent of changes in feed moisture in the range of 11 to 14%. The other responses evaluated were highly influenced by this change in moisture. Changes in screw speed in the range of 150 to 250 rpm, highly affected the torque, longitudinal expansion, and average puncturing force of extrudates. Changes in feed rate in the levels of 4 to 6 kg/h highly impacted on the integral of the curve, and moderately affected the torque and the average puncturing force of brown rice extruded snacks.

The interaction effect between feed moisture and screw speed was the key to maximize expansion properties. The highest sectional expansion with the highest extrudate porosity was obtained when brown rice grains were ground in a roller mill, the feed moisture was conditioned to 11%, and the screw speed was operated at 250 rpm. This combination also generated low torque values, low puncturing forces, and integral of the curve, when the feed rate was fixed at 4 kg/h. The significant input variables enabled the prediction and consequently, the design of brown rice extruded snacks with acceptable expansion and texture characteristics.

ACKNOWLEDGEMENTS

REFERENCES

AKDOGAN, H. Pressure, torque, and energy responses of a twin screw extruder at high moisture contents. **Food Research International**. v. 29, n. 5, p. 423-429, 1996.

ALAM, M. S.; PATHANIA, S.; SHARMA, A. Optimization of the extrusion process for development of high fibre soybean-rice ready-to-eat snacks using carrot pomace and cauliflower trimmings. **LWT - Food Science and Technology**. v. 74, p. 135-144, 2016.

ALVAREZ-MARTINEZ, L.; KONDURY, K. P.; HARPER, J. M. A General Model for Expansion of Extruded Products. **Journal of Food Science**. v. 53, n. 2, p. 609-615, 1988.

AOAC. **Official Methods of Analysis of AOAC International**. 18th ed. AOAC International: Gaithersburg, 2005.

BOUVIER, J.-M.; CAMPANELLA, O. H. Quality analysis of extrusion-textured food products. In: BOUVIER, J.-M.; CAMPANELLA, O. H. (Eds.). **Extrusion Processing Technology**. John Wiley & Sons, Ltd: Chichester, 2014. p. 311-349.

BOUZAZA, D.; ARHALIASS, A.; BOUVIER, J. M. Die design and dough expansion in low moisture extrusion-cooking process. **Journal of Food Engineering**. v. 29, n. 2, p. 139-152, 1996.

BRADFORD, M. M. A rapid and sensitive method for the quantitation of microgram quantities of protein utilizing the principle of protein-dye binding. **Analytical Biochemistry**. v. 72, n. 1, p. 248-254, 1976.

BRENNAN, C.; BRENNAN, M.; DERBYSHIRE, E.; TIWARI, B. K. Effects of extrusion on the polyphenols, vitamins and antioxidant activity of foods. **Trends in Food Science & Technology**. v. 22, n. 10, p. 570-575, 2011.

DEHGHAN-SHOAR, Z.; HARDACRE, A. K.; BRENNAN, C. S. The physico-chemical characteristics of extruded snacks enriched with tomato lycopene. **Food Chemistry**. v. 123, n. 4, p. 1117-1122, 2010.

HARPER, J. M. Food extruders and their applications. In: MERCIER, C.; LINKO, P.; HARPER, J. M. (Eds.). **Extrusion Cooking**. American Association of Cereal Chemists. Inc.: St. Paul, 1989. p. 1-16.

LENTH, R. V. Quick and Easy Analysis of Unreplicated Factorials. **Technometrics**. v. 31, n. 4, p. 469-473, 1989.

LIU, C.; ZHANG, Y.; LIU, W.; WAN, J.; WANG, W.; WU, L.; ZUO, N.; ZHOU, Y.; YIN, Z. Preparation, physicochemical and texture properties of texturized rice produce by Improved Extrusion Cooking Technology. **Journal of Cereal Science**. v. 54, n. 3, p. 473-480, 2011.

LIU, H. J.; CHANG, B. Y.; YAN, H. W.; YU, F. H.; LIU, X. X. Determination of Amino Acids in Food and Feed by Derivatization with 6-Aminoquinolyl-N-Hydroxysuccinimidyl Carbamate and Reversed-Phase Liquid Chromatographic Separation. **Journal of AOAC**

INTERNATIONAL. v. 78, n. 3, p. 736-743, 1995.

MONTGOMERY, D. C. Fitting regression models. In: **Design and analysis of experiments**. 8th ed. Wiley: Hoboken, 2013a. p. 449-477.

MONTGOMERY, D. C. Two-level fractional factorial designs. In: MONTGOMERY, D. C. (Ed.). **Design and analysis of experiments**. 8th ed. Wiley: Hoboken, 2013b. p. 320-393.

PARDHI, S. D.; SINGH, B.; NAYIK, G. A.; DAR, B. N. Evaluation of functional properties of extruded snacks developed from brown rice grits by using response surface methodology. **Journal of the Saudi Society of Agricultural Sciences**. v. 18, n. 1, p. 7-16, 2019.

PASTOR-CAVADA, E.; DRAGO, S. R.; GONZÁLEZ, R. J.; JUAN, R.; PASTOR, J. E.; ALAIZ, M.; VIOQUE, J. Effects of the addition of wild legumes (Lathyrus annuus and Lathyrus clymenum) on the physical and nutritional properties of extruded products based on whole corn and brown rice. **Food Chemistry**. v. 128, n. 4, p. 961-967, 2011.

RAUWENDAAL, C. Extruder Hardware. In: RAUWENDAAL, C. (Ed.). **Polymer Extrusion**. 5th ed. Hanser Publications: Cincinnati, 2014. p. 49-83.

ROBIN, F.; DUBOIS, C.; PINEAU, N.; LABAT, E.; THÉODULOZ, C.; CURTI, D. Process, structure and texture of extruded whole wheat. **Journal of Cereal Science**. v. 56, n. 2, p. 358-366, 2012.

SINGH, B.; SEKHON, K. S.; SINGH, N. Effects of moisture, temperature and level of pea grits on extrusion behaviour and product characteristics of rice. **Food Chemistry**. v. 100, n. 1, p. 198-202, 2007.

SONG, S.; LEE, J. E.; SONG, W. O.; PAIK, H.-Y.; SONG, Y. Carbohydrate Intake and Refined-Grain Consumption Are Associated with Metabolic Syndrome in the Korean Adult Population. **Journal of the Academy of Nutrition and Dietetics**. v. 114, n. 1, p. 54-62, 2014.

SUMARGO, F.; GULATI, P.; WEIER, S. A.; CLARKE, J.; ROSE, D. J. Effects of processing moisture on the physical properties and in vitro digestibility of starch and protein in extruded brown rice and pinto bean composite flours. **Food Chemistry**. v. 211, p. 726-733, 2016.

VARGAS-SOLÓRZANO, J. W.; CARVALHO, C. W. P.; TAKEITI, C. Y.; ASCHERI, J. L. R.; QUEIROZ, V. A. V. Physicochemical properties of expanded extrudates from colored sorghum genotypes. **Food Research International**. v. 55, p. 37-44, 2014.

WAGNER, J. R.; MOUNT, E. M.; GILES, H. F. Single Screw Extruder: Equipment. In: WAGNER, J. R.; MOUNT, E. M.; GILES, H. F. (Eds.). **Extrusion: The Definitive Processing Guide and Handbook**. 2nd ed. William Andrew Publishing: Oxford, 2014. p. 17-46.

YAĞCı, S.; GÖĞÜŞ, F. Response surface methodology for evaluation of physical and functional properties of extruded snack foods developed from food-by-products. **Journal of Food Engineering**. v. 86, n. 1, p. 122-132, 2008.

ZHOU, Z.; ROBARDS, K.; HELLIWELL, S.; BLANCHARD, C. The distribution of phenolic acids in rice. **Food Chemistry**. v. 87, n. 3, p. 401-406, 2004.

CONCLUSÃO GERAL

O design de novos alimentos a partir de matérias primas convencionais e não convencionais, através do cozimento por extrusão, é uma das áreas de atuação do laboratório de extrusão de alimentos e propriedades físicas da Embrapa Agroindústria de Alimentos. Dentro do marco desta área de atuação, o presente doutorado focalizou-se no desenvolvimento de extrudados expandidos a partir de cereais integrais. A força motriz por trás deste projeto relacionou-se com a compreensão do papel das fibras e lipídios na formação de material fundido dentro do extrusor e seu impacto na viscosidade de cisalhamento do fundido, acúmulo de pressão na matriz frontal, grau de expansão e formação de células de ar no material extrudado.

Após um estudo bibliográfico abrangente sobre a estrutura dos grãos, secagem dos grãos, tipos de moinho e processos de extrusão, optou-se por elaborar extrudados expandidos a partir de grãos integrais de arroz, milho, sorgo, centeio e trigo, em um extrusor de parafuso único, dado que essa tecnologia é comumente empregada no setor industrial de *snacks* extrudados. Para diferenciar o processo conduzido neste doutorado de outros processos utilizados na produção de *snacks* extrudados ricos em fibras, foi escolhido usar diferentes tipos de moinhos (discos, rolos e martelos). O tipo de moinho como variável independente afeta bastante tanto as propriedades físicas do material de alimentação quanto as variáveis dependentes de extrusão. Outra característica que diferenciou o processo realizado no presente doutorado foi superar as desvantagens de extrudar materiais ricos em fibras e lipídios (materiais com baixa processabilidade). Para isso, os cereais integrais foram previamente secos (na faixa de 6 a 11% de umidade em base úmida) antes de serem submetidos a processos de moagem de etapa única (moinhos sem placa de peneiramento). Nesse estágio, procurou-se maximizar o fracionamento das estruturas botânicas dos grãos, a fim de melhorar a homogeneidade do tamanho das partículas nos materiais de alimentação e a qualidade dos produtos finais em termos de expansão e textura.

As condições experimentais de extrusão de parafuso único foram previamente exploradas através de uma série de experimentos elementares: acoplamento do parafuso com diferentes taxas de compressão (3: 1, 4: 1 e 5: 1) e aquecimento do barril com diferentes perfis de temperatura (50, 110, 140 °C e 50, 90, 120 °C), a fim de conseguir processabilidade dos diferentes materiais de alimentação e maximizar a expansão dos extrudados. Esses objetivos foram alcançados através do processo de cozimento por extrusão a baixas umidades de alimentação, na faixa de 11 a 14% (base úmida), dado que as fibras naturais e os lipídeos presentes nos cereais integrais já atuam como lubrificantes entre as partículas e entre as superfícies internas do extrusor e as partículas que compõem o material de alimentação. Todos os processos, desde a secagem e moagem ao processo de extrusão, foram realizados visando a redução do número de etapas durante cada processo e sem a geração de subprodutos.

Com base nos resultados das curvas de secagem, o tempo para atingir a umidade de equilíbrio foi o mais alto para o grão de milho ($D_{eff} = 4.18 \times 10^{-10}$ m²/s) e o mais baixo para o grão de aveia ($D_{eff} = 7.35 \times 10^{-10}$ m²/s). De acordo com o perfil de viscosidade pelo RVA, o processo de secagem altera os picos de gelatinização e gelificação da fração amido em todos os grãos. Mudanças nas curvas de viscosidade evidenciaram que a secagem do centeio e do sorgo, sob as condições deste estudo, promovem um leve teor de amido danificado. O arroz, o sorgo, o milho secado e o trigo secado apresentaram partículas com distribuição unimodal. A aveia, o centeio, o milho não secado e o trigo não secado apresentaram partículas com distribuição bimodal. O arroz integral mostrou a mais estreita distribuição de tamanho de partículas, e o centeio a mais ampla. Do ponto de vista da extrudabilidade, os materiais de alimentação devem

apresentar alta homogeneidade nas partículas para garantir um fluxo aceitável de partículas na seção de transporte do parafuso. O fluxo de partículas foi melhorado quando os grãos foram secos até 6% de umidade, evidenciado pelas reduções nos valores D_{90}.

O grau de enchimento do parafuso foi correlacionado positivamente com a porosidade interpartícula (v) do material de alimentação ($r = +0,9879$). Para uma vazão mássica de partículas a 4 kg/h, v e o grau de enchimento do parafuso foram maiores para os produtos do moinho de rolos do que para os produtos do moinho de discos. As partículas de centeio moídas em rolos apresentaram maior v (72,9%), e as partículas de arroz integral moídas em discos, as menores (54,7%). O processo de secagem significativamente diminuiu a v dos produtos moídos de aveia e centeio. As partículas de milho moídas em discos, produziram extrudados com a maior expansão volumétrica (13,66). As partículas de arroz integral moídas em rolos, produziram extrudados com a maior expansão seccional (11.12). As partículas de sorgo e centeio do moinho de rolos, produziram extrudados com expansões seccionais e volumétricas mais altas do que as partículas do moinho de discos. As partículas de trigo do moinho de discos, produziram extrudados com a maior densidade aparente (240,6 kg/m³). As partículas de centeio do moinho de discos, produziram extrudados com a maior força média de perfuração (6,17 N) e o maior trabalho de crocância (0,82 N · mm). Extrudados de arroz integral produzidos a partir de partículas do moinho de rolos, e extrusados de milho produzidos a partir de partículas do moinho de discos ou rolos, apresentaram as menores forças médias de perfuração (~ 1,89 N) e o menor trabalho de crocância (~ 0,24 N · mm). A variabilidade em v em função da ação combinada do tipo cereal e do tipo de moinho pode ser usada para preparar materiais de alimentação com grau variável de cozimento por extrusão, dado que o grau de enchimento do parafuso (portanto, v) pode ser associado com o acumulo de pressão dentro do extrusor. Além disso, de acordo com o grau de cozimento por extrusão e misturas apropriadas de diversos grãos, pode ser possível otimizar as propriedades de expansão e textura dos *snacks* extrusados de cereais integrais.

As partículas do moinho de rolos foram mais adequadas para uma correlação negativa entre a v do material de alimentação e o torque fornecido ao parafuso durante o processamento de extrusão de arroz integral ($r = -0,8952$). As partículas de arroz integral do moinho de discos apresentaram menor v e geraram valores de torque mais altos que os materiais do moinho de rolos. v diminuiu ainda mais e o torque aumentou ainda mais, alterando a umidade dos grãos antes da moagem de 9 para 6%. Ao alterar a umidade de alimentação de 11 para 14%, v aumentou apenas nos materiais do moinho de rolos. O torque diminuiu com um incremento na umidade de alimentação, independentemente da umidade dos grãos antes da moagem. De acordo com o tipo de moinho e a umidade da alimentação, as partículas de arroz integral apresentaram comportamento diferente durante o processo de extrusão. Foi observada alta instabilidade de torque quando os materiais do moinho de discos foram processados a baixa umidade de alimentação. Por outro lado, o torque foi estável com materiais do moinho de rolos extrudados a 14% da umidade de alimentação. Para obter extrudados com boa expansão, recomenda-se preparar arroz integral usando moinho de rolos e extrudar a 11% de umidade de processo. Os resultados apresentados podem refletir o grau de anisotropia dos extrudados de acordo com a preparação do material particulado. Materiais de alimentação com alta v podem produzir extrusados menos anisotrópicos (torque baixo e estável), contribuindo para um uso mais eficiente da energia.

A umidade dos grãos antes da moagem nos níveis de 9 a 11% não afetou as variaveis dependentes de extrusão e as propriedades de expansão e textura dos extrudados de arroz integral. A força média de perfuração não foi influenciada pelas mudanças na umidade de extrusão na faixa de 11 a 14%. A umidade de alimentação nesta faixa altamente afetou as demais respostas avaliadas. Mudanças na velocidade do parafuso na faixa de 150 a 250 rpm altamente afetaram o torque, a expansão longitudinal e a força média de perfuração dos

extrudados. Mudanças na taxa de alimentação nos níveis de 4 a 6 kg/h altamente influenciou a integral da curva, no entanto moderadamente afetou o torque e a força média de perfuração dos *snacks* extrudados de arroz integral. O efeito de interação entre a umidade da alimentação e a velocidade do parafuso foi a chave para maximizar as propriedades de expansão. A maior expansão seccional com a maior porosidade extrudada foi obtida quando os grãos de arroz integral foram moídos em um moinho de rolos, a umidade da alimentação foi condicionada a 11% e a velocidade do parafuso foi fixada em 250 rpm. Essa combinação também gerou baixos valores de torque, baixas forças de perfuração e baixos valores de integral da curva, quando a taxa de alimentação foi fixada em 4 kg/h. As variáveis de entrada significativas possibilitaram a previsão e, consequentemente, o design de *snacks* extrudados de arroz integral com características aceitáveis de expansão e textura.

Ainda há muito a ser feito para melhorar a expansão dos extrudados à base de cereais integrais. Primeiro, pode se explorar outras tecnologias ou formas de secagem para melhorar o fracionamento das camadas externas e o germe dos grãos, como por exemplo, o uso de ultrassom na faixa de 20-300 kHz, aplicado isoladamente ou em combinação com a secagem. Aliás, as ondas ultrassónicas podem deformar as camadas externas e a endosperma dos grãos, criar canais microscópicos, reduzir a camada limite de difusão e acelerar a transferência de massa convectiva. Em segundo lugar, explorar outros tipos de moinhos não contemplados neste estudo, como por exemplo, moinho de bolas, moinho de discos com pines, ou moinho de rolos com outros padrões de canelado na superfície dos rolos. Em quanto aos parâmetros de processamento por extrusão monorosca, pode ser explorado umidades de alimentação na faixa de 9 – 11% em combinação com o uso de parafusos com relação de compressão menores a 5:1. Os lipídeos naturais e as fibras insolúveis já desempenham o role de plastificantes, sendo necessário menores teores de umidades de alimentação para atingir boa expansão.
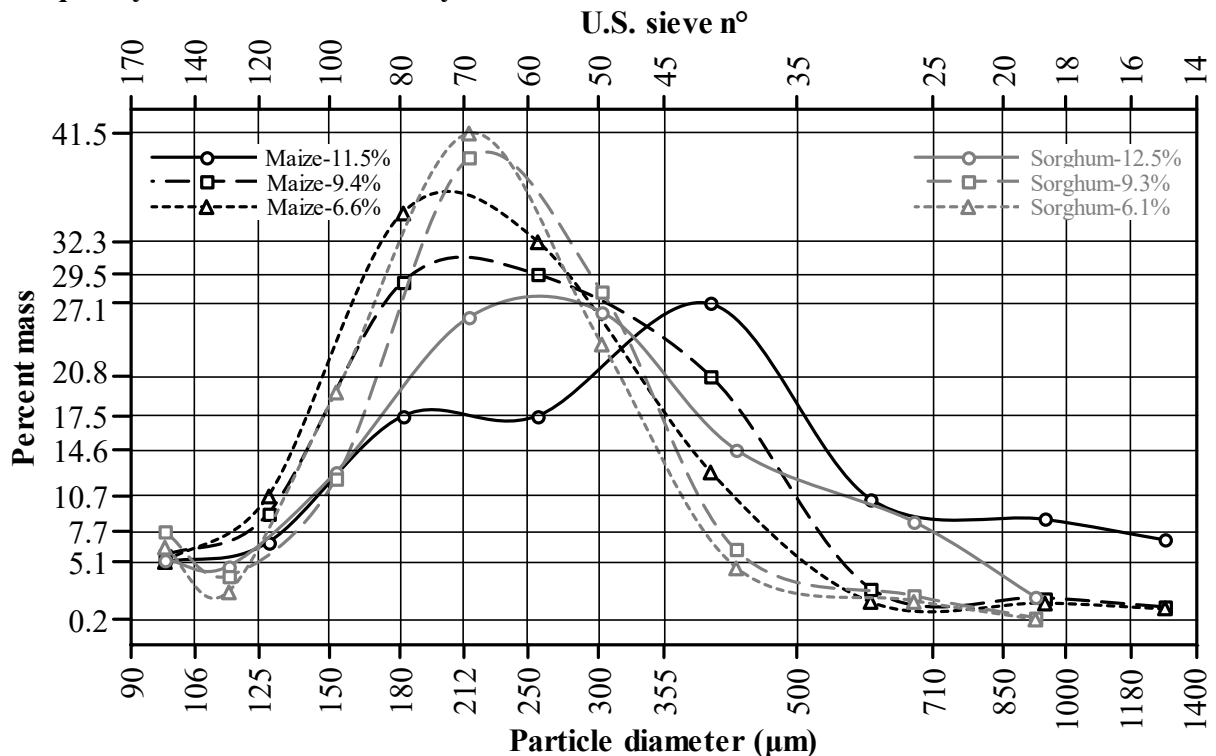
ANNEXES

ANNEXE A – Sieving analysis results, frequency distribution curves by mass, and particle-size parameters for wholemeals of brown rice and oats

Particle-size values

U.S. sieve		Mass retained (g) at variable GM						Para-meter	Particle-size parameters at variable GM					
Mesh	Opening	GM_0		GM_9		GM_6			GM_0		GM_9		GM_6	
n°	μm	1	2	1	2	1	2		1	2	1	2	1	2
Brown rice														
230	63	0.48	0.19	0.09	0.07	0.11	0.09	D_{10}	98.8	100.9	99.1	100.7	98.1	99.8
200	75	2.00	1.21	0.85	0.47	0.73	0.42	D_{50}	174.7	178.4	170.1	172.6	164.0	168.3
170	90	11.51	11.64	13.63	13.07	14.73	13.82	D_{90}	292.9	295.1	268.9	270.7	265.2	266.1
120	125	23.86	23.53	26.20	25.81	28.55	27.32	D_{mass}	215.1	218.8	207.5	210.1	202.4	205.5
80	180	33.79	32.08	33.00	33.73	32.82	34.03	σ^2	7333	7317	5891	5958	5771	5699
60	250	16.48	19.33	18.23	18.67	15.99	17.37	σ	85.6	85.5	76.8	77.2	76.0	75.5
50	300	7.80	7.90	6.40	6.80	5.81	5.88	Sp	1.111	1.088	0.998	0.985	1.018	0.988
40	425	3.76	3.89	1.77	1.91	1.60	1.60	Un	0.398	0.391	0.370	0.367	0.375	0.367
Oats														
200	75	0.50	0.11	0.45	0.23	0.52	0.12	D_{10}	129.4	130.6	123.9	123.9	97.8	96.7
170	90	0.34	0.13	1.03	1.62	15.58	17.43	D_{50}	404.7	423.0	279.9	298.7	224.2	228.3
120	125	33.43	33.76	41.69	40.02	30.13	28.22	D_{90}	1256	1318	946	957	819	827
60	250	17.23	16.15	18.06	17.73	26.05	26.06	D_{mass}	739.2	760.3	600.4	617.5	476.9	482.0
30	600	34.66	34.67	32.18	33.17	26.49	26.64	σ^2	326020	343042	250922	261421	216265	231208
14	1400	10.66	11.48	6.01	6.43	1.60	1.82	σ	571.0	585.7	500.9	511.3	465.0	480.8
10	2000	2.24	2.58	0.75	0.87	0.13	0.21	Sp	2.783	2.806	2.935	2.790	3.219	3.198
8	2380	1.00	1.15	0.23	0.28	0.00	0.00	Un	0.772	0.770	0.834	0.828	0.975	0.998

GM: grain moisture prior milling (wet basis); subscripts 0, 9, and 6 refer to the grains with initial moisture, dried up to 9%, and dried up to 6%; D: diameter; subscripts 10, 50, and 90, refer to quantiles (small particle, median, and large particle diameters, respectively); D_{mass}: average particle size by mass; σ^2: variance; σ: standard deviation; Sp: span; Un: uniformity.

Frequency distribution curves by mass
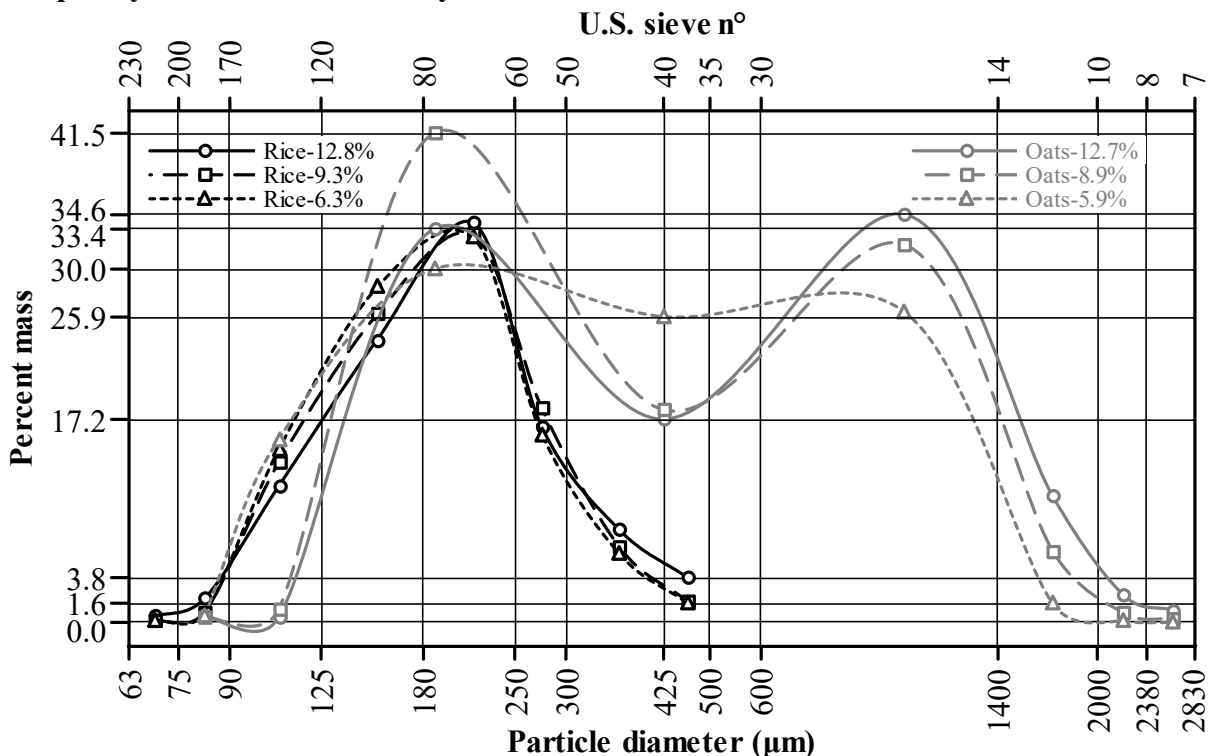
ANNEXE B – Sieving analysis results, frequency distribution curves by mass, and particle-size parameters for wholemeals of maize and sorghum

Particle-size values

U.S. sieve		Mass retained (g) on top of sieves						Para-meter	Particle-size parameters					
Mesh	Opening	GM_0		GM_9		GM_6			GM_0		GM_9		GM_6	
n°	μm	1	2	1	2	1	2		1	2	1	2	1	2
Maize														
170	90	5.09	4.36	5.62	4.86	5.16	4.72	D_{10}	119.8	123.7	112.3	113.9	111.7	113.5
140	106	6.77	6.59	9.19	9.68	10.76	10.30	D_{50}	272.7	276.2	197.2	197.7	180.1	182.7
100	150	17.52	17.42	28.89	28.88	34.95	34.42	D_{90}	826.1	833.7	372.5	373.0	336.3	337.5
70	212	17.53	17.87	29.52	29.65	32.50	33.70	D_{mass}	433.4	438.5	280.1	281.4	254.6	257.3
50	300	27.08	27.27	20.87	20.87	12.83	12.83	σ^2	105887	106424	57883	59786	60878	62519
35	500	10.42	10.63	2.78	2.77	1.68	1.66	σ	325.4	326.2	240.6	244.5	246.7	250.0
25	710	8.72	8.90	2.02	1.99	1.60	1.65	Sp	2.590	2.570	1.320	1.310	1.247	1.226
16	1180	6.96	7.10	1.23	1.33	1.10	1.17	Un	0.751	0.744	0.859	0.869	0.969	0.972
Sorghum														
170	90	5.29	2.74	7.70	5.55	6.36	4.74	D_{10}	115.5	122.4	108.4	120.7	117.7	138.0
140	106	4.70	4.76	3.92	2.35	2.53	1.94	D_{50}	219.9	226.9	194.1	196.0	185.1	184.0
120	125	12.69	13.26	12.24	15.18	19.63	22.01	D_{90}	445.1	453.0	298.5	300.8	289.6	251.3
80	180	25.82	25.44	39.54	39.04	41.71	42.19	D_{mass}	304.2	311.3	244.9	249.6	232.6	224.1
60	250	26.25	27.07	28.15	28.87	23.72	23.07	σ^2	30915	30617	16004	16274	15161	12661
45	355	14.59	15.64	6.14	6.78	4.61	4.56	σ	175.8	175.0	126.5	127.6	123.1	112.5
35	500	8.50	8.73	2.25	2.32	1.77	1.81	Sp	1.499	1.457	0.980	0.919	0.929	0.616
20	850	2.10	2.15	0.36	0.39	0.17	0.19	Un	0.578	0.562	0.516	0.511	0.529	0.502

GM: grain moisture prior milling (wet basis); subscripts 0, 9, and 6 refer to the grains with initial moisture, dried up to 9%, and dried up to 6%; *D*: diameter; subscripts 10, 50, and 90, refer to quantiles (small particle, median, and large particle diameters, respectively); D_{mass}: average particle size by mass; σ^2: variance; σ: standard deviation; *Sp*: span; *Un*: uniformity.

Frequency distribution curves by mass

ANNEXE C – Sieving analysis results, frequency distribution curves by mass, and particle-size parameters for wholemeals of rye and wheat

Particle-size values

U.S. sieve		Mass retained (g) on top of sieves						Para-meter	Particle-size parameters					
Mesh	Opening	GM_0		GM_9		GM_6			GM_0		GM_9		GM_6	
n°	μm	1	2	1	2	1	2		1	2	1	2	1	2
Rye														
200	75	16.65	17.76	29.90	30.80	30.45	30.29	D_{10}	49.5	46.4	27.7	26.9	27.3	27.4
170	90	10.78	9.87	5.20	5.21	6.47	6.80	D_{50}	256.3	257.0	172.7	169.9	158.0	157.5
120	125	25.36	24.95	38.79	37.89	44.38	44.05	D_{90}	1157.7	1163.5	740.6	738.2	511.9	518.3
40	425	9.52	9.59	9.48	9.45	9.28	9.17	D_{mass}	627.1	627.2	370.6	367.9	305.1	305.6
30	600	25.78	25.73	14.98	14.85	9.42	9.53	σ^2	351909	351153	200518	202504	184685	185274
14	1400	8.12	8.26	1.78	1.76	0.50	0.51	σ	593.2	592.6	447.8	450.0	429.7	430.4
10	2000	2.29	2.36	0.23	0.20	0.12	0.12	Sp	4.324	4.346	4.127	4.187	3.067	3.117
8	2380	1.41	1.29	0.06	0.09	0.00	0.00	Un	0.946	0.945	1.208	1.223	1.408	1.409
Wheat														
270	53	9.16	8.62	13.17	12.63	12.68	12.40	D_{10}	59.6	60.6	44.2	46.1	46.0	47.1
230	63	9.73	9.80	8.09	8.70	7.70	7.54	D_{50}	154.4	156.3	144.8	145.2	144.9	144.3
170	90	8.62	9.05	9.65	9.42	9.55	10.31	D_{90}	679.2	691.7	450.8	455.0	366.4	370.1
120	125	29.17	28.08	31.47	31.39	33.21	33.24	D_{mass}	342.1	347.1	263.3	264.8	243.2	243.7
70	212	21.43	21.98	23.39	23.45	25.92	25.51	σ^2	125657	127536	66594	67735	51180	53018
40	425	11.14	11.44	10.83	10.94	9.74	9.79	σ	354.5	357.1	258.1	260.3	226.2	230.3
20	850	7.93	8.05	3.27	3.36	1.66	1.71	Sp	4.012	4.038	2.808	2.816	2.211	2.238
14	1400	2.74	2.83	0.42	0.41	0.12	0.15	Un	1.036	1.029	0.980	0.983	0.930	0.945

GM: grain moisture prior milling (wet basis); subscripts 0, 9, and 6 refer to the grains with initial moisture, dried up to 9%, and dried up to 6%; *D*: diameter; subscripts 10, 50, and 90, refer to quantiles (small particle, median, and large particle diameters, respectively); D_{mass}: average particle size by mass; σ^2: variance; σ: standard deviation; *Sp*: span; *Un*: uniformity.
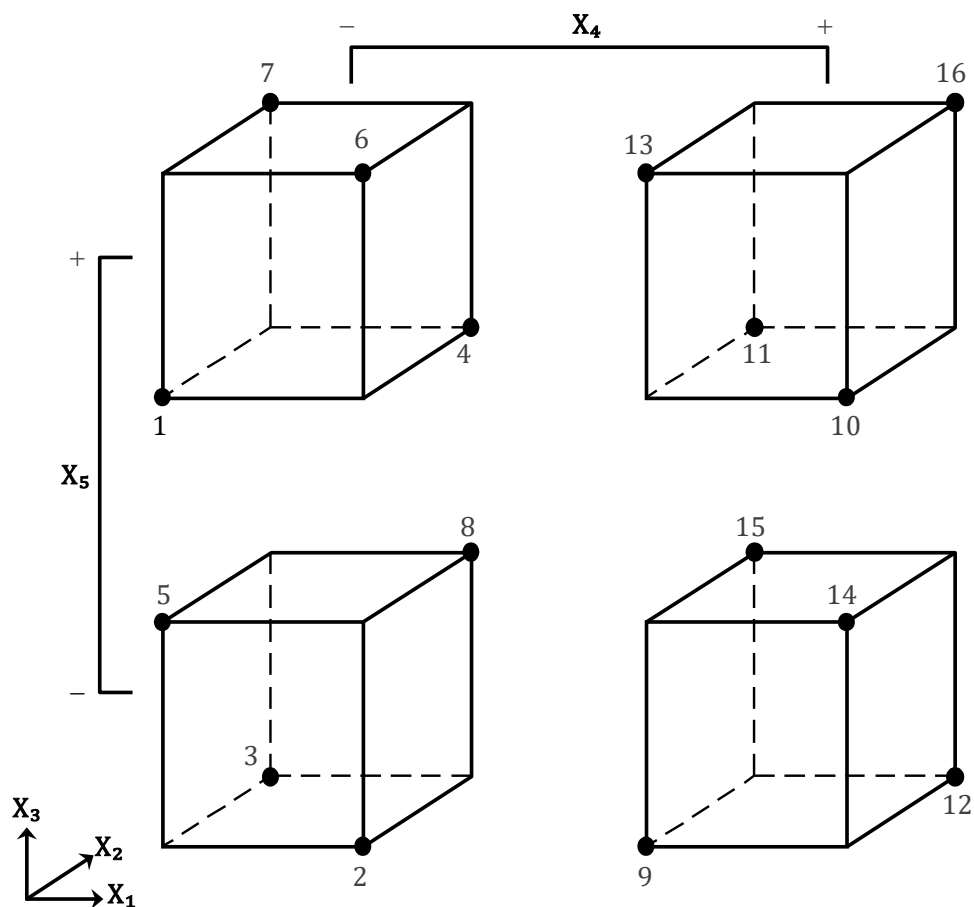
Frequency distribution curves by mass
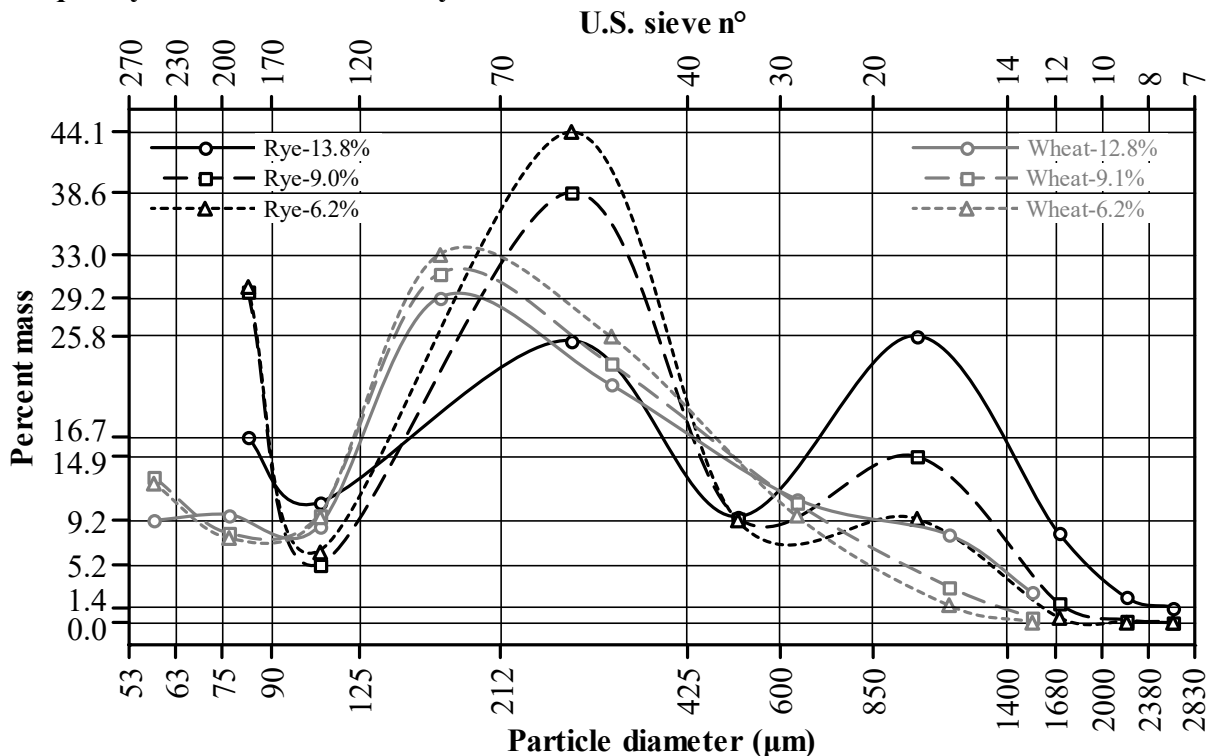
ANNEXE D – Scanned images of whole-grain cereal extruded snacks
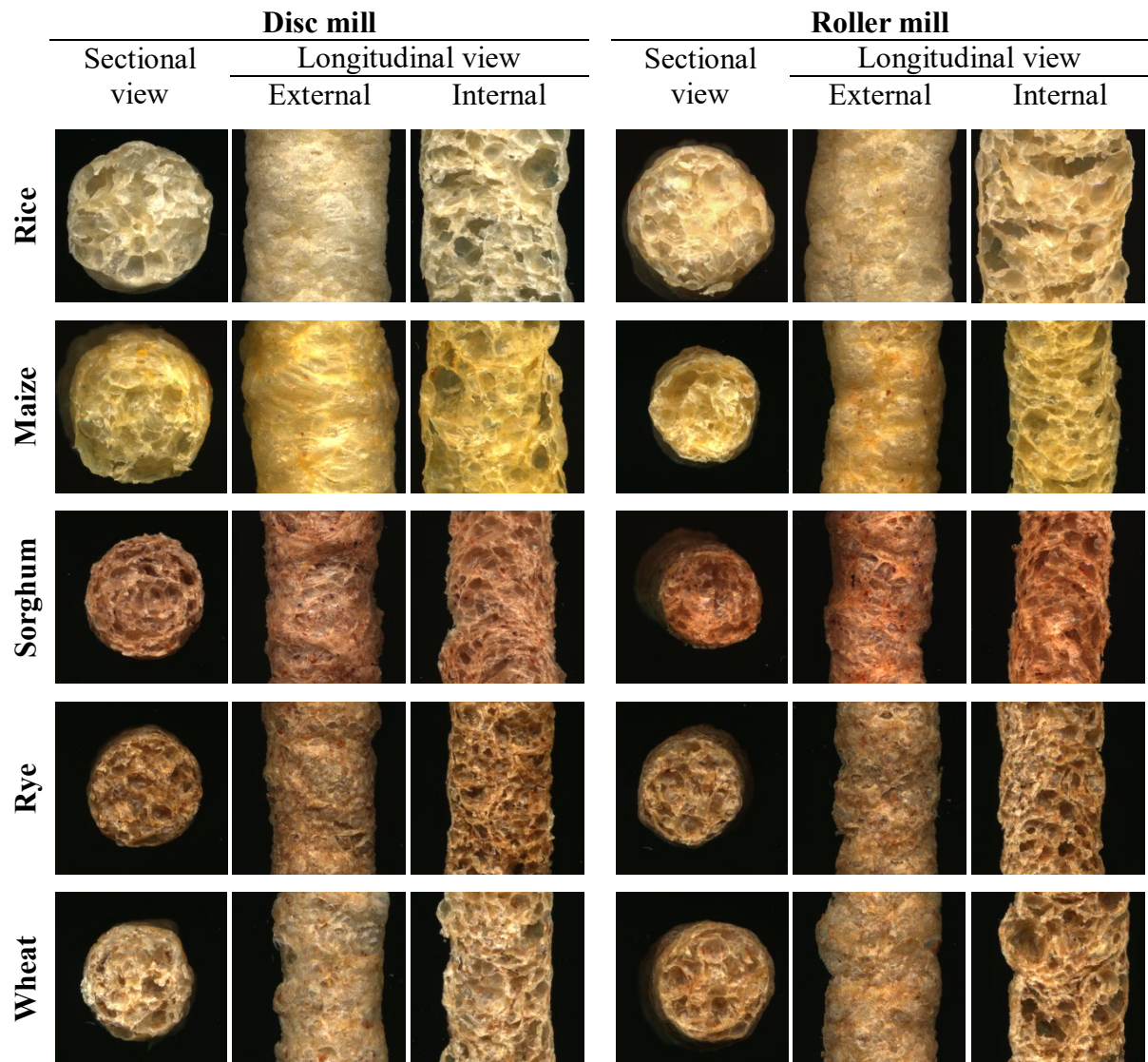
ANNEXE E – The 2_V^{5-1} design for the brown rice extrusion experiment

Actual levels for the 2_V^{5-1} design

Standard order	Grain moisture X_1 %	Grinder type X_2	Feed moisture X_3 %	Screw speed X_4 rpm	Feed rate X_5 kg/h
1	9	Disc	11	150	6
2	11	Disc	11	150	4
3	9	Roller	11	150	4
4	11	Roller	11	150	6
5	9	Disc	14	150	4
6	11	Disc	14	150	6
7	9	Roller	14	150	6
8	11	Roller	14	150	4
9	9	Disc	11	250	4
10	11	Disc	11	250	6
11	9	Roller	11	250	6
12	11	Roller	11	250	4
13	9	Disc	14	250	6
14	11	Disc	14	250	4
15	9	Roller	14	250	4
16	11	Roller	14	250	6

ANNEXE F – Scanned images of brown rice extruded snacks